Impact of elevated pCO_2 on the ecophysiology of *Mytilus edulis*

Auswirkungen erhöhter pCO_2 Werte auf die Ökophysiologie der Miesmuschel *Mytilus edulis*

Dissertation
zur Erlangung des akademischen Grades
Dr. rer. nat.
der Mathematisch-Naturwissenschaftlichen Fakultät
der Christian-Albrechts-Universität zu Kiel
vorgelegt von

Jörn Thomsen
Kiel, 2012

Referent: Prof. Dr. Frank Melzner

Koreferent: Prof. Dr. Arne Körtzinger

Tag der mündlichen Prüfung: 24.04.2012

Zum Druck genehmigt am: 24.04.2012

Summary

Increasing atmospheric CO_2 concentrations equilibrate with the surface water of the oceans and thereby increase seawater pCO_2 and decrease [CO_3^{2-}] and pH. This process of ocean acidification is expected to cause a drastic change of marine ecosystem composition and a decrease in calcification ability of various benthic invertebrates. The studied area, Kiel Fjord, is characterized by high pCO_2 variability due to upwelling of O_2 depleted and CO_2 enriched bottom water. Within less than 50 years, eutrophication of the Baltic Sea has drastically increased the mean pCO_2 in the fjord. The observed increase and also the rate of this acidification process is much higher than it is expected for the global ocean as a consequence of increasing atmospheric CO_2 concentrations. In contrast to other areas subjected to elevated pCO_2, calcifying invertebrates inhabit Kiel fjord and the benthic community is dominated by the blue mussel *Mytilus edulis*. Mussel larvae settle in the period of the year when highest pCO_2 (800-2300 µatm) are encountered, which is, at the same time, the main growth period due to highest phytoplankton densities.

In laboratory experiments, calcification rates of *M. edulis* are maintained at elevated pCO_2 levels which are expected to occur by the year 2300. Only at high pCO_2 above 3000 µatm, calcification is significantly reduced. One possible reason for this tolerance is the fact that even under control conditions, the extracellular body fluids (haemolymph and extrapallial fluid, EPF) of *M. edulis* are characterized by low pH and [CO_3^{2-}] and high pCO_2. Therefore, the EPF which is in direct contact with the shell is undersaturated with calcium carbonate also at current, low seawater pCO_2. Under elevated pCO_2, mussels do not buffer the extracellular acidosis by means of bicarbonate accumulation. Thus haemolymph pH and [CO_3^{2-}] are reduced even further. Calcification might not be affected by the extracellular acidosis, as an amorphous calcium carbonate (ACC) precursor is most probably formed in intracellular vesicles. Since mussels are able to efficiently regulate the intracellular pH, reduced extracellular pH might therefore have only little impact on the initial calcification process. On the other hand, the production of the organic shell components, e.g. the periostracum, consumes high amounts of energy. Especially in young thin shelled life stages with a higher organic shell content most of the energy allocated to growth is required for shell production.

Under elevated pCO_2, mussels initially (two months acclimation) up - regulate their metabolic rates which may indicate higher energy demand for ion regulatory processes. Long-term acclimated animals (12 months acclimation) probably switch to an energetically less expensive compensation and do not exhibit elevated aerobic metabolism. However, long-term acclimated mussels are characterized by lower filtration rates. As consequence, after both intermediate and long-term exposure, the scope for growth is reduced in high pCO_2 acclimated animals. Additionally, after intermediate and also long-term acclimation to elevated pCO_2, protein metabolism is increased, as indicated by an elevation of ammonia excretion rates. This mode of energy generation is less efficient than oxidation of lipid or carbohydrate and may contribute to lower energy availability for growth and calcification. Similar to other aquatic animals, ammonia excretion in mussels seems to be facilitated by NH_3 diffusion through

Rhesus (Rh) and ammonium transporter (Amt) protein channels and subsequent acid-trapping by separate proton excretion.

In order to test the importance of energy supply and elevated pCO_2 on mussel calcification, juvenile *M. edulis* were exposed to a crossed experimental design for seven weeks. Higher food supply enables mussels to calcify also under highly elevated pCO_2. In general food supply is the most important factor which determines the growth rates of mussels whereas pCO_2 has only a minor effect. In a simultaneous field study, mussels were transplanted to the energy rich high pCO_2 inner fjord and to the outer parts of the fjord at lower pCO_2 and particulated organic carbon concentrations. Similar to the laboratory experiment, mussels exhibit much higher growth rates in the high pCO_2 inner fjord with its higher particulate organic carbon concentrations. This reveals the importance of energy availability impacting CO_2 tolerance of *M. edulis*.

Mussels seem to be relatively tolerant to elevated pCO_2 both in laboratory experiments and under current high pCO_2 conditions in Kiel Fjord. The high energy availability present in the eutrophicated habitat may support the tolerance to elevated pCO_2. In the future, increasing atmospheric CO_2 concentrations will drastically elevate pCO_2 level in this habitat. The benthic life stages seem to be able to cope with the expected levels but plantonic larvae might be vulnerable. However, *M. edulis* exhibit a high adaptation potential to the rate of acidification in the recent past and might be able to adapt also to higher levels in future. In order to predict the success of *M. edulis* in future, also effects of elevated temperature and the response of their main predators to these conditions needs to be considered.

Zusammenfassung

Die steigenden CO_2 Konzentration der Atmosphäre und die folgende Äquilibrierung mit dem Oberflächenwasser der Ozeane führen zu erhöhten pCO_2 und sinkenden Karbonationen Konzentrationen ($[CO_3^{2-}]$) und pH Werten. Die sogenannte Ozeanversauerung hat vermutlich weitreichende Auswirkungen auf die marinen Ökosysteme und führt möglicherweise dazu, dass die Kalzifizierungsraten insbesondere benthischer Wirbelloser abnimmt. Das Untersuchungsgebiet der Kieler Förde weist, durch den Auftrieb bodennahen Wassers mit niedriger O_2 Sättigung und hohen CO_2 Konzentrationen, bereits heutzutage hohe und variable pCO_2 Werte auf. Innerhalb der letzten 50 Jahre hat die Eutrophierung zu einer deutlichen Erhöhung der pCO_2 Werte in der Förde geführt. Damit ist sowohl das Ausmaß als auch die Geschwindigkeit der Versauerung höher, als es für die weltweiten Ozeane im Zuge des zukünftigen CO_2 Anstiegs zu erwarten ist. Im Gegensatz zu anderen Gebieten, die vergleichbar erhöhten pCO_2 Werten ausgesetzt sind, leben zahlreiche kalzifizierende Wirbellose in der Förde und die Miesmuschel *Mytilus edulis* dominiert die benthische Gemeinschaft. Die Larven der Muscheln siedeln insbesondere in der Jahreszeit in der die höchsten pCO_2 Werte (800-2300 µatm) auftreten. Aufgrund der hohen Phytoplanktonkonzentrationen ist dies ebenfalls die Zeit der höchsten Wachstumsraten.

In Laborversuchen ist *M. edulis* in Lage die Kalzifizierungsraten unter erhöhten pCO_2 Werten, die für das Jahr 2300 erwartet werden, aufrechtzuerhalten. Extrazelluläre Flüssigkeiten (Hämolymphe und extrapalliale Flüssigkeit, EPF) weisen auch unter Kontrollbedingungen hohe pCO_2 Werte und niedrige pH und $[CO_3^{2-}]$ auf. Die EPF, die in direktem Kontakt zur Schale steht, ist demnach auch bei niedrigem Meerwasser pCO_2 mit Kalziumkarbonat untersättigt. Bei erhöhtem Meerwasser pCO_2 säuert sich die Hämolymphe an und wird nicht durch Bikarbonat gepuffert. Die Ansäuerung des extrazellulären Raumes hat vermutlich deshalb nur geringe Auswirkungen auf die Kalzifizierung, da ein amorpher Kalziumkarbonatvorläufer bereits in intrazellulären Vesikeln gebildet wird. Muscheln können den intrazellulären pH weitestgehend unabhängig vom Außenmedium regulieren, weshalb die extrazelluläre Ansäuerung die Schalenbildung nur geringfügig beeinflusst. Allerdings benötigt die Synthese der organischen Schalenbestandteile sehr viel Energie. Insbesondere in jungen, dünnschaligen Lebensstadien, die Schaleen mit einem höheren Organikanteil aufweisen, wird der größte Teil der für das Wachstum benötigten Energie in die Schalenbildung investiert.

Unter erhöhtem pCO_2, weisen Muscheln zunächst höhere metabolische Raten auf, was möglicherweise auf einen erhöhten Energiebedarf für aktive Ionentransportprozesse hinweist. Nach langer Akklimation scheinen sie auf eine effizientere Regulation zu wechseln und der aerobe Stoffwechsel ist nicht mehr erhöht. Allerdings nimmt die Filtrationsleistung ab. In beiden Fällen ist demnach die Energie, die für das Wachstum zur Verfügung steht, reduziert. Außerdem ist nach mittlerer und Langzeit-Akklimierung der Proteinstoffwechsel erhöht, erkennbar an der höheren Ammoniumexkretion. Diese Art der Energiegewinnung ist weniger effizient als Lipid- und kohlenhydratstoffwechsel und könnte zu einer verminderten Energieverfügbarkeit beitragen. Wie auch in anderen aquatischen Tieren scheint die Ammoniumexkretion in Muscheln durch Rhesus (Rh) und

Ammoniumtransporter (Amt) Kanalproteine und eine anschließende Protonierung gefördert zu werden.

Die Bedeutung von Energieversorgung und erhöhtem pCO_2 auf die Kalzifizierung ist in einem gekreuzten Versuchsansatz getestet worden. Höhere Futterzugabe ermöglicht den Muscheln die Kalzifizierung auch unter hohen pCO_2. Generell ist die Futterzufuhr von größerer Bedeutung für das Wachstums während pCO_2 nur einen geringen Effekt hat. In einem zeitgleich durchgeführten Feldexperiment sind junge Muscheln in die Innenförde mit ihren hohen pCO_2 und in die Außenförde mit niedrigeren pCO_2 und partikulären organischen Kohlenstoffkonzentrationen verpflanzt worden. In Übereinstimmung mit dem Laborexperiment, weisen die Tiere in der inneren Förde trotz des höheren pCO_2 deutlich höhere Wachstumsraten als die in der Außenförde auf. Dieses Ergebnis betont die Bedeutung der Energieverfügbarkeit für die Toleranz von *M. edulis* gegenüber der Ozeanversauerung.

Muscheln scheinen gegenüber erhöhten pCO_2 Werten in Laborexperimenten aber auch innerhalb der Kieler Förde relativ tolerant zu sein. Die hohe Energieverfügbarkeit in dem eutrophierten Habitat der Kieler Förde könnte die Toleranz gegenüber hohen pCO_2 Werten fördern. Allerdings werden die steigenden CO_2 Konzentrationen der Atmosphäre die pCO_2 Werte der Förde zukünftig deutlich erhöhen. Während die benthische Lebensphase gegenüber den erwarteten Werten tolerant zu sein scheint, könnten the planktischen Larven sensibler sein. Allerdings wies *M. edulis* eine hohe Anpassungsrate an die Versauerung der jüngeren Vergangenheit auf und könnte dementsprechend auch in der Lage sein, sich an zukünftige Bedingungen anzupassen. Um verlässlich vorherzusagen, ob *M. edulis* auch in Zukunft erfolgreich sein wird, ist es notwendig auch die Effekte erhöhter Temperaturen und die Auswirkungen solcher Bedingungen auf die Haupträuberorgansismen zu berücksichtigen.

.

Abbreviations

A	absorbed energy
A_C	carbon alkalinity
A_T	total alkalinity
CO_3^{2-}	carbonate
C_T	total dissolved inorganic carbon
DM	dry mass
DOC	dissolved organic matter
DOM	dissolved organic carbon
EPF	extrapallial fluid
FM	fresh mass
HCO_3^-	bicarbonate
HL	haemolymph
H^+-ATPase	vesicular proton pump
MO_2	aerobic metabolic rate
Na^+/K^+-ATPase	sodium potassium ATPase
NHE	sodium proton exchanger
NH_3	ammonia
NH_4^+	ammonium
NH_3/NH_4^+	total ammonia
O:N	oxygen to nitrogen ratio
pCO_2	carbon dioxide partial pressure
PFA	paraformaldehyde
pHe	extracellular pH (haemolymph/blood)
pHi	intracellular pH
pH_{NBS}	pH on the NBS scale
pH_T	pH on the total scale
POC	particulate organic carbon
R	respired energy
SFDM	shell free dry mass
SfG	Scope for Growth
U	excreted energy

1. Introduction

1.1 Ocean acidification

The combustion of fossil fuels leads to an increase of atmospheric carbon dioxide (CO_2) concentrations. Since the beginning of the industrial revolution, CO_2 concentrations increased from 285 ppm to 390 ppm today, whereas it remained relatively stable for the last 420,000 years (Petit et al. 1999, Fig. 1.1). Especially, the increase rate probably exceeds those of former high atmospheric CO_2 periods in earth history (Petit et al. 1999). The International Panel on Climate Change (IPCC) published a number of scenarios which calculate the CO_2 amounts emitted by human activities depending on social and technological development. Scenario A2 is based on business as usual development with slow technological progress, whereas B1 assumes rapid change to a society dominated by a service and information economy. According to these scenarios, the atmospheric CO_2 concentration is expected to rise to concentration between 650 ppm (scenario B1) and up to 970 ppm (scenario A2) until the year 2100 (IPCC 2007). Since CO_2 is a greenhouse gas its accumulation in the atmosphere causes a global warming. As a second consequence, increasing atmospheric CO_2 leads to increasing dissolution in the ocean surface water according to Henry´s law. About 50% of the anthropogenic CO_2 has been already taken up by the ocean water and this process is going to continue in future (Sabine et al. 2004).

The physical dissolution (characterized by K_0) is accompanied by a chemical reaction of CO_2 with the water molecules which forms carbonic acid (H_2CO_3). Carbonic acid is not stable but dissociates to bicarbonate and one proton is released. This proton can react with the carbonate ions of the seawater and forms a second bicarbonate. The carbon species are in chemical equilibrium to each other and the conversion can be described by two dissociation constants K_1 and K_2.

$$CO_2 + H_2O \overset{K_0}{\leftrightarrow} H_2CO_3 \overset{K_1}{\leftrightarrow} H^+ + HCO_3^- \overset{K_2}{\leftrightarrow} 2H^+ + CO_3^{2-} \quad (1)$$

Dissolved CO_2, HCO_3^- and CO_3^{2-} are the components of the carbonate system. The sum of the three species is called dissolved inorganic carbon (C_T)

$$C_T = CO_2 + HCO_3^- + CO_3^{2-} \quad (2)$$

As a consequence of the CO_2 uptake by the oceans and the net proton generation, oceanic pH decreases. Fig 1.1 depicts the pH decrease of the surface ocean in response to an increase of atmospheric CO_2 concentrations from pre-industrial values up to 550 µatm. Present day global mean pH is 8.1 which is about 0.1 units below pre-industrial values and is expected to decrease further depending on the increase of CO_2 concentrations, which will result in a pH decrease of -0.46 units in 2100 (scenario A2, Caldeira and Wickett 2005). In contrast to the relative stable open ocean, in coastal areas pH is highly variable as a consequence of upwelling or other biogeochemical processes (Feely et al. 2008, Provoost et al. 2010).

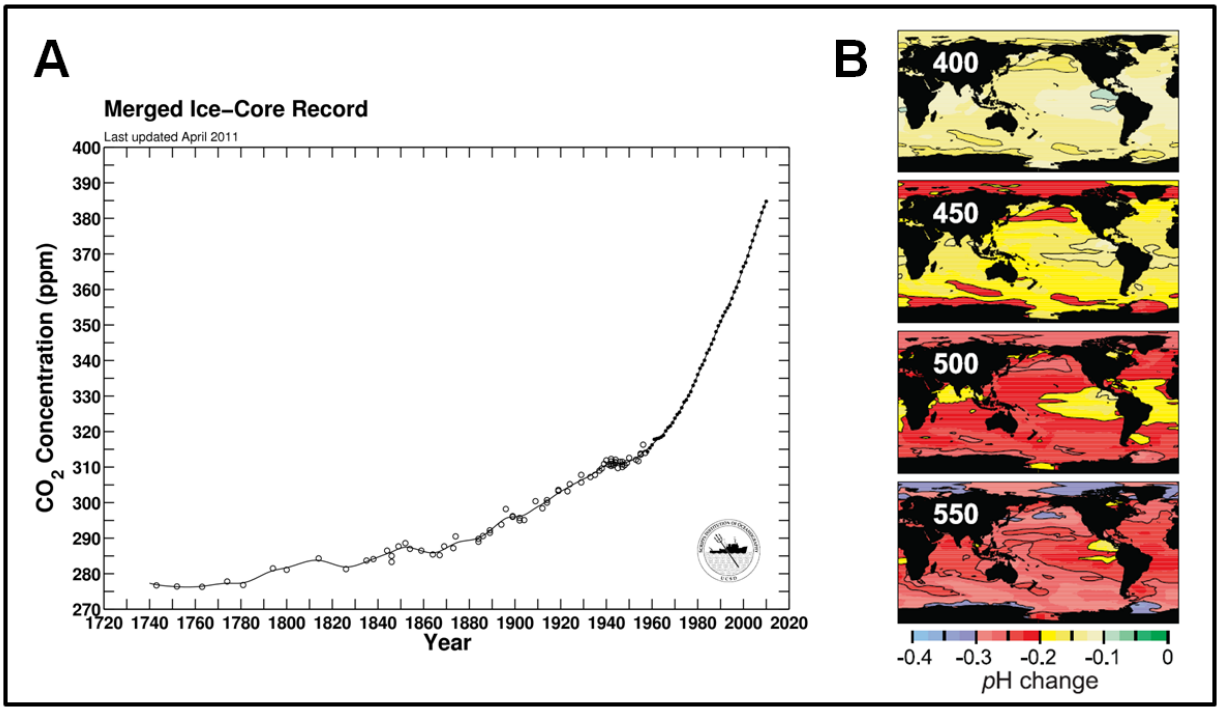

Figure 1.1: Atmospheric CO_2 concentration over the last 300 years. The data set combines concentrations from ice cores and measured atmospheric values, (http://scrippsco2.ucsd.edu/home/index.php), (A), projected pH change of ocean surface water for atmospheric CO_2 concentrations between 400 and 550 µatm in comparison to pre-industrial values (Cao and Caldeira 2008), (B).

The ocean pH is buffered by the alkalinity which is the sum of weak bases and balances the charge differences between anions and cations (Dickson et al. 1981). The total alkalinity (A_T) comprises all weak bases, whereas the major component of this buffering system is the carbonate alkalinity (A_C) with its components HCO_3^- and CO_3^{2-}.

$$A_T = [HCO_3^-] + 2[CO_3^{2-}] + [B(OH)_4^-] + [OH^-] + [HPO_3^{2-}] + 2[PO_4^{3-}] + [SiO(OH)_3^-] + [NH_3] + [HS^-] + \ldots$$

$$- [H^+]_F - [HSO_4^-] - [HF] - [H_3PO_4] - \ldots \quad (3)$$

$$A_C = [HCO_3^-] + 2[CO_3^{2-}] \quad (4)$$

Due to the high pH dependency of the chemical conversion a lowering of ocean pH has also strong influence on the components of the C_T. At current pCO_2 levels $[CO_2]$ contributes about 1%, $[HCO_3^-]$ 91% and $[CO_3^{2-}]$ 8% to C_T. In a future, more acidified ocean, the amount of CO_3^{2-} strongly declines whereas $[CO_2]$ and $[HCO_3^-]$ increase as depicted in a Bjerrum Plot (Fig. 1.2).

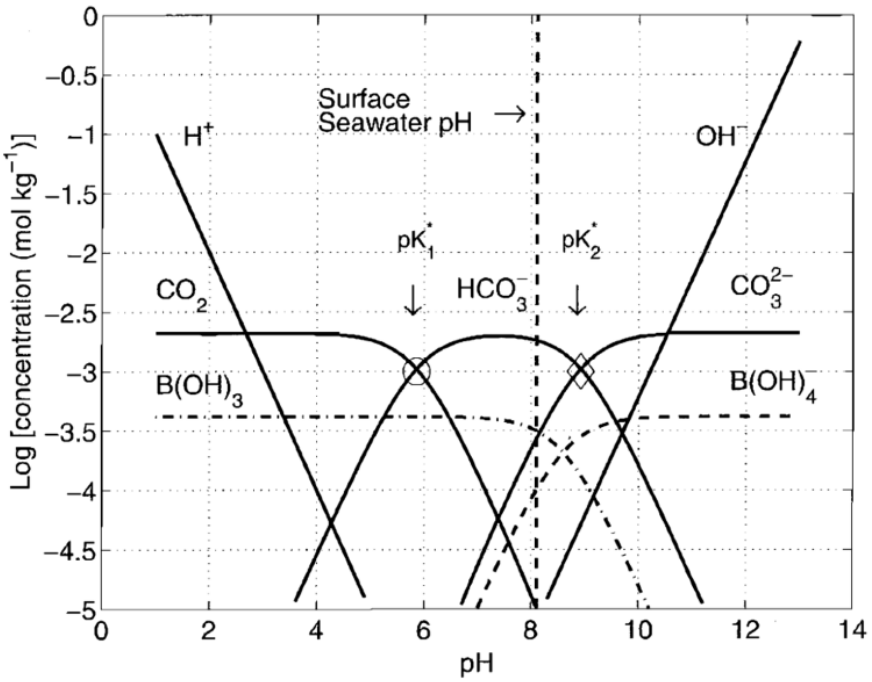

Figure 1.2: The Bjerrum plot depicts the pH dependency on concentrations of the three carbonate system species CO_2, HCO_3^- and CO_3^{2-}. The dashed line corresponds to present day mean ocean surface pH, pK1 and pK2 are the negative common logarithms of the first and second dissociation constants (from Zeebe and Wolf-Gladrow 2001)

The shift in the carbonate chemistry due to ocean acidification results in lowered $[CO_3^{2-}]$. As a consequence, the calcium carbonate saturation state Ω is going to decrease. Omega is the product of $[Ca^{2+}]$ and $[CO_3^{2-}]$ divided by a stoichiometric solubility coefficient which is specific for each of the two major carbonate polymorphs, calcite or aragonite (equation 4).

$$\Omega = \frac{[Ca^{2+}] \times [CO_3^{2-}]}{K_{sp}} \qquad (5)$$

The solubility of the polymorphs differs: calcite is more stable and therefore higher saturation states are encountered for the surface water (Fig 1.3). At today's CO_2 concentrations surface oceans are supersaturated, but higher future pCO_2 is going to lower Ω. In certain ocean areas undersaturation with respect to both polymorphs might occur (Yamamoto-Kawai et al. 2009). According to the temperature dependence of the kinetics, even today large variance of $[CO_3^{2-}]$ is observed for different parts of the oceans whereby cold temperated polar regions are characterized by low saturations states of Ωaragonite <2. In future, these areas are expected to become undersaturated first of all ocean areas (Yamamoto-Kawai et al. 2009).

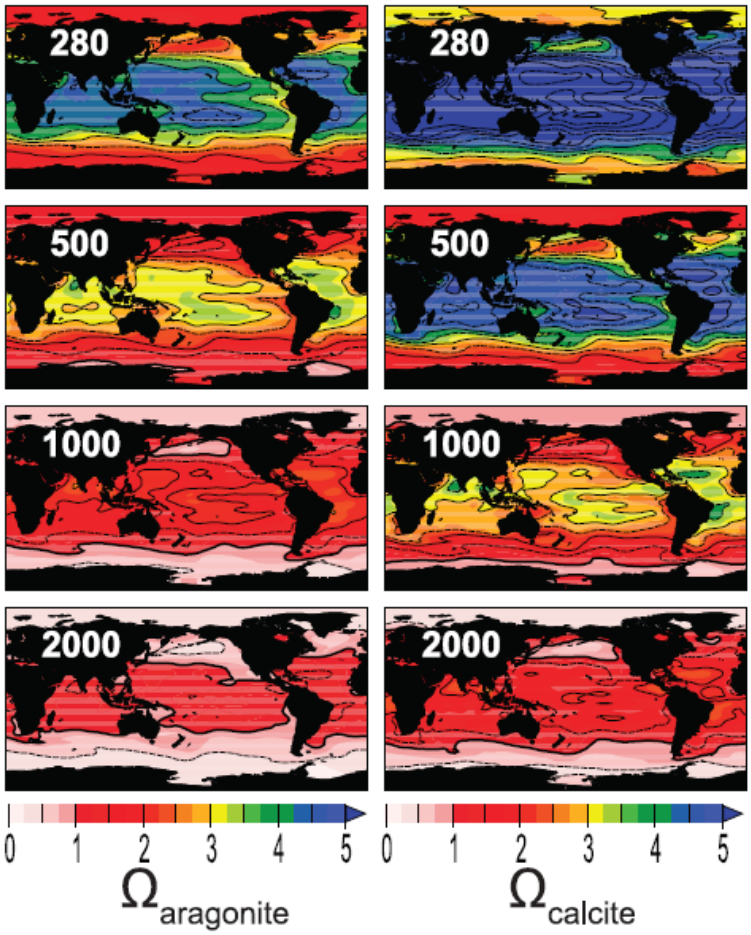

Figure 1.3: Aragonite and calcite saturation state (Ω) for of the surface ocean modeled for atmospheric CO_2 concentration between 280 (pre-industrial) and 2000 ppm. Saturation state of both polymorphs is highest in the warmer tropical areas and lowest in the cold arctic and antarctic oceans. Surface aragonite under-saturation is expected for CO_2 concentration of 1000 ppm (Cao and Caldeira 2008).

1.2 Biological impact of ocean acidification

Ocean acidification (OA) is expected to affect marine organisms and may cause a shift in marine communities, whereby especially calcifying organisms seem to be most sensitive. First observations for the sensitivity of the calcification process to ocean acidification were made for the planktonic coccolithophores (Riebesell et al. 2000) and benthic warm water corals (Gattuso et al. 1998, Langdon et al. 2000) which exhibit lower calcification rates under elevated pCO_2. These results were also confirmed for other marine taxa such as echinoderms (Shirayama and Thornton 2005), pteropods (Comeau et al. 2009, Lischka et al. 2011), bivalves (Berge et al. 2006, Gazeau et al. 2007, Ries et al. 2009), foraminifera (Haynert et al. 2011) and coralline red algae (Martin et al. 2008, Büdenbender et al. 2011). In some species even survival rates were reduced under an increased pCO_2 to values between 560 and 1000 µatm (Shirayama and Thornton 2005, Dupont et al. 2008, Talmage and Gobler 2009).

Higher sensitivity to ocean acidification is expected to be a general feature of larval stages compared to juvenile or adults (Kurihara et al. 2008b). Reduced survival rates (Talmage and Gobler et al. 2010) or deformation of larvae (Kurihara et al. 2007, 2008a,b) have been observed. In most species survival was not effected but growth or calcification rates were reduced or delayed in bivalves (Miller et al. 2010, Gazeau et al. 2010,2011, Gaylord et al. 2011, Bechmann et al. 2011), echinoderms (Stumpp et al. 2011a,b, Martin et al. 2011) and crustaceans (Walther et al. 2011, Bechmann et al. 2011).

However, responses differ between two closely related oyster species or even between populations of the same species (Parker et al. 2010, 2011). In conclusion, laboratory experiments revealed that vulnerability to ocean acidification is highly species specific and can also differ between early and late ontogenetic stages.

Due to their relative short duration time or simplification of complex species interactions the predictive power of laboratory experiments is limited. Therefore naturally CO_2 enriched habitats provide the possibility to overcome these limitations and investigate responses of ecosystems or species under natural conditions. In these habitats, the carbonate chemistry strongly deviates from the surrounding areas and may therefore allow a forecast of the possible changes in the benthic communities as a consequence of ocean acidification. High CO_2 concentrations are encountered at hydrothermal vents (Tunnicliffe et al. 2009), areas with volcanic CO_2 release (Hall-Spencer et al. 2008, Fabricius et al. 2011) and in coastal upwelling systems (Feely et al. 2008, Wootton et al. 2009). All these study sites have in common that the diversity of the benthic communities were decreased at low pH. Fabricius et al. (2011) observed reduced number of coral species at the high CO_2. Although some species were able to cope with low pH, the overall diversity was reduced. In the Mediterranean Sea, volcanic CO_2 causes a pH gradient at the Island Ischia (Hall-Spencer et al. 2008). Along this gradient, overall species number and the number of calcifying invertebrates in particular decrease with higher pCO_2 (Hall-Spencer et al. 2008, Cigliano et al. 2010, Kroeker et al. 2011). Similarly, Wootton and co-workers reported the decrease of mussel abundance and size in response to a pH decrease over an eight year period (Wootton et al. 2009). In contrast, at these sites, non calcifying autrothrophs such as seagrass or algae increased their shoot density or their biomass (Hall-Spencer et al. 2008, Wootton et al. 2009, Fabricius et al. 2011). These data indicate that also under more natural conditions calcifiers respond most sensitive to elevated pCO_2. At the same time, non calcifying species may benefit from the higher C_T availability (in case of algae and seagrasses) or from the lower space competition with calcifiers.

1.3 Physiological response to elevated pCO_2

In general, adult teleost fish (Larsen et al. 1997, Melzner et al. 2009a,b), crustaceans (Spicer et al. 2007, Ries et al. 2009, Fehsenfeld et al. 2011) and cephalopods (Gutowska et al. 2008, 2010a) are much more tolerant to ocean acidification. None of the investigated species exhibited reductions of somatic growth or calcification rates (Franke et al. 2011). These taxa are characterized by high routine metabolic rates which require well developed acid-base regulatory capacities in order to extrude metabolically produced acid loads (Melzner et al. 2009a). In order to maintain a full oxygenation of the respiratory pigments blood or haemolymph pH needs to be controlled and is buffered by active bicarbonate accumulation to counteract the respiratory acidosis during exercise (Pörtner et al. 1991, Pörtner 1994). Increased seawater CO_2 is compensated in a similar manner as it has been reported for fish (Larsen et al. 1997, Michaelidis et al. 2007), decapod crustacean (Spicer et al. 2007, Pane and Berry 2007) and cephalopods (Gutowska et al. 2010a). This is also confirmed by experimental data which revealed upregulation of ion and acid-base transport related genes under elevated pCO_2 by means of ATP driven processes (Deigweiher et al. 2009). Permanently elevated bicarbonate levels

may have also pathological effects. In some species increased production of internal calcium carbonate structures has been observed which might be a detrimental effect of elevated blood/haemolymph bicarbonate levels (Gutowska et al. 2008, Checkley et al. 2009, Ries et al. 2009). The disruption of olfactory response observed in fish might also be a result of this change of blood composition (Munday et al. 2009a, Dixson et al. 2010, Nilsson et al. 2012). In adult fish and cephalopod, the gills are the pre-dominant sites of ion and acid-base regulation (Evans et al. 2005, Hu et al. 2010). Since these organs are not fully developed in the embryo, these early ontogenetic stages might be more sensitive, e.g. cephalopods display reduced growth under high pCO_2 (Hu et al. 2011). Most benthic species have lower metabolic rates, do not rely on oxygen binding pigments and experience much smaller pCO_2 fluctuations during routine metabolism, therefore have much lower acid-base regulatory capacities. Only limited extracellular pH buffering by HCO_3^- accumulation have been reported for a sea urchin (Stumpp et al. 2011), bivalves (Michaelidis et al. 2005) and sipunculids (Pörtner et al. 1998) and no pH regulation was observed in echinoderms (Miles et al. 2006, Henroth et al. 2010). According to these results the ability to actively control the pH of extracellular fluids seems to be an important indicator for the tolerance towards ocean acidification stress (Pörtner 2008, Melzner et al. 2009a).

In species with high metabolic rates, oxygen consumption remained unchanged under elevated ambient pCO_2 (Gutowska et al. 2010a). In contrast, those species with low ion regulatory and aerobic capacities may change their metabolic rates as a responds to elevated pCO_2. Metabolic depression is one possible meachanism which could play a role under ocean acidification stress - similar to the responds to stressors like emersion or hypoxia (Pörtner et al. 2005). It describes downregulation of energy demand and especially aerobic metabolism and in some cases switch to anaerobic pathways (Guppy and Whithers 1999). This process enables organisms to survive prolonged unfavorable abiotic conditions by reducing the loss of energy necessary to maintain e.g. membrane potential (Boutilier and St-Pierre 2000). One trigger for metabolic depression is a reduction of intracellular pH (Hand 1999), but in recent years it is also suggested that reduced extracellular pH may play a role (Pörtner et al. 2000). Reduced haemolymph pH is documented during valve closure e.g. during emersion and is accompanied by lower oxygen tensions (Famme 1980). Under these conditions, oxygen consumption decreases (Famme 1980). In fact, lower aerobic metabolism has been observed for the mussel *M. galloprovincialis* under elevated pCO_2 (Michaelidis et al. 2005).

1.4 *Mytilus edulis*

Mussels of the genus *Mytilus* are common at the boreal coastlines of the southern and northern oceans and are important reef builders, thereby provide a habitat for a diverse community (McDonald et al. 1991, Vermeij 1992). As mussel beds have a large filtration capacity they act as an important trophic link between the pelagic and benthic systems (Kautsky and Evans 1987, Dankers and Zuidema 1995). Especially in the Baltic Sea, *Mytilus spp* (*edulis* and *trossulus*) are some of the most important benthic organisms which accounts for up to 80% of shell-free animal biomass and even enhances species diversity (Jansson and Kaustky 1977, Norling and Kautsky 2008). The larval stages

disperse in the water column by passive drift and primarily rely on yolk until the filtration apparatus is developed (Newell 1989). Although *M. edilus* is a marine species it tolerates a wide salinity range, albeit the lowest tolerated salinity depends on the population. Whereas in an oceanic population growth was impaired at salinities below 24 (Bayne 1965), successful development was observed for an estuarine population at 14 (Innes and Haley 1977). For the White Sea population, larvae survival at the veliger stage was not affected at salinities between 5 and 45 g kg^{-1} (Saranchoya and Flyachinskaya 2001). Nevertheless, larvae size is reduced at low salinities (Innes and Haley 1977). The next developmental stage is the pediveliger. This stage has already developed a foot which allows the larvae to crawl on the substrate. The competent larvae attach to a suitable substrate and the benthic life period starts. The main predators of mussels at the adult stage are asteroids such as *Asterias rubens*, decapod crustaceans such as *Carcinus maenas* and mammalians such as the common eider duck *Somateria mollisima* (Ameyaw-Akumfi and Hughes 1987, Bustnes and Erikstad 1990, Reusch and Chapman 1997, Enderlein et al. 2003). In the Baltic, mussels settle in the low saline Gulf of Finland at a salinity of 4.5 which is the lowest tolerated value (Westerbom et al. 2002). Although survival is not affected by the brackish conditions of the Baltic, inhabiting mussels are characterized by smaller sizes and thinner shells which might indicate an impairment of the physiology (Kautsky et al. 1990, Tedengren et al. 1990). At reduced salinities, mussel metabolism switches to higher protein turnover which is energetically less efficient and might be the cause for lower growth rates (Tedengren and Kautsky 1990). Filtration rates are only affected during acute salinity changes but increase back to control levels after acclimation (Böhle 1972). Due to the semi-sessile lifestyle in sub- and intertidal mussel beds, the species is able to tolerate various abiotic and biotic stresses like air exposure, salinity changes, cold and heat stress, hypoxia and predation pressure (Williams 1970, Booth et al. 1984, Walsh et al. 1984, Wang and Widdows 1993, Silva and Wright 1994).

In former time the *Mytilus* species were mainly referred to as *M. edulis*, but has now been described as a complex which consists of *M. edulis* and *M. trossulus* (Koehn et al. 1991). Genetic analysis evidenced that the Northern Europe shores are not only inhabited by *M. edulis* but also by *M. trossulus* and their hybrids (Väinölä and Strelkov 2011). In the Baltic, no reproduction barriers are detected therefore the two species form a hybrid swarm (Riginos and Cunningham 2005, Stuckas et al. 2009).

1.5 Biomineralization

Calcification is the process which is expected to be affected the most by ocean acidification. Nevertheless, the underlying mechanisms in molluscs are still not fully understood. Calcification in *M. edulis* starts within the first hours after fertilization. At the veliger stage a shell gland and later on mantle cells secrete the larval shells called prodissochond I and II, respectively, which consist of amorphous and aragonitic $CaCO_3$ (Kniprath et al. 1980, Newell 1989, Medakovic 2000, Weiss et al. 2002). After settlement, the pediveliger metamorphoses into the juvenile mussel which secretes calcite for shell length growth (Medakovic et al. 1997). In juvenile and adult *M. edulis* two major polymorphs form the shell, the outer, calcitic ostracum and the inner, aragonitic nacre (hypostracum) which is produced for shell thickening. The thin prismatic myostracum is located between these two major

layers. The whole shell is covered by an organic layer, the periostracum, which is secreted by epithelial mantle cells in the periostracal groove between outer and middle fold and protects the mineralized shell from the external environment (Bubel 1973, Zhang et al. 2006). Its major component is the soluble protein precursor periostracin. This precursor is sclerotized by tyrosinase in the quinone-tanning process (Waite and Andersen 1978, 1980). The protein cover is an efficient protective barrier against abiotic corrosion and biotic like fouling impacts from the ambient seawater (Michaelis 1978, Scardino et al. 2003, Tunnicliffe et al. 2009).

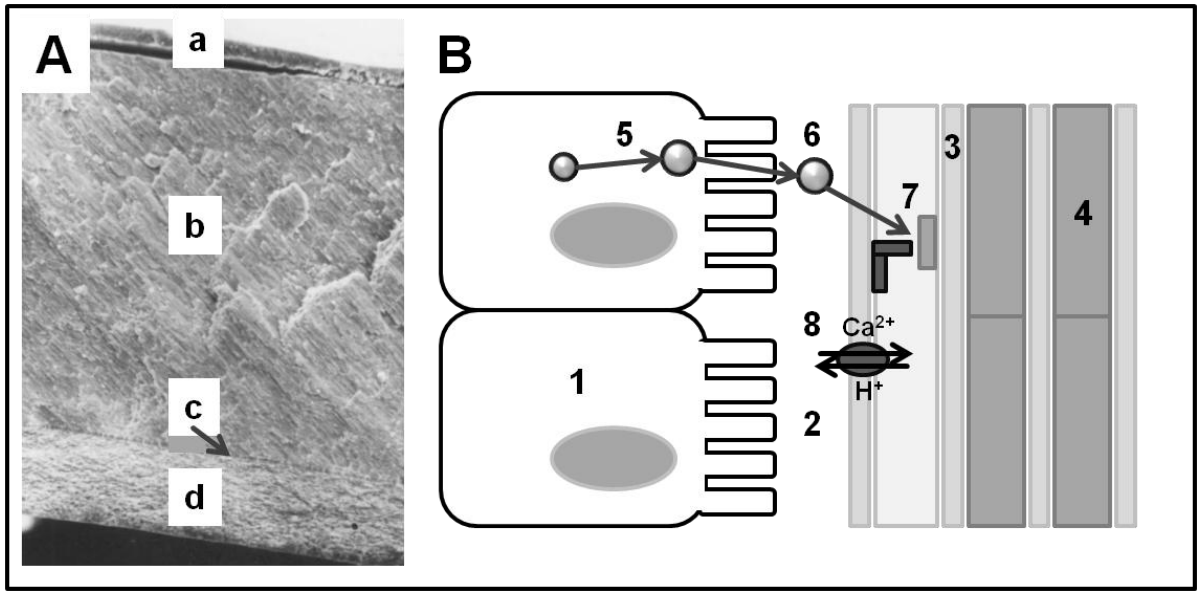

Figure 1.4: Section through the shell of an adult *M. edulis*, proteinous periostracum (a), calcitic ostracum (b), prismatic myostracum (arrow, c), aragonitic hypostracum (d), (Feng et al. 2000), (A); hypothetical calcification process for nacre according to Weiss 2010, 1 mantle epithelium, 2 extrapallial fluid, 3 chitin layer and interlamellar layer, 4 final nacre crystal sheet, 5 intracellular ACC production and vesicular transport, 6 secreted ACC vesicle, 7 calcification/nucleation of $CaCO_3$ on the silk hydrogel initiated by Pif proteins, 8 possible involvement of acidic aspartate rich proteins in $Ca^{2+}/HCO_3^-/H^+$ translocation across the chitin layer (B)

The exact mechanisms of calcification in molluscs are still elusive. It is obvious that the final biomineralization step occurs in the extrapallial space between the outer mantle and the periostracum. Nevertheless, the former hypothesis that the initial precipitation of $CaCO_3$ occurs in the external compartment of the EPF has become less probable. The extrapallial fluid (EPF) is not, as suggested earlier, supersaturated with respect to calcium carbonate (Misogianes and Chasteen 1979) and contains high concentrations of Mg^{2+} which inhibit $CaCO_3$ precipitation (Zeebe and Sanyal 2002). Similar to other marine organisms is has been suggested that an amorphous calcium carbonate (ACC) precursor is formed in intracellular vesicles and is then secreted by the mantle into the extrapallial space and is embedded into the matrix (Neff 1972, Addadi et al. 2003, Weiner et al. 2005, Jacob et al. 2088, Jacob et al. 2011, Weiner and Addadi 2011). The subsequent nucleation and conversion into polymorphs such as nacre is crucially mediated and stabilized by specific matrix proteins such as Nacrein and Pif which are secreted by the mantle (Miyamoto et al. 1996, Falini et al. 1996, Suzuki et al. 2009). The calcification process itself takes place in a space between the old shell and a chitin sheet which separates the calcification front from the bulk EPF (Weiss 2010, Fig. 1.4). The space in which the crystals are finally produced is initially filled with a gel of silk-like proteins (Addadi et al.

2006). These proteins and chitin order the crystal structure and enclose every crystal (Matsushiro and Miyashita 2004). In adult mussels, the absolute contribution of the organic component to total shell weight is only 0.1-5% (Jörgensen 1976, Yin et al. 2005). However, due to the much higher energetic costs for protein synthesis compared to $CaCO_3$ precipitation, the matrix production accounts for a much higher proportion of the total costs required for shell formation (Palmer 1992).

It is important to notice that shell formation in mussels is not terminated at a certain age. Mussels continue growing for their whole life and the precipitated shell is not entirely fixed but is subjected to periodic formation and degradation processes. During air exposure and valve closure, EPF pH decreases and inner nacre layers dissolve indicated by increasing [Ca^{2+}] (Crenshaw 1969, 1972). Additionally, mussels exhibit a phenotypic plasticity in order to respond to environmental requirements, by means of increased shell thickness under e.g. high wave exposure and predation stress (Leonard et al. 1999, Arkester and Martel 2000). Further mussels are able to repair shells damaged by e.g. the boring polychaete *Polydora ciliata* (Michaelis 1978, Uozumi and Suzuki 1979).

Calcification in bivalves requires considerable amounts of energy and therefore is closely related to the physiology of the animals. Further, as the ACC precursor is produced in intracellular vesicles, protons generated during this first step of calcification need to be removed from the intracellular space. This emphasizes that intracellular pH regulation is directly related to calcification.

1.6 Ammonia excretion mechanisms

In bivalves such as *Mytilus edulis*, NH_4^+ is the most important nitrogenous end product and excretion rates are varying around 0.1-2.45 µmol g^{-1} h^{-1} drymass depending on season and condition (Sadok et al. 1995 and references therein). It has been suggested that ammonia passively diffuses across the gill epithelium (Sadok et al. 1995). Increased NH_4^+ excretion rates in response to short-term exposure (20-24h) to elevated pCO_2 have been observed for *M. edulis* and *M. galloprovincialis* (Lindinger et al.1984, Michaelidis et al. 2005). The net excretion of H^+ in form of the protonated NH_4^+ may therefore contribute to the intracellular pH homeostasis during environmental hypercapnia.

In the past, the exact mechanism of NH_3/NH_4^+ transport across the lipid cell membrane remained elusive. The rate of simple diffusion would be limited as charged (NH_4^+) and polarized (NH_3) have a really low diffusion throught lipid bilayer. Recent studies therefore suggest the involvement of the Rhesus (Rh) protein in this process (Bishop et al. 2010, Weihrauch et al. 2004, Fig. 1.5). It is suggested that the Rhesus channels facilitate the diffusion of either charged NH_4^+ or polarized NH_3 (see Weiner and Verlander 2010 and references therein). In the latter case, NH_3 is trapped in the boundary layer by protonation in order to avoid diffusion back into the cytoplasm. The required proton can be either delivered by a proton pump (V-type ATPase) or by sodium-proton exchanger (NHE) (Shih et al. 2008, Wu et al. 2009, Wright and Wood 2009). Transport of NH_4^+ into the epithelial cells on the basolateral side is probably achieved by the Na^+/K^+-ATPase when the potassium is substituted by NH_4^+ (Knepper 2008, Pagliarani et al. 2008). Since ouabain (Na^+/K^+-ATPase inhibitor) has only a

partially inhibitory effect it can be considered that also on the basolateral side other pathways are present (Weihrauch et al. 1998).

The expression of Rh proteins is documented in varies tissues which are involved NH_4^+ transport in numerous vertebrate taxa (Wright and Wood 2009, Weiner and Verlander 2010). Certain isoforms such as Rhbg and Rhcg are expressed in the mammal kidney epithelia cells where NH_3/NH_4^+ is accumulated in the tubule lumen (Brown et al. 2009, Weiner and Verlander 2010, Bishop et al. 2010). Their non mammal counterparts have been observed in the gills and ionocytes in adult and embryonic fish which are cell types involved in ion regulation (Wright and Wood 2009). Expression levels of Rh-proteins are modulated during treatment with elevated environmental CO_2 and NH_4^+ (Nawata et al. 2010). Additionally, Rh like proteins have been also sequenced in the invertebrates *Carcinus* and *Manduka* and even in unicellular algae (Soupene et al. 2002, Weihrauch et al. 2004, Weihrauch 2006). The wide distribution of Rh proteins in a broad range of organisms emphasizes their conserved importance for physiological processes such NH_3/NH_4^+ transport or even CO_2 diffusion (Musa-Aziz et al. 2009).

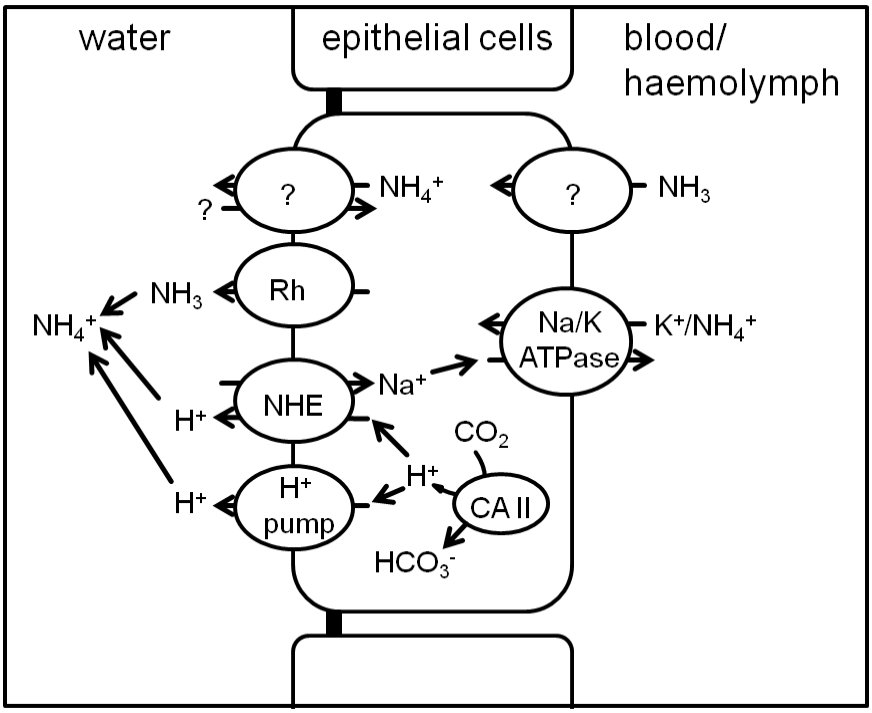

Figure 1.5: Hypothetical model for ammonium excretion involving Rh proteins in marine organisms (Weihrauch et al. 2004). Basolateral transport of NH_3/NH_4^+ into the cytosol might be conducted via Rh isoforms or Na^+/K^+-ATPase by substitution of potassium with NH_4^+. The apical excretion is carried out either by NH_4^+ exchange against an unknown positively charged ion presumable Na^+ or via gaseous NH_3 through Rh channels. In the latter case, NH_3 is trapped in the boundary layer by protonation. The required protons can be provided by H^+-ATPase or NHE (sodium-proton-exchanger).

1.7 The Baltic Sea and Kiel Fjord

The Baltic Sea is a semi enclosed marginal sea and ranges from middle to northern Europe with an overall surface area of 415 km^2 (HELCOM 2003). The Baltic has three deep basins (Åland 290 m, Landsort 459 m and Gotland Deep 239 m) but in general is shallow which results in a mean depth of 60 m. Water exchange with the North Sea is only possible through the channels of the Danish Straits (She et al. 2006). The high freshwater input from the surrounding land masses and net precipitation cause a gradual decline of the salinity along a gradient from west to north-east leading to surface values between 20 (Kattegat) and 2 (Gulf of Finland and Gulf of Bothnia) (Rohde 1988). The strong salinity differences results in a strong halocline between the low saline surface water and the high saline water below. Combination of halocline and the seasonal thermocline causes a strong stratification of the water body which inhibits the vertical exchange of dissolved nutrient and gaseous components. Therefore, the deep water in the central Baltic Proper is only ventilated by inflow events from the North Sea which transports O_2 rich water into the deep basins (Meier et al. 2006).

Kiel Fjord is part of the Kiel Bight which is located in the western Baltic Sea in proximity to the Danish Straits. Therefore, the marine influence of the North Sea is much stronger than in the central parts of the Baltic. Salinity ranges between 10 and 20 g kg^{-1} with mean values of about 15 g kg^{-1} at the surface and about 18 g kg^{-1} in the bottom water. Since seawater alkalinity is related to salinity, the buffer capacity is lower (1900-2100 µmol kg^{-1}) compared to the open ocean (2300-2400 µmol kg^{-1}, Beldowski et al. 2010). Similar to the Baltic proper strong stratification causes a decline of the O_2 concentrations in the bottom water (Hansen et al. 1999). In contrast to the basins, due to a maximal depth of less than 30 m, vertical mixing in autumn and winter is sufficient to replenish oxygen concentration of the whole water column (Hansen et al. 1999). Seasonal hypoxia is a natural process in this area but subpynocline water oxygen concentrations remained at about 250 µmol kg^{-1} until 1960 (Babenerd 1990). Enhanced productivity and following degradation of organic matter causes annual depletion of the oxygen concentration down to 100 µmol kg^{-1} or less (Babenerd 1990, HELCOM 2003, Conley et al. 2007). In conclusion, the eutrophication of the Baltic Sea, which has started in the 1960s, drastically amplified the oxygen depletion.

Due to the salinity gradient from almost full marine conditions in the Kattegat down to 2 g kg^{-1} in the Bothnian Bay, the Baltic is characterized by a transition from marine to freshwater species. In Kiel Fjord, marine organisms like *Mytilus edulis* (Phylum Mollusca), *Amphibalanus improvisus* and *Carcinus maenas* (Phylum Arthropoda, class crustacea) and *Asterias rubens* (Phylum Echinodermata, class Asterioidea) dominate the hard-bottom benthos community (Enderlein and Wahl 2004, Dürr and Wahl. 2004). Without predation the habitat would become a *M. edulis* monoculture (Enderlein and Wahl 2004, Reusch and Chapman 1997). Due to the low diversity, the prey-predator interactions are relatively simple, whereby *A. rubens* and *C. maenas* preferentially prey on mussels which on the other hand find a size refuge at a shell length >50 mm (Ameyaw-Akumfi and Hughes 1987, Reusch and Chapman 1997).

1.8 Questions and research hypothesis

What is the natural pCO_2 variability in a coastal habitat like Kiel Fjord?

Research on the effects of ocean acidification on marine biota is based on the assumption that present day seawater pH is relative stable and seawater pCO_2 corresponds to atmospheric values. Most studies applied a seawater pCO_2 range which resembles the atmospheric pCO_2 that might be reached according to worst case scenarios. In general, such constant pCO_2 which is close to equilibrium with the atmosphere is only observed for the open oceans. These conditions may not mimic the natural pCO_2 range which is encountered in coastal habitats. Hypoxic water masses which are not in contact with the atmosphere are always characterized by increased dissolved CO_2 concentrations. Therefore, transport of these water masses to the surface causes a drastic increase of pCO_2 and decreased pH and [CO_3^{2-}] (Feely et al. 2008). Due to the pronounced hypoxic zones in the bottom water layers of the western Baltic Sea, it can be expected that similar patterns can be observed here. During this thesis, the carbonate chemistry variability was assessed for the Fjord.

Hypopthesis: Kiel Fjord carbonate chemistry is highly variable as a consequence of seasonal bottom water hypoxia.

Are mussels able to maintain calcification rates under elevated pCO_2?

It is expected that calcification rates of marine organisms decrease in response to ocean acidification. Especially bivalves are thought to react sensitive and calcification is linearly reduced in response to short-term increases in seawater pCO_2 (Gazeau et al. 2007). According to these results no calcification would be possible at pCO_2 values above 1800 µatm. On the other hand, reduced but positive calcification rates were obtained for *Mytilus galloprovincialis* grown at 5000 µatm for 90 days (Michaelidis et al. 2005). Additionally, cultivation of adult mussels is complicated and requires high algae supply, otherwise only low growth rates are obtained in laboratory experiments (Berge et al. 2006, Ries et al. 2009). These results highlight the need to conduct experiments with adequate acclimation time and nutrition and under a realistic pCO_2 range which resembles present day but also near-future levels. These experiments were conducted which may allow prediction of the vulnerability of *M. edulis* to ocean acidification.

Hypothesis: M. edulis *is adapted to moderately elevated pCO_2 and is able to continue calcification at these levels.*

What are the physiological responses of *M. edulis* to elevated pCO_2?

Invertebrates with low metabolic rates are expected to respond most sensitive to elevated pCO_2 since their ability to regulate the acid-base status of extracellular fluids is limited (Melzner et al. 2009a). Reduced extracellular pH might elicit a depression of the aerobic metabolism (Pörtner et al. 2008). Results obtained for the Mediterranean mussel *M. galloprovincialis* suggest lowered oxygen consumption, higher ammonia excretion and dissolution of the shell carbonate which causes a partial compensation of the pH decrease (Michaelidis et al. 2005).

Recent studies suggest that metabolic rates of benthic invertebrates can also increase under elevated pCO_2 (Wood et al 2009, Stumpp et al. 2011). If this is also observed for mussels this would imply that growth reductions can be a consequence of lowered Scope for Growth rather than metabolic depression. In the frame of this thesis, experiments were conducted in order to assess the extracellular acid-base status and metabolic response of *M. edulis* under a realistic pCO_2 range.

Hypothesis: Extracellular acid-base status is unregulated and Scope for Growth is reduced under CO_2 stress.

What biotic and abiotic factors determine the tolerance of mussels to elevated pCO_2?

Several studies investigated the benthic communities along gradients of naturally acidified seawater in the Mediterranean and tropical seas (Hall-Spencer et al. 2008, Fabricius et al. 2011, Rodolfo-Metalpa et al. 2011). In general abundances of calcifying organisms and species diversity were lowered at high ambient pCO_2. Nevertheless, some species like mussels are able to survive at these sites and continue to calcify (Rodolfo-Metalpa et al. 2011). This tolerance may result from protection of the calcium carbonate structure by the organic periostracum cover. The production of this proteinaceous layer consumes a lot of energy which might be limited in oligotrophic areas of the ocean such as the Mediterranean. I conducted field and laboratory studies with focus on the effects of elevated pCO_2 and also energy availability.

Hypothesis: Organic covers protect external $CaCO_3$ structures from dissolution and higher energy supply causes higher tolerance to sublethal CO_2 stress.

What are the mechanisms of mussels to excrete nitrogenous waste products?

It has been examined that mussels are ammonotelic animals. Nevertheless the mechanisms by which NH_3 or NH_4^+ are excreted are not known. It has been proposed that NH_3 diffuses passively from the haemolymph via the gills or NH_4^+/Na^+ are exchanged actively (Mangum et al. 1978, Sadok et al. 1995). Since NH_3 is polarized, diffusion rate across the lipid bilayer would be limited. A recent publication suggests that Rhesus proteins act as channel for gaseous NH_3 diffusion in marine crustaceans (Weihrauch et al. 2004). It is not known if molluscs express similar genes and if the kidney is involved in the excretion. I examined the expression of genes which may play a role in ammonia excretion.

Hypothesis: NH_3/NH_4^+ excretion does not depend on passive diffusion, rather is an actively regulated process and requires certain transport proteins.

2. Material and Methods

2.1 Biogeochemical analyses

2.1.1 Monitored of the carbonate chemistry of Kiel Fjord

From April 2009 until August 2011 Fjord surface pH was measured weekly from a footbridge in front of the IFM-GEOMAR (54°19.8'N; 10°9.0'E) in about 10 cm water depth using a WTW 340i pH-meter and a WTW SenTix 81-electrode which was calibrated with Radiometer IUPAC precision pH buffer 7 and 10 (S11M44, S11 M007). Salinity and temperature were measured with a WTW cond 315i salinometer and a WTW TETRACON 325 probe.

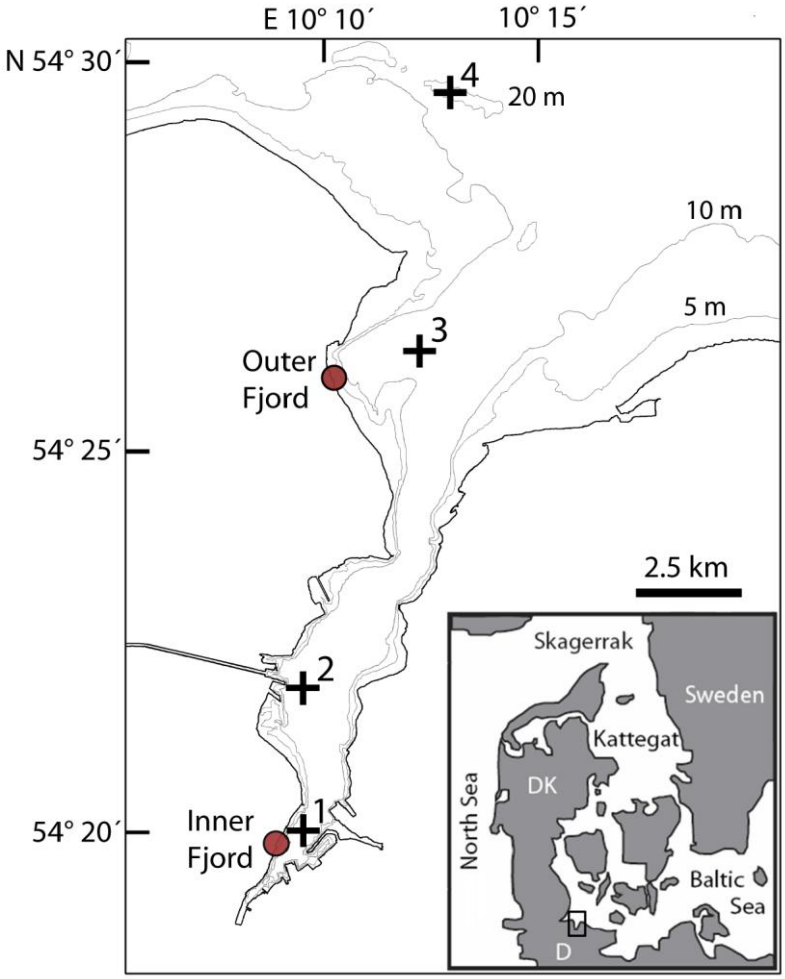

Figure 2.1: Map of Kiel Fjord, crosses and numbers (1-4) indicate the stations of the carbonate chemistry monitoring in 2009/10. Brown circles give the coordination of the field experiment in the inner and outer fjord in summer/autumn 2010.

Using R/V Polarfuchs a monitoring was conducted on weekly (station 1) and bi-weekly (stations 2-4) cruises between April 2009 to March 2010 (Fig. 2.1). On these cruises, two samples (500 mL) were taken at each station from both surface (about 1 m depth) and bottom water (1 m above sea floor, i.e.

11-20 m). Seawater samples were poisoned with saturated mercuric chloride solution and stored at room temperature until analysis according to SOP1[1]. Additionally, water samples for nutrient determination (PO_4^{3-}, H_4SiO_4) were collected in 10 mL Falcon tubes and stored at -20°C.

During the field growth experiment, weekly measurements of pH (NBS scale), salinity and temperature were conducted at the experimental sites in the inner Fjord (station IF, 54°19.8'N; 10°9.0'E, Fig. 2.1) and bi-weekly in the outer Kiel Fjord (station OF, 54°.25´N, 10°10´O, Fig. 2.1) as described above. Additionally, water samples were taken from 1m depths with a water sampler for determination of the carbon chemistry.

In 2009 and 2010, carbonate chemistry was also monitored at the Boknis Eck Time Series station (BETS, 54°31'N; 10°09'E). The station has a depth of 28 m and water is routinely sampled from 1, 5, 10, 15, 20 and 25 m and analyzed for e.g. nutrient and [O_2]. The carbonate system monitoring was carried out only for water depths of 1, 10, 20 and 25 m.

2.1.2 Seawater analysis

Seawater samples for carbonate chemistry monitoring were analyzed for C_T and A_T. A_T was measured by means of a potentiometric open-cell titration with hydrochloric acid using a VINDTA autoanalyzer (Mintrop et al., 2000; Dickson et al., 2007). C_T was determined coulometrically (Dickson et al., 2007) using a SOMMA autoanalyzer. Additionally, pH on the total scale (pH_T) and C_T were determined for samples taken in the laboratory and field experiment stud. For this purpose, pH was measured using a Metrohm 6.0262.100 electrode and 626 Metrohm pH meter and C_T was determined with an AIRICA C_T analyzer (Marianda, Kiel, Germany). pH_T was determined using Tris/HCl and AMP/HCl seawater buffers mixed for salinity 15 according to Dickson et al. (2007) in a 21°C water bath. Accuracy and precisionof A_T and C_T measurements was ensured by using certified reference material (Dickson et al. 2003).

Analyses for PO_4^{3-} and H_4SiO_4 were carried out spectrophotometrically using a U-2000 spectrophotometer (Hitachi-Europe, Krefeld, Germany) (Hansen and Koroleff 1999).

Seawater carbonate system parameters (Ω, pCO_2) were calculated using the CO2sys program (Dickson et al., 2003; Lewis and Wallace, 1998). For calculations, the $KHSO_4$ dissociation constant published by Dickson et al. (1990) have been used. Dissociation constants K1 and K2 were used according to Mehrbach et al. (1973) refitted by Dickson and Millero 1987 or Roy et al. (1993). The deviation between both set of constants for a pCO_2 calculation is below 3.5%.

Particulate organic carbon (POC) and particulate organic nitrogen (PON) concentrations were determined for 500 mL water samples. Subsequently, samples were filtered on pre-combusted GF/F (VWR, Darmstadt, Germany) filters using a vacuum pump (0.2 bar) and stored at -20°C. Before analysis, filters were treated with fuming hydrochloric acid, dried (60°C, 6 h) and wrapped in tin boats. The amount of POC and PON were quantified gas chromatography in an elemental analyser Euro Vector 3000 (EuroVector, Milan, Italy) according to Sharp (1974). A calibration curve was obtained by

measurements of an acetanilide standard (71.09% C, 10.36% N) and a certified Bodenstandard (3.5% C, 0.216% N) with C:N ratios of 7 and 16, respectively.

2.2 Animals

For experiments using juvenile and adult *Mytilus edulis*, specimens were collected directly from Kiel Fjord (54°19.8´N; 10°9.0´E, Fig. 2.1, brown circle ´Inner Fjord´). Animals were collected using a scratcher or by hand from sub tidal depths. Depending on the purpose of the experiment, the mean sizes of the collected animals varied between 15 and 50 mm shell length.

Freshly settled mussels were collected on submersed PVC panels in the Fjord. For this purpose, 5x5 cm PVC settlement panels which were roughed on one side using sandpaper (grain 60) were suspended in the fjord (IF station) at one meter water depth. After 10 days, panels were removed from the fjord and all settled organisms other than 100 settled *M. edulis* larvae were removed using a stereo microscope. The panels were stored in aquaria until transfer to the experimental aquaria or the field sites.

For studies conducted in Winnipeg, Manitoba, Canada, adult specimens of *M. edulis* were obtained from a local grocery store (Superstore). Animals were kept in 5 L aquaria in order to acclimate to experimental conditions for at least 2 days and were fed a commercial food for filter feeding organisms.

2.3 Laboratory experiments

2.3.1 General experimental setup

All experiments were conducted in the climate chambers of the IFM-GEOMAR. According to the seasonal cycle and the water temperatures of Kiel Fjord, air temperatures were adjusted to values between 8 and 17°C. Seawater salinity varied according to the natural variation in the Fjord, without any attempts to control it.

Experiments with adult mussels were performed in a flow-through seawater system under a 14:10 h light/dark cycle. Seawater from Kiel Fjord was filtered through a series of 50, 20, and 5 µm water filters, UV-sterilized and subsequently pumped at a rate of 5 L min^{-1} into a storage tank of 300 L volume. The water was aerated and mixed by a pump to ensure that air saturated water was pumped up to a header tank which supplied 12 experimental aquaria (volume = 16 L each) by gravity feed. The flow rate was adjusted to 50 or 100 mL min^{-1} $aquarium^{-1}$ depending on the experiment. Overflow drain pipes in the storage tank, header tank, and every aquarium ensured constant water levels in the system.

For the experiments with freshly settled mussel larvae, aquaria without flow-through were used. Single panels were transferred into 500 mL aquaria in a 17°C constant temperature room. Aquaria were filled with 0.2 µm filtered and UV-radiated seawater from the fjord. Water exchange of 400 mL (80%) was performed daily using CO_2 and temperature pre-equilibrated water.

2.3.2 CO_2 manipulation

In both setup systems, the experimental aquaria were continuously aerated using a central automatic CO_2 mixing-facility (Linde Gas & HTK Hamburg, Germany) in order to establish constant pCO_2 levels. This custom built gas-mixing facility determines the CO_2 content of inflowing ambient air of the pressurized air at IFM-GEOMAR and automatically adds pure CO_2 to produce five different CO_2-air mixtures which were introduced into the experimental aquaria at a rate of 0.8 L min^{-1} using aquarium diffuser stones (Dohse, Grafschaft-Gelsdorf, Germany). Ambient air (ca. 390 ppm, 390 µatm pCO_2) was used for the control treatment. The air of the elevated CO_2 treatments contained 1120, 2400 and 4000 ppm which corresponds to seawater pCO_2 levels between 390 and 4000 µatm (approximately 39-405 Pa).

2.3.3 Nutrition

During the first Tto-weeks incubation, mussels were fed with an algae suspension (DT's Live Marine Phytoplankton Premium Blend) which was pumped into the header tank using a peristaltic pump at a rate of 1 mL min^{-1} to maintain stable concentrations of 1000-4000 cells mL^{-1} within the experimental aquaria. The algae suspension contained *Nannochloropsis oculata* (40%), *Phaeodactylum tricornutum* (40%), and *Chlorella sp*. (20%).

In all subsequent experiments, *Rhodomonas sp.* was supplied to the experimental aquaria. For this purpose, *Rhodomonas sp.* was cultured in 7 L of 0.2 µm filtered seawater enriched with Provasolis seawater medium (Ismar et al. 2008). 5 mL of 0.2 µm filtered solutions of potassium dihydrogen orthophosphate and ammoniumnitrate were added to the culture media to final concentrations of 0.036 mmol L^{-1} P and 0.55 mmol L^{-1} N, respectively. The culturing was performed in plastic bags at 20°C and under constant illumination. Correlation of measured *Rhodomonas* cell number and POC and PON amount revealed a carbon and nitrogen content of 45 pg C $cell^{-1}$ and 9.6 pg N $cell^{-1}$, respectively. This results in a molar C:N ratio of 6.1.

In the experiments, using the flow-through set up, one seven litre bag of culture was supplied per day which was filled up to 16 L in order to ensure constant algae supply during the entire day. Depending on the cell densities in the bag the amount of supplied algae slightly differed during and between the experiments. *Rhodomonas* concentrations in the headertank and in the aquaria were regularly monitored during the experiments using a particle counter (Z2 Coulter® Particle count and size analyzer, Beckman Coulter™, Krefeld, Germany). In the close system set up, three feeding treatments were established by addition of exact cell numbers of *Rhodomonas spp.* algae to the experimental aquaria. For this purpose, *Rhodomonas* culture densities were measured in 1:20 and 1:40 dilutions using a particle counter to calculate the culture volume which had to be added in order to reach the desired cell densities in the aquaria. Cell concentrations of the *Rhodomonas* culture was measured in in a coulter counter (Z2 Coulter Particle count and size analyzer, Beckman Coulter, Krefeld, Germany) in order to calculate the required volume to add exact cell number. In weekly intervals, algae cell concentrations were increased and the number of mussels was reduced in order to compensate for mussel growth (Supplementary Table S1). Initial algal supply in the different food treatments was

5,000, 2,500 and 500 cells mL^{-1}, respectively, which was increased up to 40,000, 20,000 and 4,000 cells mL^{-1} during the last week. The ratio of 10:5:1 between the feedings levels was maintained during the entire experiment. Weekly, POC content of the supplied algae and of algae following a 24 h incubation was analyzed from water samples pooled from two aquaria of the same pCO_2 and feeding treatment. Differences between supplied and remaining POC were used to calculate POC uptake by the mussels.

2.4 Field experiments

2.4.1 Larval settlement

Monthly, settlement substrata were exposed to natural colonization at the IFM-GEOMAR pier at a depth of 1 m, approximately 50 m North of the carbonate chemistry sampling site. Settlement substrata were made of grey PVC manually roughed by grain 60 sandpaper to facilitate attachment. Each unit consisted of three differently oriented, 5 cm x 5 cm surfaces: vertical, horizontal upwards and horizontal downwards. The units were allowed to rotate freely around their vertical axis. The use of a biologically widely accepted material and the different orientations in space maximized our capacity to sample a large proportion of the propagules settling in a particular month. After retrieving the substrata at the end of a 4-week-exposure, they were gently rinsed to remove unattached organisms, then foulers were identified to the lowest taxonomic level possible (genus or species), and % cover per taxon was estimated. The level of replication was three.

2.4.2 Mussel shell growth

Individually tagged young (13 - 22 mm) blue mussels (*M. edulis*) from Kiel Fjord were placed into a net on 31.01.2007 and subsequently submerged into a container containing ambient seawater supplemented with 20 mg L^{-1} $MnCl_2$ for 6-24 h (with breaks from 26.07.07 to 23.08.07, from 07.11.07 to 29.11.07 and from 19.12.07 to 10.01.08). In these treatment phases, the mussels incorporated manganese during precipitation of their shells (Barbin et al., 2008). The days between the $MnCl_2$ markings the mussel net was freely suspended at the IFM-GEOMAR jetty in Kiel Fjord at about 1 m water depth, enabling the mussels to filter feed in their natural environment. After 12 months (on 05.02.08) the soft tissue of the mussels was removed and the left valve of one individual (initial shell length: 16.1 mm, final shell length: 46.6 mm) was prepared for electron micro probe (EMP) measurements: The shell was cut along the axis of maximum growth using a cut-off wheel and shell sections were embedded in a two component epoxy resin (Buehler, EPO-THIN, Low Viscosity Epoxy Resin) on a brass-slide. After hardening at 50°C, the sections were ground with sand paper (grading (p): 240-600) and polished with diamond paste (grading 0.5-0.01 µm). EMP analyses were carried out at IFM-GEOMAR Kiel, Germany, using a JEOL JXA 8200 “Superprobe” applying Wavelength Dispersive Spectrometry (WDS), using a focused beam, a resolution between 3 µm x 3 µm and 10 µm x 10 µm and an integration time per point of 400 ms.

Field growth experiments:

For the field growth study, settlement panels were treated in the same way as stated above in the section Animals. Panels were transferred to the experimental sites and suspended at 1 m depths. Both field sites are characterized by similar salinity, temperature, light exposure and are sheltered from wave action. The number of replicates was 6. Despite the shelter, two panels were lost at station OF during storms. Water chemistry (pH_T, C_T) and POC concentrations were monitored bi-weekly at both stations. The experiment lasted from July 23th to November 19th 2010 (18 weeks), when the panels were removed from the water.

2.5 Determination of whole animal performance

2.5.1 Growth and calcification

For determination of initial size of settled larvae (shell length, $CaCO_3$ and total organic content) a subsample of specimens was sampled directly from the panels after removal from the Fjord and stored in seawater with 4% paraformaldehyde (PFA). For measurements of weekly growth rates, 5-6 individuals were sampled at each sampling day from each aquarium and were similarly treated. Shell length was measured using a stereo microscope equipped with a MicroPublisher 3.3 RTV camera and the image analysis software Image Pro Plus 5.0.1. Final $CaCO_3$ and total organic content (TOC = SFDM + organic shell components, OSC) was determined as described above by weighing single specimens with a precision balance (accuracy ± 1 µg, Sartorius, Göttingen, Germany) after drying at 60°C and ashing at 500°C for 20 h. Additionally, shell free drymass (SFDM) was dissected from carefully opened, frozen specimens and dried at 60°C. Comparison of SFDM and total organic content was performed using a regression of both parameters against shell length.

Shell length of juvenile mussels were measured using a calliper to the nearest of ±0.1 mm. SFDM and total shell mass including ISC and OSC were measured with a balance (accuracy ± 0.1 mg) after drying at 60°C overnight. Determination of ISC and OSC was performed by measuring the mass difference after drying at 60°C overnight and after ashing at 500°C for 20 h.

2.5.2 Determination of metabolic rates

Respiration and NH_4^+ excretion rates measurements were performed in 100 mL plexiglas chambers which were placed in a 100 L water bath. 0.2 µm filtered and UV-sterilized seawater was equilibrated with a specific pCO_2 for 24 h before and during the measurements. 4 replicate chambers (3 replicates with mussels, one chamber without mussels serving as a bacterial control) were combined in four measuring circuits using gas - tight Tygon tubing (R-3603, Saint-Gobain, France). Each chamber contained 10 randomly chosen mussels from one replicate aquarium. Transfer from aquaria to the chambers lasted less than one minute and measurements started after half an hour of acclimation to experimental conditions. During the incubation period in the respiratory chambers, mussel valves remained open.

2.5.3 Oxygen consumption

MO_2 of *M. edulis* was measured using an intermittent-flow system. Water inside the respirometry chambers was continuously circulated using a peristaltic pump (MCP ISM 404, ISMATEC, Switzerland) at a rate of 2 mL s^{-1}. Oxygen concentrations were recorded every 5 minutes using fibre-optic oxygen sensors (needle-type optodes, Presens, Regensburg, Germany) inserted into the tubing of the measuring circuit via a plastic y-piece. One measuring interval lasted 45 minutes. Between measuring intervals, chambers were flushed with seawater from the water bath for 3 h using 5 W submersible pumps (Eheim, Deizisau, Germany). The whole incubation lasted for 20 h per pCO_2 treatment, with 6 MO_2 determinations per replicate chamber per aquarium. NH_4^+ concentrations in the water bath were always below one µmol L^{-1} at the end of an incubation.

For calculation of oxygen consumption rates, the linear decrease of oxygen concentration during measuring intervals between 5 and 35 minutes was considered; $[O_2]$ maximally decreased to 65% air saturation (average: 74%). The observed decrease of oxygen concentration resulted in an increase of C_T and therefore pCO_2 in the closed chambers. Depending on oxygen consumption rates in the different pCO_2 treatments, seawater pCO_2 in the chambers increased by 40-180 µatm (<10% of the initial pCO_2) during incubations. The results of 6 separate runs per chamber measured during the whole incubation interval were averaged. Over the course of 20h incubations, consumption rates slightly decreased in the last runs at all pCO_2 levels. Molar oxygen consumption rates (MO_2) are expressed as µmol O_2 g^{-1} SFDM h^{-1}.

2.5.4 Ammonium excretion

Seawater ammonium (NH_4^+) concentrations were determined prior to, and following the respiration trials. An initial 10 mL water samples was taken from every chamber before closing for oxygen consumption measurements, after 1h incubation, a second sample was taken. Additionally, excretion rates were assessed in a stop-flow experiment during the growth period one week earlier (Dec 10th). Seawater flow-through was stopped and mussels were incubated in closed aquaria. Following 8.5 h of incubation, 10 mL water samples were taken from each replicate aquarium.

Ammonium concentrations were determined according to Holmes et al. (1999). 2.5 mL of a reagent which contains orthophthaldialdehyde, sodium sulfite, and sodium borate, were added to the water samples. After two hours incubation, samples were measured using a Kontron SFM25 fluorometer at an excitation and emission wavelength of 360 and 422 nm, respectively. Ammonium excretion rates ($NH_4^+{}_{ex}$) are expressed as µmol NH_4^+ g^{-1} SFDM h^{-1}.

Additionally, excretion rates were determined for mussels placed in plastic aquaria containing 180 ml water with different pH (7, 8 and 9) and pCO_2 (380 and 4000 µatm) levels. Water pCO_2 was aerated with air containing 380 and 4000 ppm and water pH was adjusted by addition of HCl (pH 7, 380 ppm) or NaOH (pH 9, 380 ppm and pH 8 at 4000 ppm). After 30 minutes a first sample and after two additional hours a second sample was taken. Seawater analyses were carried out as stated above and differences between both samples were to calculate excretion rates. An aquarium without mussels for each treatment was used as a control.

2.5.5 Calculation of O:N ratio, metabolic energy turnover and energetic contents

The atomic ratio of oxygen uptake and excreted nitrogen was calculated from MO_2 and $NH_4^+{}_{ex}$.

$O:N = MO_2\ NH_4^+{}_{ex}^{-1}$

Aerobic energy loss was calculated using a mean oxycaloric equivalent of 0.44 J µmol O_2^{-1} representing a mixed, but protein dominated, catabolism of hydrocarbons, lipids, and proteins as metabolic substrates (Lauff and Wood 1996). Calculations were performed without consideration of potential changes in the fraction of the three substrates to total metabolism in the different pCO_2 treatments. Energy loss by NH_4^+ excretion was calculated using an energy value of 0.347 J µmol^{-1} NH_4^+ according to Elliott and Davison (1975). Total metabolic energy loss (E_{NET}, J g^{-1} SFDM h^{-1}) was calculated from aerobic energy metabolism and nitrogen excretion:

$E_{NET} = MO_2 \times 0.44J + NH_4^+{}_{ex} \times 0.347J$

Energy contents of supplied *Rhodomonas* and seawater POC was estimated using the conversion factor of 46 J mg^{-1} POC (Salonen et al. 1976). Mussel SFDM and OSC (periostracum+organic) was converted to caloric equivalents using the conversion factor 23 J mg^{-1} (Brey et al. 1988). Similarly, the inorganic shell component (ISC) was converted into energy equivalents using a factor of 2 J mg^{-1} $CaCO_3$ (Palmer 1992).

2.6 Determination extracellular acid-base status and ion concentrations

Haemolymph (HL) and extrapallial fluid (EPF) were sampled bubblefree from the posterior adductor muscle or from the extrapallial cavity between the mantle tissue and the shell using a syringe.

pH_{NBS} of *M. edulis* haemolymph was measured either using fiber-optic sensors (optodes, PreSens, Regensburg, Germany) or with an pH microelectrode (WTW Mic-D). For the optode measurements a fiber-optic sensors was installed in the tip of 1 mL syringes (Gutowska and Melzner, 2009) which was palced in a 12° water bath. Samples were filtered through a glassfiber filter at the syringe tip to remove haemocytes. The sensors were calibrated in ambient sea water which was adjusted to four different pH_{NBS} values between 6.9 and 7.8 with HCl and NaOH. Optodes were calibrated against a WTW 340i pH meter and a SenTix 81 electrode, calibrated with Radiometer precision buffers (S11M44, S11 M007). In the other case, pH_e was measured within a cap using a microelectrode (WTW Mic-D) and a WTW 340i pH meter. The slight offset of the WTW pH_{NBS} electrodes with respect to pH_{NBS} values calculated from A_T and C_T measurements on the same water bodies were corrected by using the following linear relationship (eq. (2), n=95, r^2=0.9593):

$$pH_{corrected} = 0.9398\,pH_{measured} + 0.556$$

Haemolymph C_T was measured in two 100 µL subsamples with a Corning 965 CO_2 analyzer. To correct for instrument drift 100 µL of distilled water were measured prior to each sample determination. Thus, a precision and accuracy of 0.1 mM could be reached. To determine *in vitro* non-bicarbonate

buffer (NNB)- values of extracellular fluid, 600 µL samples pooled from 10 animals were equilibrated with humidified CO_2 gas mixtures (pCO_2 57, 142, 405, 564 Pa) for 1h using the gas mixing facility and a gas mixing pump (Wösthoff, Bochum, Germany). Incubations were performed in a shaking water bath at 12°C, using a glass flask (120 mL) as an incubator. pH and C_T were measured using a microelectrode (WTW Mic-D) and Corning 965 CO_2 analyzer, respectively, as described above.
Body fluid pCO_2, bicarbonate, and carbonate concentrations were calculated from measured pH and C_T values according to the rearranged versions of the Henderson-Hasselbalch equation:

$$\mathrm{p}CO_2 = C_T\left(10^{ph-pK'_1}\alpha_{CO_2} + \alpha_{CO_2}\right)^{-1}$$

$$\left[HCO_3^{2-}\right] = 10^{pH-pK'_1}\alpha_{CO_2}\mathrm{p}CO_2$$

$$\left[CO_3^{2-}\right] = 10^{pH-pK'_2}\left[HCO_3^{-}\right]$$

α is the CO_2 solubility coefficient and pK'_1 and pK'_2 are the first and second apparent dissociation constants of carbonic acid. α_{co2} was calculated (Weiss, 1974) and pK'_2 (Roy et al., 1993) was chosen according to experimental temperature and salinity. pK'_1 was calculated from pH_{NBS}, C_T, and pCO_2 measured in vitro in body fluids of both species using equation (6) (Albers and Pleschka, 1967):

$$pK'_1 = pH - \log\left(\frac{C_T}{\mathrm{p}CO_2\alpha_{CO_2}} - 1\right)$$

A linear relationship was found for pK'_1 in relation to pH_{NBS}. The regression for pK'_1 for *M. edulis* haemolymph was $pK'_1 = -0.1795pH + 7.5583$ (r^2=0.5). The calculated values for pK'_1 in *M. edulis* differed between 6.20±0.03 in control and 6.27±0.02 in 405 Pa pCO_2 treated animals. For determination of acid-base status *of M. edulis* sampled directly from Kiel Fjord during 2009, the linear regression for pK_1 was adjusted for Fjord temperature and salinity.
Protein concentration in the haemolymph was determined using a Thermo Multiskan spectrum photometer (Waltham, Massachusetts, USA) and BSA standard solutions (Bradford, 1976). Prior to measurements samples were centrifuged to remove haemocytes (100 g, 25 min, 2°C). The total cation concentrations of water and body fluid were measured using a Dionex ICS-2000 ion chromatograph, a CS18 column and methane sulfonic acid as eluent. Samples were centrifuged for 20 minutes at 100 g and 4°C to remove haemocytes. The supernatant was transferred into a new cap and frozen at -20°C. Prior to measurement, body fluid and ambient seawater samples were diluted 1:100 with de-ionized water. A calibration curve was obtained by measuring a dilution series of 1:50, 1:100, 1:200, 1:300, 1:400, and 1:500 of the IAPSO seawater standard (International Association for the Physical Sciences of the Oceans, batch: P146; 12.05.05; salinity: 34.992; K15: 0.99979).

2.7 Biochemical and molecular work

2.7.1 Na^+/K^+-ATPase and H^+-ATPase activity

The measurement was performed using the method described by Schwartz et al. (1969). It is based on the coupled reaction of pyruvate kinase and lactate dehydrogenase.
Ca. 100 mg of the frozen tissue (mantle, gill and kidney) were homogenized in 1 mL ice-cold extraction buffer which contained imidazole 50 mM, sucrose 250 mM, EDTA 1 mM, β-mercaptoethanol 1 mM and desoxycholic acid 5 mM using a DUALL hand homogenizer (Kleinfeld Labortechnik, Gehrden, Germany). Subsequently, the homogenate was centrifuged at 1000 g at 0°C for 10 minutes. Ten µL of the supernatant were added to 990 µLl of each reaction buffer containing 100 mM imidazole, pH 7.8, NaCl 80 mM, KCl 20 mM, $MgCl_2$ 5 mM, ATP 5 mM, NADH 0.24 mM, PEP 2 mM, and a PK/LDH-enzyme mix (AppliChem) with 14 U/mL PK and 17 U/mL LDH activity. The specific fraction of Na^+/K^+-ATPase activity (NA) of total activity (TA) is determined by addition of 5 mM ouabain. H^+-ATPase activity corresponds to the lowering of activity after addition of 100 nM Bafilomycin. The photometric measurement of the supernatant was performed using a DU 650 spectrophotometer (Beckman, Krefeld, Germany) at λ= 339 nm for 10 min at 16°C. Activity is calculated as µmol ATP per gram of freshmass and hour using an extinction coefficient for NADH of 6.31 mM^{-1} cm^{-1}.

2.7.2 Tissue and haemolymph ammonia concentration

Haemolymph (500 and 1000 µL) was sampled from the posterior adductor muscle (PAM) and frozen at -20°C. Afterwards, mussels were opened by cutting the PAM and tissue samples of gill, kidney, mantle, foot, PAM and hepatopancreas were dissected and similarly frozen at -20°C. After weighing, frozen tissues were cut using a scissor and transferred into in1.5 mL MilliQ. Samples were homogenized using an ULTRA-TURRAX (IKA, Germany) and 3.5 mL MilliQ (Millipore, USA) were added. Samples were stored at -20°C until analysis. Prior to the analyses haemolymph samples were diluted 1:10 for controls and 1:20 for high environmental ammonia treated animals. Homogenized tissue samples were diluted by 1:5. Determination of ammonia was carried out using a gas-sensitive NH_3 electrode (Thermo Orion, Cambridgeshire, England) and a digital mV/pH meter (type 646, Knick, Germany). 30 µL of a 10 M NaOH solution were added to each samples exact prior to determination. During measurements, samples were mixed by a magnetic stirrer.

2.7.3 Molecular work

Tissue samples of kidney, foot and gill were dissected from the animals and directly used for RNA extraction. Tissue were homogenized in RLT buffer with mercaptoethanol using hand homogenizers Total RNA was extracted using the Quiagen RNA plus Mini Kit according to the manufacturrer's instructions. Additionally, for some samples extraction was performed using TRIzol Reagent ® (Invitrogen). This protocol includes chloroform, isopropanol and 70% ethanol washing steps. The extracted total RNA was quantified with a Nanodrop Bioanalyzer. 0.5 µg total RNA were treated with DNAse (DNAse 1 amplication grade, Invitrogen) and 10 µL of the digested RNA were used for cDNA synthesis (iScript cDNA synthesis kit, Biorad). Primer were generated using the *Mytilus* mantle

transcriptome (Philipp et al., PLos One in press, Melzner et al. unpublished) with Primer 3 software and tested using conventional PCR in order to test amplification of single bands. Sequences were verified using the BLAST algorithm (blast.ncbi.nlm.nih.gov) and revealed high similarities to their invertebrate and vertebrate homologs.

Table 2.1: List of primers used in the quantitative real-time PCR

Gene	Abbreviation	fragment size	Primer sequence 5´-3´	Blasthit
Na/proton exchanger	NHE	133	CCCTGCTCAATGATGGAGTTA	AY607752.1
			CCACCAAGGGCAATGATAA	
Rhesus protein	Rh	200	GGATACCAGATGCTTGCCTTAG	XM_002741103.1
			TCATTACTTTTCCCATTCTCATACTT	
Ammoniumtransporter	AMT	184	TGTGTATGGGGTGTCGGTTAC	AY713399.1
			TTGGTCTTCCTCGCTCTATGA	
Na^+/K^+-ATPase	NKA	69	TGGACGACAACTTCAGGGAAT	JN010430.1
			AAACTCTTTCTCCAAGACCTCCTAATT	
Carbonic anhydrase II	CA	194	TCAGATGGTTTGGCGGTATT	XM_001507011.2
			GTTGTCAGCGACCCATCATA	
V-type ATPase	HAT	203	CAAACCCCAAAACACCTGTA	XM_623492.3
			TGCCTGCTGATTCTGGTTAC	
18s ribosomal RNA	18s	244	CTGGCACGGGGAGGTAGT	L33455.1
			AGGTCAGGAGCAGGCAGTAA	

Quantitative real time PCR was carried out as two steps PCR using a Biorad MJ mini cycler and sso fast EvaGreen Supermix (Biorad). For quantification of the gene product, standard curves were generated for each tested gene by dilution of samples after reamplification, gelextraktion, gelelectrophoresis and quanitifcation to concentration of 100 pg, 10 pg, 1 pg, 100 fg and 10 fg. The volume used in real time PCR reactions was 15 µL in total. The protocol was 95° 3min for Taq activation, and 40 cycles with 95° for 15 sec and 54° for 20 sec. Melting curve analysis was conducted with steps of one degree per 0.05 sec from 50 to 95° and finally 95° for one min. This volume contained 7.5 µL EvaGreen Supermix buffer mix, 1.2 µL of forward and reverse primer, 4.1 µL water and 1 µL template. For controls no template was added to the mix. No contaminations were detected.

3. Publications

List of publications and declaration of my contribution to the following manuscripts:

Publication 1

Thomsen, Jörn; Gutowska, Magdalena A.; Saphörster, Julia; Heinemann, Agnes; Trübenbach, Katja; Fietzke, Jan; Hiebenthal, Claas; Eisenhauer, Anton; Körtzinger, Arne; Wahl, Martin, Melzner, Frank (2010) *Calcifying invertebrates succeed in a naturally CO_2-rich coastal habitat but are threatened by high levels of future acidification*. Biogeoscience

I designed and conducted the laboratory experiments and measured pH variability in Kiel Fjord. I wrote the manuscript together with the last author, all co-authors helped revise the manuscript.

Publication 2

Thomsen, Jörn; Melzner, Frank (2010) *Moderate seawater acidification does not elicit long-term metabolic depression in the blue mussel* Mytilus edulis. Marine Biology

I designed and performed the experiment and wrote the manuscript together with the co-author.

Publication 3

Thomsen, Jörn; Casties, Isabel; Pansch, Christian; Körtzinger, Arne; Melzner, Frank (submitted) *Food availability outweighs ocean acidification effects in the mussel* Mytilus edulis.

I designed and performed the experiments together with the co-authors, conducted the carbonate system monitoring and wrote the manuscript together with the last author, all co-authors helped revise the manuscript.

Calcifying invertebrates succeed in a naturally CO_2 enriched coastal habitat but are threatened by high levels of future acidification

Jörn Thomsen[1]

Magdalena A. Gutowska[2]

Julia Saphörster[1]

Agnes Heinemann[1,3]

Katja Trübenbach[2]

Jan Fietzke[3]

Claas Hiebenthal[4]

Anton Eisenhauer[3]

Arne Körtzinger[5]

Martin Wahl[4]

Frank Melzner[1*]

Corresponding author: Frank Melzner, fmelzner@ifm-geomar.de

[1]Biological Oceanography, Leibniz -Institute of Marine Sciences (IFM-GEOMAR), Kiel 24105, Germany

[2]Institute of Physiology, Christian-Albrechts-University Kiel, Germany

[3]Marine Geosystems, Leibniz-Institute of Marine Sciences (IFM-GEOMAR), Kiel 24148, Germany

[4]Marine Ecology, Leibniz-Institute of Marine Sciences (IFM-GEOMAR), Kiel 24105, Germany

[5]Chemical Oceanography, Leibniz-Institute of Marine Sciences (IFM-GEOMAR), Kiel 24105, Germany

Abstract:

CO_2 emissions are leading to an acidification of the oceans. Predicting marine community vulnerability towards acidification is difficult, as adaptation processes cannot be accounted for in most experimental studies. Naturally CO_2 enriched sites thus can serve as valuable proxies for future changes in community structure. Here we describe a natural analogue site in the Western Baltic Sea. Seawater pCO_2 in Kiel Fjord is elevated for large parts of the year due to upwelling of CO_2 rich waters. Peak pCO_2 values of >230 Pa (>2300 µatm) and pH values of <7.5 are encountered during summer and autumn, average pCO_2 values are ~70 Pa (~700 µatm). In contrast to previously described naturally CO_2 enriched sites that have suggested a progressive displacement of calcifying auto- and heterotrophic species, the macrobenthic community in Kiel Fjord is dominated by calcifying invertebrates. We show that blue mussels from Kiel Fjord can maintain control rates of somatic and shell growth at a pCO_2 of 142 Pa (1400 µatm, pH = 7.7). Juvenile mussel recruitment peaks during the summer months, when high water pCO_2 values of ~100 Pa (~1000 µatm) prevail. Our findings indicate that calcifying keystone species may be able to cope with surface ocean pH values projected for the end of this century. However, owing to non-linear synergistic effects of future acidification and upwelling of corrosive water, peak seawater pCO_2 in Kiel Fjord and many other productive estuarine habitats could increase to values >400 Pa (>4000 µatm). These changes will most likely affect calcification and recruitment, and increase external shell dissolution.

1. Introduction

Future ocean acidification will most likely impact ocean ecosystems by differentially modulating species fitness and biotic interactions. Decreases in pH predicted for the next century have been shown to affect several marine taxa (Fabry et al., 2008). In short to intermediate (days-weeks) CO_2 perturbation experiments, calcifying marine invertebrate groups have been shown to react sensitively to simulated ocean acidification (Dupont et al., 2008; Pörtner et al., 2004; Kurihara, 2008b). Current hypotheses derived from experimental work suggest that there could be (i) direct effects of carbonate chemistry on calcification rate and shell integrity and that (ii) CO_2 induced disturbances in extracellular acid-base equilibria can lead to metabolic disturbances, which then impact growth and calcification rate, and, ultimately, fitness (Pörtner et al., 2004; Fabry et al., 2008; Melzner et al., 2009).

However, as most laboratory experiments cannot account for species' genetic adaptation potential, they are limited in their predictive power. Naturally CO_2 enriched habitats have thus recently gained attention as they could more accurately serve as analogues for future, more acidic ecosystems. The most prominent example, the volcanic CO_2 vents off of Ischia, Italy, have been shown to exert a negative influence on calcifying communities, with certain taxa (scleractinian corals, sea urchins, coralline algae) absent and seagrasses dominating in the acidic parts of the study site (Hall-Spencer et al., 2008). Another study conducted by Tunicliffe et al. (2009) revealed effects of low seawater pH on mussels living near hydrothermal vents. Shell thickness and length growth was reduced compared to specimens originate from areas with high pH conditions. Additionally, calcification in the low pH environment was only possible for animals with an intact periostracum and damage of it lead to complete dissolution of carbonate shells. Upwelling regions could also serve as natural analogue sites. 'Corrosive' upwelling of CO_2 enriched Pacific seawater onto the American shelf has recently been demonstrated (Feely et al., 2008). In shelf seas, seasonal stratification of water masses, respiration in deeper layers and subsequent upwelling of CO_2 enriched waters also results in an acidification of coastal surface waters. Our study site in the Western Baltic Sea is such a habitat: summer hypoxia and anoxia develop in bottom water layers, and strong upwelling events have been measured and modelled along the coasts (Hansen et al., 1999; Lehmann et al., 2002). However, prior to this study no detailed measurements of coastal carbonate system variability have been available for this system.

Here, we present first measurements of carbonate system variability in the shallow water habitats of Kiel Fjord. We also present field data on settlement success of invertebrate larvae and discuss growth rates of blue mussels in Kiel Fjord. Further, we conducted two laboratory experiments using the dominant benthic calcifier, the blue mussel *Mytilus edulis*, as a model species. In a first experiment (2 weeks duration), we studied haemolymph ion- and acid base regulation in larger mussels to test whether this species is able to control the carbonate system speciation in its extracellular fluids. In a second experiment (8 weeks duration), we exposed small and medium sized mussels to elevated seawater pCO_2 under an optimized feeding regime to test the hypothesis, whether disturbances in acid-base equilibria impact growth and calcification performance. We analyze shell morphology and microstructure from long-term acclimated mussels (Exp. 2) in order to determine whether formation of 'control' shell material is possible under acidified conditions.

2. Material & Methods

2.1 Field study

2.1.1 Determination of carbonate system parameters

Water samples from Kiel Fjord were taken for determination of total alkalinity (A_T) and total dissolved inorganic carbon (C_T). A_T was measured by means of a potentiometric open-cell titration with hydrochloric acid using a VINDTA autoanalyzer (Mintrop et al., 2000; Dickson et al., 2007). C_T was determined coulometrically (Dickson et al., 2007) using a SOMMA autoanalyzer. Both A_T and C_T measurements were measured against Certified Reference Material provided by Andrew Dickson of the Scripps Institution of Oceanography (http://andrew.ucsd.edu/co2qc/) yielding an overall precision (accuracy) of about 1 (2) µmol kg^{-1} and 1.5 (3) µmol kg^{-1}, respectively. Seawater carbonate system parameters (Ω, pCO_2) were calculated using the CO2sys program (Dickson et al., 2003; Lewis and Wallace, 1998). Dissociation constants K_1 and K_2 (Mehrbach et al., 1973; Dickson and Millero, 1987), $KHSO_4$ dissociation constant (Dickson, 1990) and the NBS scale [mol kg^{-1} H_2O] were used. The measured pH_{NBS} values of the experiments were corrected by a correlation of pH_{NBS} calculated from A_T and C_T for every experiment. Kiel Fjord surface pCO_2 values were estimated from weekly measured pH_{NBS} values (42 weeks between 01.04.2008 and 01.04.2009). For this purpose, measured pH_{NBS} was correlated with pCO_2 values calculated from measured A_T and C_T values (eq. (1), N = 9, see table 1 for A_T and C_T values, r^2=0.94):

$$\mathrm{p}CO_2 = -281.14\,pH_{NBS} + 2291.3 \quad (1)$$

where pCO_2 is the seawater pCO_2 in Pa, pH_{NBS} is the measured seawater pH value.

2.1.2 Larval settlement in Kiel Fjord

Between January and November 2008, settlement substrata were exposed monthly to natural colonization at the IFM-GEOMAR pier at a depth of 1 m, approximately 50 m north of the carbonate chemistry sampling site. Settlement substrata were made of grey PVC manually roughed using grain 60 sandpaper to facilitate attachment. Three separate settlement units were used; each consisted of three differently oriented, 5 cm x 5 cm surfaces: vertical, horizontal upwards, horizontal downwards. The units were allowed to rotate freely around their vertical axis. The use of a biologically widely accepted material and the different orientations in space maximized our capacity to sample a large proportion of the propagules settling in a particular month. After retrieving the substrata at the end of a 4-week-exposure, they were gently rinsed to remove unattached organisms, then foulers were identified to the lowest taxonomic level possible (genus or species), and % cover per taxon was estimated.

2.1.3 Mussel shell growth using $MnCl_2$ as a marker

Individually tagged young (13 to 22 mm) blue mussels (N = 50) from Kiel Fjord were placed into a net on 31.01.2007 and subsequently submerged into a container containing ambient seawater supplemented with 20 mg l^{-1} $MnCl_2$ for 6 to 24 h (with breaks from 26.07.07 to 23.08.07, from 07.11.07 to 29.11.07 and from 19.12.07 to 10.01.08). In these treatment phases, the mussels incorporated manganese during precipitation of their shells (Barbin et al., 2008). No mortality due to the $MnCl_2$ marking has been observed. The days between the $MnCl_2$ markings the mussel net was freely suspended at the IFM-GEOMAR jetty in Kiel Fjord at about 1 m water depth, enabling the mussels to filter feed in their natural environment. After 12 months (on 05.02.08) the soft tissue of the mussels was removed and the left valve of one individual (initial shell length: 16.1 mm, final shell length: 46.6 mm) was prepared for electron micro probe (EMP) measurements: The shell was cut along the axis of maximum growth using a cut-off wheel and shell sections were embedded in a two component epoxy resin (Buehler, EPO-THIN, Low Viscosity Epoxy Resin) on a brass-slide. After hardening at 50°C, the sections were ground with sand paper (grading (p): 240 to 600) and polished with diamond paste (grading 0.5 to 0.01 µm). EMP analyses were carried out at IFM-GEOMAR Kiel, Germany, using a JEOL JXA 8200 “Superprobe” applying Wavelength Dispersive Spectrometry (WDS), using a focused beam, a resolution between 3 µm x 3 µm and 10 µm x 10 µm and an integration time per point of 400 ms.

2.2 Laboratory experiments

2.2.1 Animals

Mytilus edulis were collected from a subtidal population in Kiel Fjord (54°19.8'N; 10°9.0'E). For extracellular acid-base status experiments (Exp. 1), large specimens with a shell length of 76 ± 5 mm were used. The long-term growth and calcification trial (Exp. 2) was conducted with mussels of 5.5 ± 0.6 (“small”) and 13.3 ± 1.4 mm (“medium”) shell length. Mussels were collected in March and April 2008 (acid-base regulation) and May 2009 (growth and calcification). Prior to experimentation, shells were cleaned of epibionts and animals were acclimated to the experimental settings for one to two weeks.

2.2.2 Experimental setup

Experiments were performed in a flow-through seawater system under a 14:10 h light/dark cycle. Seawater from Kiel Fjord was filtered through a series of 50, 20, and 5 µm water filters, UV-sterilized and subsequently pumped at a rate of 5 L min^{-1} into a storage tank of 300 l volume. The water was aerated and mixed by a pump to ensure that air saturated water was pumped up to a header tank which supplied 12 experimental aquaria (volume = 16 L each) by gravity feed. The flow rate was adjusted to 100 mL min^{-1} $aquarium^{-1}$. Overflow drain pipes in the storage tank, header tank, and every aquarium ensured constant water levels in the system. The experimental aquaria were continuously aerated using a central automatic CO_2 mixing-facility (Linde Gas & HTK Hamburg, Germany). This custom built gas-mixing facility determines the CO_2 content of inflowing ambient air and automatically

adds pure CO_2 to produce five different CO_2-air mixtures. CO_2-enriched air with a pCO_2 of 57, 85, 113, 142 and 405 Pa (i.e. 560, 840, 1120, 1400, 4000 µatm) was injected into the experimental aquaria at a rate of 0.8 L min^{-1} using aquarium diffuser stones (Dohse, Grafschaft-Gelsdorf, Germany). Ambient air (ca. 39 Pa / 385 µatm pCO_2) was used as a control.

2.2.3 Experimental protocol

Exp. 1: Two *M. edulis* experimental runs lasted for 14 days each at a constant water temperature of 12°C (Exp. 1). Temperature in the storage tank was kept constant using heaters (Eheim, Deizisau, Germany) or a flow-through cooler (TITAN 1500, Aqua Medic, Bissendorf, Germany). In the first run (Exp. 1a, 29.04.-16.05.2008) only the five lower pCO_2 levels were used, in the second run (Exp. 1b, 28.05.-12.06.2008) all six levels were used. Six mussels were placed in each of the experimental aquaria (biomass, total wet mass per aquarium = 246 ± 35 g). Mussels were fed with an algae suspension (DT's Live Marine Phytoplankton Premium Blend) which was pumped into the header tank using a peristaltic pump at a rate of 1 ml min^{-1} to maintain stable concentrations of 1000 to 4000 cells mL^{-1} within the experimental aquaria. Previous work established that blue mussels display maximum filtration rates when exposed to such algae densities (Riisgard et al., 2003). The algae suspension contained *Nannochloropsis oculata* (40%), *Phaeodactylum tricornutum* (40%), and *Chlorella sp*. (20%). At the end of the experimental period, animals were gently removed from the aquaria. Extracellular fluid samples were taken within two min after removal from the aquaria. Haemolymph samples of *M. edulis* were drawn anaerobically with a syringe from the posterior adductor muscle after valves were opened and blocked with a pipette tip. Two samples were taken from each animal. The first sample (200 µL) was used for pH determination and the second (500 µL) for measurement of total dissolved inorganic carbon (C_T) and ion composition (see below). Water samples were taken from the aquaria for the determination of ionic composition, A_T, and C_T. Similarly to haemolymph samples, extrapallial fluid (EPF) was sampled from the extrapallial space by gently inserting a syringe needle between shell and the pallial attachment. For comparison of EPF and haemolymph acid-base status, mussels were sampled from the field on 30 August 2010. Prior to measurements, mussels were stored in a flow-through aquarium to avoid sampling stress artefacts.

Exp. 2: In a long-term growth experiment, mussels were exposed for 2 months to three pCO_2 levels (39, 142, and 405 Pa / 385, 1400, 4000 µatm) in four replicate aquaria for each treatment level at a mean temperature of 13.8 ± 0.6°C between 14.05.-13.07.2009. Each replicate contained eight mussels of 5.5 mm (‘small’) and 13 mm (‘medium’) shell length. Initial total biomass per replicate aquarium was 14 ± 0.5 g. Mussels were continuously fed with a *Rhodomonas sp.* suspension containing 2903 ± 1194 cells ml^{-1} which was introduced into each aquarium at a rate of 100 ml min^{-1}. *Rhodomonas sp.* was cultured in 0.2 µm filtered seawater enriched with Provasolis seawater medium (Ismar et al., 2008), phosphate, and nitrate at a final concentration of 0.036 mmol L^{-1} P and 0.55 mmol L^{-1} N in plastic bags at 7.5 L each under constant illumination. Mean algae concentrations in the experimental aquaria were 820 ± 315 cell mL^{-1}. Shell length and fresh mass of the mussels were measured at the beginning of the experiment and after 8 weeks using a calliper (± 0.1 mm) and a precision balance (± 1 mg). Somatic dry and shell mass were measured after drying the animals for

24h at 80°C using a precision balance (± 1 mg, Sartorius, Germany). Similar determinations were carried out for control mussels from Kiel Fjord collected at the sampling site of our experimental animals.

2.2.4 Monitoring of carbonate system

Daily measurements were conducted to monitor pH, salinity, and temperature in the aquaria and the same parameters were determined weekly in Kiel Fjord (54°19.8'N; 10°9.0'E). pH was measured with a WTW 340i pH-meter and a WTW SenTix 81-electrode which was calibrated with Radiometer IUPAC precision pH buffer 7 and 10 (S11M44, S11 M007). Salinity and temperature were measured with a WTW cond 315i salinometer and a WTW TETRACON 325 probe. Additionally, water samples for A_T and C_T measurements were taken from the aquaria and analyzed as stated in section 2.1.1.

2.2.4 Determination of extracellular acid-base and ion status:

In Exp. 1, *M. edulis* haemolymph (HL) pH_{NBS} was measured in a 12°C water bath using fiber-optic sensors (optodes, PreSens, Regensburg, Germany) which were installed in the tip of 1 ml syringes (Gutowska and Melzner, 2009). Samples were filtered through a glassfiber filter at the syringe tip to remove haemocytes. The sensors were calibrated in ambient sea water which was adjusted to four different pH_{NBS} values between 6.9 and 7.8 with HCl and NaOH. Optodes were calibrated against a WTW 340i pH meter and a SenTix 81 electrode, calibrated with Radiometer precision buffers (S11M44, S11 M007). For comparison of haemolymph and extrapallial pH samples were measured within a cap using a microelectrode (WTW Mic-D) and a WTW 340i pH meter. The slight offset of the WTW pH_{NBS} electrodes with respect to pH_{NBS} values calculated from A_T and C_T measurements on the same water bodies were corrected by using the following linear relationship (eq. (2), N = 95, $r^2 = 0.96$):

$$pH_{corrected} = 0.9398\, pH_{measured} + 0.556 \quad (2)$$

Haemolymph C_T was measured in two 100 µL subsamples with a Corning 965 CO_2 analyzer. To correct for instrument drift 100 µL of distilled water were measured prior to each sample determination. Thus, a precision and accuracy of 0.1 mM could be reached. To determine *in vitro* non-bicarbonate buffer (NBB) - values of extracellular fluid, 600 µL samples pooled from 10 animals were equilibrated with humidified CO_2 gas mixtures (pCO_2 57, 142, 405, 564 Pa / 560, 1400, 4000, 5570 µatm) for 1h using the gas mixing facility and a gas mixing pump (Wösthoff, Bochum, Germany). Incubations were performed in a shaking water bath at 12°C, using glass flasks (120 ml) as incubators. pH_{NBS} and C_T were measured using a microelectrode (WTW Mic-D) and Corning 965 CO_2 analyzer, respectively, as described above.

Body fluid pCO_2, bicarbonate, and carbonate concentrations were calculated from measured pH and C_T values according to the rearranged versions of the Henderson-Hasselbalch equation:

$$\mathrm{p}CO_2 = C_T\left(10^{ph-pK'_1}\alpha_{CO_2} + \alpha_{CO_2}\right)^{-1} \quad (3)$$

$$\left[HCO_3^{2-}\right] = 10^{pH-pK'_1}\alpha_{CO_2}\mathrm{p}CO_2 \quad (4)$$

$$\left[CO_3^{2-}\right] = 10^{pH-pK'_2}\left[HCO_3^{-}\right] \quad (5)$$

where α is the CO_2 solubility coefficient and pK'_1 and pK'_2 are the first and second apparent dissociation constants of carbonic acid. α_{co2} was calculated (Weiss, 1974) and pK'_2 (Roy et al., 1993) was chosen according to experimental temperature and salinity. pK'_1 was calculated from pH_{NBS}, C_T, and pCO_2 measured *in vitro* in the body fluid using equation (6) (Albers and Pleschka, 1967):

$$pK'_1 = pH - \log\left(\frac{C_T}{\mathrm{p}CO_2\alpha_{CO_2}} - 1\right) \quad (6)$$

A linear relationship was found for pK'_1 in relation to pH_{NBS}. The regression for pK'_1 for *M. edulis* haemolymph was $pK'_1 = -0.1795\ pH + 7.5583$ ($r^2 = 0.5$). The calculated values for pK'_1 differed between 6.20 ± 0.03 in control and 6.27 ± 0.02 in 405 Pa pCO_2 treated animals. Protein concentration in the haemolymph was determined using a Thermo Multiskan spectrum photometer (Waltham, Massachusetts, USA) and BSA standard solutions (Bradford, 1976). Prior to measurements samples were centrifuged to remove haemocytes (100 g, 25 min, 2°C). The total cation concentrations of water and body fluid were measured using a Dionex ICS-2000 ion chromatograph, a CS18 column and methane sulfonic acid as eluent. Samples were centrifuged for 20 minutes at 100 g and 4°C to remove haemocytes. The supernatant was transferred into a new cap and frozen at -20°C. Prior to measurement, body fluid and ambient seawater samples were diluted 1:100 with de-ionized water. A calibration curve was obtained by measuring a dilution series of 1:50, 1:100, 1:200, 1:300, 1:400, and 1:500 of the IAPSO seawater standard (International Association for the Physical Sciences of the Oceans, batch: P146; 12.05.05; salinity: 34.992; K15: 0.99979).

2.2.5 Shell morphology and shell microstructure

Shell morphology was assessed for 20 randomly chosen, medium sized mussels from each treatment in experiment 2. Mussel shells were checked for external and internal shell dissolution under low magnification (8 fold magnification) using a stereomicroscope. Shell umbones were photographed at 18 times magnification and analyzed for signs of external dissolution (50 fold magnification). Images were analyzed for the extent of dissolution at the umbo with an accuracy of 1 mm^2 (the large uncertainty is due to the curvature of the shell). Severity of dissolution was graded according to the following scale, the 'dissolution index': 0 = no dissolution, 1 = periostracum abrasion, 2 = calcite dissolution visible, 3 = massive dissolution of calcite, multi – layered, often with round dissolution pits. Other dissolution spots on the outer shell surface were not quantified.

Microstructure of shell cross sections at two different positions of the shell of randomly chosen *M. edulis* (N = 5) from experiment 2 (medium size) that were characterized by similar final shell lengths

was investigated. Shells were perforated every 2 mm along the longitudinal axis (i.e. anterior-posterior axis) using a 1 mm diameter drill. They could then be manually fractured in a controlled fashion. Shell analysis was performed exclusively on intact cross sections in between drilled holes. We found that such a procedure produces high quality cross sections. Position one (at 75% shell length) is located anterior to the pallial line (PL) and consists of aragonite and calcite layers. Position two (at 95% shell length) lies posterior to the PL and is solely composed of calcite. Both positions are located in shell regions formed during the experiment. The shell fractions were coated with gold-palladium and examined using scanning electron microscopy (SEM, Nanolab 7, Zeiss). The thickness of the different crystal layers (aragonite, calcite) and the number of the aragonite platelets were quantified.

2.3 Statistical analyses:

Regression analysis was performed with SigmaPlot 10. Statistical analyses were performed using STATISTICA 8. Differences between treatments were analyzed using one- and two-way ANOVA and the Tukey post-hoc test for unequal N. Relative quantities were arcsine transformed prior to analysis. For shell morphology analysis of dissolved shell area and the dissolution index, non-parametric Kruskal-Wallis and subsequent Dunn's Multiple Comparisons Tests were used. Values in graphs and tables are means ± standard deviation.

3. Results & Discussion

3.1. Habitat carbonate system speciation and calcifying communities

The western Baltic Sea is characterized by low salinity (10 to 20) and relatively low A_T of 1900 to 2150 µmol kg^{-1}. Thus, the calcium carbonate saturation state (Ω) typically is much lower than in the open ocean. Our A_T and C_T measurements in 2008 and 2009 indicate that Ω_{arag} did not exceed a value of one in Kiel Fjord surface waters during summer and autumn. Even Ω_{calc} dropped below one on multiple occasions (Table 1, Fig. 1A). Minimum values for Ω_{arag} (Ω_{calc}) were 0.35 (0.58) in September 2008. Low Ω is associated with high surface pCO_2 during the summer and autumn months, caused by upwelling of CO_2-rich deeper water masses (Hansen et al., 1999). Kiel Fjord surface pCO_2 exceeds present average ocean pCO_2 values during large parts of the year. Habitat pCO_2 varies between 38 and 234 Pa (375 and 2309 µatm), pH_{NBS} varies between 7.49 and 8.23. Using a correlation of weekly measured surface pH_{NBS} and calculated pCO_2 from A_T and C_T measurements, we estimate that in 34%, 23% and 9% of 42 weeks investigated, pCO_2 exceeded pre-industrial pCO_2 (28 Pa, 280 µatm) by a factor of three (>85 Pa, >840 µatm), four (>113 Pa, >1120 µatm) and five (>142 Pa, >1400 µatm), respectively.

Given the particular carbonate system variability of the habitat it is surprising that blue mussel (*Mytilus edulis*) beds and associated calcifying benthic species (e.g. the barnacle *Amphibalanus improvises* and the echinoderm *Asterias rubens*) are common features in Kiel Fjord and the Western Baltic. *M. edulis* forms a shell consisting of an inner aragonite (nacre) and outer calcite layer, covered and protected by an organic layer, the periostracum. Despite an extensive organic matrix surrounding the

calcite and aragonite crystals, 95-99.9% of the shell's mass is comprised of $CaCO_3$ (Yin et al., 2005). *M. edulis* constitutes more than 90% of the macrofauna biomass in many habitats in the Western Baltic (Reusch and Chapman, 1997; Enderlein and Wahl, 2004). Competitive dominance is achieved primarily through very high rates of recruitment (spatfall) and high rates of juvenile growth (Dürr and Wahl, 2004). Previous results indicate that *M. edulis* (2 to 3 cm shell length) are characterized by shell growth rates of ca. 4 mm $month^{-1}$ during the summer months in Kiel Fjord (Kossak, 2006). Our EMP analysis of a $MnCl_2$ marked mussel confirms these earlier findings and indicates that weekly shell increments in the field can exceed 1 mm $week^{-1}$ during May to October (Fig. 2). Settlement of juvenile mussels in 2008 occurred exactly when highest pCO_2 values were encountered in the habitat (Fig. 1C): peak settlement took place in July and August, at an average surface pCO_2 of 98 Pa (967 µatm). Other calcifying invertebrates (e.g. the barnacle *Amphibalanus improvisus*) also settled abundantly between May and October 2008 in Kiel Fjord (Fig. 1C). When settlement plates are not exchanged regularly, mussels have been found to dominate the species assemblage (>0.99 by biomass) in Kiel Fjord within ~10 weeks in summer (Enderlein and Wahl, 2004).

3.2 *M. edulis* extracellular acid-base status (Exp. 1)

In order to better understand the success of *M. edulis* in Kiel Fjord, a chemically and physiologically challenging habitat, we studied haemolymph pH_{NBS} (pH_e) and ion regulation (Exp. 1) and, subsequently growth and calcification performance (Exp. 2). We found that mussels do not regulate pH_e when exposed to elevated seawater pCO_2. pH_e followed the non-bicarbonate buffer line when displayed in a Davenport–diagram (Fig. 3, Table 3), suggesting that buffering by extracellular proteins (1.2 ± 0.4 mg mL^{-1}, N=8 control mussels) is the sole mechanism to stabilize pH_e. The buffer value of the haemolymph is low (0.49 mM HCO_3^- pH^{-1}, Fig. 3), matching findings from other populations of the same species (Booth et al., 1984; Lindinger et al., 1984). Significant reductions in pH_e were found at 142 and 405 Pa (Table 3, Fig. 3A). No significant changes in the concentration of haemolymph Mg^{2+} and Ca^{2+} were observed with respect to treatment pCO_2 (Table 3). While it was proposed that mytilid mussels use HCO_3^- derived from their shells to buffer pH_e (Lindinger et al., 1984; Michaelidis et al., 2005), our results clearly demonstrate that in flow-through seawater experimental designs, *M. edulis* do not maintain extracellular [HCO_3^-] above that of ambient seawater. This is in contrast to the more active cephalopod molluscs, which greatly elevate extracellular [HCO_3^-] in order to stabilize pH_e to conserve haemocyanin blood oxygen transport (Gutowska et al., 2010). However, while *M. edulis* does not possess a pH sensitive respiratory pigment, uncompensated pH_e might negatively impact shell formation: comparing control extracellular pH of haemolymph drawn from the posterior adductor muscle with that of the extrapallial fluid (EPF), the fluid that fills the space between mantle and shell surface, indicates that both fluids are characterized by a very similar carbonate system speciation (Table 3B). Assuming that pH_e in the EPF always behaves like that of haemolymph, it is very likely that the inner shell layers (nacre), which primarily consist of aragonite, are in contact with a fluid that is highly under saturated with $CaCO_3$: haemolymph [CO_3^{2-}] is much lower than in seawater at any given seawater pCO_2 (see Figure 3B). As in addition, only 15% of total EPF [Ca^{2+}] has been found to be freely dissolved Ca^{2+} (Misogianes and Chasteen, 1979), Ω_{arag} would be even lower at the inner shell interface. Therefore, even under control conditions at high seawater pH, calcification proceeds in a

high pCO_2 compartment. This fact and the high measured Mg^{2+} concentrations in the EPF even accentuate the importance of a microenvironment at the side of calcification suitable to facilitate precipitation of calcium carbonate. Recent findings suggest that certain proteins excreted from mantle tissue are probably able to generate these conditions which are required for biomineralisation (Suzuki et al. 2009, Weiss 2010).

3.3 *M. edulis* growth and calcification (Exp. 2)

To estimate the long-term repercussions of decreased pH_e on the energy budget and the calcification machinery, we conducted a growth trial under optimized feeding conditions (Exp. 2). Previous studies suggested that in mytilid bivalves (*M. galloprovincialis)*, uncompensated reductions in pH_e may be causally related to reductions in metabolism (metabolic depression) and somatic growth (Michaelidis et al., 2005). In our 8 week growth study, shell length growth was high under control conditions (3.3 to 4.6 mm $month^{-1}$ in small vs. medium mussels), fully matching summer field growth rates for mussels of the same size classes in Kiel Fjord (Kossak, 2006). Initial mussel shell length and pCO_2 had significant effects on shell length growth and shell mass increment (see Table 4 for ANOVA results). While shell mass and length growth were similar in control and 142 Pa treated medium sized mussels, both parameters were significantly reduced at 405 Pa (Fig. 4A). In the smaller size group, length growth was significantly reduced at 405 Pa as well. There were no significant differences in shell mass growth in small mussels, although a trend towards lower shell mass was apparent in the 405 Pa group as well (Fig. 4B). However, when displaying shell mass vs. shell length in comparison to wild-type mussels collected from the sampling site in Kiel Fjord (grey symbols in Fig. 4A,B), it appears that all experimental groups lie within the 95% prediction band of the shell mass vs. length function. This indicates that exposure to elevated pCO_2 does not result in the production of a grossly abnormal, thinner shell phenotype; rather, shell growth is slowed proportionally. Regardless of the decreased rates of shell growth at higher pCO_2 (405 Pa), all treatment mussels increased their shell mass at least by 150% during the 8 week trial, even at Ω_{arag} (Ω_{calc}) as low as 0.17 (0.28) (Fig. 4E). This is in contrast to a previous study that has suggested a high sensitivity of mussel calcification to elevated pCO_2: during acute exposure, a linear correlation between $CaCO_3$ precipitation rate and seawater pCO_2 (and $[CO_3^{2-}]$) has been observed in *M. edulis* from the Western Scheldt. A reduction in calcification by about 50% was found at a pCO_2 of ca. 100 Pa (ca. 1000 µatm), net shell dissolution was observed at pCO_2 higher than ca. 180 Pa (ca. 1800 µatm, Gazeau et al., 2007). Clearly, acclimation, adaptation and food availability or quality could be responsible factors for the observed differences between both studies. Somatic growth was not significantly affected by pCO_2 in our experiment (Fig. 4F). This may primarily be due to high variability encountered between replicates, but also could point at a higher capacity for somatic growth vs. shell accretion under hypercapnic conditions. Findings pointing in this direction have recently been obtained for an echinoderm species, where somatic growth was up-regulated under acidified conditions while calcification was suppressed (Gooding et al., 2009).

3.4 *M. edulis* shell microstructure and morphology (Exp. 2)

SEM analyses of shell cross-sections from mussels with a similar final length from all growth trial treatments (Table 5), illustrates that there are no significant changes in calcite and aragonite layer

thickness in newly formed shell parts when pCO_2 is elevated. While calcite layer thickness is also comparable between 39 Pa and 405 Pa mussels, a significant decrease in the thickness of individual aragonite platelet layers, from 0.60 to 0.38 µm, was evident in the 405 Pa treatment. This indicates that high levels of acidification result in changes in shell microstructure that are not detected by simple shell mass vs. shell length regression analysis. As mentioned above, it needs to be emphasized that nacre (aragonite) platelet layers on the inner side of the shell (Fig. 4C) are in contact with an extrapallial fluid (EPF) that is most likely characterized by Ω_{arag} of <0.4 even under control conditions. Our shell microstructure analysis (Table 5) indicates that even at 405 Pa, the same number of aragonite platelets can be formed as in control animals of the same length. Thus, mussels must possess a powerful calcification machinery to construct and maintain shell integrity in an EPF that is highly under saturated with $CaCO_3$.

M. edulis seems to be well adapted to form shell material even under highly acidified conditions when the newly formed material is protected by an intact periostracum. However, fractures of the periostracum seem to be fairly common, even in control mussels and especially at the umbo region and other older parts of the shell (Fig 5). Mussels occur in dense beds in Kiel Fjord (see Fig 1D) and the umbo region is often in close contact to other mussels or the substrate. Friction in a wave swept environment then probably causes an abrasion of the organic cover. Such fractures can then act as nucleation sites for external shell dissolution. We found some degree of periostracum damage and / or shell dissolution at the umbo region in 58 out of 60 medium sized mussels analyzed from Exp. 2. Dissolution area was smallest (<2 mm^2) in control mussels and significantly increased at 142 and 405 Pa (Fig 6A). While shell damage was primarily restricted to periostracum abrasion in the control group (dissolution index = 1, Fig 5A), significantly more calcite dissolution was observed in the 405 Pa group (dissolution index = 3, Fig 5C, Fig. 6B). Dissolution spots (e.g. Fig 7) could be demonstrated in a range of mussels at 39, 142 and 405 Pa, mainly in old parts of the shell, indicating that periostracum damage and subsequent external dissolution also occurs in the natural habitat (Fig 7A-F). As we did not screen our experimental mussels for periostracum damage prior to the experiment incubation, it is difficult to assess the magnitude of shell dissolution during the incubation. In two mussels (one at 142 Pa, one at 405 Pa), dissolution spots could also be witnessed in newly formed shell parts (Fig.7C,G to I). It is unclear, whether elevated seawater pCO_2 itself can disrupt the protective function of the periostracum. Future studies need to take this possibility into consideration.

3.5 Conclusion

In summary, our laboratory studies demonstrate that calcification in this economically and ecologically important bivalve species can be maintained at control rates even when seawater Ω_{arag} is lower than 0.5 (pCO_2 142 Pa, 1400 µatm). 56 to 65% of control calcification rates can be obtained at a seawater pCO_2 of 405 Pa (4000 µatm), a pCO_2 that is twice as high as that producing zero calcification in an already mentioned acute study on a North Sea population (Gazeau et al., 2007). This could be due to physiological differences between North- and Baltic Sea populations of *M. edulis*; however, our and other studies indicate that it is more likely that long-term acclimation to elevated pCO_2 increases the

ability to calcify in *Mytilus* spp. (Michaelidis et al., 2005; Ries et al., 2009). We also show evidence that uncompensated extracellular pH at moderately elevated pCO_2 (142 Pa, 1400 µatm) does not significantly impair growth and calcification, suggesting that there is no causal relationship between acid-base status and metabolic depression in this species at levels of ocean acidification that can be expected in the next few hundred years (IPCC, 2007). Rather, we show in a companion study that moderate levels of acidification (pCO_2 113 to 240 Pa, 1120 to 2400 µatm) increase metabolic rates, potentially indicating increased costs for calcification and cellular homeostasis (Thomsen and Melzner, 2010).

While current levels of CO_2 enrichment may still permit the dominance of calcifying communities in habitats such as Kiel Fjord, future increases in pCO_2 could deplete their tolerance capacity: an increase in seawater pCO_2 from 39 to 78 Pa (385 to 770 µatm) due to future ocean acidification will elevate C_T by approximately 90 µmol kg^{-1} (i.e. at S = 20, A_T = 2060 µmol kg^{-1}, T = 20°C), but leave A_T unaffected. Simple model calculations illustrate, how additional increases in C_T due to respiration in deeper water masses and subsequent upwelling would affect the carbonate system speciation in Kiel Fjord (Fig. 1B): adding 100 µmol kg^{-1} of C_T to the values measured in 2008 and 2009 (see Table 1) and leaving A_T unaltered results in dramatic increases in pCO_2; Peak pCO_2 values would shift from ca. 230 to >440 Pa (>4300 µatm), average pCO_2 for the measurements in Table 1 would shift from ca. 104 Pa to 248 Pa (2450 µatm). As pCO_2 is generally highest in the summer months, mussel recruitment could be one of the first processes to be affected: Kurihara and colleagues (Kurihara et al. 2008a) demonstrated a high CO_2 sensitivity of larval *M. galloprovincialis*, with an increased prevalence of shell malformation at a pCO_2 of ca. 200 Pa (ca. 2000 µatm). Such values could be reached within the next decades in Kiel Bay (Fig. 1B). However, older mussels would probably be affected just as well: considering that abrasions of the periostracum are very common among *M. edulis* in Kiel Fjord, enhanced external shell dissolution may compromise fitness of older mussels during long-term exposure to seawater highly under saturated with $CaCO_3$ by negatively influencing shell stability. In addition, increased external shell dissolution might favour settlement of the shell boring polychaete *Polydora ciliata* which can more easily penetrate shell parts with damaged periostracum (Michaelis, 1978). *P. ciliata* boring may render mollusc shells more vulnerable to crab predation (Blöcher 2008). In addition, invasion of the extracellular space by microorganisms through minute shell fractures seems possible. Long-term experiments (>6 months) are necessary to test these hypotheses.

Coastal upwelling habitats such as Kiel Bay or the West coast of the United States (Feely et al., 2008) can be important ‘natural analogues’ to understand how ecosystems might be influenced by future ocean acidification. In contrast to a natural analogue study that shows a progressive displacement of calcifying organisms by photoautotrophic communities along a CO_2 gradient in the Mediterranean (Hall-Spencer et al., 2008), we show that communities dominated by calcifying invertebrates can thrive in CO_2 enriched (eutrophic, ‘energy dense’) coastal areas. However, such habitats, which are quite common along the world’s coasts (Diaz and Rosenberg, 2008), will be exposed to rates of change in seawater pCO_2 that go well beyond the worst scenarios predicted for surface oceans (Caldeira and Wickett, 2003).

4. Acknowledgements

The authors wish to thank Ulrike Panknin for culturing algae, supervising the long-term experiment, and laboratory work associated with this project, Hans-Ulrik Riisgard (University of Southern Denmark) for his suggestion on how to improve filtration efficiency and experimental design, Renate Schütt for marking mussels with $MnCl_2$ and carrying out the settlement plate work and Susann Grobe for carbonate chemistry analysis. This study was funded by DFG Excellence Cluster 'Future ocean' grants to AK, FM and MW, This work is a
contribution to the German Ministry of Education and Research (BMBF) funded project ''Biological Impacts of Ocean ACIDification''(BIOACID) subproject 3.1.3 awarded to FM and MAG and is a contribution to the ''European Project on Ocean Acidification'' (EPOCA) that received funding from the European Community's Seventh Framework Programme (FP7/2007 to 2013) under grant agreement no 211384.

5. References

Albers, C., and Pleschka, K.: Effect of temperature on CO_2 transport in elasmobranch blood., Respiration Physiology, 2, 261-273, 1967.

Barbin, V., Ramseyer, K., and Elfman, M.: Biological record of added manganese in seawater: a new efficient tool to mark in vivo growth lines in the oyster species *Crassostrea gigas*, Int J Earth Sci, 97, 193-199, 2008.

Blöcher, N.: Ökologische und biologische Aspekte des *Polydora ciliata*- Aufwuchses auf *Littorina littorea*. MSc Thesis, University of Kiel, 2008

Booth, C. E., McDonald, D. G., and Walsh, P. J.: Acid-base-balance in the sea mussel, *Mytilus-edulis* .1. Effects of hypoxia and air-exposure on hemolymph acid-base status, Marine Biology Letters, 5, 347-358, 1984.

Bradford, M. M.: Rapid and sensitive method for quantitation of microgram quantities of protein utilizing principle of protein-dye binding, Analytical Biochemistry, 72, 248-254, 1976.

Caldeira, K., and Wickett, M. E.: Anthropogenic carbon and ocean pH, Nature, 425, 365-365, 2003.

Diaz, R. J., and Rosenberg, R.: Spreading dead zones and consequences for marine ecosystems, Science, 321, 926-929, 2008.

Dickson, A. G., and Millero, F. J.: A comparison of the equilibrium-constants for the dissociation of carbonic-acid in seawater media, Deep-Sea Research Part a-Oceanographic Research Papers, 34, 1733-1743, 1987.

Dickson, A. G.: Standard potential of the reaction - $AgCl_S$+1/2 H_2 = Ag_S+HCl_{Aq} and the standard acidity constant of the ion HSO_4- in synthetic sea-water from 273.15-K to 318.15-K, Journal of Chemical Thermodynamics, 22, 113-127, 1990.

Dickson, A. G., Afghan, J. D., and Anderson, G. C.: Reference materials for oceanic CO_2 analysis: a method for the certification of total alkalinity, Marine Chemistry, 80, 185-197, 2003.

Dickson, A. G., Sabine, C. L., and Christian, J. R.: Guide to best practices for ocean CO_2 measurements PICES Special Publications 191 pp., 2007.

Dupont, S., Havenhand, J., Thorndyke, W., Peck, L., and Thorndyke, M.: Near-future level of CO_2-driven ocean acidification radically affects larval survival and development in the brittlestar *Ophiothrix fragilis*, Mar Ecol-Prog Ser, 373, 285-294, 2008.

Dürr, S., and Wahl, M.: Isolated and combined impacts of blue mussels (*Mytilus edulis*) and barnacles (*Balanus improvisus*) on structure and diversity of a fouling community, Journal of Experimental Marine Biology and Ecology, 306, 181-195, 2004.

Enderlein, P., and Wahl, M.: Dominance of blue mussels versus consumer-mediated enhancement of benthic diversity, Journal of Sea Research, 51, 145-155, 2004.

Fabry, V. J., Seibel, B. A., Feely, R. A., and Orr, J. C.: Impacts of ocean acidification on marine fauna and ecosystem processes, Ices Journal of Marine Science, 65, 414-432, 2008.

Feely, R. A., Sabine, C. L., Hernandez-Ayon, J. M., Ianson, D., and Hales, B.: Evidence for upwelling of corrosive "acidified" water onto the continental shelf, Science, 320, 1490-1492, 2008.

Gazeau, F., Quiblier, C., Jansen, J. M., Gattuso, J. P., Middelburg, J. J., and Heip, C. H. R.: Impact of elevated CO_2 on shellfish calcification, Geophysical Research Letters, 34, 2007.

Gooding, R. A., Harley, C. D. G., and Tang, E.: Elevated water temperature and carbon dioxide concentration increase the growth of a keystone echinoderm, Proceedings of the National Academy of Sciences of the United States of America, 106, 9316-9321, 2009.

Gutowska, M. A., and Melzner, F.: Abiotic conditions in cephalopod (*Sepia officinalis*) eggs: embryonic development at low pH and high pCO_2, Marine Biology, 156, 515-519, 2009.

Gutowska, M. A., Melzner, F., Langenbuch, M., Bock, C., Claireaux, G., and Portner, H. O.: Acid-base regulatory ability of the cephalopod (*Sepia officinalis*) in response to environmental hypercapnia, J Comp Physiol B, 180, 323-335, 2010.

Hall-Spencer, J. M., Rodolfo-Metalpa, R., Martin, S., Ransome, E., Fine, M., Turner, S. M., Rowley, S. J., Tedesco, D., and Buia, M. C.: Volcanic carbon dioxide vents show ecosystem effects of ocean acidification, Nature, 454, 96-99, 2008.

Hansen, H. P., Giesenhagen, H. C., and Behrends, G.: Seasonal and long-term control of bottom-water oxygen deficiency in a stratified shallow-water coastal system, Ices Journal of Marine Science, 56, 65-71, 1999.

IPCC: Climate Change (2007) The Physical Science Basis. Contribution of Working Group I to the Fourth Assessment Report of the Intergovernmental Panel on Climate Change, Cambridge University Press, Cambridge, United Kingdom and New York, NY, USA..

Ismar, S. M. H., Hansen, T., and Sommer, U.: Effect of food concentration and type of diet on *Acartia* survival and naupliar development, Marine Biology, 154, 335-343, 2008.

Kossak, U.: How climate change translates into ecological change: Impacts of warming and desalination on prey properties and predator-prey interactions in the Baltic Sea, Ph.D. dissertation, IFM-GEOMAR, Christian-Albrechts-Universität, Kiel, 97 pp., 2006.

Kurihara, H.: Effects of CO_2-driven ocean acidification on the early developmental stages of invertebrates, Mar Ecol-Prog Ser, 373, 275-284, 2008.

Kurihara, H., Asai, T., Kato, S., and Ishimatsu, A.: Effects of elevated pCO_2 on early development in the mussel Mytilus galloprovincialis, Aquatic Biology, 4, 225-233, 2009.

Lehmann, A., Krauss, W., and Hinrichsen, H. H.: Effects of remote and local atmospheric forcing on circulation and upwelling in the Baltic Sea, Tellus A, 54, 299-316, 2002.

Lindinger, M. I., Lauren, D. J., and McDonald, D. G.: Acid-base-balance in the sea mussel, *Mytilus edulis*. 3. Effects of environmental hypercapnia on intracellular and extracellular acid-base-balance, Marine Biology Letters, 5, 371-381, 1984.

Mehrbach, C., Culberso, C. H., Hawley, J. E., and Pytkowic, R. M.: Measurement of apparent dissociation-constants of carbonic-acid in seawater at atmospheric-pressure, Limnology and Oceanography, 18, 897-907, 1973.

Melzner, F., Gutowska, M. A., Langenbuch, M., Dupont, S., Lucassen, M., Thorndyke, M. C., Bleich, M., and Portner, H. O.: Physiological basis for high CO2 tolerance in marine ectothermic animals: pre-adaptation through lifestyle and ontogeny?, Biogeosciences, 6, 2313-2331, 2009.

Michaelidis, B., Ouzounis, C., Paleras, A., and Pörtner, H. O.: Effects of long-term moderate hypercapnia on acid-base balance and growth rate in marine mussels *Mytilus galloprovincialis*, Mar Ecol-Prog Ser, 293, 109-118, 2005.

Michaelis, M.: Zur Morphologie und Ökologie von *Polydora ciliata* und *P. ligni* (Polychaeta, Spionidae), Helgoländer wiss. Meeresunters., 31, 102-116, 1978.

Mintrop, L., Perez, F. F., Gonzalez-Davila, M., Santana-Casiano, M. J., and Körtzinger, A.: Alkalinity determination by potentiometry: Intercalibration using three different methods, Ciencias Marinas, 26, 23-37, 2000.

Misogianes, M. J., and Chasteen, N. D.: Chemical and Spectral Characterization of the Extrapallial Fluid of Mytilus-Edulis, Analytical Biochemistry, 100, 324-334, 1979.

Pörtner, H. O., Langenbuch, M., and Reipschläger, A.: Biological impact of elevated ocean CO_2 concentrations: Lessons from animal physiology and earth history, Journal of Oceanography, 60, 705-718, 2004.

Reusch, T. B. H., and Chapman, A. R. O.: Persistence and space occupancy by subtidal blue mussel patches, Ecological Monographs, 67, 65-87, 1997.

Ries, J. B., Cohen, A. L., and McCorkle, D. C.: Marine calcifiers exhibit mixed responses to CO_2-induced ocean acidification, Geology, 37, 1131-1134, 2009.

Riisgard, H. U., Kittner, C., and Seerup, D. F.: Regulation of opening state and filtration rate in filter-feeding bivalves (*Cardium edule*, *Mytilus edulis*, *Mya arenaria*) in response to low algal concentration, Journal of Experimental Marine Biology and Ecology, 284, 105-127, 2003.

Roy, R. N., Roy, L. N., Vogel, K. M., Porter-Moore, C., Pearson, T., Good, C. E., Millero, F. J., and Campbell, D. M.: The dissociation constants of carbonic acid in seawater at salinities 5 to 45 and temperatures 0 to 45° C, Marine Chemistry, 44, 249-267, 1993.

Thomsen, J., and Melzner, F.: Seawater acidification does not elicit metabolic depression in the blue mussel *Mytilus edulis*, Marine Biology, submitted, 2010.

Weiss, R. F.: Carbon dioxide in water and seawater: the solubility of a non-ideal gas, Marine Chemistry, 2, 203-215, 1974.

Yin, Y., Huang, J., Paine, M. L., Reinhold, V. N., and Chasteen, N. D.: Structural characterization of the major extrapallial fluid protein of the mollusc *Mytilus edulis*: Implications for functions, Biochemistry, 44, 10720-10731, 2005.

Figure legends

Figure 1: (A) Surface pH_{NBS} in Kiel Fjord at the site of the experimental mussel population (54°19.8'N; 10°9.0'E) in 2008 and 2009. Stars and numbers indicate dates for which accurate determinations of total alkalinity (A_T) and dissolved inorganic carbon (C_T) are available, see Table 1. (B) Kiel Fjord pCO_2 replotted from Table 1, and calculated after addition of 50 (2) and 100 (3) µmol kg^{-1} of C_T to C_T from Table 1. A doubling in surface pCO_2 will result in an increase in C_T by about 90 µmol kg^{-1} in this habitat, see text (C) Settlement of marine invertebrates on vertically suspended PVC plates. Plates (N = 3 each) were exchanged monthly and aufwuchs was quantified. (D) Image of typical vertical hard substrate in Kiel Fjord dominated by calcifying communities.

Figure 2: Manganese marks in the calcite of the shell of a wild *Mytilus edulis* from Kiel Fjord illustrating weekly shell length growth between 07.02.2007 (line 1) and 05.04.2008 (line 9). Shell $[Mn^{2+}]$ in arbitrary units (a.u.).

Figure 3 (Exp. 1): (A) haemolymph acid-base status in relation to environmental pCO_2 (Davenport-diagram) for treatment groups under pCO_2 levels of 39 Pa (ca. 385 µatm, N = 12), 142 Pa (ca. 1400 µatm, N = 12) and 405 Pa (ca. 4000 µatm, N = 6). Isobars represent haemolymph pCO_2. NBB = non - bicarbonate buffer line. Mussels cannot significantly elevate $[HCO_3^-]$ to compensate pH_e. See also Table 4 A for ANOVA tables; (B) Calculated haemolymph $[CO_3^{2-}]$ at seawater pCO_2 values of 39, 142 and 405 Pa (385, 1400, 4000 µatm). Black lines indicate seawater $[CO_3^{2-}]$ and the corresponding $CaCO_3$ saturation state (Ω_{arag}).

Figure 4 (Exp. 2): (A) and (B): Shell mass vs. shell length relationships of small and medium experimental mussels at the beginning of the experiment (black) and after 8 weeks (red, orange, green; means and standard deviation). The grey symbols represent individual mussels from the collection site, the dashed line gives the 95% prediction interval for the shell mass vs. length relationship of wild mussels. (C): SEM cross-section of *M. edulis* shell (detail), showing calcite (C) and aragonite (A) layers. Aragonite layers are in direct contact with the extrapallial fluid (EPF, E). Scale bar = 10 µm. (D), (E), (F): Percent shell mass and length, as well as somatic (dry mass) growth over the entire 8 week period. See Table 5 for ANOVA tables.

Figure 5 (Exp. 2): External shell dissolution at the umbo region. Images of umbones of medium sized shells taken under reflected (A, C, E) and transmitted (B, D, F) illumination to quantify shell dissolution area and severity. In D and F, dissolution spots are visible as darker regions, as corroded shell material blocks the light stronger than intact crystal structures. (A and D) 39 Pa (385 µatm), dissolution index = 1, (B and E) 142 Pa (1400 µatm), dissolution index = 2, (C and F) 405 Pa (4000 µatm), dissolution index = 3; scale bars = 2.5 mm.

Figure 6 (Exp. 2): (A) shell dissolution area at the umbo region (mm^2) of medium sized mussels, (B) shell dissolution index; N = 20 mussels randomly chosen from the 4 replicate treatments, asterisks indicate significant differences from control (39 Pa, 385 µatm) using Dunn's test. See table 5 for Kruskal-Wallis test results.

Figure 7 (Exp. 2): Example of a medium sized mussel (405 Pa, 4000 µatm) with dissolution spots on old and newly formed parts of the shell. (A, B, C) overview, reflected light (A), transmission light (B), position of close-up areas 1 and 2 (C) which are depicted in (D-I). Close up area 1 (D to F) is located on pre-experimental shell parts (black trace in C indicates the size of the mussel at the start of the experiment), close-up area 2 (G to I) on newly formed shell material. D and G are reflected light pictures, E and H are transmission images, F and I combined reflected and transmission images. White spots are corroded calcite material that is visible when the periostracum is fractured. These spots appear dark when viewed under transmission light. Scale bars: A to C: 5 mm, D to F: 1 mm, G to I: 0.5 mm.

Table legends

Table 1: Kiel Fjord surface seawater carbonate system speciation 2008 to 2009. Total alkalinity (A_T) and dissolved inorganic carbon (C_T) were measured by potentiometric titration using the VINDTA system and coulometric titration after CO_2 extration using the SOMMA system. Carbonate system speciation was calculated using the CO2SYS program. See Fig. 1A for corresponding surface pH_{NBS}.

Table 2: Seawater carbonate system speciation during experimental trials (mean ± SD, 14 and 3 determinations for pH, S, T and A_T, C_T). Salinity (S) was 11.8 ± 0.4 and temperature (T) 12.5°C ± 0.5°C in Exp. 1 (duration 2 weeks), S = 15.0 ± 0.6 and T = 13.8°C ± 0.6°C in Exp. 2 (duration: 8 weeks).

Table 3: (A) Exp.1 haemolymph acid-base status and ion concentrations of large mussels in relation to treatment pCO_2. Significant differences from control (39 Pa, 385 µatm treatment) in bold, mean values ± SD. (B) Haemolymph (HL) vs. extrapallial fluid (EPF) acid-base status in 11 mussels sampled from Kiel Fjord at an ambient seawater pCO_2 of ca. 50 Pa (ca. 500 µatm) (30.08.2010) at T = 15.7°C, S = 14.6, pH_{NBS} = 8.04.

Table 4: ANOVA results. (A) Exp. 1: One-factorial ANOVAs for extracellular acidbase and ion status of large mussels (factor: seawater pCO_2, $pCO_{2\,sw}$). Significant Post-hoc tests ($p<0.05$, Tukey HSD) indicated in the manuscript figures and tables. Six seawater *p*CO2 levels (39 to 405 Pa / 385 to 4000 µatm), N = 12 replicates for 39 to 142 Pa, N = 6 replicates for 405 Pa. (B) Exp. 2: Two-factorial ANOVAs for shell and somatic growth (factors: seawater pCO_2 and initial size). Significant Post-hoc tests ($p<0.05$, Tukey HSD) indicated in the manuscript figures and tables. Three seawater pCO_2 levels (39, 142 and 405 Pa / 385, 1400 and 4000 µatm) and two size classes (small, medium), N = 4 replicate aquaria for each treatment. (C) Exp. 2: One-factorial ANOVAs for shell microstructure (SEM) analysis of medium sized mussels (factor: seawater pCO_2, pCO_2sw). Significant Post-hoc tests ($p<0.05$, Tukey HSD) indicated in the manuscript. Three seawater pCO_2 levels (39, 142, 405 Pa), N = 5 replicate mussels analyzed. (D) Exp. 2: Kruskal-Wallis test results for comparison of shell dissolution area at the umbo and shell dissolution severity at the umbo vs. pCO_2 (39, 142, 405 Pa), N = 20 replicate medium sized mussels analyzed. Significant Dunn's multiple comparison tests are indicated in Fig. 6.

Table 5 (Exp. 2): Shell microstructure analysis using SEM. N = 5 mussels of similar final length (medium size) were cross sectioned at 75 and 95% shell length. Mean values ± SD, significant differences from control (39 Pa, 385 µatm) in bold. Both cross sections are located in parts of the shell that have been newly formed during the experimental incubation.

Figure 1

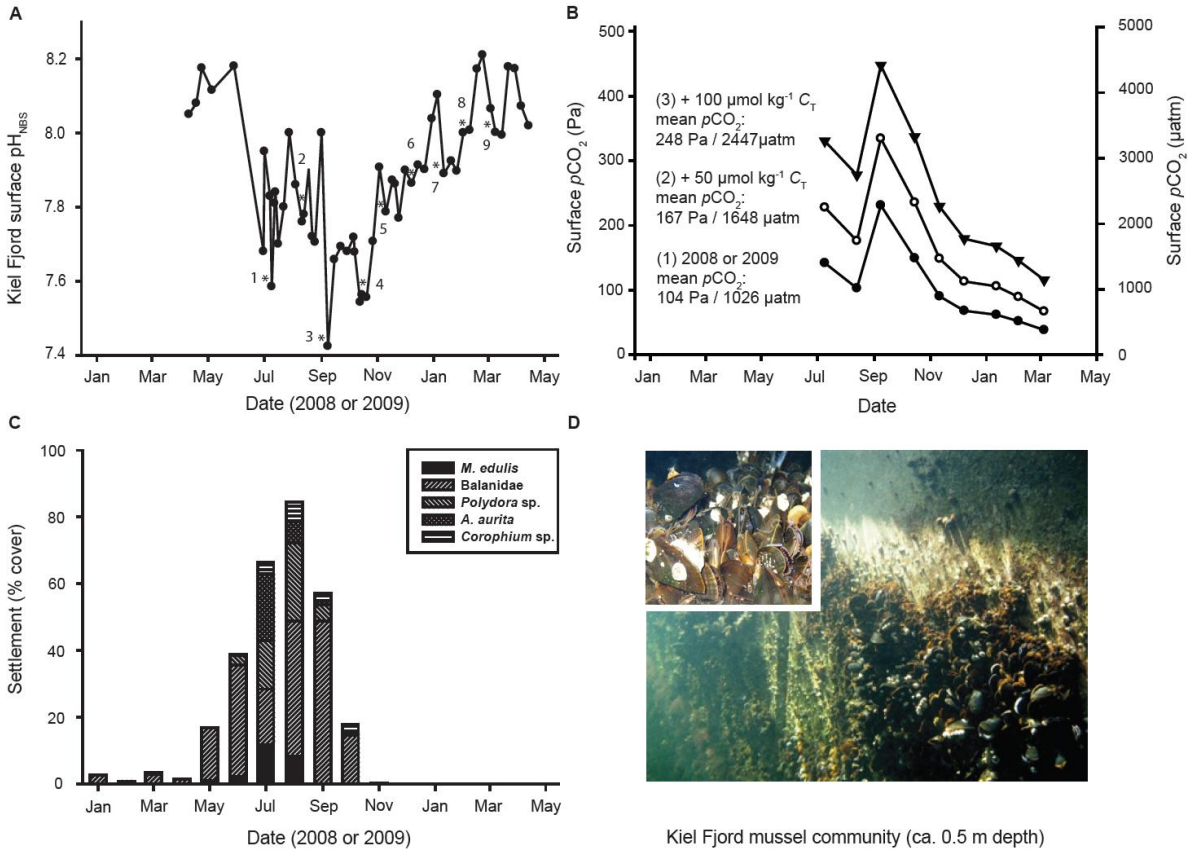
A
Kiel Fjord surface pH$_{NBS}$
8.2
8.0
7.8
7.6
7.4
Jan Mar May Jul Sep Nov Jan Mar May
Date (2008 or 2009)
1
2
3
4
5
6
7
8
9
B
Surface pCO_2 (Pa)
500
400
300
200
100
0
5000
4000
3000
2000
1000
0
Surface pCO_2 (µatm)
(3) + 100 µmol kg^{-1} C_T
mean pCO_2:
248 Pa / 2447µatm
(2) + 50 µmol kg^{-1} C_T
mean pCO_2:
167 Pa / 1648 µatm
(1) 2008 or 2009
mean pCO_2:
104 Pa / 1026 µatm
Jan Mar May Jul Sep Nov Jan Mar May
Date
C
Settlement (% cover)
100
80
60
40
20
0
M. edulis
Balanidae
Polydora sp.
A. aurita
Corophium sp.
Jan Mar May Jul Sep Nov Jan Mar May
Date (2008 or 2009)
D
Kiel Fjord mussel community (ca. 0.5 m depth)

Figure 2

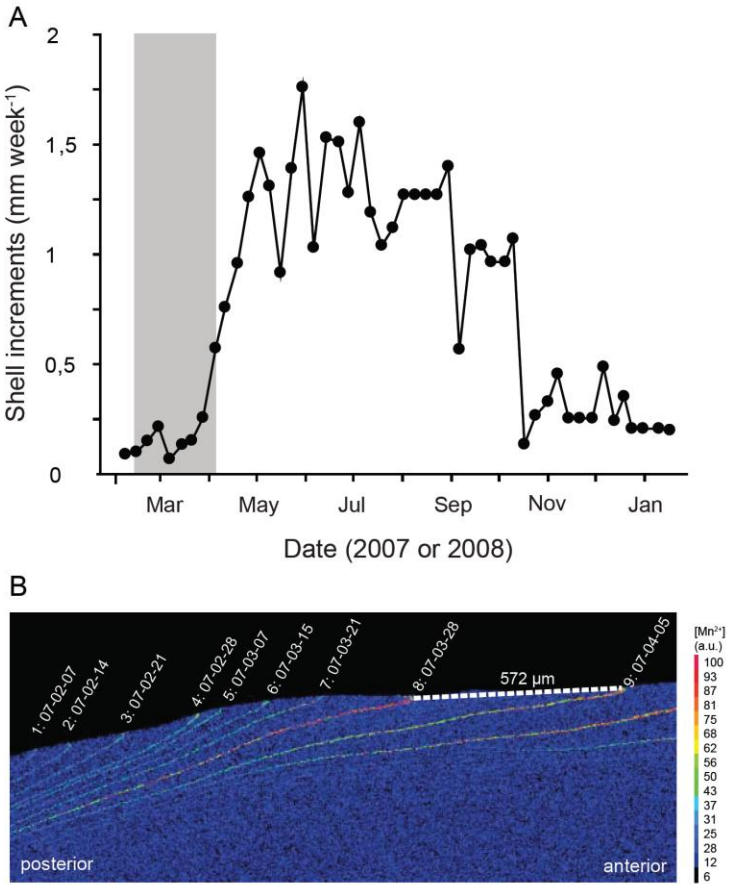
A
Shell increments (mm week-1)
2
1,5
1
0,5
0
Mar
May
Jul
Sep
Nov
Jan
Date (2007 or 2008)
B
1: 07-02-07
2: 07-02-14
3: 07-02-21
4: 07-02-28
5: 07-03-07
6: 07-03-15
7: 07-03-21
8: 07-03-28
572 µm
9: 07-04-05
posterior
anterior
[Mn2+] (a.u.)
100
93
87
81
75
68
62
56
50
43
37
31
25
28
12
6

Figure 3

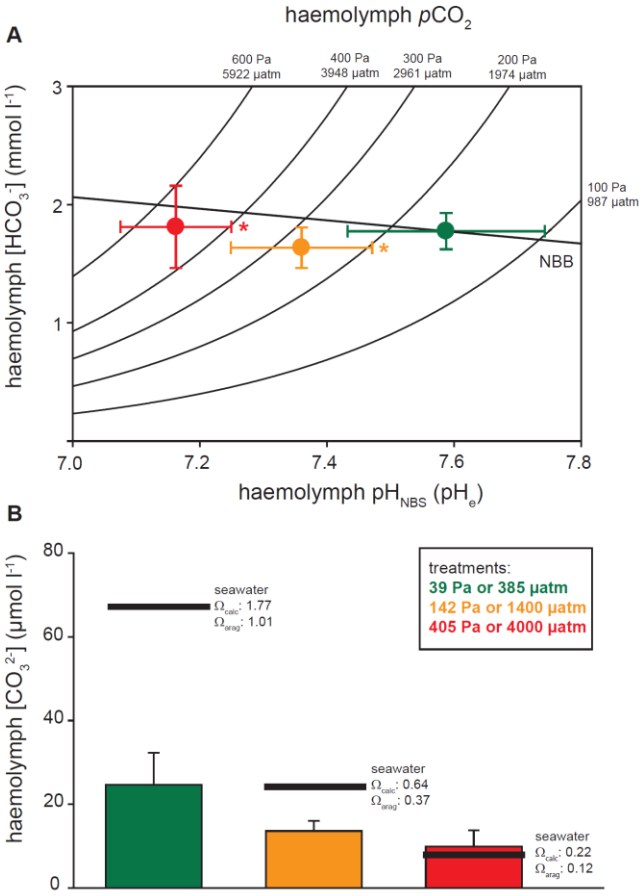
A
haemolymph pCO_2
600 Pa
5922 µatm
400 Pa
3948 µatm
300 Pa
2961 µatm
200 Pa
1974 µatm
100 Pa
987 µatm
NBB
haemolymph $[HCO_3^-]$ (mmol l^{-1})
haemolymph pH_{NBS} (pH_e)
B
haemolymph $[CO_3^{2-}]$ (µmol l^{-1})
seawater
Ω_{calc}: 1.77
Ω_{arag}: 1.01
treatments:
39 Pa or 385 µatm
142 Pa or 1400 µatm
405 Pa or 4000 µatm
seawater
Ω_{calc}: 0.64
Ω_{arag}: 0.37
seawater
Ω_{calc}: 0.22
Ω_{arag}: 0.12

Figure 4

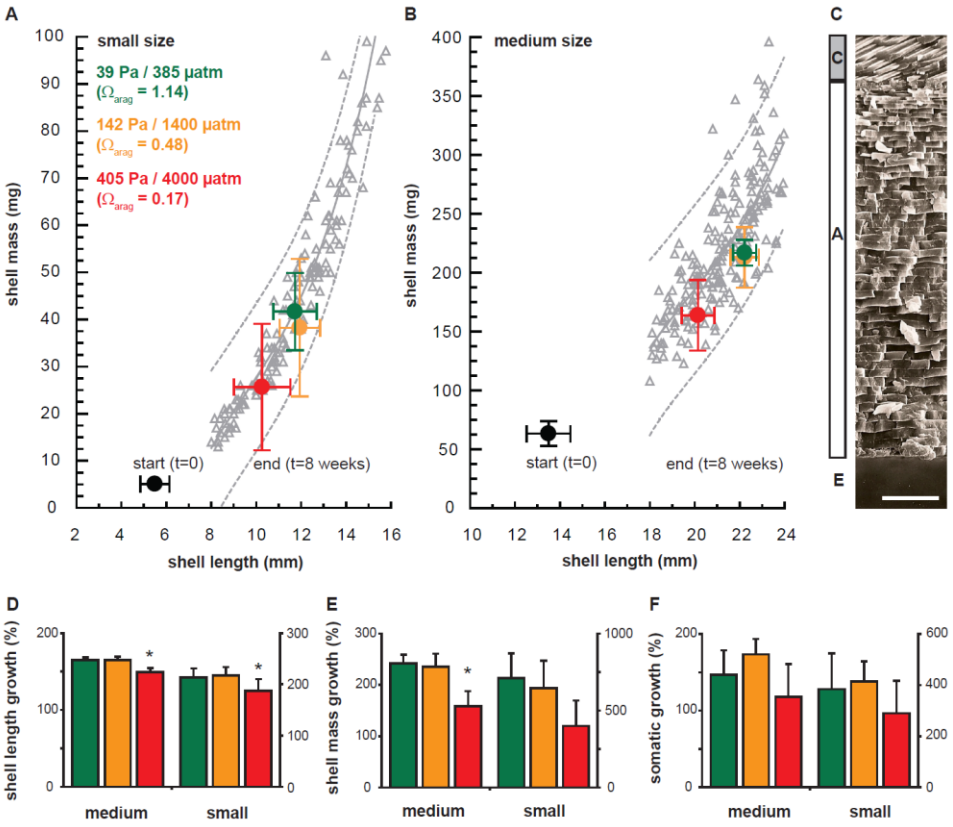
A
small size
39 Pa / 385 µatm
(Ωarag = 1.14)
142 Pa / 1400 µatm
(Ωarag = 0.48)
405 Pa / 4000 µatm
(Ωarag = 0.17)
shell mass (mg)
shell length (mm)
start (t=0)
end (t=8 weeks)
B
medium size
shell mass (mg)
shell length (mm)
start (t=0)
end (t=8 weeks)
C
C
A
E
D
shell length growth (%)
medium
small
E
shell mass growth (%)
medium
small
F
somatic growth (%)
medium
small

Figure 5

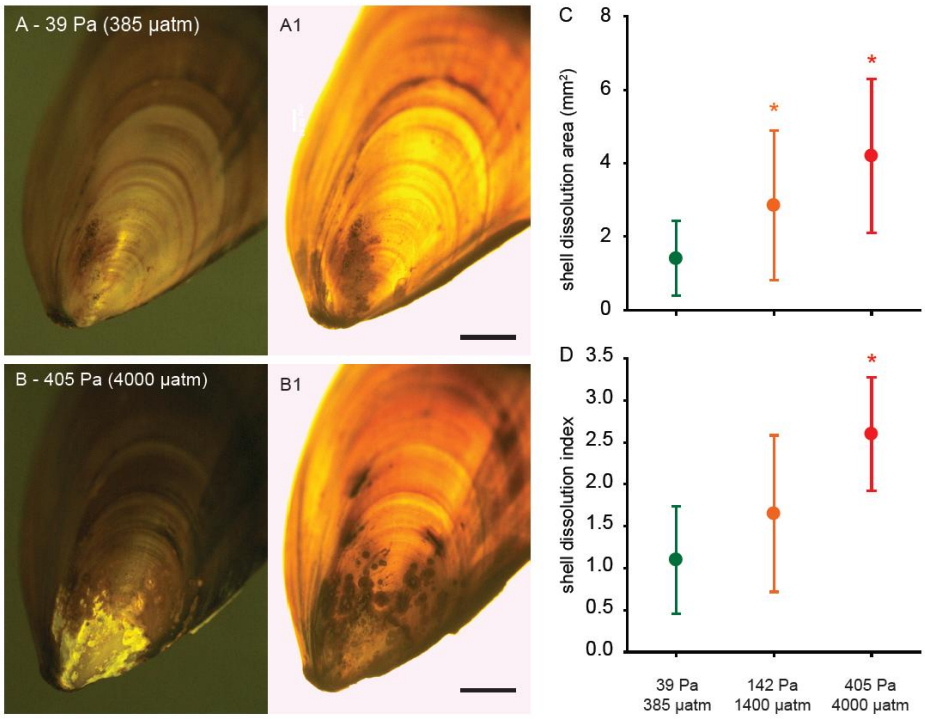
A - 39 Pa (385 µatm)
A1
B - 405 Pa (4000 µatm)
B1
C
shell dissolution area (mm²)
0
2
4
6
8
*
*
D
shell dissolution index
0.0
0.5
1.0
1.5
2.0
2.5
3.0
3.5
*
39 Pa
385 µatm
142 Pa
1400 µatm
405 Pa
4000 µatm

Figure 6

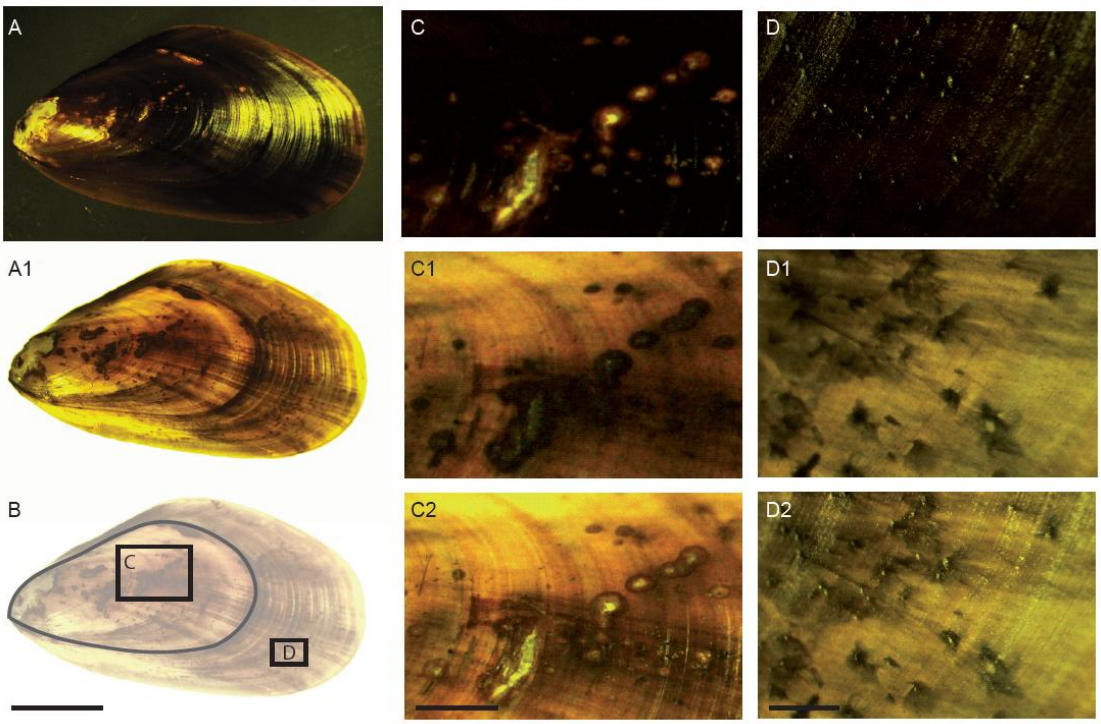

Table 1: Kiel Fjord surface seawater carbonate system speciation 2008/2009

#	Date	S	T (°C)	pH_{NBS}	A_T (µmol kg^{-1})	C_T (µmol kg^{-1})	pCO_2 (Pa)	pCO_2 (µatm)	Ω_{calc}	Ω_{arag}
1	09.07.2008	17	14.6	7.68	1955.2	1973.1	143	1411	0.79	0.47
2	13.08.2008	16	18.7	7.83	1913.7	1891.5	104	1026	1.21	0.72
3	08.09.2008	19	15.5	7.49	2044.9	2106.3	234	2309	0.58	0.35
4	15.10.2008	17	14.1	7.67	2018.4	2041.3	150	1480	0.79	0.47
5	11.11.2008	22	11.5	7.86	2063.3	2037.2	91	898	1.22	0.74
6	08.12.2008	20	7.1	7.98	2123.7	2088.2	68	671	1.34	0.8
7	12.01.2009	18	3.9	8.01	2078.3	2053.0	62	612	1.18	0.69
8	05.02.2009	17	3.3	8.10	2113.2	2075.3	52	513	1.36	0.79
9	05.03.2009	15	3.5	8.23	2067.7	2008.3	39	385	1.67	0.96

Table 2: Seawater carbonate system speciation during experimental trials.

Exp. 1:							
Treatment	**pH_{NBS}**	**A_T (µmol kg^{-1})**	**C_T (µmol kg^{-1})**	**pCO_2 (Pa)**	**pCO_2 (µatm)**	**Ω_{calc}**	**Ω_{arag}**
39 Pa / 385 µatm	8.05 ±0.03	1901.4 ±42.2	1841.5 ±36.2	47 ±2	464 ±20	1.77 ±0.13	1.01 ±0.08
57 Pa / 560 µatm	7.89 ±0.04	1903.5 ±40.8	1873.5 ±31.3	67 ±5	661 ±49	1.31 ±0.16	0.75 ±0.09
85 Pa / 840 µatm	7.81 ±0.03	1905.6 ±40.3	1891.8 ±34.7	80 ±3	789 ±30	1.09 ±0.09	0.62 ±0.05
113 Pa / 1120 µatm	7.70 ±0.03	1906.2 ±38.9	1914.3 ±34.1	106 ±5	1046 ±49	0.86 ±0.07	0.49 ±0.04
142 Pa / 1400 µatm	7.56 ±0.06	1906.1 ±39.3	1943.9 ±53.7	150 ±31	1480 ±306	0.64 ±0.09	0.37 ±0.05
405 Pa / 4000 µatm	7.08 ±0.02	1890.8 ±25.1	2077.5 ±12.0	431 ±35	4254 ±345	0.22 ±0.01	0.12 ±0.01
Exp.: 2							
Treatment	**pH_{NBS}**	**A_T (µmol kg^{-1})**	**C_T (µmol kg^{-1})**	**pCO_2 (Pa)**	**pCO_2 (µatm)**	**Ω_{calc}**	**Ω_{arag}**
39 Pa / 385 µatm	8.13 ±0.02	1966.1 ±3.2	1891.2 ±5.3	50 ±3	493 ±29	1.94 ±0.04	1.14 ±0.04
142 Pa / 1400 µatm	7.72 ±0.06	1968.1 ± 4.9	1984.4 ±12.3	135 ±20	1332 ±197	0.81 ±0.09	0.48 ±0.06
405 Pa / 4000 µatm	7.26 ±0.04	1970.2 ±4.3	2125.8 ±12.6	395 ±22	3898 ±217	0.28 ±0.02	0.17 ±0.01

Table 3 (Exp. 1): extracellular acid-base and ion status in haemolymph (HL) and extrapallial fluid (EPF).

a) experimental animal haemolymph acid-base status

Treatment (Pa / µatm)	pH_{NBS}	$[HCO_3^-]$ (mmol l^{-1})	$[CO_3^{2-}]e$ (µmol l^{-1})	pCO_2e (Pa)	pCO_2e (µatm)	$[Na^+]e$ % of SW	$[K^+]e$ % of SW	$[Mg^{2+}]e$ % of SW	$[Ca^{2+}]e$ % of SW
39 Pa / 385 µatm	7.59 ±0.16	1.77 ±0.15	24.6 ±7.6	169.7 ±76.7	1675 ±757	100.9 ±1.9	128.9 ±15.2	104.4 ±2.0	110.5 ±6.7
57 Pa / 560 µatm	7.53 ±0.15	1.78 ±0.13	22.4 ±7.4	171.8 ±90.6	1694 ±894	99.4 ±4.4	117.0 ±10.3	102.0 ±6.2	103.6 ±5.7
85 Pa / 840 µatm	7.54 ±0.17	1.61 ±0.13	20.5 ±8.7	175.3 ±78.9	1730 ±779	103.3 ±5.9	120.7 ±18.2	105.9 ±6.0	109.1 ±8.4
113 Pa / 1120 µatm	7.43 ±0.12	1.79 ±0.30	18.0 ±8.0	243.6 ±75.1	2404 ±741	102.5 ±2.7	130.4 ±7.3	102.7 ±5.4	106.3 ±5.4
142 Pa / 1400 µatm	**7.36** **±0.11**	1.64 ±0.17	**13.6** **±2.4**	272.0 ±99.3	2684 ±980	102.9 ±2.4	130.4 ±25.9	103.6 ±5.4	110.3 ±4.2
405 Pa / 4000 µatm	**7.16** **±0.09**	1.81 ±0.35	**9.8** **±3.9**	**496.0** **±31.8**	**4895** **±314**	**108.2** **±1.3**	134.8 ±11.5	108.2 ±1.2	113.1 ±2.6

b) haemolymph (HL) vs. extrapallial fluid (EPF) acid-base status

Fluid	pH_{NBS}	$[HCO_3^-]$ (mmol l^{-1})	$[CO_3^{2-}]e$ (µmol l^{-1})	pCO_2e (Pa)	pCO_2e (µatm)
HL	7.59 ±0.05	1.74 ±0.20	30.9 ±6.6	152.7 ±23.2	1506.7 ±228.9
EPF	7.54 ±0.10	1.80 ±0.16	29 ±7.0	183.4 ±52.1	1809.8 ±513.9

Table 4: ANOVA and Kruskal-Wallis test results

A) Extracellular acid-base and ion status (Exp. 1)

	Factor	F	p
Extracellular pH	pCO_2 sw	$F_{(5,56)}$=172494	**<0.001**
Extracellular [HCO_3^-]	pCO_2 sw	$F_{(5,54)}$=1.80	>0.12
Extracellular [CO_3^{2-}]	pCO_2 sw	$F_{(5,53)}$=4.366	<**0.003**
Extracellular pCO_2	pCO_2 sw	$F_{(5,54)}$=16.6874	**<0.001**
Extracellular [K^+]	pCO_2 sw	$F_{(5,55)}$=1.67	>0.15
Extracellular [Na^+]	pCO_2 sw	$F_{(5,56)}$=5.01	**<0.001**
Extracellular [Ca^{2+}]	pCO_2 sw	$F_{(5,56)}$=2.28	>0.05
Extracellular [Mg^{2+}]	pCO_2 sw	$F_{(5,56)}$=1.97	>0.09

B) Shell and somatic growth (Exp. 2)

a) shell length growth vs. seawater pCO_2 (pCO_2 sw) and initial size (size)

	SS	Degr. Of Freedom	MS	F	p
Intercept	6.436.372	1	6.436.372	7.864.467	0.0000
size	636.529	1	636.529	777.761	**0.0000**
pCO_2 sw	16.563	2	8.281	10.119	**0.001135**
size * pCO_2 sw	0.541	2	0.271	0.331	0.722615
Error	14.731	18	0.818		

b) dry mass growth vs. seawater pCO_2 (pCO_2 sw) and initial size (size)

	SS	Degr. Of Freedom	MS	F	p
Intercept	7.465.653	1	7.465.653	8.174.232	0.0000
size	3.838.226	1	3.838.226	4.202.520	**0.0000**
pCO_2 sw	63.247	2	31.624	34.625	0.053424
size * pCO_2 sw	32.676	2	16.338	17.889	0.195616
Error	164.397	18	9.133		

c) shell mass growth vs. seawater pCO_2 (pCO_2 sw) and initial size (size)

	SS	Degr. Of Freedom	MS	F	p
Intercept	323798.4	1	323798.4	1.996.641	0.0000
size	160413	1	160413	989.156	**0.0000**
pCO_2 sw	5566.3	2	2783.1	17.162	**0.000067**
size * pCO_2 sw	1930.4	2	965.2	5.952	**0.010375**
Error	2919.1	18	162.2		

C) Shell microstructure (SEM) analysis (Exp. 2)

	Factor	F	p
Initial shell length	pCO_2 sw	$F_{(2,12)}$=2.90	>0.09
Final shell length	pCO_2 sw	$F_{(2,12)}$=0.10	>0.93
95% shell length: calcite thickness	pCO_2 sw	$F_{(2,12)}$=0.85	>0.44
75% shell length: calcite thickness	pCO_2 sw	$F_{(2,12)}$=1.45	>0.27
75% shell length: aragonite thickness	pCO_2 sw	$F_{(2,12)}$=0.35	>0.70
75% shell length: number of aragonite layers	pCO_2 sw	$F_{(2,12)}$=0.10	>0.91
75% shell length: thickness of aragonite layers	pCO_2 sw	$F_{(2,12)}$=56.8	**<0.02**

D) Shell dissolution analysis (Exp. 2)

a) dissolution area at umbo vs. pCO_2

group	N mussels	Sum of ranks	Mean of ranks
39 Pa	20	35.5	1.8
142 Pa	20	64.6	3.2
405 Pa	20	83.0	4.2
Kruskal-Wallis Statistic = 19.49, **p<0.0001**			

b) dissolution index at umbo vs. pCO_2

group	N mussels	Sum of ranks	Mean of ranks
39 Pa	20	36.7	1.8
142 Pa	20	56.9	2.8
405 Pa	20	89.5	4.5
Kruskal-Wallis Statistic = 25.41, **p<0.0001**			

Table 5 (Exp. 2): SEM shell microstructure analysis of medium sized mussels

Treatment	Initial shell length (mm)	Final shell length (mm)	95% shell length calcite thickness (µm)	75% shell length calcite thickness (µm)	aragonite thickness (µm)	Layers of aragonite (n)	aragonite layer thickness (µm)
39 Pa / 385 µatm	12.4 ±1.8	21.4 ±1.2	95.6 ±14.0	99.2 ±9.1	9.6 ±2.8	15.8 ±3.7	0.6 ±0.11
142 Pa / 1400 µatm	12.4± 1.3	21.2 ±0.9	101.5 ±17.3	87.4 ±6.0	10.2 ±6.2	15.4 ±6.8	0.62 ±0.13
405 Pa / 4000 µatm	14.1± 0.5	21.1 ±1.7	109.6 ±19.2	99.7 ±19.6	7.5 ±6.2	17.2 ±9.3	**0.38 ±0.13**

Moderate seawater acidification does not elicit long-term metabolic depression in the blue mussel *Mytilus edulis*

Jörn Thomsen*
Frank Melzner

Biological Oceanography
Leibniz -Institute of Marine Sciences (IFM-GEOMAR)
Hohenbergstr 2, 24105 Kiel, Germany

*Corresponding author: jthomsen@ifm-geomar.de

Keywords: hypercapnia, metabolism, growth, calcification, oxygen consumption, NH_4^+ excretion

Abstract:

Marine organisms are exposed to increasingly acidic oceans, as a result of equilibration of surface ocean water with rising atmospheric CO_2 concentrations. In this study, we examined the physiological response of *Mytilus edulis* from the Baltic Sea, grown for two months at 4 seawater pCO_2 levels (39, 113, 243 and 405 Pa / 385, 1120, 2400 and 4000 µatm). Shell and somatic growth, calcification, oxygen consumption and NH_4^+ excretion rates were measured in order to test the hypothesis, whether exposure to elevated seawater pCO_2 is causally related to metabolic depression. During the experimental period, mussel shell mass and shell free dry mass (SFDM) increased at least by a factor of two and three, respectively. However, shell length and shell mass growth decreased linearly with increasing pCO_2 by 6-20 and 10-34%, while SFDM growth was not significantly affected by hypercapnia. We observed a parabolic change in routine metabolic rates with increasing pCO_2 and the highest rates (+60%) at 243 Pa. NH_4^+ excretion rose linearly with increasing pCO_2. Decreased O:N ratios at the highest seawater pCO_2 indicate enhanced protein metabolism which may contribute to intracellular pH regulation. We suggest that reduced shell growth under severe acidification is not caused by (global) metabolic depression but is potentially due to synergistic effects of increased cellular energy demand and nitrogen loss.

1. Introduction:

Equilibration of surface ocean waters with increasing atmospheric CO_2 concentrations is causing an increase in seawater pCO_2 (hypercapnia) and a shift in the marine carbonate system towards lower pH values and lower carbonate (CO_3^{2-}) ion concentrations (Cao and Caldeira 2008). While ocean acidification is a global phenomenon, seasonal effects, such as upwelling of hypoxic and hypercapnic waters are superimposed onto slowly progressing acidification in many coastal habitats, e.g. along the Pacific coastline and in the Western Baltic Sea (Feely et al. 2008). High seawater pCO_2 values of >200 Pa (100 Pa = 987 µatm) can be encountered in Kiel Fjord surface waters during summer and autumn (Thomsen et al. 2010). Additionally, brackish habitats such as the Baltic Sea exhibit lower [CO_3^{2-}] and, consequently, lower calcium carbonate saturation states (Ω) when compared to the open ocean. Baltic seawater is often under saturated with respect to aragonite even at low seawater pCO_2. Both, low Ω and seasonal acidification events are conditions that might be potentially adverse for shell growth and calcification of mussels (Fabry et al. 2008). Nevertheless, blue mussels (*Mytilus edulis*) can be found in high densities in Kiel Fjord (Enderlein and Wahl 2004) and juvenile settlement of this species occurs when highest seawater pCO_2 values are encountered in summer (Thomsen et al. 2010). This implies a certain resistance of *M. edulis* to acidified seawater.

Previous work with the mussel *M. galloprovincialis* has simultaneously determined growth and respiration and revealed a depression of both parameters in response to long-term (13 weeks) hypercapnic stress of about 500 Pa (Michaelidis et al. 2005). The reduction of physiological performance was concluded to be causally related to an uncompensated extracellular acidosis (Michaelidis et al. 2005). During short-term exposure, calcification in *M. edulis* has been found to decrease linearly with increasing pCO_2 and net shell dissolution has been observed at levels above 180 Pa (Gazeau et al. 2007).

It has been hypothesized that hypercapnia elicits a reduction of aerobic metabolism in marine organisms (metabolic depression) as a result of acid-base disturbances (Pörtner et al. 2004). Whereas intracellular pH (pHi) decreases in marine metazoans are typically compensated rapidly, extracellular pH (pHe) remains uncompensated in some species and has been hypothesized to be the trigger for metabolic depression (Pörtner et al. 1998). Several studies, performed under a broad range of seawater pCO_2 (100-1000 Pa), seem to confirm the reductions of oxygen consumption under elevated pCO_2 in different invertebrate taxa (Langenbuch and Pörtner 2002; Michaelidis et al. 2005; Rosa and Seibel 2008). However, unchanged or even increased oxygen consumption has been observed in some species as well (Gutowska et al. 2008; Wood et al. 2008; Melzner et al. 2009; Munday et al. 2009; Comeau et al. 2010). Studies which investigated calcification under elevated pCO_2 obtained similar heterogeneous responses; reduced, conserved, or even increased calcification rates have been measured in different phyla (Michaelidis et al. 2005; Berge et al. 2006; Gutowska et al. 2008; Wood et al. 2008; Ries et al. 2009; Comeau et al. 2010). Maintained (and increased) rates of calcification under hypercapnia may be causally related to partial or full pHe compensation, as the pHe regulatory response results in an accumulation of extracellular bicarbonate. This might alter the transport kinetics of HCO_3^- across calcifying epithelia or directly increase Ω at the site of calcification. Increased calcification has so far only been observed in species that perform strong pHe regulatory

responses (cephalopods: Gutowska et al. 2008; Gutowska et al. 2009, decapod crustaceans: Ries et al. 2009, fish: Checkley et al. 2009). In contrast, *M. edulis* does not actively elevate extracellular [HCO_3^-] above seawater [HCO_3^-] and does not compensate pHe (Thomsen et al. 2010).

Responses of mussel metabolism towards various short-term abiotic stressors, such as rapid salinity change, hypercapnia, or toxin exposure, have been the focus of several studies (Lindinger et al. 1984; Tedengren and Kautsky 1986). Generally, mussels respond with a decreased O:N ratio, as a result of either decreased metabolism, increased NH_4^+ excretion rates or a combination of both (Lindinger et al. 1984; Tedengren and Kautsky 1987; Michaelidis et al. 2005). In general, O:N ratios are considered a common indicator for the proportion of the three metabolic substrates, carbohydrates, lipids, and proteins, used in energy metabolism (Mayzaud and Conover 1988). Although absolute values vary for different species, regions, and seasons, lower O:N ratios indicate a higher fraction of protein metabolism whereas a higher ratio indicates an elevated turnover of carbohydrates and lipids (Mayzaud and Conover 1988).

This study was performed in order to estimate the long-term effects of elevated seawater pCO_2 levels on the parameters of shell and somatic growth as well as aerobic metabolism in Baltic blue mussels (*Mytilus edulis*). Specifically, we tested the hypothesis; whether elevated pCO_2 elicits metabolic depression at realistic levels of seawater acidification. For this purpose, we investigated shell length and mass growth, somatic growth, respiration and NH_4^+ excretion rates of mussels following a 2 month acclimation period at 4 different seawater pCO_2 levels under optimized feeding conditions.

2. Material and Methods:

2.1 Animal collection and experimental setup:

Subtidal *Mytilus edulis* individuals were sampled from Kiel Fjord (54°19.8'N; 10°9.0'E) at a water temperature of 10.6°C on Oct 26th 2009. 13 equally sized mussels were randomly placed into each of 16 experimental aquaria. Morphometric data were measured for a subsample of mussels (n=12). Mean shell length and shell mass at the start of the experimental incubation were 15±0.2 mm and 109±19 mg, respectively. Total fresh mass at the beginning of the incubation period was 1.6±0.04 g aquarium^{-1}. During the acclimation phase, low mortality was observed, in total six mussels died (3% mortality) 1 at 38 Pa, 2 at 113 Pa, 3 at 243 Pa).

2.2 Experimental procedure:

The long-term acclimation of the mussels was performed in a flow-through seawater setup. Mussels were incubated in 16 aquaria (volume=16L) that were supplied with filtered and UV-radiated seawater from a single header tank. Various seawater pCO_2 in the experimental aquaria (4 replicate aquaria per treatment) were achieved by aeration with CO_2-enriched air, pCO_2 levels were 39, 113, 243 and 405 Pa (380, 1120, 2400 and 4000 µatm). Flow rates from a header tank into the experimental aquaria were adjusted to 50 mL min^{-1} aquarium^{-1}. Seawater perfusing the experimental aquaria contained a *Rhodomonas* suspension enabling continuous food supply. *Rhodomonas* were cultured in Provasolis medium II according to Ismar et al. (2008) in 0.2 µm filtered N (0.55 mmol L^{-1}) and P (0.036 mmol L^{-1})

enriched seawater. Algae concentration was monitored at weekly intervals using a Coulter Counter (Z2, Beckman Coulter™). Cells densities were 5955±3889 cells mL^{-1} in the inflowing water and 2330±482 cells mL^{-1} in the outflow of the aquaria. In all aquaria, algae concentration never fell below 1500 cells mL^{-1}. The mussels were simultaneously cultured in the 4 CO_2 treatments for 8 weeks between October and December 2009.

Measurements of physiological rates were performed on subsequent days from December 16th to 20th, additional NH_4^+ excretion rates were determined on Dec 10th. Following experimentation, mussel morphometric parameters were assessed. Mussel shell length was measured with an accuracy of 0.1 mm. Shell mass and shell free dry mass (SFDM) were measured using a balance with an accuracy of 0.1 mg after mussels were dried in an oven at 80°C for 24 h.

2.3 Water chemistry parameter monitoring:

Water pH_{NBS}, salinity, and temperature were monitored daily in the setup during the entire incubation period using a WTW 340i pH-analyzer and a WTW SenTix 81-electrode for pH and WTW cond 315i salinometer and a WTW TETRACON 325 probe for salinity and temperature. Water parameters measured during the growth period are displayed in Table 1. pH_{NBS} values were stable and differed between pCO_2 treatments over the entire experimental duration. During the 8 week incubation period, water temperature decreased in the aquaria due to winter cooling of the Fjord water, from 9.7 to ca. 8°C, whereas salinity was less variable at values around 18.1±1.0 g kg^{-1}.

Total alkalinity (A_T) and total dissolved inorganic carbon (C_T) were analyzed in water samples taken from the experimental aquaria during the growth phase and in the respiration setup using VINDTA and SOMMA autoanalyzers (Dickson et al. 2007). Measured values were corrected for instrument shift using DICKSON seawater standard as reference material (Dickson et al. 2003). Carbonate system parameters were calculated from measured A_T and C_T values using CO2SYS software (Lewis and Wallace 1998). Dissociation constants K_1 and K_2 were chosen according to Mehrbach et al. (1973) as refitted by Dickson and Millero (1987) and $KHSO_4$ dissociation constant after Dickson (1990).

2.4 Measurements of oxygen consumption and ammonium excretion

Respiration and NH_4^+ excretion rates measurements were performed at 8.3°C in 100 mL plexiglas chambers which were placed in a 100 L water bath. 0.2 µm filtered and UV-sterilized seawater was equilibrated with a specific pCO_2 for 24 h before and during the measurements. 4 replicate chambers (3 replicates with mussels, one chamber without mussels serving as a bacterial control) were combined in four measuring circuits using gas - tight Tygon tubing (R-3603, Saint-Gobain, France). Each chamber contained 10 randomly chosen mussels from one replicate aquarium. Transfer from aquaria to the chambers lasted less than one minute and measurements started after half an hour of acclimation to experimental conditions. During the incubation period in the respiratory chambers, mussel valves remained open.

2.4.1 Oxygen consumption (MO_2):

MO_2 of *M. edulis* was measured using an intermittent-flow system. Water inside the respirometry chambers was continuously circulated using a peristaltic pump (MCP ISM 404, ISMATEC, Switzerland) at a rate of 2 mL s^{-1}. Oxygen concentrations were recorded every 5 minutes using fibre-optic oxygen sensors (needle-type optodes, Presens, Regensburg, Germany) inserted into the tubing of the measuring circuit via a plastic y-piece. One measuring interval lasted 45 minutes. Between measuring intervals, chambers were flushed with seawater from the water bath for 3 h using 5 W submersible pumps (Eheim, Deizisau, Germany). The whole incubation lasted for 20h per pCO_2 treatment, with 6 MO_2 determinations per replicate chamber per aquarium. NH_4^+ concentrations in the water bath were always below one µmol L^{-1} at the end of an incubation.

For calculation of oxygen consumption rates, the linear decrease of oxygen concentration during measuring intervals between 5 and 35 minutes was considered; [O_2] maximally decreased to 65% air saturation (average: 74%, see Fig. 3 for typical respiration traces). The observed decrease of oxygen concentration resulted in an increase of C_T and therefore pCO_2 in the closed chambers. Depending on oxygen consumption rates in the different pCO_2 treatments, seawater pCO_2 in the chambers increased by 4-18 Pa (<10% of the initial pCO_2) during incubations. The results of 6 separate runs per chamber measured during the whole incubation interval were averaged. Over the course of 20 h incubations, consumption rates slightly decreased in the last runs at all pCO_2 levels. Molar oxygen consumption rates (MO_2) are expressed as µmol O_2 g^{-1} SFDM h^{-1}.

2.4.2 Ammonium excretion:

Seawater ammonium (NH_4^+) concentrations were determined prior to, and following the respiration trials. An initial 10 mL water samples was taken from every chamber before closing for oxygen consumption measurements, after 1h incubation, a second sample was taken. Additionally, excretion rates were assessed in a stop-flow experiment during the growth period one week earlier (Dec 10th). Seawater flow-through was stopped and mussels were incubated in closed aquaria. Following 8.5 h of incubation, 10 mL water samples were taken from each replicate aquarium.

Ammonium concentrations were determined according to Holmes et al. (1999). 2.5 ml of a reagent which contains orthophthaldialdehyde, sodium sulfite, and sodium borate, were added to the water samples. After two hours incubation, samples were measured using a Kontron SFM25 fluorometer at an excitation and emission wavelength of 360 and 422 nm, respectively. Ammonia (NH_3) was not measured since its concentration is negligible (Körner et al. 2001). At seawater pH values of 8-7.1, NH_3 concentrations are in the range of 0.2-2% of total [NH_3 + NH_4^+]. Ammonium excretion rates ($NH_4^+{}_{ex}$) are expressed as µmol NH_4^+ g^{-1} SFDM h^{-1}.

2.5 Calculation of O:N ratio and metabolic energy loss:

2.5.1 O:N ratio:

The atomic ratio of oxygen uptake and excreted nitrogen was calculated from MO_2 and $NH_4^+{}_{ex}$.

O:N = MO_2 $NH_4^+{}_{ex}^{-1}$

2.5.2 Metabolic energy loss:

Aerobic energy loss was calculated using a mean oxycaloric equivalent of 0.44 J µmol O_2^{-1} representing a mixed, but protein dominated, catabolism of hydrocarbons, lipids, and proteins as metabolic substrates (Lauff and Wood 1996). Calculations were performed without consideration of potential changes in the fraction of the three substrates to total metabolism in the different pCO_2 treatments. Energy loss by NH_4^+ excretion was calculated using an energy value of 0.347 J µmol^{-1} NH_4^+ according to Elliott and Davison (1975). Total metabolic energy loss (E_{NET}, J g^{-1} SFDM h^{-1}) was calculated from aerobic energy metabolism and nitrogen excretion:

$E_{NET} = MO_2 \times 0.44J + NH_4^+{}_{ex} \times 0.347J$

2.6 Statistics:

Data were analyzed by quadratic or linear regression using SIGMA PLOT 10. Data sets were analyzed for normality and Cook´s distance. ANCOVA (STATISTICA 8) was performed to compare NH_4^+ excretion rates obtained by the two different methods. All graphically represented values are means of pooled sub replicates (from 4 replicated aquaria of each treatment). The error in the equations of regression equations is the standard error of the mean.

3. Results:

M. edulis were continuously fed with a *Rhodomonas* suspension which enabled high growth. Mean shell length of control mussels increased from 15.0±0.2 mm to 22.9±0.3 mm, thus by about 7.9±0.3 mm (Fig. 1A). Mussels from higher pCO_2 treatments displayed reduced growth. With increasing pCO_2 shell length decreased linearly. Shell length increment of 113 and 405 Pa treated mussels was reduced to 7.4±0.9 and 6.3±0.3 mm, respectively. This corresponds to shell length growth reductions of 6-20% compared to control mussels.

Similar results were obtained for *M. edulis* shell mass growth. Mussels from all treatments accreted shell mass. From an inital mass of 109±19 mg, 319±6.6 mg was reached in the 39 Pa treatment, corresponding to an increase of 290% (Fig. 1B). Similar to shell length, shell mass increment decreased linearly with increasing pCO_2. Final shell mass ranged from 297±21.5 mg to 243.7±15.5 mg between the 113 and 405 Pa treatments. Thus, shell mass growth rates were reduced by 10 to 36% with elevated pCO_2. SFDM increased from 17.8±5.5 mg to mean values of 56-60.3 mg with no significant differences between pCO_2 groups (Fig. 1C). Thus, somatic growth of *M. edulis* was not significantly reduced by elevated seawater pCO_2.

Effects of long-term hypercapnia on oxygen consumption of *M. edulis* are shown in Fig. 2A: mussels raised at a control pCO_2 of 39 Pa displayed mean oxygen consumption rates of 19.8±1.7 µmol O_2 g^{-1} h^{-1}. Increasing pCO_2 led to a change of respiration rates which followed a quadratic function (see figure caption for regression). Measured respiration rates peaked in the 243 Pa treatment. A further

elevation in pCO_2 to 405 Pa led to decreased oxygen uptake, but still slightly elevated MO_2 when compared to the control condition.

A linear correlation between sea water pCO_2 and NH_4^+ excretion was found. Mussels placed in the respiration chambers displayed mean NH_4^+ excretion rates of 1.13±0.24 µmol NH_4^+ g^{-1} h^{-1} in the control treatment (Fig. 2B). When mussels were subjected to higher seawater pCO_2, NH_4^+ excretion increased to values of 2.12±0.41 in the 405 Pa treatment. Mussel NH_4^+ excretion measured in the stop-flow experiment resulted in similar mean values (control: 1.22±0.24) and an identical slope of NH_4^+ excretion increase with increasing water pCO_2 (ANCOVA, $F_{(1,25)}$= 0.2034, p=0.656).

Oxygen uptake and nitrogen excretion measurements were used to calculate the O:N ratio of the mussels. In the lower pCO_2 treatments, the O:N ratio increased slightly with rising pCO_2 as a result of increasing oxygen uptake and reached a maximum in the 243 Pa treatment (Fig. 2C). In the highest treatment (405 Pa), O:N values decreased due to decreasing respiration rates despite elevated NH_4^+ excretion. The mean O:N values for control mussels were 17.9±2.6 and 21±2.7 at 243 Pa. Mussels from the 405 Pa treatment were characterized by O:N values of 12.3±1.6.

Calculations of the energy lost by respiration and NH_4^+ excretion per g drymass and h are displayed in Tab 2. Correlated to rising oxygen consumption rates, the amount of energy lost by the experimental animals increased at elevated pCO_2. Control mussels lost a total of 9.10±0.82 J g^{-1} SFDM h^{-1} of energy, which slightly increased in the treatments up to 243 Pa and started to decrease at 405 Pa. The linear rise of NH_4^+ excretion at elevated pCO_2 resulted in a rising energy loss from 0.39±0.08 to 0.74±0.14 J g^{-1} h^{-1} in the 39 and 405 treatment, respectively. Due to the different order of magnitude between the two fluxes, increased nitrogen excretion only had a minor impact on the total energy loss (Tab 2). Energy loss by ammonium excretion was calculated to contribute ca. 5 % to total energy loss.

4. Discussion:

Long-term acclimation of *Mytilus edulis* from the Western Baltic Sea to elevated seawater pCO_2 resulted in an increase of aerobic metabolic rates during moderate hypercapnia, rather than metabolic depression. As our companion study demonstrated that *M. edulis* does not control pHe when exposed to seawater acidification (Thomsen et al. 2010), it is clear that there is no causal relationship between metabolic depression and extracellular acid-base status under moderate acidification scenarios. Oxygen consumption and NH_4^+ excretion in hypercapnic treatments remained elevated above control rates, whereas shell growth declined during 2 months of incubation under elevated pCO_2. Our control respiration and NH_4^+ excretion rates were in the range of published results for *Mytilus spp.* (Tedengren et al. 1990; Okumus and Stirling 1994; Michaelidis et al. 2005).

Up to a certain seawater pCO_2, mussels increase metabolic rates (<243 Pa). Beyond this pCO_2 metabolism starts to decrease, but remains above control rates. Similar effects of hypercapnia on respiration rates have already been observed for other marine taxa at comparable pCO_2 levels, such as an ophiuroid echinoderm and tropical teleost fish species (Wood et al. 2008; Munday et al. 2009). In contrast, Michaelidis et al. (2005) reported a drop of respiration rates for *Mytilus galloprovincialis* during short- and long-term incubation at a pCO_2 of ca. 500 Pa. These findings are not contradictory to

our results since the course of oxygen consumption in our experiment described a downward trend at higher pCO_2. Thus, it is possible that at pCO_2 >405 Pa a downregulation of MO_2 may be encountered. During prolonged emersion or in a hypoxic/anoxic environment, extracellular pCO_2 values in bivalve extracellular fluids rise and are coupled with decreases in pO_2 in the seawater encased by the closed shell valves (Famme 1980; Wang and Widdows 1993). Therefore, down regulation of energy demand and aerobic metabolism at very high pCO_2 may result from evolutionary adaptation of mussels to fluctuating pCO_2 in intertidal habitats. During 8h air exposure at 12°C mussel haemolymph pH decreased by 0.4 units and at the same time haemolymph pCO_2 raises up to 440 Pa (Booth et al. 1984). Highly elevated extracellular pCO_2 could serve as a signal for cellular metabolic depression, a process that prevents fatal thermodynamic imbalances and cell death during short-/ intermediate term abiotic stress (Guppy and Withers 1999).

O:N ratios around 20 indicate that amino acid catabolism dominates Baltic Sea *M. edulis* aerobic metabolism. Pure protein metabolism can be expected at a ratio of 3-16, balanced lipid and protein degradation occurs at O:N = 50-60 (Mayzaud and Conover 1988). This is in agreement with the results of studies that compared Baltic and North Sea *M. edulis* metabolism. These studies revealed lower O:N ratios in Baltic mussels, resulting from increased NH_4^+ excretion as a consequence of osmoregulatory demands (Tedengren and Kautsky 1986; Tedengren et al. 1990). It has been hypothesized that this lowered ratio explains reduced growth rates of Baltic mussels in the field due to enhanced unfavourable protein metabolism. Higher amino acid metabolism is energetically less efficient compared to turnover of carbohydrate and lipid as it implies a continuous energy loss by enhanced excretion of, in the case of mussels, ammonium (Tedengren and Kautsky 1986). Additionally, relatively low O:N ratios observed in this study may result from the high protein content of the diet which enabled high protein metabolism (Kreeger and Langdon 1993; Hatcher et al. 1997). The mussels of this study were fed with *Rhodomonas* sp. which is characterized by a high nitrogen content (Berggreen et al. 1988). However, increasing respiration and NH_4^+ excretion lead to an almost unchanged O:N ratio which indicates no dramatic proportional change in metabolic substrate choice in the treatments up to 243 Pa. Rather, parallel increases in metabolic rate and NH_4^+ excretion indicate an absolute rise of protein metabolism during hypercapnia. Only very high seawater pCO_2 (405 Pa) causes a marked reduction of the O:N ratio which might indicate a larger fraction of protein metabolism in these mussels.

Increased NH_4^+ excretion rates of mussels have been already observed by Lindinger et al. (1984) and Michaelidis et al. (2005) during short-term (20-24h) incubation at pCO_2 between 500 and 4000 Pa. Our results confirm these short-term findings for the long-term acclimation process in mussels subjected to elevated pCO_2. The authors of the former study proposed a contribution of the positively charged ion to proton excretion under elevated pCO_2 (Lindinger et al. 1984). Increased metabolic formation of NH_3 by protein breakdown and following extrusion as NH_4^+ can serve as an intracellular pH regulatory mechanism (Boron 2004). Increases in NH_4^+ excretion suggest a significant contribution of this mechanism to proton removal in *M. edulis*, as NH_4^+ excretion almost doubled at the highest pCO_2. This may have the added benefit that protein degradation probably supports HCO_3^- production and thereby pHi regulation as already suggested for sipunculids and the mussel *M. galloprovincialis*

(Langenbuch and Pörtner 2002; Michaelidis et al. 2005). Studies that analyzed NH_4^+ and CO_2 excretion in fish gill concluded that CO_2 excretion lowers pH in the boundary layer of the gill and thereby facilitates passive NH_3 diffusion (Wright et al. 1989; Wilkie 2002). Hypercapnia might have a similar effect on the boundary layer, thereby enabling higher nitrogen excretion rates. However, since in *Mytilus* spp. extracellular pH decreases during hypercapnia while pHi is maintained, this increases the driving force for H^+ flux into the intracellular space. In fact, high levels of seawater acidification even lead to a reversal of the proton gradient from the extra- to the intracellular space (Michaelidis et al. 2005). Thus, cellular acid extrusion effort needs to be upregulated (Boron 2004; Michaelidis et al. 2005). One possibility pathway of NH_4^+ excretion is via primary active transport, e.g. by basolateral Na^+/K^+-ATPase transporting NH_4^+ (instead of K^+) into epithelial cells (Wilkie 1997; Knepper 2008; Pagliarani et al. 2008). Subsequently, nitrogen extrusion from the intracellular compartment is performed either by diffusion of uncharged NH_3 or as charged NH_4^+. In the first case, NH_3 is protonated in the seawater boundary layer on the apical side of the cells. This can be a result by either separate H^+ transport via V-type H^+-ATPase and Na^+/H^+ exchanger or by hydration of CO_2 via carbonic anhydrase (Wilkie 2002; Kaloyianni et al. 2005; Nawata et al. 2007; Knepper 2008). In the latter case, NH_4^+ may be removed by an apical Na^+/NH_4^+ exchanger as described for marine fish (Wilkie 1997). Irrespective of the mechanism, active transport of base and acid equivalents across the cell membranes needs to be increased in order to achieve pHi compensation when pHe is decreased. This has been already reported for the energy budget in isolated perfused fish gill where energy expenditure for ion regulation rose during hypercapnia (Deigweiher et al. 2009).

The observed reduction of mussel shell growth rates is in accordance with the results of Michaelidis et al. (2005) and our own findings from a similar experiment performed in summer 2009 (Thomsen et al. 2010). We found significant CO_2 induced reductions in shell length and shell mass growth at high pCO_2 (405 Pa). However, we did not find significant decreases in SFDM, indicating that somatic growth is not as strongly affected by elevated pCO_2 as the calcification process. The elevated ion regulatory activity necessary to achieve a new steady state for intracellular pH homeostasis may force *M. edulis* to allocate a surplus of energy to cellular ion and pH homeostasis. At elevated pCO_2 levels of 113 Pa and 243 Pa total energy expenditure in *M. edulis* rose by 42% and 58% above control level. Therefore decreased shell growth may be a consequence of increased energy demand and, potentially, energy re-allocation during hypercapnia. Mussels shift towards protein/amino acid metabolism as indicated by an increase in NH_4^+ excretion. Increased energy loss cannot be balanced by an increased energy uptake by means of elevated filtration rates. *M. edulis* filtration rates remain on control levels at elevated seawater pCO_2 (Saphörster, Thomsen, Melzner. unpublished). In general, mussel shell growth rate does not only depend on the food energy content but is more closely correlated to the nitrogen/protein content (Kreeger and Langdon 1993; Kreeger et al. 1996). Increased protein turnover and thereby elevated loss of nitrogen as NH_4^+ at higher pCO_2 cannot be compensated by increased nitrogen uptake by enhanced filtration activity during hypercapnia. Thus, mussel metabolism might be ultimately impaired by an increasing nitrogen limitation. The high growth and protein accretion efficiency of *M. edulis* mainly results from a high recycling rate of protein degradation products (Hawkins 1985; Hawkins et al. 1989; Bayne and Hawkins 1997). Therefore decreased shell growth rates may in part also be related to increased protein breakdown and nitrogen loss since

calcified structures of bivalve shells are enclosed by an organic matrix consisting of proteins and chitin (Matsushiro and Miyashita 2004; Addadi et al. 2006). A reduced capacity to form matrix structures might in turn have adverse effect on the deposition of calcium carbonate crystals. It has been previously described that elevated pCO_2 has an impact on protein turnover in several marine organisms leading to lowered synthesis or even enhanced degradation (Langenbuch and Pörtner 2003; Langenbuch et al. 2006; Wood et al. 2008). On the other hand, it cannot be excluded that the progressively more acidic environment of the extrapallial fluid (c.f. Thomsen et al. 2010), which is in direct contact with the newly formed nacre layers, negatively impacts the energetics of $CaCO_3$ deposition and / or organic matrix formation, or even the interaction between organic and mineral phase construction. Thus, the observed decreases in shell growth could be partly explained by higher maintenance requirements for cellular homeostasis and a shift towards unfavourable nitrogen cycling causing reduced protein accretion rates. As a consequence, calcification may not necessarily be affected exclusively by lowered [CO_3^{2-}] in body fluids and ambient seawater but also in a secondary fashion by lowered net protein deposition.

According to our results, the general hypothesis of metabolic depression in mussels might only be valid for very high levels of hypercapnia and does not play a role at seawater pCO_2 values predicted for the most parts of the oceans within the next ca. 50-100 years (Cao and Caldeira 2008). At moderate seawater pCO_2 (<243 Pa) mussels try to compensate unfavourable abiotic conditions such as intracellular acid loads instead of decreasing their activity. Overall, mussel metabolism rises and shell growth rates decrease while somatic growth is preserved under elevated seawater pCO_2. This will be particularly important for the Kiel Fjord mussel population, which is exposed to very high seawater pCO_2 in summer and autumn. Seawater pCO_2 >200 Pa have been recorded during summer and autumn 2008 as a result of upwelling of hypoxic-hypercapnic bottom waters. Synergistic effects of future ocean acidification and this natural phenomenon can potentially increase seawater pCO_2 to values above 400 Pa, given a doubling in surface pCO_2 by the year 2100 (see Thomsen et al. 2010). Additionally, elevated metabolic rates due to ocean warming will probably challenge the energy budgets of *M. edulis* even more, leaving less energy for growth of calcified structures. It remains to be established, to what degree energy allocation into reproduction will be compromised during exposure to hypercapnia as well. It has been already revealed that mussel reproduction is highly susceptible to environmental stress such as extreme temperatures and elevated pCO_2 (Petes et al. 2007; Whitman Miller et al. 2009; Gazeau et al. 2010). While the capacity of *M. edulis* to calcify at high rates in seawater highly undersaturated with $CaCO_3$ is astonishing, it is also likely that this feature is costly and may only be possible in eutrophic habitats. Future studies clearly need to address (i) the role of energy supply to maintain high rates of growth and calcification under elevated seawater pCO_2 and (ii) identify the cellular processes that lead to increased metabolic demands. It is likely that the combined action of elevated temperature and high seawater pCO_2 can negatively impact the fitness of *M. edulis* in coastal upwelling habitats in the next decades.

Acknowledgements:

We thank Ullrike Panknin for her technical support with algae culturing and monitoring of experimental water parameters, Peter Fritsche for the help with the ammonium measurements, and Sebastian Fessler for supporting the carbonate system measurements. We like to thank Magdalena A. Gutowska for her advice to improve the manuscript. This study was funded by the DFG Excellence cluster ´Future Ocean´ and the German 'Biological impacts of ocean acidification (BIOACID)' project 3.1.3, funded by the Federal Ministry of Education and Research (BMBF, FKZ 03F0608A).

References:

Addadi L, Joester D, Nudelman F, Weiner S (2006) Mollusk shell formation: A source of new concepts for understanding biomineralization processes. Chemistry-a European Journal 12: 981-987

Bayne BL, Hawkins AJS (1997) Protein metabolism, the costs of growth, and genomic heterozygosity: Experiments with the mussel *Mytilus galloprovincialis* Lmk. Physiological Zoology 70: 391-402

Berge JA, Bjerkeng B, Pettersen O, Schaanning MT, Oxnevad S (2006) Effects of increased sea water concentrations of CO_2 on growth of the bivalve *Mytilus edulis* L. Chemosphere 62: 681-687

Berggreen U, Hansen B, Kiorboe T (1988) Food size spectra, ingestion and growth of the copepod *Acartia tonsa* during development - Implications for determination of copepod production. Marine Biology 99: 341-352

Booth CE, McDonald DG, Walsh PJ (1984) Acid-base-balance in the sea mussel, *Mytilus-edulis* .1. Effects of hypoxia and air-exposure on hemolymph acid-base status. Marine Biology Letters 5: 347-358

Boron WF (2004) Regulation of intracellular pH. Advances in Physiology Education 28: 160-179

Cao L, Caldeira K (2008) Atmospheric CO_2 stabilization and ocean acidification. Geophysical Research Letters 35

Checkley DM, Dickson AG, Takahashi M, Radich JA, Eisenkolb N, Asch R (2009) Elevated CO_2 Enhances Otolith Growth in Young Fish. Science 324: 1683-1683

Comeau S, Jeffree R, Teyssie JL, Gattuso JP (2010) Response of the arctic pteropod *Limacina helicina* to projected future environmental conditions. Plos One 5: e11362

Deigweiher K, Hirse T, Bock C, Lucassen M, Pörtner HO (2009) Hypercapnia induced shifts in gill energy budgets of Antarctic notothenioids. Journal of Comparative Physiology B: Biochemical, Systemic, and Environmental Physiology

Dickson AG (1990) Standard potential of the reaction - $AgCl_S$+1/2 H_2 = Ag_S+HCl_{Aq} and the standard acidity constant of the ion HSO_4- in synthetic sea-water from 273.15-K to 318.15-K. Journal of Chemical Thermodynamics 22: 113-127

Dickson AG, Afghan JD, Anderson GC (2003) Reference materials for oceanic CO_2 analysis: a method for the certification of total alkalinity. Marine Chemistry 80: 185-197

Dickson AG, Millero FJ (1987) A comparison of the equilibrium-constants for the dissociation of carbonic-acid in seawater media. Deep-Sea Research Part A-Oceanographic Research Papers 34: 1733-1743

Dickson AG, Sabine CL, Christian JR (2007) Guide to best practices for ocean CO_2 measurements. . PICES Special Publications

Elliott JM, Davison W (1975) Energy equivalents of oxygen-consumption in animal energetics. Oecologia 19: 195-201

Enderlein P, Wahl M (2004) Dominance of blue mussels versus consumer-mediated enhancement of benthic diversity. Journal of Sea Research 51: 145-155

Fabry VJ, Seibel BA, Feely RA, Orr JC (2008) Impacts of ocean acidification on marine fauna and ecosystem processes. Ices Journal of Marine Science 65: 414-432

Famme P (1980) Effect of shell valve closure by the mussel *Mytilus edulis* L. on the rate of oxygen consumption in declining oxygen-tension. Comparative Biochemistry and Physiology a-Physiology 67: 167-170

Feely RA, Sabine CL, Hernandez-Ayon JM, Ianson D, Hales B (2008) Evidence for upwelling of corrosive "acidified" water onto the continental shelf. Science 320: 1490-1492

Gazeau F, Gattuso JP, Dawber C, Pronker AE, Peene F, Peene J, Heip CHR, Middelburg JJ (2010) Effect of ocean acidification on the early life stages of the blue mussel *Mytilus edulis*. Biogeoscience 7: 2051-2060

Gazeau F, Quiblier C, Jansen JM, Gattuso JP, Middelburg JJ, Heip CHR (2007) Impact of elevated CO_2 on shellfish calcification. Geophysical Research Letters 34

Guppy M, Withers P (1999) Metabolic depression in animals: physiological perspectives and biochemical generalizations. Biological Reviews 74: 1-40

Gutowska MA, Melzner F, Langenbuch M, Bock C, Claireaux G, Portner HO (2009) Acid-base regulatory ability of the cephalopod (*Sepia officinalis*) in response to environmental hypercapnia. Journal of Comparative Physiology B-Biochemical Systemic and Environmental Physiology 180: 323-335

Gutowska MA, Pörtner HO, Melzner F (2008) Growth and calcification in the cephalopod *Sepia officinalis* under elevated seawater pCO_2. Marine Ecology-Progress Series 373: 303-309

Hatcher A, Grant J, Schofield B (1997) Seasonal changes in the metabolism of cultured mussels (*Mytilus edulis* L.) from a Nova Scotian inlet: the effects of winter ice cover and nutritive stress. Journal of Experimental Marine Biology and Ecology 217: 63-78

Hawkins AJS (1985) Relationships between the synthesis and breakdown of protein, dietary absorption and turnovers of nitrogen and carbon in the blue mussel, *Mytilus edulis*-L. Oecologia 66: 42-49

Hawkins AJS, Widdows J, Bayne BL (1989) The relevance of whole-body protein-metabolism to measured costs of maintenance and growth in *Mytilus edulis*. Physiological Zoology 62: 745-763

Holmes RM, Aminot A, Kerouel R, Hooker BA, Peterson BJ (1999) A simple and precise method for measuring ammonium in marine and freshwater ecosystems. Canadian Journal of Fisheries and Aquatic Sciences 56: 1801-1808

Ismar SMH, Hansen T, Sommer U (2008) Effect of food concentration and type of diet on *Acartia* survival and naupliar development. Marine Biology 154: 335-343

Kaloyianni M, Stamatiou R, Dailianis S (2005) Zinc and 17 beta-estradiol induce modifications in Na^+/H^+ exchanger and pyruvate kinase activity, through protein kinase C in isolated mantle/gonad cells of *Mytilus galloprovincialis*. Comparative Biochemistry and Physiology C-Toxicology & Pharmacology 141: 257-266

Knepper MA (2008) PHYSIOLOGY Courier service for ammonia. Nature 456: 336-337

Körner S, Das SK, Veenstra S, Vermaat JE (2001) The effect of pH variation at the ammonium/ammonia equilibrium in wastewater and its toxicity to *Lemna gibba*. Aquatic Botany 71: 71-78

Kreeger DA, Hawkins AJS, Bayne BL (1996) Use of dual-labeled microcapsules to discern the physiological fates of assimilated carbohydrate, protein carbon, and protein nitrogen in suspension-feeding organisms. Limnology and Oceanography 41: 208-215

Kreeger DA, Langdon CJ (1993) Effect of dietary-protein content on growth of juvenile mussels, *Mytilus trossulus* (Gould 1850). Biological Bulletin 185: 123-139

Langenbuch M, Bock C, Leibfritz D, Pörtner HO (2006) Effects of environmental hypercapnia on animal physiology: A ^{13}C NMR study of protein synthesis rates in the marine invertebrate *Sipunculus nudus*. Comparative Biochemistry and Physiology A-Molecular & Integrative Physiology 144: 479-484

Langenbuch M, Pörtner HO (2002) Changes in metabolic rate and N excretion in the marine invertebrate *Sipunculus nudus* under conditions of environmental hypercapnia: identifying effective acid-base variables. Journal of Experimental Biology 205: 1153-1160

Langenbuch M, Pörtner HO (2003) Energy budget of hepatocytes from Antarctic fish (*Pachycara brachycephalum* and *Lepidonotothen kempi*) as a function of ambient CO_2: pH-dependent limitations of cellular protein biosynthesis? Journal of Experimental Biology 206: 3895-3903

Lauff RF, Wood CH (1996) Respiratory gas exchange, nitrogenous waste excretion, and fuel usage during aerobic swimming in juvenile rainbow trout. Journal of Comparative Physiology B-Biochemical Systemic and Environmental Physiology 166: 501-509

Lewis E, Wallace DWR (1998) Program developed for CO_2 system calculations. Oak Ridge, Oak Ridge National Laboratory ORNL/CDIAC-105

Lindinger MI, Lauren DJ, McDonald DG (1984) Acid-base-balance in the sea mussel, *Mytilus edulis*. 3. Effects of environmental hypercapnia on intracellular and extracellular acid-base-balance. Marine Biology Letters 5: 371-381

Matsushiro A, Miyashita T (2004) Evolution of hard-tissue mineralization: comparison of the inner skeletal system and the outer shell system. Journal of Bone and Mineral Metabolism 22: 163-169

Mayzaud P, Conover RJ (1988) O:N atomic ratio as a tool to describe zooplankton metabolism. Marine Ecology-Progress Series 45: 289-302

Mehrbach C, Culberso CH, Hawley JE, Pytkowic RM (1973) Measurement of apparent dissociation-constants of carbonic-acid in seawater at atmospheric-pressure. Limnology and Oceanography 18: 897-907

Melzner F, Göbel S, Langenbuch M, Gutowska MA, Pörtner HO, Lucassen M (2009) Swimming performance in Atlantic Cod (*Gadus morhua*) following long-term (4-12 months) acclimation to elevated seawater pCO_2. Aquatic Toxicology 92: 30-37

Michaelidis B, Ouzounis C, Paleras A, Pörtner HO (2005) Effects of long-term moderate hypercapnia on acid-base balance and growth rate in marine mussels *Mytilus galloprovincialis*. Marine Ecology-Progress Series 293: 109-118

Munday PL, Crawley NE, Nilsson GE (2009) Interacting effects of elevated temperature and ocean acidification on the aerobic performance of coral reef fishes. Marine Ecology-Progress Series 388: 235-242

Nawata CM, Hung CCY, Tsui TKN, Wilson JM, Wright PA, Wood CM (2007) Ammonia excretion in rainbow trout (*Oncorhynchus mykiss*): evidence for Rh glycoprotein and H^+-ATPase involvement. Physiological Genomics 31: 463-474

Okumus I, Stirling HP (1994) Physiological energetics of cultivated mussel (*Mytilus edulis*) populations in 2 Scottish west-coast sea lochs. Marine Biology 119: 125-131

Pagliarani A, Bandiera P, Ventrella V, Trombetti F, Manuzzi MP, Pirini M, Borgatti AR (2008) Response of Na^+-dependent ATPase activities to the contaminant ammonia nitrogen in *Tapes philippinarum*: Possible ATPase involvement in ammonium transport. Archives of Environmental Contamination and Toxicology 55: 49-56

Petes LE, Menge BA, Murphy GD (2007) Environmental stress decreases survival, growth, and reproduction in New Zealand mussels. Journal of Experimental Marine Biology and Ecology 351: 83-91

Pörtner HO, Langenbuch M, Reipschläger A (2004) Biological impact of elevated ocean CO_2 concentrations: Lessons from animal physiology and earth history. Journal of Oceanography 60: 705-718

Pörtner HO, Reipschlager A, Heisler N (1998) Acid-base regulation, metabolism and energetics in *Sipunculus nudus* as a function of ambient carbon dioxide level. Journal of Experimental Biology 201: 43-55

Ries JB, Cohen AL, McCorkle DC (2009) Marine calcifiers exhibit mixed responses to CO_2-induced ocean acidification. Geology 37: 1131-1134

Rosa R, Seibel BA (2008) Synergistic effects of climate-related variables suggest future physiological impairment in a top oceanic predator. Proceedings of the National Academy of Sciences of the United States of America 105: 20776-20780

Tedengren M, Andre C, Johannesson K, Kautsky N (1990) Genotypic and phenotypic differences between Baltic and North-Sea populations of *Mytilus edulis* evaluated through reciprocal transplantations .3. Physiology. Marine Ecology-Progress Series 59: 221-227

Tedengren M, Kautsky N (1986) Comparative-study of the physiology and its probable effect on size in blue mussels (*Mytilus edulis* L) from the North-Sea and the northern Baltic proper. Ophelia 25: 147-155

Tedengren M, Kautsky N (1987) Comparative stress response to diesel oil and salinity changes of the blue mussel, *Mytilus edulis* from the Baltic and North Seas. Ophelia 28: 1-9

Thomsen J, Gutowska MA, Saphörster J, Heinemann A, Trübenbach K, Fietzke J, Hiebenthal C, Eisenhauer A, Körtzinger A, Wahl M, Melzner F (2010) Calcifying invertebrates succeed in a naturally CO_2 enriched coastal habitat but are threatened by high levels of future acidification. Biogeoscience Discussions 7: 5119-5156

Wang WX, Widdows J (1993) Metabolic responses of the common mussel *Mytilus edulis* to hypoxia and anoxia. Marine Ecology-Progress Series 95: 205-214

Whitman Miller A, Reynolds AC, Sobrino C, Riedel GF (2009) Shellfish face uncertain future in high CO_2 world:Influence of acidification on oyster larvae calcification and growth in estuaries. Plos One 4: e5661

Wilkie MP (1997) Mechanisms of ammonia excretion across fish gills. Comparative Biochemistry and Physiology a-Physiology 118: 39-50

Wilkie MP (2002) Ammonia excretion and urea handling by fish gills: Present understanding and future research challenges. Journal of Experimental Zoology 293: 284-301

Wood HL, Spicer JI, Widdicombe S (2008) Ocean acidification may increase calcification rates, but at a cost. Proceedings of the Royal Society B-Biological Sciences 275: 1767-1773

Wright PA, Randall DJ, Perry SF (1989) Fish gill water boundary-layer - a site of linkage between carbon-dioxide and ammonia excretion. Journal of Comparative Physiology B-Biochemical Systemic and Environmental Physiology 158: 627-635

Figure legends

Figure 1: Shell length (A), shell mass (B) and shell free dry mass (SFDM)(C) of *M. edulis* grown at 4 different pCO_2 treatments for 2 months. Each dot represents the mean of the mussels from a replicate aquarium, Black lines give linear function of shell length and shell mass. Long dashed lines are 95% confidence intervals. The single point left of the vertical line displays the initial shell length, shell mass and SFDM. (A) Shell length = -0.0045(±0.001) pCO_2 + 22.9544(±0.2106), R^2=0.6177, F=22.6244, p<0.01; (B) Shell mass = -0.2170(±0.032) pCO_2 + 321.7090(±7.01), R^2=0.7532, F=46.7735, p<0.01; (C) SFDM = -0.0067(±0.0124) pCO_2 + 59.3475(±2.748), R^2=0.0203, F=0.2906, p=0.598; N=16

Figure 2: Oxygen consumption (A), NH_4^+ excretion (B) and O:N ratio (C) of *M. edulis* as a function of 4 different pCO_2 levels. (A) Dots display means of 6 repeated measurements of 10 mussels from every replicate aquarium. Long dashed lines give 95% confidence intervals. -0.0005(±0.0002) * pCO_2^2 + 0.1971(±0.0656) * pCO_2 + 11.5505(±4.7267), R^2=0.458, F=5.2253 p<0.05, N=11; (B) Dots represent measurements of ammonium excretion in the respiration trial. NH_4^+ = 0.0025(±0.0007) pCO_2 + 1.113(±0.1668) R^2=0.4788, F=11.1054, p<0.01, N=12. Triangles represent ammonium excretion in the stop-flow experiment 0.0025(±0.0006) pCO_2 + 1.1681(±0.1361) R^2=0.5041, F=16.2457, p<0.01, N=16; (C) The ratio was calculated from measured molar oxygen consumption and ammonium excretion rates. Long dashed lines give the 95% confidence interval. O:N = -0.0003(±0.00009) * pCO_2^2 + 0.1159(±0.0352) * pCO_2 + 11.6953(±2.533), R^2= 0.6089, F=8.7858 p<0.01, N=11

Figure 3: Representative courses of air saturation in the respiration chambers during measuring intervals between 5 and 35 minutes. Triangles represent the O_2 concentration change of a bacterial control. Black and white dots represent courses for mussels of the 39 and 243 Pa pCO_2 treatments, respectively.

Table legends

Table 1: Carbonate system parameter during 2 month incubation in the four pCO_2 treatments. Values display means and standard deviation

Table 2: Metabolic energy loss by (J g^{-1} SFDM h^{-1}) of *M. edulis* subjected to 4 pCO_2 treatments.

Figure 1

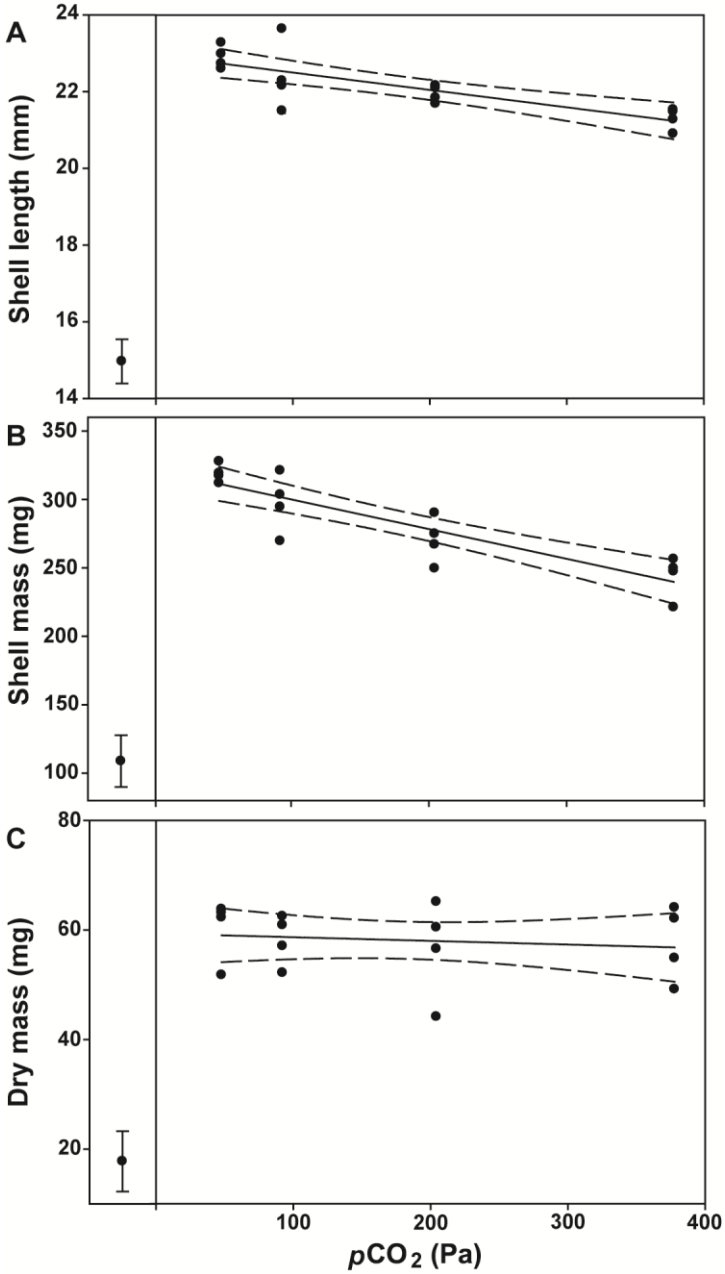
A
Shell length (mm)
24
22
20
18
16
14
B
Shell mass (mg)
350
300
250
200
150
100
C
Dry mass (mg)
80
60
40
20
100
200
300
400
pCO2 (Pa)

Figure 2

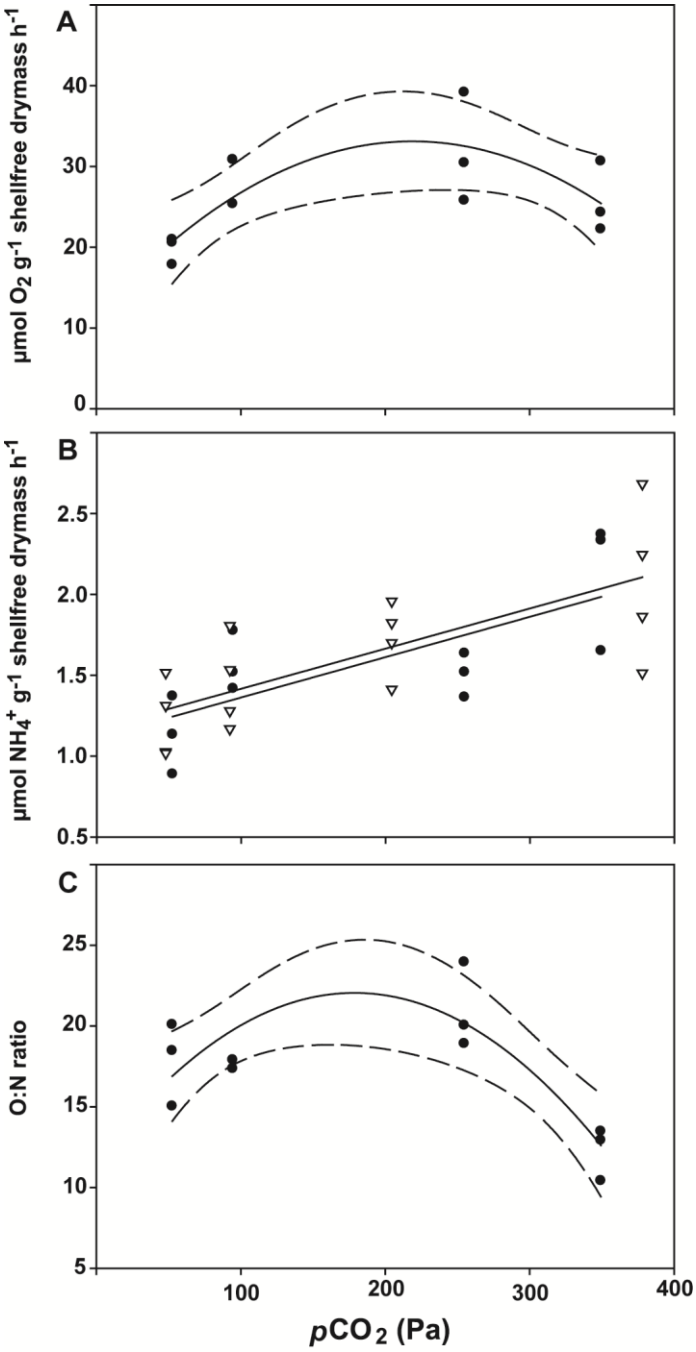
A
B
C
µmol O_2 g^{-1} shellfree drymass h^{-1}
µmol NH_4^+ g^{-1} shellfree drymass h^{-1}
O:N ratio
pCO_2 (Pa)
0
10
20
30
40
0.5
1.0
1.5
2.0
2.5
5
10
15
20
25
100
200
300
400

Figure 3

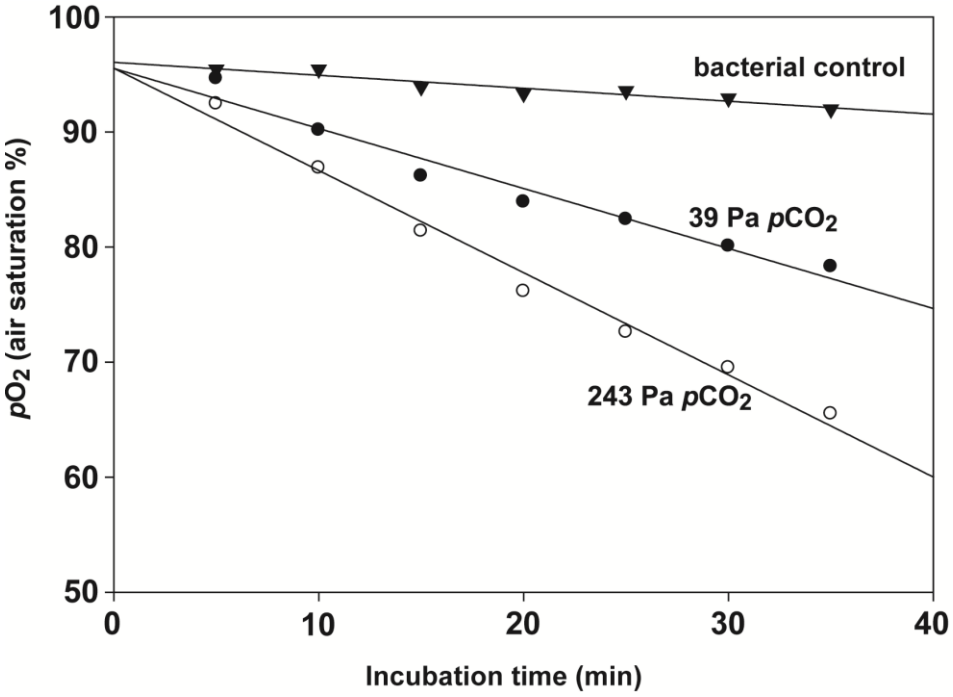
100
90
80
70
60
50
0
10
20
30
40
pO_2 (air saturation %)
Incubation time (min)
bacterial control
39 Pa pCO_2
243 Pa pCO_2

Table 1

pCO_2 treatment (Pa)	pH_{NBS}	A_T (μmol kg^{-1})	C_T (μmol kg^{-1})	pCO_2 (Pa)	Ω_{ca}	Ω_{ar}
39	8.03 ± 0.04	2044.6 ± 52.4	1968.9 ± 21.7	47.8 ± 5.3	1.86 ± 0.20	1.11 ± 0.12
113	7.70 ± 0.04	2040.7 ± 23.4	2031.1 ± 27.3	92.2 ± 6.9	1.02 ± 0.06	0.61 ± 0.04
243	7.38 ± 0.06	2051.0 ± 29.2	2124.1 ± 13.9	204.3 ± 26.6	0.50 ± 0.07	0.30 ± 0.04
405	7.14 ± 0.08	2044.3 ± 22.2	2213.9 ± 26.7	377.8 ± 24.1	0.27 ± 0.02	0.16 ± 0.01

Table 2

pCO_2 treatment (Pa)		39	113	243	405
Energy loss by respiration	mean	8.71	12.36	13.99	11.32
(J g^{-1} h^{-1})	sd	0.75	1.70	2.99	1.93
Energy loss by NH_4^+ excretion	mean	0.39	0.55	0.52	0.74
(J g^{-1} h^{-1})	sd	0.08	0.06	0.05	0.14
Total energy loss	mean	9.10	12.92	14.51	12.06
(J g^{-1} h^{-1})	sd	0.82	1.79	3.04	2.03
Fraction of NH_4^+ excretion	mean	4.30	4.29	3.67	6.12
of total energy (%)	sd	0.63	0.09	0.42	0.82

Food availability outweighs ocean acidification effects in the mussel *Mytilus edulis*

Jörn Thomsen[1,*]

Isabel Casties[1,*]

Christian Pansch[1]

Arne Körtzinger[2]

Frank Melzner[1]

[1]Marine Ecology, Leibniz-Institute of Marine Sciences (IFM-GEOMAR), Kiel 24105, Germany

[2]Chemical Oceanography, Leibniz-Institute of Marine Sciences (IFM-GEOMAR), Kiel 24105, Germany

*These authors contributed equally to this work

Abstract:

Ocean acidification is expected to decrease calcification rates of benthic calcifiers[1-5]. On regional scales, the progressing global acidification[6] can be amplified by upwelling processes and eutrophication[7,8]. In the Western Baltic Sea, high pCO_2 is encountered seasonally; however, calcifiers, such as the mussel *Mytilus edulis*, dominate the benthic community[8]. This contrasts with previous field studies from other CO_2 enriched subtropical and tropical habitats[1,9]. Here we show that high energy availability in the Western Baltic leads to the high resilience of mussels to high pCO_2. In a laboratory experiment, mussel growth rates chiefly depended on the supplied food with only minor impacts of pCO_2. Eutrophication of the Baltic causes adverse carbonate chemistry but leads to much higher productivity at the same time[10]. At a high pCO_2 field site, mussel growth exceeded that encountered at a low pCO_2 station by a factor of 7. Due to higher organic carbon concentrations at the pCO_2 high site, mussels outcompeted barnacles on settlement panels. Mussels benefit from high energy availability in this coastal habitat and have adapted within less than 50 years to high and fluctuating CO_2 partial pressures without losing their dominant position in the benthic habitat[11]. We conclude that benthic stages of *M. edulis* tolerate very high ambient pCO_2 when food supply is abundant and that species interactions and specific biotic and abiotic factors such as nutritional supply need to be considered when predicting species vulnerability to ocean acidification.

Increasing atmospheric CO_2 concentrations are reducing ocean pH[6]. However, in coastal areas surface pCO_2 can deviate most strongly from the atmospheric values as a consequence of local processes such as upwelling[7] and eutrophication[10]. In Kiel Fjord, Western Baltic Sea, transport of low pO_2 bottom water to the surface leads to pCO_2 values up to 2300 µatm[8]. Additionally, the Western Baltic Sea is characterized by a permanently low calcium carbonate saturation state (Ω), which is due to the low prevalent seawater alkalinity[4,8]. Future ocean acidification will therefore lead to very high summer and autumn seawater pCO_2 in estuarine coastal habitats, with regular occurrence of pCO_2 values of >2000 µatm likely by the year 2100[8].

Ocean acidification is expected to lower biomineralisation rates of calcifiers[2-5], but recent studies also revealed unchanged or even increased calcification rates at high pCO_2 indicating a considerable potential for acclimation[12]. As most of the present laboratory studies only covered a relative short fraction of the total lifespan of long lived metazoans, their predictive power is limited. Therefore, naturally CO_2 enriched habitats provide the possibility to investigate long-term acclimation or even adaptation to elevated pCO_2. A gradual decline of the number of calcifying species has been observed along a natural pCO_2 gradient in the Mediterranean Sea[1]; similar observations were made along a tropical pCO_2 gradient[9]. In contrast, benthic metazoan communities in Kiel Fjord are dominated by calcifying invertebrates such as *Mytilus edulis* and *Amphibalanus improvisus*[8].

Calcification is a complex, biologically controlled process. Shell $CaCO_3$ and a diverse set of shell organic matrix molecules are produced intracellularly and are exported to sites of incipient biomineralization[13]. Further, a number of invertebrates protect their external shells from the surrounding water with chemically robust organic covers such as the periostracum in the case of bivalves[14]. Therefore, shell production is not necessarily related to external [CO_3^{2-}] but is an energetically costly process, primarily due to the production of the organic components[15]. Increased metabolic rates and shifts of cellular energy budgets towards ion regulation required for cellular homeostasis under elevated pCO_2 may thereby reduce the energy available for growth and calcification[16-19].

Here we tested, whether increased energy supply enables mussels to overcome energetic constraints under elevated pCO_2 in a laboratory and an accompanying field study. Mussels, freshly settled on PVC panels in Kiel Fjord, were transferred into experimental aquaria and incubated at four pCO_2 (range 470-3350 µatm,) and three feeding levels for seven weeks (Supplementary Table S1+S2). Feeding regime and pCO_2 had significant effects on shell length, inorganic shell component (ISC) and total organic component (TOC) growth (Fig. 1). The observed growth was described best using a two factorial linear model (see Fig. 1 caption). However, AIC analysis revealed that single factor models based on food supply, explained most of the variability encountered in the experiment (Supplementary table S3). The inorganic shell component (ISC) growth was significantly affected by food level and pCO_2 (Two-way ANOVA: factor food supply: $F_{(2,72)}=40.6$, $p<0.01$, factor pCO_2: $F_{(3,72)}=3.27$, $p<0.05$, interaction: $F_{(6,72)}=1.07$, $p>0.5$, Fig. 1D), whereas total organic component (TOC) growth was significantly influenced by food supply but not by pCO_2 (Two-way ANOVA: factor food supply: $F_{(2,72)}=51.84$, $p<0.01$, factor pCO_2: $F_{(3,72)}=1.19$, $p=0.32$, interaction: $F_{(6,72)}=1.02$, $p>0.5$, Fig. 1D). Settled mussels consisted of about 20% organic and 80% inorganic ($CaCO_3$) material whereby approx. 50%

of the produced organic mass corresponded to the structural organic material of the shell (OSC), i.e. matrix proteins and carbohydrates as well as the outer periostracum. The remaining organic mass corresponded to somatic tissue (shell free drymass, SFDM, Supplementary Fig. S1). We estimate that about 60% of the total energy necessary for body growth was invested into synthesis of organic and inorganic shell components (Supplementary Table S4). Our study demonstrates the ability of freshly settled *M. edulis* to calcify under highly elevated pCO_2 when nutritional supply is sufficient and confirms results obtained for adult mussels[8,16,20]. Whereas the shell mineralogy of freshly settled *M. edulis* is similar to that of older mussels[21], the organic shell component is much higher in younger (>10%, Supplementary Table S4) than in fully grown mussels (1-6%[22], Supplementary Table S5). As the production of organic components requires high amounts of energy (Supplementary Fig. S2), downregulation of shell formation processes can contribute significantly to energy conservation during unfavourable, low food periods or during exposure to very high ambient pCO_2 [23]. No mortality was encountered in our experiment (Fig S1). This is in contrast to high mortality observed in metamorphosed larvae of other bivalve larvae[3].

In the field, long-term monitoring confirmed that inner Kiel Fjord (IF) is characterized by elevated mean pCO_2 values and a large seasonal pCO_2 variability[8]. Occasional upwelling of hypoxic bottom water in late summer and autumn leads to increased pCO_2 and lowered pH (Fig. 2, Supplementary Table S5). Whereas elevated pCO_2 values persist at the surface due to the slow air-sea equilibration time-scale of the carbonate system, physically dissolved oxygen rapidly equilibrates with the atmosphere resulting in pO_2 >50% air saturation (C. Clemmesen, GEOMAR, unpublished data 2006-2011). Along a gradient along the axis of Kiel Fjord, average surface pCO_2 and variability decreased towards the fjord opening (from 706±461 µatm at station 1 to 447±162 µatm at station 4, Fig. 2a). Permanently low surface $\Omega_{aragonite}$ was measured and undersaturation (i.e., $\Omega_{aragonite}<1$) occurred in 35 out of 55 weeks investigated (Supplementary Table S6). High pCO_2 values are a consequence of aerobic degradation in the bottom water during the seasonal stratification, a natural seasonal process in the Baltic that has been greatly amplified by eutrophication over the last 50 years [10,24].

In order to test whether the observed pCO_2 gradient in the Fjord would influence calcification rates of *M. edulis*, we transferred settlement panels with freshly settled mussels to the inner and the outer fjord area. The field growth study demonstrated that high energy availability at the high pCO_2 IF station enabled higher growth and calcification rates and almost complete mussel dominance of the benthic community when compared to the low pCO_2 outer fjord area (Fig. 3+4). Although the mean pCO_2 at IF was significantly higher in comparison to station OF (969±420 µatm vs. 599±283 µatm, Tab. 1, Fig. 4f, paired t test $t=2.46$, $p<0.05$, $N=7$), shell length growth rates were much higher with 1.1 mm $week^{-1}$ (IF) vs. 0.5 mm $week^{-1}$ (OF, Supplementary Fig. 3). Final shell lengths and masses at IF of 18.3±6.8 mm and 226±169.4 mg exceeded those encountered at OF by far (9.4±3.4 mm and 33.0±22.8 mg, Fig. 4). Settlement panels were almost completely dominated by *M. edulis* at both stations and only the barnacle *Amphibalanus improvisus* was able to exclusively cover smaller parts of the panels at station OF (Fig. 3+Supplementary Fig. S4, Supplementary Table S7). Barnacles, thought to be even more tolerant to acidification than mussels[25], were outcompeted at station IF. Whereas $CaCO_3$ production of both species was similar at station OF with 13.8±4.9 (mussels) vs. 14.2±4.3 (barnacles) g $panel^{-1}$,

mussel production exceeded that of barnacles about 12 –fold at station IF (101.2±24.3 vs. 8.0±2.9 g panel^{-1}). This is most probably due to restriction of barnacle food supply by fast growing mussels and very high recruitment intensity. High filtration and clearance rates by *M. edulis*, spatial restriction of barnacle feeding apparatus and depletion of planktonic organisms are probable causes for starvation induced high mortality (>75%) of barnacles at station IF (Tab.1).

M. edulis lacks the ability to control extracellular pH (Supplementary figure S5+Table S8), but intracellular pH is tightly regulated and maintained at control levels under acidification stress[20,26]. A causal connection between cellular ion homeostasis and calcification is given, as vesicular production of an amorphous calcium carbonate precursor (ACC) occurs intracellularly[13]. Excess intracellular protons generated during calcification then need to be excreted against an increased extracellular proton concentration, which most likely consumes more energy. Upregulation of energy demanding ion transport processes would then compromise the cellular energy budget[17]. Higher metabolic rates in response to elevated pCO_2 have in fact been observed in invertebrates[16,18]. Higher maintenance costs for intracellular homeostasis under CO_2 stress might be one main cause for the decrease in calcification rates observed in mytilid bivalves. On the other hand, seawater [CO_3^{2-}] and $CaCO_3$ saturation seem to be only of minor importance for gross calcification in *M. edulis*. However, both external[8] and internal shell dissolution[27] may occur when seawater and/or haemolymph are strongly undersaturated with $CaCO_3$. While external dissolution is related to periostracum fractures and cannot be prevented by the organism, internal dissolution is under strong biological control and closely related to energy budget constraints[27]. Therefore, in both juvenile and adult mussels, higher energy supply meets the higher energy demand under elevated pCO_2.

In Kiel Fjord, elevated pCO_2 does not decrease the productivity of calcifying metazoans, which is in contrast to other field studies along natural pCO_2 gradients [1,9]. Peak pCO_2 observed during summer months in inner Kiel Fjord can reach >2000 µatm - pCO_2 levels that have been shown to cause abnormal development of *M. galloprovincialis*[28]. However, successful settlement and highest growth rates were documented during the period of the year with most adverse carbonate system conditions, but best food supply at the same time[8]. Overall, the effect of seawater acidification seems to be marginal compared to the effect of food supply, with no reductions in growth and calcification up to a seawater pCO_2 of 2100 µatm observed in our laboratory experiment. In the field, the high particulate organic carbon (POC) concentrations in Kiel Fjord enable overcompensation of the adverse carbonate system conditions. In other coastal areas with comparable POC concentrations (e.g. the North Sea), mussels may also be able to compensate negative effects of high CO_2 by means of high energy availability. In contrast, in oligotrophic ocean regions like the Mediterranean Sea such compensatory effects might not be possible[29]. Due to the eutrophication process in the recent past of the Baltic[10,24], we conclude that the benthic community in Kiel Fjord has been subjected to a rapid change towards high ambient pCO_2 within less than 50 years, without impacting the dominant position of *M. edulis* in this habitat[11]. This implies a high tolerance to high and variable pCO_2 of mussels in general, or an expressed capacity for rapid adaptation to high pCO_2. Simulated selection of *M. trossulus* larvae under an elevated pCO_2 regime revealed significant adaptation potential within a similar period[30].

In summary, the present study demonstrates a high inherent resilience of calcifying benthic communities in estuarine, eutrophic habitats to elevated seawater pCO_2. Food supply, and not pCO_2, appears to be the primary factor driving biomass and biogenic $CaCO_3$ production, as well as community structure. Our findings emphasize the need to include additional factors such as habitat energy availability in order to predict single- and multi-species responses towards ocean acidification.

Material and methods: (SHORT)

Water chemistry of Kiel Fjord was monitored on weekly (station 1) and bi-weekly (stations 2-4) cruises using R/V Polarfuchs (Supplementary Table 6) and samples were analyzed for dissolved inorganic carbon (C_T) and alkalinity (A_T) using SOMMA and VINDTA autoanalyzers. The pH on the total scale (pH_T) and C_T of samples taken during the laboratory and the field growth experiment were measured using a Metrohm 6.0262.100 electrode and 626 Metrohm pH meter and an AIRICA C_T analyzer. Carbonate system specifications were calculated using the CO2SYS program. Particulate organic carbon (POC) was determined from 500 mL water samples which were taken from the experimental aquaria and the field stations and filtered on combusted GF/F filters. Filters were treated with hydrochloric acid, dried and analyzed with an elemental analyzer (Euro vector 3000). Settlement panels were suspended in Kiel Fjord at station IF for 10 days. Panels were removed, cleaned from fouling organisms other than 100 freshly settled *M. edulis* and stored in separate aquaria. For the laboratory experiment, single panels were transferred to 500 mL aquaria at 17°C. The experiment lasted for 7 weeks and four pCO_2 treatments (470, 1020, 2110, 3350 µatm) and three feeding levels (low, intermediate, high) were established. On a weekly basis, the amount of supplied food was steadily increased and the number of specimens per aquarium was reduced in order to compensate for mussel growth. The ratio between the feeding levels of 1:5:10 was maintained constant throughout the experiment. Shell lengths were measured weekly and final inorganic (ISC) and total organic (TOC) components of mussels were determined by weighing after samples were dried (60°C, 24h) and ashed (500°C, 24h). Energetic contents of supplied *Rhodomonas* and of mussel biomass were calculated according to literature values. In the field study, settlement panels were transferred to inner fjord (IF) and outer fjord (OF) stations. Water carbonate chemistry (pH, pCO_2, Ω) and POC were monitored bi-weekly and mussels were sampled for determination of shell length and mass growth. Finally, panels were removed from the water after an incubation period of 18 weeks. Coverage of mussels and barnacles was determined using ImageJ software and total $CaCO_3$ production per panel was determined after ashing. Extracellular acid-base status of *M. edulis* haemolymph was determined for mussels directly sampled from the inner fjord. pH was measured using a pH microelectrode and C_T with a Corning 965 C_T analyzer. Extracellular pCO_2, $[HCO_3^-]$ and $[CO_3^{2-}]$ were calculated according to the Henderson-Hasselbalch-Equation. See full methods for details.

Acknowledgements:

The authors like to thank D. Rossoll, H. Ossenbrügger, K. Trübenbach, L. Töpfer, H. Mempel and Captain and Crew of RV Polarfuchs for supporting carbonate chemistry sampling and S. Grobe, T. Steinhoff, S. Fessler, and V. Saderne for help with the measurements. P. Fritsche and A. Stuhr provided nutrient data, A. Zavisic measured POC and P. Schubert contributed the map of Kiel Fjord. Further, we acknowledge U. Panknin for maintaining *Rhodomonas* cultures and R. Schütt for species analysis on the settlement panels. This study was funded by the DFG Excellence Cluster ´Future Ocean´ and the German ´Biological impacts of ocean acidification (BIOACID)` project 3.1.3, funded by the Federal Ministry of Education and Research (BMBF, FKZ 03F0608A).

References:

1. Hall-Spencer, J. M. *et al*. Volcanic carbon dioxide vents show ecosystem effects of ocean acidification. *Nature*, 454, 96-99 (2008).
2. Wootton, J. T., Pfister, C. A. & Forester, J. D. Dynamic patterns and ecological impacts of declining ocean pH in a high-resolution multi-year dataset. *P. Natl. Acad. Sci. USA*, 105, 18848-18853 (2008).
3. Talmage, S.C. & Gobler, C.J. Effects of past, present, and future ocean carbon dioxide concentrations on the growth and survival of larval shellfish. *P. Natl. Acad. Sci. USA*,107, 17246-17251 (2010).
4. Haynert, K., Schönfeld, J., Riebesell, U. & Polovodova, I. Biometry and dissolution features of the benthic foraminifer *Ammonia aomoriensis* at high pCO_2. *Mar. Ecol.-Prog. Ser.*, 432, 53-67 (2011).
5. Lischka, S., Büdenbender, J., Boxhammer, T. & Riebesell, U. Impact of ocean acidification and elevated temperatures on early juveniles of the polar shelled pteropod *Limacina helicina*: mortality, shell degradation, and shell growth. *Biogeoscience*, 8, 919-932 2011).
6. Cao, L. & Caldeira, K. Atmospheric CO_2 stabilization and ocean acidification. *Geophys. Res. Lett.*, 35, L19609 (2008).
7. Feely, R.A. *et al*. The combined effects of ocean acidification, mixing, and respiration on pH and carbonate saturation in an urbanized estuary. *Estuar. Coast Shelf S.*, 88, 442-449 (2010).
8. Thomsen, J. *et al*. (2010). Calcifying invertebrates succeed in a naturally CO_2 enriched coastal habitat but are threatened by high levels of future acidification. *Biogeosciences*, *7*, 3879-3891.

9. Fabricius, K.E. *et al*. Losers and winners in coral reefs acclimatized to elevated carbon dioxide concentrations. *Nature Clim.* , 1, 165-169 (2011).
10. HELCOM Eutrophication in the Baltic Sea – An integrated thematic assessment of the effects of nutrient enrichment and eutrophication in the Baltic Sea region. Balt. Sea Environ. Proc. No. 115B (2009).
11. Boje, R. Die Bedeutung von Nahrungsfaktoren für das Wachstum von Mytilus edulis L. in der Kieler Förde und im Nord-Ostsee Kanal. Kieler Meeresforsch., 21, 81-100 (1965).
12. Ries, J.B., Cohen, A.L. & McCorkle, D.C. Marine calcifiers exhibit mixed responses to CO_2-induced ocean acidification. *Geology*, 37, 1131-1134 (2009).
13. Addadi, L., Politi, Y., Nudelman, F., & Weiner, S. Biomineralization design strategies and mechanisms of of mineral formation: operating at the edge of instability. in: *Engineering of crystalline materials properties* (ed. Novoa, J..J.), Springer, Heidelberg, 1-15 (2008).
14. Waite, J., Saleuddin, A., & Andersen, S. Periostracin — A soluble precursor of sclerotized periostracum in *Mytilus edulis* L. *J. Comp. Physiol B, 130*, 301-307 (1979).
15. Palmer, A. R. Calcification in marine mollusks - How costly is it. *P. Natl. Acad. Sci. USA*, 89, 1379-1382 (1992).
16. Thomsen, J. & Melzner, F. Moderate seawater acidification does not elicit long-term metabolic depression in the blue mussel *Mytilus edulis*. *Mar. Biol.*, 157, 2667-2676 (2010).
17. Deigweiher, K., Hirse, T., Bock, C., Lucassen, M. & Pörtner, H.O. Hypercapnia induced shifts in gill energy budgets of Antarctic notothenioids. *J. Comp. Physiol. B*, 180, 347-359 (2009).
18. Stumpp, M., Wren, J., Melzner, F., Thorndyke, M.C. & Dupont, S. CO_2 induced seawater acidification impacts sea urchin larval development I: Elevated metabolic rates decrease scope for growth and induce developmental delay. *Comp. Biochem. Phys. A*, 160, 331-340 (2011).
19. Hu, M. Y.-A. *et al*. Elevated seawater pCO_2 differentially affects branchial acid-base transporters over the course of development in the cephalopod *Sepia officinalis*. *Am. J. Physiol.-Reg. I*, 300, R1100-R1114 (2011).
20. Michaelidis, B., Ouzounis, C., Paleras, A.,& Pörtner, H.O. Effects of long-term moderate hypercapnia on acid-base balance and growth rate in marine mussels *Mytilus galloprovincialis*. *Mar. Ecol.-Prog. Ser.*, 293, 109-118 (2005).

21. Medaković, D., Popović, S., Gržeta, B., Plazonić, M. & Hrs-Brenko, M. X-ray diffraction study of calcification processes in embryos and larvae of the brooding oyster *Ostrea edulis. Mar. Biol.*, 129, 615-623 (1997).
22. Jörgensen, C. Growth efficiencies and factors controlling size in some mytilid bivalves, especially *Mytilus edulis* L.: Review and interpretation. *Ophelia*, 15, 175-192 (1976).
23. Gazeau, F. *et al*. Effect of ocean acidification on the early life stages of the blue mussel *Mytilus edulis*. *Biogeosciences*, 7, 2051-2060 (2010).
24. Babenerd, B. Increasing oxygen deficiency in Kiel Bay (Western Baltic). *Mar. Res*., *33*, 121-140 (1991).
25. Pansch, C., Nasrolahi, A., Appelhans Y.S. & Wahl. M. Impacts of ocean warming and acidification on the larval development of the barnacle *Amphibalanus improvisus*. J. Exp. Mar. Biol. Ecol. in press
26. Zange, J., Grieshaber, M.K. & Jans, A.W. The regulation of intracellular pH estimated by ^{31}P-NMR spectroscopy in the anterior byssus retractor muscle of *Mytilus edulis* L. *J. Exp. Biol.*, 150, 95-109 (1990).
27. Melzner, F. *et al*. Interactive effects of of food supply and seawater pCO_2 on calcification and internal shell dissolution in the blue mussel *Mytilus edulis. Plos One, 6, e24223* (2011).
28. Kurihara, H., Asai, T., Kato, S. & Ishimatsu, A. Effects of elevated pCO_2 on early development in the mussel *Mytilus galloprovincialis*. *Aquat. Biol.*, 4, 225-233 (2008).
29. Rodolpho-Metalpa, R. *et al*. Coral and mollusc resistance to ocean acidification adversely affected by warming. Nature Clim., 1, 308-312 (2011).
30. Sunday, J.M., Crim, R.N., Harley, C.D.G. & Hart, M.W. Quantifying rates of evolutionary adaptation in response to ocean acidification. *Plos One*, 6, e22881 (2011).

Figure legends

Figure 1: *Mytilus edulis* shell and somatic growth during the experiment. Weekly measured shell length of mussels from the four pCO_2 and three feeding treatments (A-C). Shell length growth could best be described with the following two factorial linear regression: shell length growth (µm) = 1312.2 (±150.6) - 0.148 (± 0.06) pCO_2 (µatm) + 46.83 (±3.81) energy supply (J), R^2=0.66, $F_{(2,81)}$=78.4, p<0.01; (A-C). Final shell $CaCO_3$ growth (filled bars) and total organic growth (SFDM+OSC, striped bars, $CaCO_3$: Two-way ANOVA: factor energy: F(2,72)=40.6, p<0.01, factor pCO_2: F(3,72)=3.27, p<0.05, interaction: $F_{(6,72)}$=1.07, p<0.5, total organic: Two-way ANOVA: factor energy: F(2,72)=51.84, p<0.01, factor pCO_2: F(3,72)=1.19, p>0.05, interaction: $F_{(6,72)}$=1.02, p<0.5; (D), n=7 for all treatments. bars represent means ± SD.

Figure 2: Box-whisker-plot of Kiel Fjord pCO_2 in 2009/2010 measured at stations 1-4 in surface (light grey, s) and bottom (dark grey, b) water samples. Circles depict individual measurements (A); Time course of surface pH_{NBS} in inner Kiel Fjord (station IF) between 2008 and 2010, data from 2008-2009 adopted from Thomsen et al. 2010 (B).

Figure 3: Map of Kiel Fjord with representative settlement plates from the outer Fjord (OF) and the inner Fjord (IF) and the average carbonate system speciation during the field study, Numbers 1-4 indicate the stations of the carbonate system monitoring program, the brown circles indicate the positions of stations OF and IF, original size of the PVC panels 5cm x 5cm (panels are fully overgrown with mussels and barnacles). Pictures are drawn to scale, scale bar 5cm **.**

Figure 4: Results of the field study (outer Fjord: white, inner Fjord: black): Final mean $CaCO_3$ mass of *M. edulis* per settlement plate (A), Final shell mass and length of individual *M. edulis* grown at the outer and inner Fjord (B), POC concentrations (C), Mean values for abiotic conditions during the experimental period at both sites (D-F), $\Omega_{aragonite}$ (D), pH_{total} (E), pCO_2 in µatm (F); bars represent means ± SD.

Table legend

Table 1: Abiotic seawater conditions and carbonate system parameters (measured: Sal, T, POC, C_T, pH and calculated: A_T, pCO_2, $\Omega_{calcite}$ and $\Omega_{aragonite}$) at the field sites (A), final morphometry of individual specimens, plate coverage and $CaCO_3$ production on the settlement panels at the end of the field study (B), values exceeding 100% coverage result from secondary settlement of *M. edulis* spat on existing mussel beds, see panels in Fig. 3, POC and PON concentration and C:N ratio at the field sites; values represent means ± SD

Figure 1

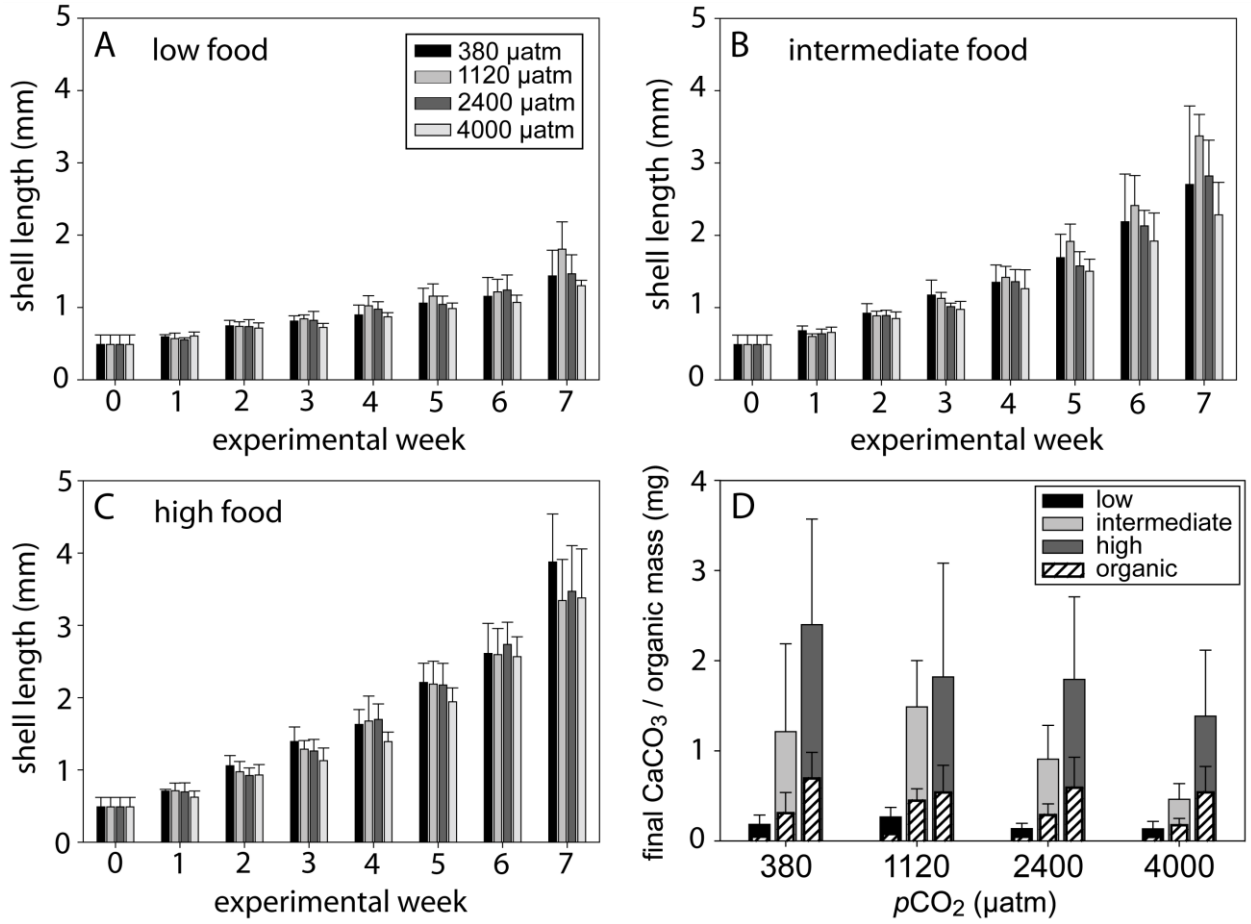
A
low food
380 µatm
1120 µatm
2400 µatm
4000 µatm
shell length (mm)
experimental week
B
intermediate food
C
high food
D
low
intermediate
high
organic
final CaCO3 / organic mass (mg)
pCO2 (µatm)
380
1120
2400
4000

Figure 2

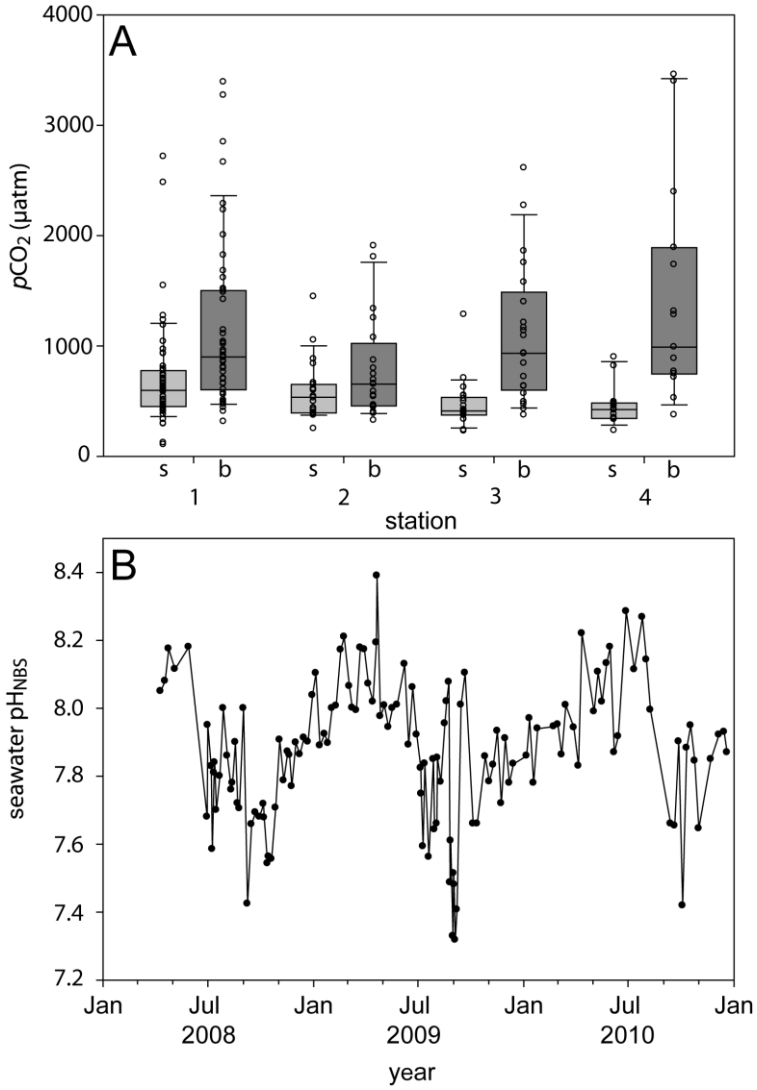
A
4000
3000
2000
1000
0
pCO_2 (µatm)
s
b
1
2
3
4
station
B
8.4
8.2
8.0
7.8
7.6
7.4
7.2
seawater pH_{NBS}
Jan
Jul
2008
2009
2010
year

Figure 3

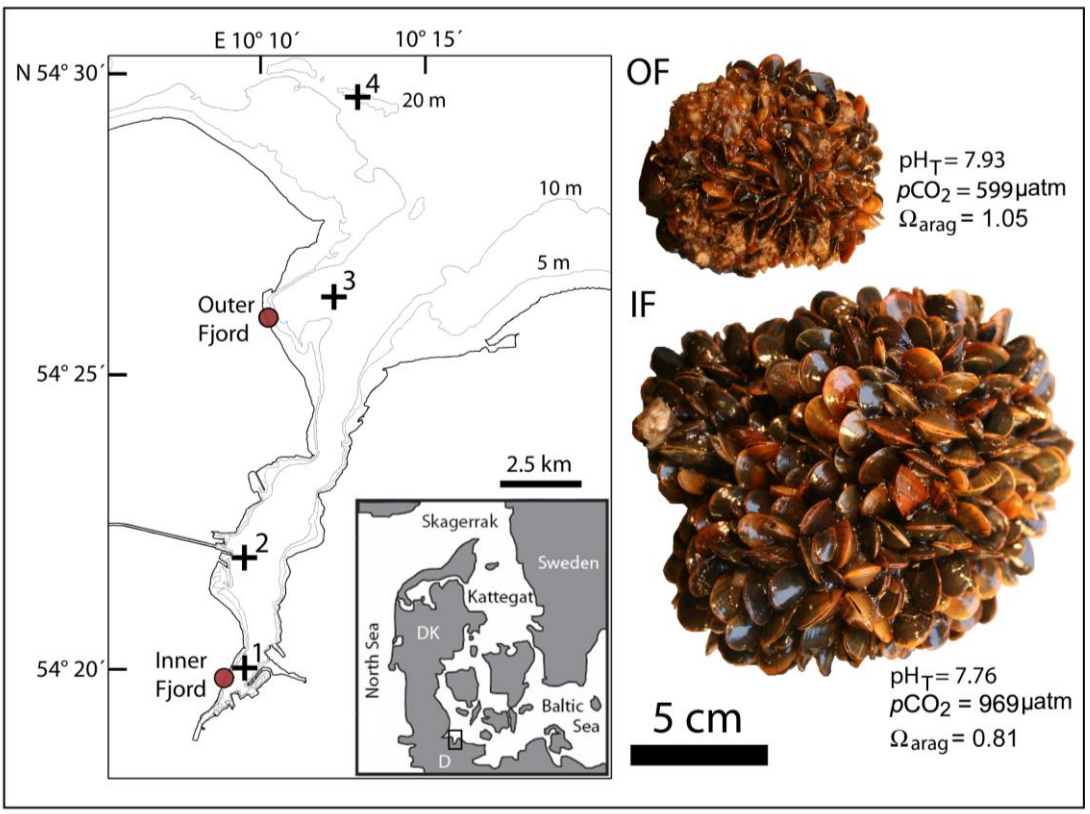
E 10° 10´
10° 15´
N 54° 30´
54° 25´
54° 20´
4
20 m
10 m
5 m
3
Outer
Fjord
2
1
Inner
Fjord
2.5 km
Skagerrak
Sweden
Kattegat
DK
North Sea
Baltic
Sea
D
OF
pH$_T$ = 7.93
pCO$_2$ = 599 µatm
Ω$_{arag}$ = 1.05
IF
pH$_T$ = 7.76
pCO$_2$ = 969 µatm
Ω$_{arag}$ = 0.81
5 cm

Figure 4

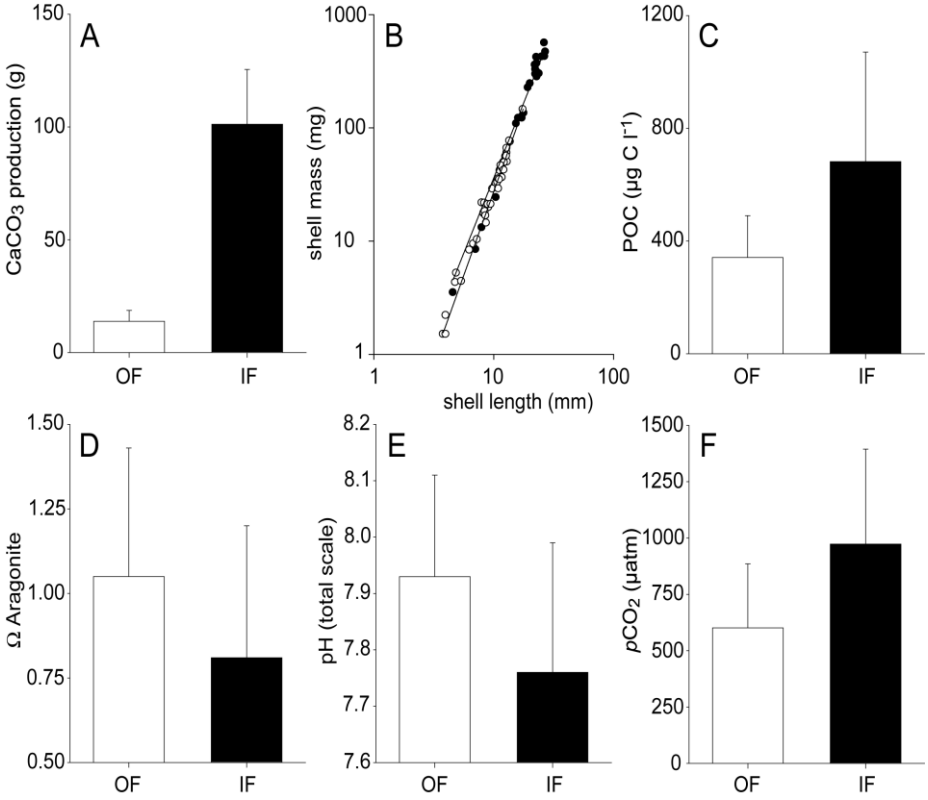
A
B
C
D
E
F
CaCO3 production (g)
shell mass (mg)
shell length (mm)
POC (µg C l-1)
Ω Aragonite
pH (total scale)
pCO2 (µatm)
OF
IF
150
100
50
0
1000
10
1
1
10
100
1200
800
400
1.50
1.25
1.00
0.75
0.50
8.2
8.1
8.0
7.9
7.8
7.7
7.6
1500
1250
1000
750
500
250

Table 1

A			carbonate system parameters					
site	Salinity	Temperature °C	C_T µmol kg^{-1}	A_T µmol kg^{-1}	pH total scale	pCO_2 µatm	Ω calcite	Ω aragonite
Inner Fjord	16.2 ± 2.0	13.2 ± 3.0	1996.5 ± 104.8	2021.1 ± 95.1	7.76 ± 0.23	969 ± 420	1.38 ± 0.68	0.81 ± 0.39
Outer Fjord	16.0 ± 1.4	12.5 ± 2.8	1829.1 ± 99.8	1945.5 ± 56.8	7.93 ± 0.18	599 ± 283	1.79 ± 0.65	1.05 ± 0.38

B	single specimens				settlement plates			
site	shell length mm	shell mass mg	drymass mg	mussel coverage %	barncale coverage %	barnacle survival %	mussel $CaCO_3$ g plate^{-1}	barnacle $CaCO_3$ g plate^{-1}
Inner Fjord	18.3 ± 6.8	226.6 ± 169.4	51.1 ± 42.2	166.7 ± 25.8	66.7 ± 44.6	24.2 ± 22.4	101.2 ± 24.3	8.0 ± 2.9
Outer Fjord	9.4 ± 3.4	33.0 ± 22.8	5.8 ± 4.3	87.5 ± 25.0	95.0 ± 10.0	62.5 ± 14.4	13.8 ± 4.9	14.2 ± 4.3

C	nutrition		
site	POC µg l^{-1}	PON µg l^{-1}	C:N molar ratio
Inner Fjord	682 ± 388	92 ± 46	8.8 ± 1.8
Outer Fjord	342 ± 148	50 ± 23	8.1 ± 0.7

Supplementary information:

Supplementary Figure S1: Energetic content (J) of the $CaCO_3$ mass (filled bars) and total organic mass (SFDM+OSC, striped bars) of settled *M. edulis* larvae. Calculation was performed by converting the masses shown in Figure 1D into energy using values of 2 J mg^{-1} for $CaCO_3$ and 23 J mg^{-1} for organic mass (references 9,10, B), n=7; bars represent means ± SD

Supplementary Figure S2: Total organic content (TOC = shell free dry mass (SFDM) + OSC, black) and organic shell component (OSC = shell matrix proteins and carbohydrates + periostracum, white) of settled *M. edulis* as a function of shell length. TOC = 0.018(±0.003)*SL(mm)^2.705(±0.125), $F_{(1,84)}$=959.4, p<0.01; OSC = 0.009(±0.002)*SL(mm)^2.735(±0.127), $F_{(1,82)}$=987.2, p<0.01

Supplementary Figure S3: Bi-weekly measured shell length of settled *M. edulis* sampled during the field experiment in 2010, inner fjord (black), outer fjord (grey); bars represent means ± SD

Supplementary Figure S4: Coverage (A) and $CaCO_3$ production (B) of *M. edulis* (black) and *A. improvisus* (grey) on settlement panels at stations OF and IF; bars represent means ± SD

Supplementary Figure S5: Relationship of haemolymph pH (pH_{HL}) of *M. edulis* and ambient seawater pH_{NBS} (pH_{SW}) measured in 2009, pH_{HL} =0.413(±0.08) x pH_{SW} + 4.14(±0.64), F(1,60)=26.5 p<0.01; each data point represents mean ± SD of n=5 mussels from one sampling date (C).

Supplementary Figure S1

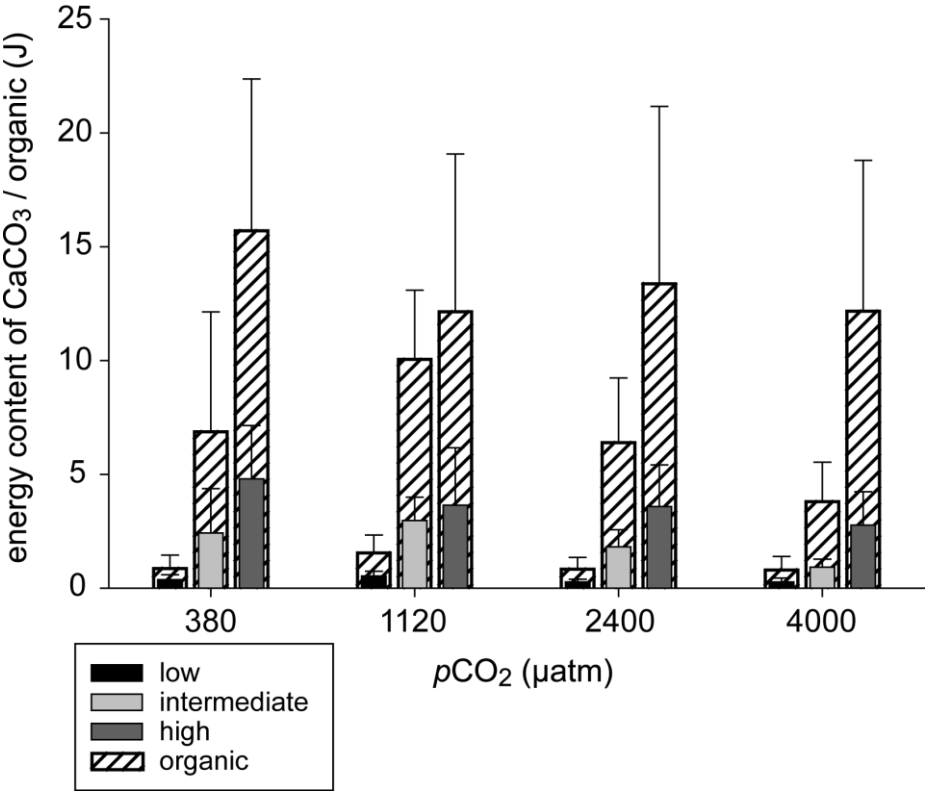

Supplementary Figure S2

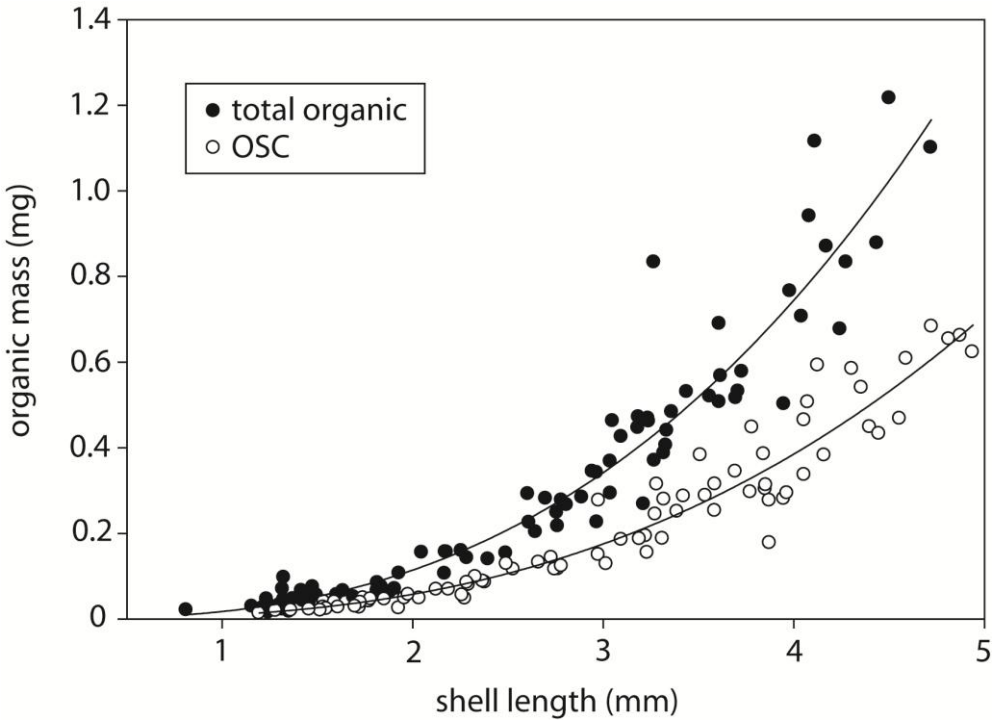

Supplementary Figure S3

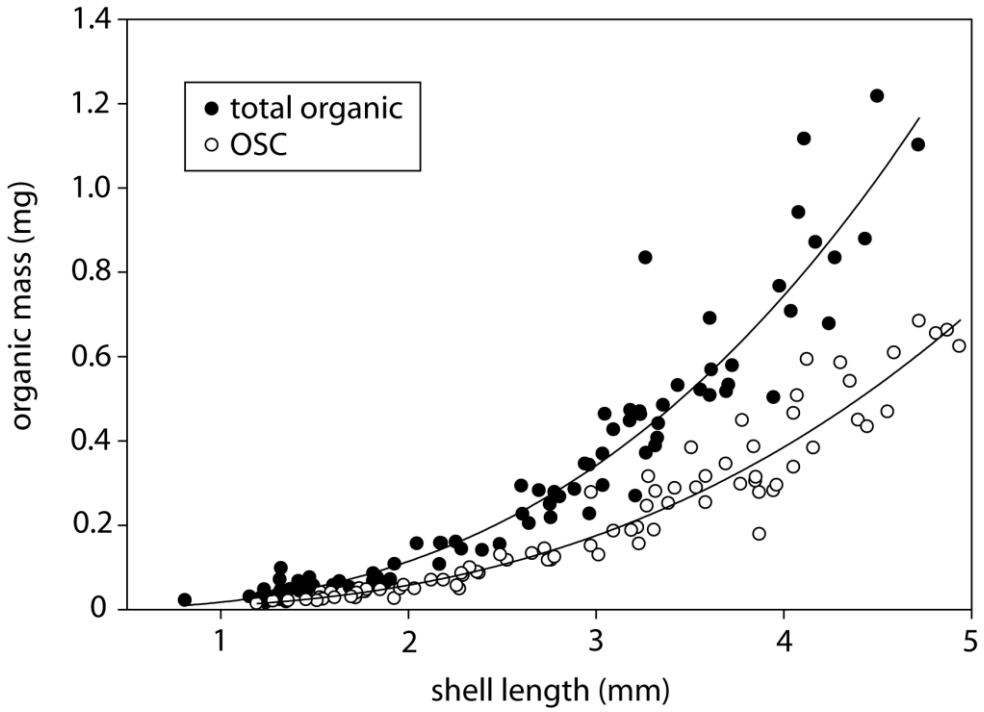

Supplementary Figure S4

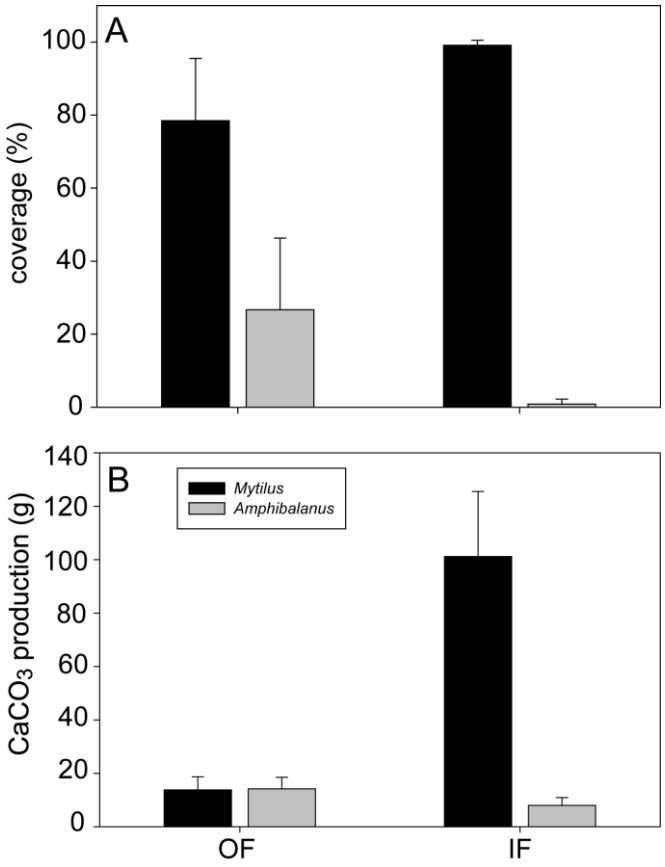

Supplementary Figure S5

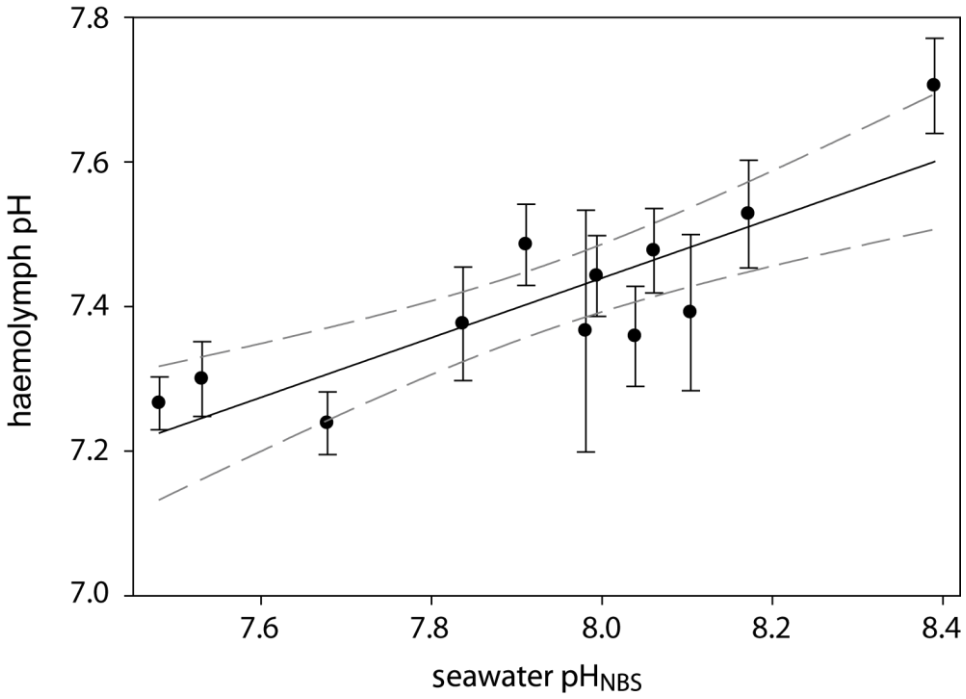

Supplementary table S1: Energy supply settings and weekly shell length growth during the laboratory experiment. Data are mean values of all pCO_2 treatments per feeding level. Shell length growth was calculated from weekly measurements and pooled for all pCO_2 treatments of one feeding level; values represent means ± SD

week	# animal per aquarium	feeding treatment	supplied algae cells mL^{-1}	supplied energy J day^{-1} $animal^{-1}$	weekly shell length growth in %
1	100	low	500	0.05	18.9 ± 4.8
		intermediate	2500	0.06	31.8 ± 6.8
		high	5000	0.09	40.2 ± 8.5
2	95	low	700	0.04	27.6 ± 6.5
		intermediate	3500	0.07	38.8 ± 7.6
		high	7000	0.15	43.6 ± 7.4
3	80	low	1500	0.02	9.8 ± 5.5
		intermediate	7500	0.09	21.6 ± 7.6
		high	15000	0.19	31.9 ± 6.0
4	50	low	2000	0.06	18.5 ± 5.4
		intermediate	10000	0.28	26.6 ± 7.7
		high	20000	0.63	27.3 ± 7.8
5	30	low	3000	0.12	13.3 ± 4.9
		intermediate	1500	0.54	26.6 ± 7.8
		high	30000	1.03	34.9 ± 4.2
6	20	low	3500	0.19	11.4 ± 5.7
		intermediate	17500	0.80	30.0 ± 4.4
		high	35000	1.56	24.0 ± 6.8
7	10	low	4000	0.38	29.6 ± 15.2
		intermediate	20000	1.57	30.0 ± 9.6
		high	40000	3.07	33.9 ± 10.1

Supplementary table S2: Carbonate system speciation during the laboratory experiment, mean salinity = 14.2±0.9, mean temperature = 17.2±0.2°C; values represent means ± SD

treatment	C_T	pH	A_T	pCO_2	Ω	Ω
µatm	µmol kg^{-1}	total scale	µmol kg^{-1}	µatm	calcite	aragonite
380	1774.8 ± 28.7	8.01 ± 0.03	1866.5 ± 30.5	472.1 ± 29.0	2.20 ± 0.11	1.29 ± 0.06
1120	1877.6 ± 44.1	7.70 ± 0.01	1899.4 ± 39.3	1021.2 ± 31.4	1.15 ± 0.06	0.67 ± 0.04
2400	1964.4 ± 41.2	7.40 ± 0.02	1914.6 ± 29.9	2114.3 ± 73.0	0.59 ± 0.04	0.35 ± 0.02
4000	2034.7 ± 31.2	7.19 ± 0.04	1924.8 ± 31.5	3350.0 ± 273.7	0.39 ± 0.04	0.23 ± 0.03

Supplementary table S3: Multiple regression of observed growth of shell length, inorganic shell component (ISC) and total organic (TOC) A; Comparison of growth model using AIC, B.

A	shell length	(µm) = 1312 (±150.6) - 0.148 (± 0.06) pCO_2 (µatm) + 46.83 (±3.81) energy supply (J)					
		r^2 = 0.66	F =78.4		p<0.001		
	CaCO3	(mg) = 0.50 (±0.17) - 0.0002 (±0.00006) pCO_2 (µatm) + 0.039 (±0.004) energy supply (J)					
		r^2 = 0.53	F =46.4		p<0.001		
	total organic	(mg) = 0.08 (±0.05) - 0.00004 (±0.00002) pCO_2 (µatm) + 0.013 (±0.0012) energy supply (J)					
		r^2 = 0.58	F= 55.2		p<0.001		
B	shell length	model	df	AIC	model quantity	chi^2	p
		Food + CO2	3	1310.882		98.90	**0.000000**
		Food	2	1314.323	0.17631	93.46	**0.000000**
		CO2	1	1404.036	0.00000	1.75	0.185918
	total organic	model	df	AIC	model quantity	chi^2	p
		Food + CO2	3	176.8151		66.83	**0.000000**
		Food	2	186.8465	0.00663	54.80	**0.000000**
		CO2	1	235.134	0.00000	4.51	**0.033698**
	CaCO3	model	df	AIC	model quantity	chi^2	p
		Food + CO2	3	-32.3182		72.43	**0.000000**
		Food	2	-30.7201	0.44976	68.83	**0.000000**
		CO2	1	34.7737	0.00000	1.34	0.247840

Supplementary table S4: Relative contribution of shell free drymass (SFDM) and shell components (organic shell component (OSC) + inorganic shell component (ISC)) to total mass (A) and energy content (B) of settled *M. edulis* in the four pCO_2 treatments.

A				
% of total mass	380	1120	2400	4000
SFDM	10	11	12	13
Shell	90	89	88	87
OSC	10	11	12	13
$CaCO_3$	79	77	76	74
B				
% of total energy content	380	1120	2400	4000
SFDM	37	38	39	39
Shell	63	62	61	61
OSC	37	38	39	39
$CaCO_3$	26	24	23	21

Supplementary table S5: Shell mass, organic shell component (OSC) and OSC in % of shell mass shell of juvenile *M. edulis* (shell length 12.4 ± 1.1mm) from Kiel Fjord including mean ± sd.

Shell mass mg	OSC mg	OSC % of shell mass
39.0	2.1	5.4
40.4	2.3	5.6
62.7	3.1	4.9
52.4	3.3	6.4
52.1	2.8	5.3
44.9	2.6	5.9
55.0	3.0	5.4
41.2	2.5	6.1
49.6	2.5	5.1
33.6	2.1	6.1
57.8	3.6	6.1
25.3	1.9	7.4
30.6	1.8	5.7
64.0	2.4	4.5
39.6	1.8	5.4
31.3	2.2	7.5
44.9	2.5	5.8
11.8	0.5	0.8

Supplementary table S6: Location of the carbonate system monitoring stations and sampling depths, mean salinity, temperature, pH, pCO_2, Ω, PO_4^{3-} and SiO_3^- measured in surface and bottom water samples during monitoring 2009/10; values represent means ± SD

station	1	2	3	4
location	54°19.8´N 10°9.0´W	54° 21.7` N 10° 09.5`O	54° 26`N 10° 12.2`O	54° 29.4` N 10° 13`O
sample depth (m)	1+18	1+11	1+15	1+20
surface				
salinity	16.17 ± 1.89	16.31 ± 1.47	16.66 ± 1.46	15.97 ± 1.11
temperature (°C)	9.58 ± 6.47	9.84 ± 6.55	9.82 ± 6.79	9.51 ± 7.37
pH (total scale)	7.91 ± 0.23	7.94 ± 0.16	8.01 ± 0.14	8.01 ± 0.15
pCO_2 (µatm)	705.5 ± 461.1	635.2 ± 308.5	508.5 ± 265.9	447.5 ± 162.4
$\Omega_{calcite}$	1.64 ± 0.75	1.70 ± 0.72	1.90 ± 0.79	1.89 ± 0.89
$\Omega_{aragonite}$	0.96 ± 0.20	1.00 ± 0.43	1.12 ± 0.48	1.12 ± 0.54
PO_4^{3-}	0.69 ± 0.52	0.38 ± 0.19	0.25 ± 0.15	0.16 ± 0.10
SiO_3^-	21.9 ± 10.4	12.2 ± 6.4	6.6 ± 4.3	3.3 ± 2.7
bottom				
salinity	18.29 ± 1.66	17.48 ± 1.57	18.69 ± 1.93	19.50 ± 2.29
temperature (°C)	8.83 ± 5.44	8.63 ± 5.81	8.11 ± 5.09	7.19 ± 5.12
pH (total scale)	7.70 ± 0.23	7.83 ± 0.20	7.70 ± 0.22	7.60 ± 0.26
pCO_2 (µatm)	1150.5 ± 759.8	945.5 ± 807.4	1184.3 ± 736.7	1516.8 ± 1071.2
$\Omega_{calcite}$	1.03 ± 0.34	1.27 ± 0.57	0.99 ± 0.46	0.79 ± 0.38
$\Omega_{aragonite}$	0.61 ± 0.20	0.75 ± 0.34	0.59 ± 0.27	0.47 ± 0.23
PO_4^{3-}	0.72 ± 0.52	0.50 ± 0.27	0.54 ± 0.27	1.07 ± 1.58
SiO_3^-	20.5 ± 8.4	13.8 ± 8.8	15.9 ± 9.6	14.5 ± 9.8

Supplementary table S7: Detected macrobenthic species and their abundances as coverage (%) or number (n) on the settlement panels removed from the Fjord on November 18th 2010; values represent means ± SD

site	species	abundance Coverage (%)/number (n)
Outer Fjord	*Mytilus edulis*	78.5 ± 17.0 %
	Amphibalanus improvisus	26.7 ± 19.6 %
	Nereis pelagica	1.25 ± 1.26
	Gammarus locusta	0.25 ± 0.50
	Polydora ciliata	0.25 ± 0.50 %
	Ceramium sp.	2.0 ± 2.0 %
	Polysiphonia sp.	0.05 ± 0.06 %
Inner Fjord	*Mytilus edulis*	99.1 ± 1.4 %
	Amphibalanus improvisus	0.9 ± 1.4 %
	Nereis pelagica	1.5 ± 2.1
	Polydora ciliata	0.03 ± 0.05 %

Supplementary table S8: Haemolymph acid-base status of *M. edulis* from the inner fjord measured in 2009 at ambient seawater temperature and salinity, n=5 at each time point; values represent means ± SD

date	pH	pCO_2	$[HCO_3^-]$	$[CO_3^{2-}]$	Temperature	Salinity
	NBS	µatm	mmol l^{-1}	µmol l^{-1}	°C	
17/02/2009	7.63 ± 0.07	1724 ± 352	2.07 ± 0.08	21.8 ± 3.3	2.5	13.1
16/03/2009	7.55 ± 0.05	2296 ± 332	2.25 ± 0.08	23.5 ± 3.0	6.1	13.7
21/04/2009	7.80 ± 0.06	1167 ± 266	2.29 ± 0.16	54.1 ± 5.6	12.1	13.5
20/05/2009	7.47 ± 0.07	2346 ± 395	1.90 ± 0.17	23.9 ± 5.4	13.6	14.9
22/06/2009	7.59 ± 0.06	1630 ± 236	1.80 ± 0.17	32.4 ± 6.0	16.0	14.9
13/07/2009	7.49 ± 0.07	2105 ± 418	1.86 ± 0.13	29.7 ± 6.3	16.9	16.5
17/08/2009	7.48 ± 0.16	2255 ± 1011	1.84 ± 0.19	33.2 ± 12.2	19.4	16.6
26/08/2009	7.42 ± 0.05	2991 ± 419	2.19 ± 0.12	31.0 ± 4.1	17.2	17.6
27/08/2009	7.36 ± 0.04	3090 ± 494	1.93 ± 0.14	23.7 ± 2.3	16.3	18.5
02/09/2009	7.38 ± 0.03	2908 ± 234	1.96 ± 0.11	25.8 ± 2.9	16.0	19.0
21/09/2009	7.50 ± 0.10	2265 ± 537	2.07 ± 0.13	36.2 ± 9.6	16.9	17.7
30/11/2009	7.59 ± 0.05	1835 ± 256	2.14 ± 0.07	29.6 ± 4.1	8.8	15.5
mean ± SD	7.52 ± 0.12	2218 ± 581	2.03 ± 0.17	30.4 ± 8.7	13.9 ± 5.2	16.0 ± 2.1

Supplementary material and methods:

Water chemistry and particulate organic carbon (POC) measurements:

The carbonate chemistry of Kiel Fjord was monitored on weekly (station 1) and bi-weekly (stations 2-4) cruises using RV Polarfuchs between April 2009 to March 2010 (Fig. 2, Supplementary Tab. S4). Two samples (500 mL) were taken at each station from both surface (about 1 m depth) and bottom water (1 m above sea floor, i.e. 11-20 m). Seawater samples were poisoned with saturated mercuric chloride solution and stored at room temperature until analysis according to SOP1[1]. Samples were analyzed for C_T and A_T by coulometric and potentiometric titration using SOMMA and VINDTA autoanalyzers, respectively[1]. Additionally, water samples for nutrient determination (PO_4^{3-}, H_4SiO_4) were collected in 10 mL Falcon tubes and stored at -20°C. Analyses were carried out spectrophotometrically using a U-2000 spectrophotometer (Hitachi-Europe, Krefeld, Germany)[2].

Weekly pH measurements (NBS scale) were conducted in the inner Fjord (station IF, 54°19.8'N; 10°9.0'E, Fig. S3b) and bi-weekly in the outer Kiel Fjord (station OF, 54°.25´N, 10°10´O, Fig 2+3, Supplementary Table S4) during the field study using a WTW 340i pH meter and a WTW Sentix 81-electrode. Salinity and temperature were measured at 10 cm depth using a WTW cond 315i salinometer and a TETRACON 325 probe. For carbonate chemistry, water samples were taken with a water sampler and pH on the total scale (pH_T) and C_T were determined using a Metrohm 6.0262.100 electrode and 626 Metrohm pH meter and an AIRICA C_T analyzer (Marianda, Kiel, Germany). pH_t was determined using Tris/HCl and AMP/HCl seawater buffers mixed for salinity 15[1] in a 21°C water bath. Accuracy of A_T and C_T measurements was ensured by using certified reference material[3]. The carbonate system speciation was calculated using the CO2SYS program[4]. For calculations, the $KHSO_4$ dissociation[5] and the carbonate system dissociation constants K_1 and K_2[6] were used.

Particulate organic carbon (POC) concentrations were monitored bi-weekly at IF and OF stations as an indicator for habitat energy supply. For POC determinations, 500 mL water samples were obtained with a water sampler from one meter depth. Subsequently, samples were filtered on combusted GF/F filters using a vacuum pump and stored at -20°C. Before analysis, filters were treated with fuming hydrochloric acid, dried (60°C, 6 h) and wrapped in tin boats. POC determinations were performed by gas chromatography in an elemental analyser Euro Vector 3000 (EuroVector, Milan, Italy).

Laboratory study:

For the laboratory study, settled *M. edulis* postlarvae were used. For this purpose, 5x5 cm PVC settlement panels which were roughed on one side using sandpaper (grain 60) were suspended in the fjord (IF station) at one meter water depth. After 10 days, panels were removed from the fjord and all settled organisms other than 100 settled *M. edulis* larvae were removed using a stereo microscope. Subsequently single plates were transferred into 500 mL aquaria in a 17°C constant temperature room. For the 7 week laboratory experiment, four pCO_2 treatments, 470, 1020, 2110 and 3350 µatm, and three feeding regimes (low, medium, high) were realized. In total, 12 different treatments with 7 replicates each were used. The pCO_2 treatment levels correspond to present day and projected future levels in this area[7]. Aquaria were filled with 0.2 µm filtered and UV-radiated seawater from the fjord

and aerated with compressed air with one of the four pCO_2 levels (see[7] for details). Water exchange of 400 mL (80%) was performed daily using CO_2 and temperature pre-equilibrated water. Measurements of salinity, temperature and pH_{NBS} were performed daily in 24 of the 84 aquaria. Carbonate system parameters (pCO_2, A_T, Ω) were calculated weekly from C_T and pH_T as described above from 250 mL water samples. Water samples were analysed within 2 hours of sampling.

Three feeding treatments were established by addition of exact cell numbers of *Rhodomonas spp.* algae to the experimental aquaria. In weekly intervals, algae cell concentrations were increased and the number of mussels was reduced in order to compensate for mussel growth (Supplementary Table S1). Initial algal supply in the different food treatments was 5,000, 2,500 and 500 cells mL^{-1}, respectively, which was increased up to 40,000, 20,000 and 4,000 cells ml^{-1} during the last week. The ratio of 10:5:1 between the feedings levels was maintained during the entire experiment. The algae cells were cultured in 0.2 µm filtered seawater with Provasoli´s enriched seawater (PES) medium and elevated phosphate (0.036 mmol L^{-1}) and nitrate (0.55 mmol L^{-1}) concentrations as previously described[3]. Once a day, *Rhodomonas* culture densities were measured using a particle counter (Z2 Coulter® Particle count and size analyzer, Beckman Coulter™, Krefeld, Germany) to calculate the culture volume which had to be added in order to reach the desired cell densities in the aquaria. Weekly, POC content of the supplied algae and of algae following a 24 h incubation was analyzed as described above. Differences between supplied and remaining POC were used to calculate POC uptake by the mussels. Correlation of measured *Rhodomonas* cell abundance and POC revealed a carbon content of 45 pg C $cell^{-1}$.

For determination of initial size (shell length, $CaCO_3$ and total organic content) and weekly growth rates, 5-6 individuals were sampled at each sampling day from each aquarium and stored in seawater with 4% paraformaldehyde (PFA). Shell length was measured using a stereo microscope equipped with a MicroPublisher 3.3 RTV camera and the image analysis software Image Pro Plus 5.0.1. Final $CaCO_3$ and total organic content was determined as described above by weighing single specimens with a precision balance (accuracy ± 1 µg, Sartorius, Göttingen, Germany) after drying at 60° C and ashing at 500°C for 20 h. Additionally, shell free drymass (SFDM) was dissected from carefully opened, frozen specimens and dried at 60°C. Comparison of SFDM and total organic content (TOC = SFDM + organic shell components, OSC) was performed using a regression of both parameters against shell length.

Energy contents of supplied *Rhodomonas* and seawater POC was estimated using the conversion factor of 46 J mg^{-1} POC[8]. Mussel SFDM and OSC (periostracum+organic) was converted to caloric equivalents using the conversion factor 23 J mg^{-1} [9]. Similarly, the inorganic shell component (ISC) was converted into energy equivalents using a factor of 2 J mg^{-1} $CaCO_3$[10].

Field study:

Haemolymph acid-base status was determined for *M. edulis* specimens (shell length about 5 cm) sampled directly at station IF in 2009. Animals were transported in ambient water into the lab and haemolymph was collected with a syringe from the posterior adductor muscle within 2 min after

sampling and transferred into 1.5 mL cap. pH_{NBS} was measured using a WTW microelectrode and C_T was measured using a Corning 965 CO_2 analyzer (Olympic Analytical, Malvern, UK), which was calibrated with $NaHCO_3$ standards. Acid-base parameters pCO_2, [HCO_3^-] and [CO_3^{2-}] were calculated according to the Henderson-Hasselbalch-Equation as described previously[7].

For the field study, settlement panels were treated in the same way as stated above for the laboratory study. Panels were transferred to the experimental sites and suspended at 1 m depths. Both field sites are characterized by similar salinity, temperature, light exposure and are sheltered from wave action. The number of replicates was 6. However, despite the shelter two panels were lost at station OF during storms. Water chemistry (pH_T, C_T) and POC concentrations were monitored bi-weekly at both stations. The experiment lasted from July 23th to November 19th 2010 (18 weeks) when the panels were removed from the water. Subsequently, plates were frozen and pictures were taken. The percentage of coverage for *M. edulis* and *A. improvisus* on both side of each panel was measured using ImageJ version 1.45. Fouling organisms were determined to the lowest possible taxonomic level. TOC and ISC of mussels and barnacles were determined after drying at 60° C over night and ashing at 500°C for 20 h, respectively. Additionally, freshly settled individuals were collected at each station every second week starting at August 11th for determination of shell length growth relationship. Final somatic drymass and shell length and mass were determined from specimens collected on November 19th.

Statistics:

Regression analyses were performed using Sigma Plot 10, all other statistics were performed with Statistica 10. Data were analyzed for normality using Shapiro-Wilks test. For the laboratory results repeated measures ANOVA and two-way ANOVA were applied. Forward stepwise multiple linear regression analysis was performed for shell length growth. For data analyses of the field study, paired t-tests and Mann-Whitney U tests were used. Figures and tables give mean values and standard deviation.

Supplementary References:

1. Dickson, A.G., Sabine, C.L. & Christian, J.R. *Guide to best practices for ocean CO_2 measurements* (Vol. 3, p. 191). PICES Special Publications (2007).
2. Hansen, H.P. & Koroleff, F. In Grasshof, K., Kremlöing, K. & Ehrhardt, M. *Methods of seawater analysis* (Wiley-VCH 1999)
3. Dickson, A.G., Afghan, J.D. & Anderson, G.C. Reference materials for oceanic CO_2 analysis: a method for the certification of total alkalinity. *Mar. Chem.*, 80, 185-197 (2003).
4. Lewis, E. & Wallace, D. W. R. Program developed for CO_2 system calculations. Oak Ridge, Oak Ridge National Laboratory ORNL/CDIAC-105 (1998).
5. Dickson, A.G. Standard potential of the reaction - AgCl(S)+1/2 H_2 = Ag(s)+HCl(Aq) and the standard acidity constant of the ion HSO_4^- in synthetic sea-water from 273.15 to 318.15-K. *J Chem. Thermodyn.,* 22, 113-127. (1990)

6. Roy, R. *et al*. The dissociation constants of carbonic acid in seawater at salinities 5 to 45 and temperatures 0 to 45°C. *Mar. Chem.*, 44, 249-267 (1993).
7. Thomsen, J. *et al*. (2010). Calcifying invertebrates succeed in a naturally CO_2 enriched coastal habitat but are threatened by high levels of future acidification. *Biogeosciences*, *7*, 3879-3891.
8. Salonen, K., Sarvala, J., Hakala, I. & Viljanen, M. The relation of energy and organic carbon in aquatic invertebrates. *Limnol. Oceanogr.*, 21, 724-730 (1976).
9. Brey, T., Rumohr, H. & Ankar, S. Energy content of macrobenthic invertebrates: general conversion factors from weight to energy. *J. Exp. Mar. Biol. Ecol.*, 117, 271-278 (1988).
10. Palmer, A. R. (1992). Calcification in Marine Mollusks - How Costly Is It. *Proceedings of the P. Natl. Acad. Sci. USA*, *89*(4), 1379-1382.

4. Discussion

In this thesis, I investigated the sensitivity of *M. edulis* to elevated pCO_2. It has been proposed that calcification is the process which is most affected by ocean acidification. For a broad range of marine taxa, calcification rates were shown to decrease in response to elevated pCO_2 (Riebesell et al. 2000, Shirayama and Thornton 2005, Kroeker et al. 2010). Studies conducted along pCO_2 gradients at naturally acidified volcanic vents observed that especially benthic, calcified invertebrates responded most sensitively to elevated pCO_2 and were absent at low mean pH < 7.8 (Hall-Spencer et al. 2008). Especially bivalves were thought to be very sensitive to elevated pCO_2. A decrease of calcification rates by 25% until the end of the century and incipient net dissolution at 1800 µatm pCO_2 has been measured in short-term experiment (Gazeau et al. 2007).

This thesis combines results of field and laboratory studies conducted with *M. edulis* from the western Baltic Sea. I carried out a long-term monitoring program to study the fluctuations in carbonate chemistry in the natural habitat of the inner Kiel Fjord mussel population and in the entire fjord (publications 1 and 3). Using a correlation of measured C_T and oxygen concentrations and data from 1957 to 2009, I can demonstrate that the increase of pCO_2 in the Kiel Fjord in the recent past is a consequence of eutrophication (discussion part 4.1).

Although, pCO_2 is much higher than in other coastal habitats, calcifying organisms inhabit Kiel Fjord and the benthic community is dominated by *M. edulis* (publications 1 and 3). Under elevated pCO_2, the extracellular pH of mussels is decreased and no signs of buffering by shell dissolution have been observed (publications 1 and 3). Arobic metabolism and nitrogen excretion rates rwere upregulated following intermediate acclimation interval (8 weeks) and constant following long-term acclimation (52 weeks, publication 2 and discussion part 4.2). The ammonium excretion mechanism in mussels seems to involve Rh- and Amt-proteins (discussion part 4.2). In laboratory experiments, protein turnover increased and Scope for Growth (SfG) decreased which may explain growth rate reductions at elevated pCO_2 (publication 2 and discussion part 4.2). Nevertheless, I have demonstrated that somatic growth and calcification rates of mussels are fairly stable also at high ambient pCO_2 (publications 1, 2 and 3). The high energy availability in the inner region of Kiel Fjord even enhanced the growth rates of mussels compared to a low pCO_2 control site. Finally, I compare my results from Kiel Fjord to the observations made for other CO_2 enriched coastal habitats (discussion part 4.3).

4.1 pCO_2 variability in the western Baltic Sea

Ocean acidification is expected to cause a significant change of the ocean chemistry and may thereby affect the marine biota. The analysis of the marine carbonate chemistry enables accurate measurements; therefore effects of rising atmospheric CO_2 concentrations are measurable even over short periods of few years. The rate of seawater pCO_2 increase appears to be similar to the increase of atmospheric pCO_2 at least in the Atlantic (Takahashi et al. 2006, 2009). As a consequence,

equilibration causes pH decreases in a linear fashion, as observed at the Hawaii Ocean Time Series (HOT) and other areas (Doney et al. 2009, Feely et al. 2009, Ishii et al. 2011). An even faster decrease of pH is documented in the areas around Iceland with an annual rate of change of -0.0024 units during the period from 1984-2009 (Olafsson et al. 2009). At both stations, aragonite saturation state is decreasing with the saturation horizon rising at a rate of 4 m y^{-1} (Olafsson et al. 2009).

Nevertheless, in contrast to the open ocean, coastal habitats are characterized by a much higher variability (Borges et al. 2006, Hofmann et al. 2011). Kiel Fjord is an example for a coastal habitat with highly variable carbonate chemistry (publication 1 and 3). Although measured peak pCO_2 are higher than in comparable habitats, high pCO_2 variability in coastal ecosystems is the rule and not an exception (Borges and Frankignoulle 1999, Borges et al. 2006, Provoost et al. 2010). Diurnal variability is known e.g. in rock pools during low tide with high pH during the day time and a similarly decrease during the night (Truchot and Duhamel-Jouve 1980, Spicer et al. 1995, Mandic et al. 2000). Nevertheless, pCO_2 variability is not only restricted to enclosed rock pools but is observed along coastal zones when deep water is transported to the surface or rivers discharge a high carbon load. In continental upwelling areas, deep water enters the shelf and is transported to the surface leading to elevated pCO_2 (Lefevre et al. 2002, Sarma 2003, Feely et al. 2008, Manzello 2010). This process is best documented for the coastal upwelling on the US west coast (Feely et al. 2008, Feely et al. 2009). The pCO_2 variability in Kiel Fjord similarly results from upwelling of high pCO_2 water to the surface. However, the process is different as it is not driven by Ekman transport but results from seaward winds which transport the surface water out of the Fjord (Myrberg and Andrejev 2003). Additionally, the affected area is much smaller compared to the California upwelling. Nevertheless, upwelling is documented for many different areas along the Baltic coast, which emphasize the importance of this process in the whole area (Siegel et al. 1994, Gidhagen 1987, Lehmann and Myrberg 2008, Myrberg and Andrejev 2003). This also implies that a similar degree of pCO_2 variability may occur at many different sites in the Baltic as the whole basin is characterized by strong stratification and consequently CO_2 enrichment in the subsurface water (Schneider et al. 2002, Wesslander et al. 2010, Frommel et al. 2012)

Similar high pCO_2 levels compared to Kiel Fjord can be observed in heterotrophic estuaries and river mouths where nutrient and dissolved organic matter (DOM) input causes high productivity and increased community respiration (Frankignoulle et al. 1996, 1998, Brasse et al. 2002, Schiettecatte et al. 2006, Cai et al. 2011). Since O_2 uptake and CO_2 release are coupled processes, $[O_2]$ and C_T are correlated and high pCO_2 levels are always encountered in hypoxic (Burnett 1997). In tropical oxygen minimum zones (OMZ), high C_T values and consequently elevated pCO_2 is observed (Brewer and Pelzer 2009, Paulmier et al. 2011). The eutrophication in the second half of the 20th century drastically enhanced the formation of seasonal or permanent hypoxic zones, so called ´dead zones´ (Rosenberg and Diaz 2008), particularly in coastal areas with a human footprint (Borges and Gypens 2010). Also in the western Baltic Sea, the seasonal oxygen depletion mainly results from enhanced nutrient input (Babenerd 1992, Conley et al. 2007, HELCOM 2009). In general, seasonal hypoxia is a natural process during the seasonal stratification in this region and is also enhanced by inflowing low O_2 bottom water from the Kattegat (Weigelt 1990). Nevertheless, the calculations by Babenerd (1992) for

O_2 concentrations in the water masses below the thermocline revealed faster oxygen decline as a result of enhanced community respiration. Therefore, eutrophication has the largest influence on seawater [O_2] in this area.

The correlation of seawater C_T and [O_2] can be used to back calculate the pCO_2 in Kiel Bay at an early stage of eutrophication. The [O_2] data by Babenerd (1992) and correlated [O_2] and C_T data measured in 2009/10 at the Boknis Eck Time Series (BETS, Hansen et al. 1999) station were used for the calculation (Fig 4.1). These data reveal the drastic increase of seawater pCO_2 in the bottom water (20+25m) at Boknis Eck within the last 50 years. According to these data, bottom water pCO_2 increased from about 750 µatm in 1957 to present levels of about 2500 µatm (Fig 4.1).

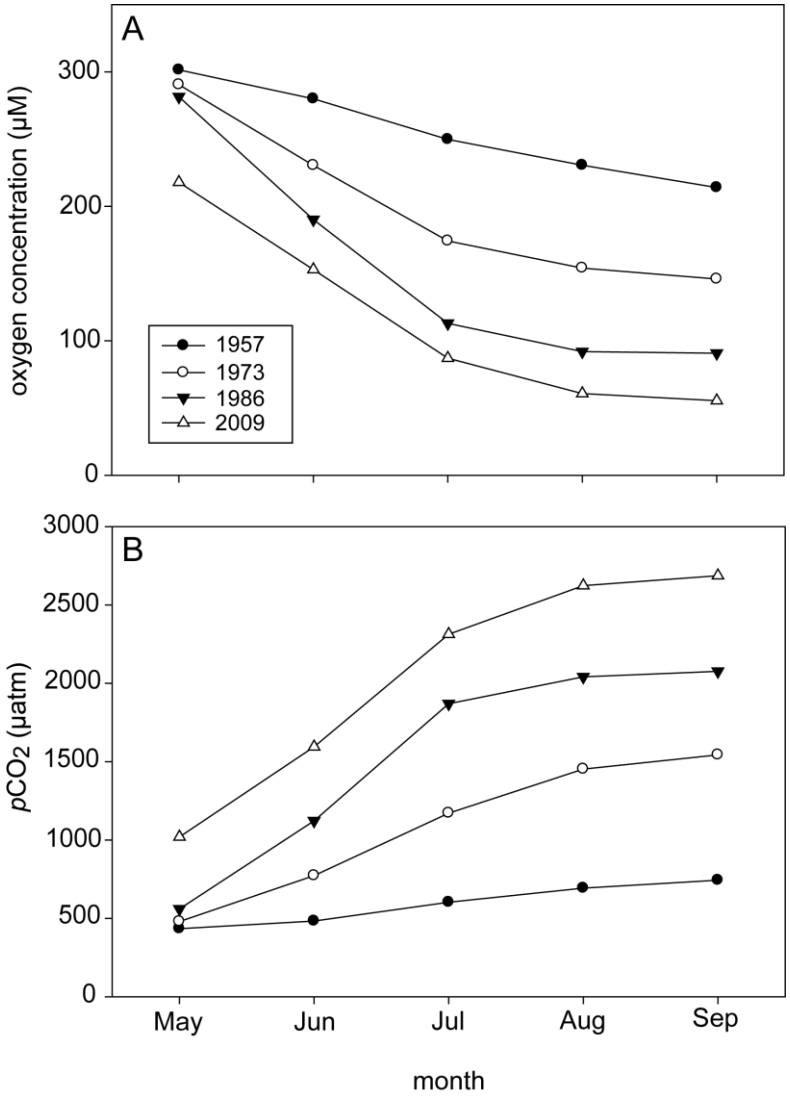

Figure 4.1: Oxygen concen-trations of the bottom water at Boknis Eck. Data for 1957, 1973 and 1986 are taken from figures in Babenerd (1992) and converted into µM. Data for 2009 were measured during the sampling at Boknis Eck and were averaged for 20 and 25 m depth (A). pCO_2 was calculated using the correlation of [O_2] and C_T in 20+25m measured in 2009/10. Initial C_T (at 100% air saturation) was calculated using mean temperature (7.2°C), salinity (20.5 g kg^{-1}) and A_T (2032 µmol kg^{-1}) measured in 2009/10 and atmospheric pCO_2 between 320 and 390 µatm. Reductions of oxygen concentrations were converted into C_T accumulation using the equation C_T=-0.71 x [O_2] + 250.8. Values were added to the respective initial C_T. Calculation of past pCO_2 was carried out using constant A_T, S and T and calculated C_T.

So far, little attention has been drawn to the fact, that future ocean acidification will especially amplify pCO_2 levels in hypoxic water masses (Brewer and Pelzer 2009). In the future, seawater C_T will be higher and sinking of particular organic matter (POM) into the subpycnocline water masses and subsequent degradation leads to a further increase of C_T. Under hypoxic conditions, low [CO_3^{2-}] and thus high CO_2 is encountered and additional CO_2 drastically elevates seawater pCO_2. This has been observed for the northern part of the Gulf of Mexico and for the East China Sea (Cai et al. 2011). Calculations confirm this pattern also for the western Baltic Sea (Melzner et al. 2012, accepted).

According to these calculations, pCO_2 has drastically increased in the bottom water and is expected to further increase. In Kiel Fjord, upwelling transports bottom water to the surface, therefore the maximal pCO_2 levels which can be observed here, are directly correlated to the bottom water pCO_2 levels. As a consequence, surface pCO_2 should have increased in a similar fashion as bottom pCO_2 and the high pCO_2 variability in Kiel Fjord may not occur for more than 50 years. In former years, maximum pCO_2 should have been below 1000 µatm, which is the mean value for the summer/autumn period today. In future, a further increase is expected in this area which might lead to mean pCO_2 levels up to 2000 µatm during summer and autumn (Melzner et al. 2012, accepted, publication 1).

In the area of Kiel Fjord, alkalinity and $[CO_3^{2-}]$ are much lower when compared to the open ocean (Beldowski et al. 2011). As a consequence calcium carbonate saturation is found to be low in the whole of Kiel Bay and the seawater is often undersaturated with respect to aragonite. At the surface, in 35 out of 55 investigated weeks, Ω for aragonite was below 1 (publications 1 and 3). Similar to the observed low saturation in polar, cold temperate oceans (Yamamoto-Kawai et al. 2009) lowest saturation values were not necessarily obtained during periods of high pCO_2 in summer/autumn, but in February with lowest seawater temperatures. The measured alkalinity values in the outer areas of the Fjord and at Boknis Eck correspond to those obtained by Beldowksi et al. (2011). In the inner Fjord, no obvious correlation of salinity and alkalinity exists, as the water is strongly influenced by the discharge of the Schwentine River which transports high amounts of dissolved organic matter and carbon (DOM/DOC) into the Fjord (Fig 4.2). These substances, such as humic acids, with pK values relevant for the alkalinity titration, presumably influence also the alkalinity titrations leading to over estimation of values (Kim and Lee 2009, Koeve et al. 2011). The influence is restricted to the inner part of the Fjord, probably due to dilution of the substances in the Fjord water (Cai et al. 1998). Nevertheless, comparison of pH values calculated from A_T and C_T were similar to directly measured values, therefore DOM does not lead to a significant error of pCO_2 calculation (Koeve et al. 2011).

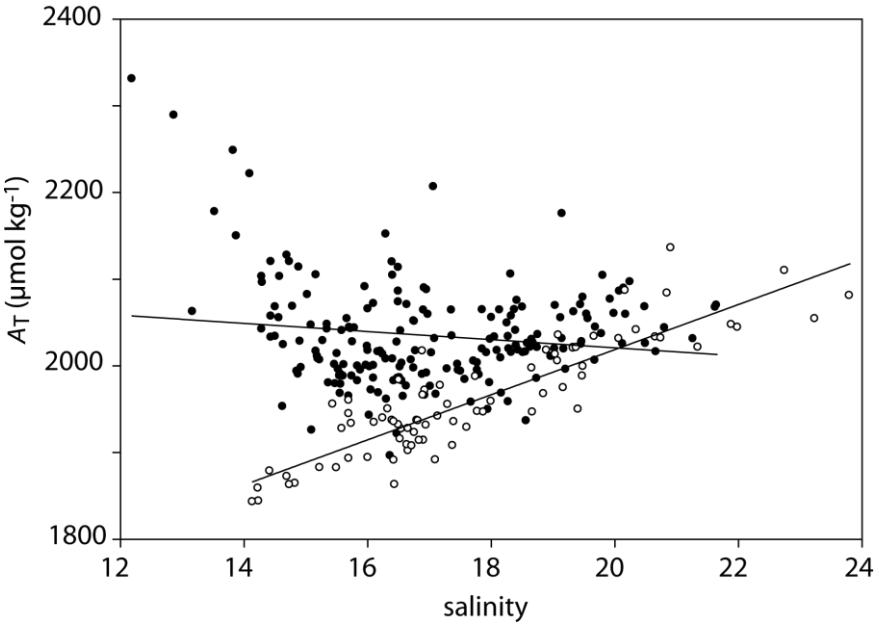

Figure 4.2: Correlation of measured A_T and salinity for station 1 and 2 in the inner Fjord (filled circles) and station 3 and 4 in the outer Fjord (open circles), A_T station 1+2 = -4.7 x salinity + 2114.8 µmol kg^{-1}, R^2=0.02, F=4.26, p<0.05; A_T station 3+4 = 26.0 x salinity + 1498.5 µmol kg^{-1}, R^2=0.78, F=265.5, p<0.01; see Fig 2.1 for a detailed overview of the locations (Thomsen et al. unpublished).

In conclusion, Kiel Fjord is characterizd by a strong seasonal variability of the pCO_2. During summer and autumn, upwelling of low O_2 bottom water leads to really high pCO_2 levels in the inner Fjord area. Increased pCO_2 results from recent eutrophication and will be drastically amplified by increasing atmospheric CO_2 concentrations (Cai, et al. 2011, Melzner et al. 2012). Further, due to the low alkalinity these areas are also characterized by higher Revelle factor. As a consequence, pH decreases are much stronger than in comparable full marine habitats. Therefore, future ocean acidification will have a major impact on the carbonate chemistry in the Baltic and in marginal, estuarine habitats in general.

4.2 Impact of elevated pCO_2 on *Mytilus edulis*

4.2.1 Calcification

It has been suggested that mussels of the genus *Mytilus* react sensitively to ocean acidification and calcification rates will decrease at elevated pCO_2 (Michaelidis et al. 2005, Berge et al. 2006, Gazeau et al. 2007). Although the main conclusion of reduced calcification was similar in these papers, contradictive results were obtained between and also within these studies. Whereas no net calcification and even dissolution was observed by Gazeau and coworkers (2007) for pCO_2 levels > 1800 µatm, *M. galloprovincialis* continued shell growth even at 5000 µatm, albeit at 45% reduced rate (Michaelidis et al. 2005). At the same time, Michaelidis et al. (2005) measured increased $[Ca^{2+}]$ and $[HCO_3^-]$ in the haemolymph which would indicate shell dissolution. Several studies which investigated the calcification response of *Mytilus* to OA were conducted under unrealistically high pCO_2 levels (Bamber 1990, Michaelidis et al. 2005, Berge et al. 2006) or without providing any acclimation time to the experimental animal population (Gazeau et al. 2007). Further, in some experiments, mussels were not or inadequately fed, which resulted in no or only low growth (Berge et al. 2006, Ries et al. 2009, Rodolfo-Metalpa et al. 2011).

The studies, which were conducted in the framework of this thesis, clearly revealed that calcification of the benthic life stage of *M. edulis* is relatively robust towards pCO_2 levels relevant for ocean acidification scenarios of the next century. The experiments presented in this thesis included pCO_2 treatment levels which correspond to values that can be expected in the habitat due to ocean acidification considering adequate acclimation time and food supply. Table 4.1 summarizes the experimental conditions and main findings of all laboratory studies on the effects of low pH or high pCO_2 on calcification of benthic *M. spp.* life stages published so far and those from this work.

According to these studies, the most drastic responses of decreasing calcification rates and net shell dissolution where obtained when mussels were subjected to rapid short-term increases in seawater pCO_2 (Gazeau et al. 2007). This is similar to results observed for other bivalve species (Waldbusser et al. 2010a,b, Mingliang et al. 2011) and highlights the importance of adequate acclimation intervals at elevated pCO_2 before measuring response variables. The response of animals subjected to a short-term pCO_2 stress drastically differs to that of long-term acclimated specimens. This is a general pattern observed during exposure to other abiotic stressors, such as desalination or temperature

(Widdows and Bayne 1971, Böhle 1972). After transfer from 34 to 18 g kg^{-1} seawater, mussel filtration rate is significantly decreased but within 8 weeks, filtration rates recover and reach control conditions (Böhle 1972). Similarly, when the mussels were acclimated to elevated pCO_2, acclimation enables conserved calcification rates at least at moderate levels up to 1500 µatm (Bamber 1990, publication 1-3). Within one week, the freshly settled mussel spat was able to continue shell calcification and somatic growth even at a pCO_2 above 3000 µatm (publication 3).

In some studies no or inadequate food was supplied. Bamber (1990) and Rodolpho-Metalpa et al. (2011) did not provide any exact initial shell length, mass and condition index data; therefore it is not possible to calculate growth for these experiments. Berge et al. (2006) and Ries et al. (2009) observed only very little growth which indicates insufficient food supply. As evidenced by the data of Melzner et al (2011) the ability to preserve existing shell nacre in adult mussels under elevated pCO_2, strongly depends on the supplied food. Therefore, drastic decreases of calcification rates, shell dissolution or even reduced survival in laboratory studies may result from starvation effects, which may not occur under natural conditions.

Table 4.1: Experimental conditions (duration, pCO_2 levels, food supply) and the main results of laboratory experiments on the calcification response and survival of *Mytilus edulis* and *galloprovincialis* under elevated pCO_2

publication	duration d/h	$p\,CO_2$ levels µatm	food supply additonal to flow-through	effect
Bamber 1990	30d	480-18000	no	reduced survival at $p\,CO_2$ >15000 µatm
		35000-110000		feeding supression at $p\,CO_2$ >7000 µatm
Michaelidis et al. 2005	90d	1100 and 5000	*Isochrysis* and *Chlorella*	45% shell length growth reduction, shell dissolution
Berge et al. 2006	44d	500, 2700, 5500 and 14000	no	reduced survival at 14000 µatm reduced calcifcation at 5500 µatm
Gazeau et al. 2007	2h	420-2300	*Isochrysis* , *Pavlova* , *Tetra-selmis* and *Thalassiosira*	linear decrease of calcifcation net dissolution at $p\,CO_2$ >1800 µatm
Ries et al. 2009	60d	410-2860	puréed brine shrimp and green algae	no effect on calcification
Melzner et al. 2011	60d	540-3990	*Rhodomonas* and no additional food	increased nacre dissolution at 4000 µatm in starved mussels
Rodolfo-Metalpa et al. 2011	22d	470 and 2300	no	lowered calcification at 2300 µatm
Publication 1	60d	490-3900	*Rhodomonas*	conserved shell growth at 1400 µatm reduced calcifcation at 4000 µatm
Publication 2	60d	480-3780	*Rhodomonas*	positive calcification, linear decrease with increasing $p\,CO_2$
Publication 3	49d	470-3350	*Rhodomonas*	conserved shell growth up to 2400 µatm lowered calcification at 4000 µatm

Anthropogenic ocean acidification changes the carbonate chemistry in three distinct ways at the same time by (1) lowering of carbonate saturation state, (2) pH decrease and (3) increasing pCO_2. It is not obvious which aspect may affect mussels and especially calcification the most.

From a geological perspective, decreasing [CO_3^{2-}] may favor the dissolution of carbonate structure as Ω becomes <1. Net calcification might be either reduced by dissolution of existing structures (Nienhuis et al. 2010) or by the reduced availability of CO_3^{2-}. The correlation of calcification rates and seawater Ω or [CO_3^{2-}] was published for corals (Langdon et al. 2000, Silverman et al. 2009) bivalves and their larval stages (Ries et al. 2009, Waldbusser et al. 2010, Gazeau et al. 2011) and pteropods (Comeau et al. 2009). According to the field and laboratory data from Kiel Fjord mussels, seawater Ω or [CO_3^{2-}] does not play an important role for calcification in adult mussels. *M. edulis* inhabits Kiel Fjord which is characterized by low and frequent $CaCO_3$ undersaturation throughout the year. Mussels even settle in the northern, low saline parts (minimum salinity: 4.5 g kg^{-1}) of the Baltic which is characterized by even lower Ω values due to the very low alkalinity (Westerbom et al. 2002, Beldowski et al. 2011). Exposed to undersaturated conditions, fractures of the periostracum lead to external shell dissolution which can not be prevented by the animals (publication 1, Fig. 5 and 6). Similar results were obtained at hydrothermal vents where mussels are able to preserve their shells in highly acidic water (pH: 5.36, Tunnicliffe et al. 2009). However, periostracum damages lead to complete dissolution of the shell $CaCO_3$ (Tunnicliffe et al. 2009). Therefore, the periostracum thickness as an indicator for its resistance may also be an important parameter for the sensitivity of bivalves towards external shell dissolution (Ries et al. 2009). While *M. edulis* possess a relative thick periostracum (35 µm) that is chemically very resistant, other bivalve species (e.g. of the family Veneridae) are characterized by a thin periostracum (<10 µm, Harper 1997). Species from this family (e.g. *Mercenaria mercenaria*) exhibit high mortality or growth reduction in water with Ωaragonite only slightly super- or undersaturated (Harper 1997, Green et al. 2004, 2009, Talmage and Gobler 2009, 2010, 2011). Planktonic pteropods without any organic cover and aragonitic shells therefore might be most vulnerable to undersaturation (Comeau et al. 2009, 2010, Lischka et al. 2011). Lischka et al. (2011) demonstrated enhanced shell degradation at elevated pCO_2 and when Ω aragonite <1.

The measurements of acid-base status in the bulk EPF revealed that shell formation occurs in an environment which is undersatured with respect to both polymorphs even at a high seawater pH (Misogianes and Chasteen 1979, publication 1). Under elevated pCO_2, EPF [CO_3^{2-}] becomes even lower which may favour dissolution of the nacre under certain conditions (Heinemann et al. 2012). As net calcification includes not only formation of new $CaCO_3$ structures but also the preservation of existing crystals this may cause net dissolution even when seawater is not undersaturated (Gazeau et al. 2007). Nevertheless, Melzner et al. (2011) observed a strong additive effect of high pCO_2 and starvation on nacre dissolution. These results show, that to a certain degree, shell dissolution is correlated to seawater [CO_3^{2-}]. But dissolution may not be of crucial importance in living animals, which are able to countermineralize, however this response may interfere with the energy budget (Melzner et al. 2011). Increased dissolution may only be observed for empty shells or in starved animals (Nienhuis et al. 2010).

Ocean acidification may impact living animals due to increasing pCO_2 and lowering of seawater pH. The latter may directly impact calcium carbonate production of organisms with limited ability for intracellular pH regulation (Suffrian et al. 2011) as observed for coccolithophores (Bach et al. 2011). In mussels, the formation of the amorhpous $CaCO_3$ precursor is probably located in intracellular vesicles

(Weiner and Addadi 2011). But in contrast to coccolithophores, molluscs are able to regulate the intracellular pH independently of the extracellular fluids or ambient seawater (Zange et al. 1990, Ellington 1993, Michaelidis et al. 2005). Under control conditions, EPF pH is low compared to seawater pH. Higher seawater pCO_2 causes significant lower pH, but the change in pH is relative moderate, e.g. EPF pH at 400 µatm is 7.52±0.04 vs. 7.34±0.09 at 2700 µatm (Heinemann et al. 2012). According to the boron isotopic data for *M. edulis*, molluscs do not increase the pH at the site of calcification as it is reported for e.g. foraminifera and corals (Bentov et al. 2009, de Noojer et al. 2009, Venn et al. 2011, Heinemann et al. 2012). Rather biomineralization is potentially facilitated by exclusion of Mg^{2+} from the precipitate (Lorens and Bender 1977, Zeebe and Sanyal 2002, Heinemann et al. 2008). Therefore the calcification process is probably not as sensitive to lowered seawater pH as in the above mentioned organisms.

In general increasing pCO_2 seems to be the most important aspect of OA for heterotrophic metazoans. These organisms maintain a CO_2 diffusion gradient between the intra- and extracellular body compartments and the ambient seawater in order to facilitate the diffusion of metabolically generated CO_2 from the tissues into the ambient water (Melzner et al. 2009a). Whereas increased acidity of the water does not affect extra- and intracellular pH (pHe, pHi) directly, increased intracellular pCO_2 would lead to reduction of pHi. Since pHi needs to be buffered in order to preserve cellular functions, an upregulation of cellular acid-base regulation is required e.g. proton extrusion from the cytosol (Madshus 1988, Boron 2004). This upregulation and the accompanied modulation of the membrane protein composition may affect the energy budgets on a cellular or even whole organism level (Deigweiher et al 2009, Martin et al. 2011, Stumpp et al. 2011a,b). Since calcification includes not only $CaCO_3$ precipitation but also requires production of an organic component that includes chitinous organic matrices, glycoproteins, silk-like proteins and periostracin, it is a costly process (Palmer 1992). Although the mass of the organic shell components contributes only to a small extent to total shell mass, its production requires a much higher fraction of the energy required for calcification (publication 3). Therefore it seems likely that calcification is down regulated as a result of an energetic trade off under elevated pCO_2. In this case, calcification is not directly affected but in a secondary fashion as a consequence of lowered energy availability (Melzner et al. 2011). This has also been suggested for sea urchin larvae. Here development is slowed down as the Scope for Growth decreases in the elevated pCO_2 treatment (Stumpp et al. 2011a). As mentioned above, fed mussels exhibit a higher ability to preserve internal nacre from dissolution than starved animals (Melzner et al. 2011). Therefore, it is also possible that calcification becomes more costly under elevated pCO_2, when crystals need to be stabilized under increasing corrosive conditions. One mechanism could be the enhancement of the organic envelope surrounding the crystals. In fact, expression of tyrosinase increases with increasing pCO_2 which may support stabilization of the shell structure under corrosive conditions (Hüning et al. accepted).

In contrast to the benthic bivalve stages studied here, pelagic bivalve larvae are more sensitive to ocean acidification and exhibit reduced calcification (Kurihara et al. 2008b, Talmage and Gobler 2009, Gazeau et al. 2010, Bechman et al. 2011, Gaylord et al. 2011). In bivalve larvae, seawater $[CO_3^{2-}]$ seems to be more important for growth and calcification than in adults (Gazeau et al. 2011). This might

be related to less efficient protection by the organic cover or to the use of amorphous $CaCO_3$, which is much more unstable compared to aragonite or calcite polymorphs (Weiss et al 2002). Additionally, larvae depend to a higher degree on seawater carbon as a source for calcification, whereas in adult mussels metabolism provides a much larger fraction (Owen et al. 2008, Gillikin et al. 2009). However, so far, for moderate acidification levels no study has addressed the question whether bivalve larval development is disturbed as observed for high pCO_2 (Kurihara et al. 2008, Bechman et al. 2010) or only slowed down indicated by smaller size and thinner shells (Gazeau et al. 2010, Gaylord et al. 2010) This has been observed for a number of different taxa including cephalopods (Martin et al. 2011, Hu et al. 2011, Stumpp et al. 2011a,b). In these studies, absolute calcification rates were reduced when they were correlated to age, but not in relation to size (Martin et al. 2011).

Similar to observations on the benthic life stage, calcification in larvae might be affected by energy limitation. The organic content of pediveliger and freshly metamorphosed specimens of *M. edulis* was much higher compared to juvenile or adult mussels (Jörgensen et al. 1976, publication 3, figure S2 and table S3). These findings should be similar at least for the late veliger stages. A higher organic content in the shell drastically increases the energy costs required for shell production (Palmer 1983, 1992). Especially in thin shelled bivalve larvae with a large surface to volume ratio, periostracum production accounts for an over proportional energy fraction of shell growth. As a consequence, reduction of calcification under high pCO_2 could save high amounts of energy.

4.2.2 Acid-base regulation

Experiments conducted under elevated pCO_2 with *M. galloprovincialis* and *M. edulis* suggested that extracellular haemolymph pH (pHe) is partly buffered by an accumulation of bicarbonate (Lindinger et al. 1984, Michaelidis et al. 2005). As increased [HCO_3^-] were always accompanied by a similar increase of [Ca^{2+}], shell dissolution seemed to be source of this buffering. This is a common pattern observed in nearly all bivalves during prolonged valve closure in response external stress such as emersion or hypoxia (Crenshaw and Neff 1969, Jokumsen and Fyhn 1982, Booth et al. 1984, Walsh et al. 1984). Whereas a partially buffering of molluscs haemolymph pH by active HCO_3^- accumulation has been observed for cephalopods (Gutowska et al. 2010a) it does not play a role in bivalves during prolonged exposure to elevated pCO_2. Although the internal shell might dissolve under certain conditions of low temperature and food availability (Melzner et al. 2011) *M. edulis* is not able to retain extracellular bicarbonate levels above those of the ambient medium. Rather internal shell dissolution leads to net transfer of base equivalents to the incubation water. This was observed for the haemolymph and also for the EPF (Heinemann et al. 2012, publication 1).

Under natural conditions, in mussels subjected to the high pH variability in Kiel Fjord, haemolymph pH seems to be solely determined by ambient seawater pCO_2 and pH. Thus elevated haemolymph bicarbonate concentrations observed in other bivalve studies (Michaelidis et al 2005, Lannig et al. 2010), may result from an accumulation due to shell dissolution in recirculating aquarium systems (Lindinger et al. 1984). Similar to all other ions, bicarbonate equilibrates between water and

haemolymph which explains the slow Ca^{2+} and bicarbonate increase observed by Michaelidis et al. (2005). According to these results, pH and ion regulation in general in *M. edulis* seems to be restricted to the intracellular space, similar to results obtained for osmoregulation (Wright and Silva 1994). It has been observed that the extracellular fluid of mussels exposed to varying salinities is iso-osmotic and iso-tonic to the ambient environment (Gilles 1972, Davenport 1979). Leakages across the membranes seem to avoid bicarbonate accumulation.

In contrast, more active species rely on oxygenated, pH sensitive respiratory pigments and therefore need to control extracellular blood or haemolymph pH (Larsen et al. 1997, Spicer et al. 2007, Gutowska et al. 2010a). The capacity to regulate extracellular acid-base status is suggested to be a general indicator for a high tolerance to ocean acidification stress (Melzner et al. 2009a). This seems to be confirmed by number of studies where elevated pCO_2 has only small effects on species performance (Gutowska et al. 2008, Munday et al. 2011). Nevertheless, species need to upregulate ion regulatory transport in e.g. gill tissue (Deigweiher et al. 2008) in order to accumulate elevated bicarbonate concentrations. As elevated bicarbonate is also lost to the environment, maintenance of high blood bicarbonate requires additional energy which impacts the energy budget of the animals (Deigweiher et al. 2009, Grosell et al. in press). At the same time, bicarbonate accumulation itself may affect these species negatively (Gutowska et al. 2010b, Munday et al. 2011, Nilsson et al. 2012). Elevated blood bicarbonate and the electrochemically required lowering of $[Cl^-]$ might disturb transepithelial signaling and thereby may affect the species survival due to e.g lowered escape response (Dixson et al. 2010, Munday et al. 2011, Nilsson et al. 2012). Additionally it leads to hypercalcification which may affect proper function of e.g. otoliths (Gutowska et al. 2010b, Maneja et al. submitted). Under elevated pCO_2, slow bicarbonate accumulation leads to a partially buffering of coelomic pH in a sea urchin species (Stumpp et al. 2012). However, although this accumulation seems to support the ability to withstand lowered seawater pH, it is seems to require high energy amounts and fails in starving animals (or vice versa) which ultimately may cause enhanced mortality (Stumpp et al. 2012).

Bivalves, maintain a CO_2 gradient of about 1000 µatm between haemolymph and seawater. As a consequence, the haemolymph exhibits a relative high pCO_2 even under high ambient pH, relative low pH and carbonate concentrations are a consequence. The intracellular regulatory capacity of mussels seems to be well developed (Zange et al. 1990, Ellington 1993, Michaelidis et al. 2005) and probably allows an energetically much more efficient response to environmental stress such as elevated pCO_2. Tissues exhibit always much higher non bicarbonate buffer capacities (-9.6 to -23.8 mmol HCO_3^- kg^{-1} drymass pH^{-1}, Walsh et al. 1984) compared to extracellular fluids (-0.49 mmol HCO_3^- L^{-1} pH^{-1}, publication 1) due to higher protein concentrations (Truchot 1976, Smith and Raven 1979, Lindinger et al. 1984, Zange et al. 1990, Gutowska et al. 2010a, publication 1). Intracellular pH seems to be quite similar in a wide range of organisms with values of about 7.0-7.4 (Madshus 1988). It is important to consider that the negative membrane potential in cells causes a permanent acid load of the intracellular lumen (Boron et al. 2004). An unregulated pHi would decrease to values of about 6.5 or about 1 pH unit below extracellular pH. Only under these conditions H^+ ions do not passively diffuse into the intracellular space (Madshus 1988, Boron et al. 2004). In *Mytilus spp*. intracellular pH values

ranging between 7.1 and 7.4 and values of 7.4 have been observed for the anterior byssal retractor muscle (ABRM, Walsh et al. 1984, Zange et al. 1990, Michaelidis et al. 2005). The membrane potential of the ARBM has been determined to be about -64 mV (Hidaka and Goto 1973). Using these data and the rearranged version of the Nernst equation from Boron (2004) it can be assumed that even at a control extracellular pH of about 7.59 (publication 1), H^+ ions chronically enter the cytosol. No proton leakage would only be observed at a pHe of 8.41 which is not realistic under natural conditions. During exposure to elevated seawater pCO_2, pHe decreases while pHi remains constant. Therefore, the acid-load of the cytosol increases. Therefore with increasing acidity, intracellular acid extrusion or base intrusion mechanisms need to be upregulated (Boron 2004).

Ion transport across a cellular membrane is always energy consuming, as it is either primarily or secondarily driven by ATP. In the case of the H^+-ATPase, ATP hydrolysis and H^+-translocation are directly linked. On the other hand, the NHE (sodium proton exchanger) is driven by the sodium gradient between intra- and extracellular space, which is established by the sodium potassium ATPase (Na^+-K^+-ATPase). Therefore, the Na^+-K^+-ATPase plays a key role and is an indicator for the general ion regulatory capacity of an animal (Gibbs and Somero 1990). Increasing gene expression, protein concentration and activity has been observed in fish and cephalopods in response to strongly elevated seawater pCO_2 (Melzner et al. 2009b, Hu et al. 2011). These findings support the hypothesis of higher ion regulatory demand under hypercapnia. Nevertheless, this general assumption may only be valid for fish, cephalopods or crustaceans which actively regulate e.g. bicarbonate concentrations in the extracellular fluids. In mussels, the restriction of pH regulation to the intracellular space requires probably much lower acid-base regulatory capacities. Therefore mussels exhibit much lower presence of Na^+-K^+-ATPase (Melzner et al. 2009a) but are competent pHi regulators.

4.2.3 Metabolic rates, scope for growth and ammonium excretion

Similar to organisms which actively elevated blood bicarbonate (Deigweiher et al. 2009) also in *Mytilus* higher energetic effort for acid-base regulation is expected under elevated pCO_2 due to lowered pHe but constant pHi. This upregulation may either cause an energy allocation which leads to a higher fraction of total energy budget required for ion regulation (Deigweiher et al. 2009) or will even increase the standard or routine metabolic rates (Stumpp et al. 2011a). Recent observations revealed elevated aerobic metabolism which might reflect higher energy demand of cellular homeostasis during environmental hypercapnia (Wood et al. 2008, Stumpp et al. 2011). The data obtained for the genus *Mytilus* revealed different responses of oxygen consumption under elevated pCO_2. Michaelidis et al. (2005) observed lowered O_2 uptake in *M. galloprovincialis* exposed to about 5000 µatm pCO_2 compared to control animals. In *M. edulis*, oxygen consumption initially increased with increasing pCO_2 to up to 160% of control rates and peaked at about 2000-2500 µatm (publication 2). At higher pCO_2 levels, respiration started to decrease, 4000 µatm treated animals had similar metabolic rates as the control. Similar results of increasing aerobic metabolism at moderately increased pCO_2 levels have been observed for a number of echinoderm, fish and mollusks species including other bivalves (Wood et al. 2008, Munday et al. 2009b, Comeau et al. 2010, Lannig et al. 2010, Stumpp et al. 2011, Beniash

et al. 2011, Cummings et al. 2012). These results are in disagreement with the hypothesis that reduced extracellular pH elicits metabolic depression (Pörtner et al. 2005) as reported earlier also for bivalves (Michaelidis et al. 2005). In these studies, pCO_2 far beyond realistic expectations have been applied and therefore do not resemble the metabolic response at moderate pCO_2.

Converting the respired oxygen into energy equivalents, much higher metabolic energy turnover is observed under elevated pCO_2. Nevertheless, the studies mentioned above only lasted for several weeks or few months and therefore do not resemble the long-term effects of ocean acidification. In mussels acclimated for twelve months to 4 different pCO_2 levels, oxygen consumption was not elevated at higher pCO_2, but algae clearance and consequently energy uptake was drastically reduced under elevated pCO_2 (Fig 4.3). As metabolic rates strongly depend on food uptake (SDA = specific dynamic action), unchanged or slightly lowered respiration might be a secondary response to lowered filtration and digestion (Thompson and Bayne 1972, 1974, Jobling 1983). Increased ion regulatory effort is probably not detectable as changed oxygen consumption on the whole animal level. It is also possible that animals were able to switch to a more energy efficient buffer mechanism during long-term acclimation.

Nevertheless, independent of wether metabolic rates are increased at unchanged food absorption (2 months, publication 2) or wether absorption decreased drastically and metabolic rates remained unchanged (12 months, Fig. 4.3). In both cases, SfG was reduced at elevated pCO_2 in *M. edulis*. This is similar to results obtained for sea urchin larvae and adults (*Strongylocentrotus droebachiensis*, Stumpp et al. 2011, 2012) and juvenile sea stars (*Asterias rubens*, Appelhans et al. in prep). It has been suggested, that the lowering of extracellular pH values in stomach or digestive tracts might affect the proper functioning of digestive enzymes with narrow pH optima and thereby lead to lowered feeding rates (Stumpp 2011). Also in *M. edulis*, digestion occurs both extra- and also intracellularly (Hawkins et al. 1983), therefore might be susceptible to the lowering of extracellular pH values.

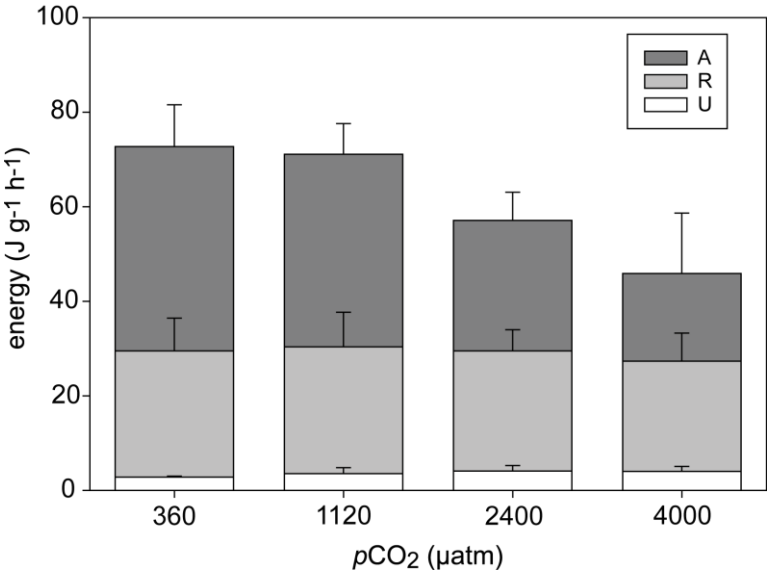

Figure 4.3: Energy budget of *M. edulis* acclimated to four pCO_2 levels between 380 and 4000 µatm for twelve months (unpublished data). Energetic equivalents were calculated for absorbed (A), respired (R) and excreted (U) energy. Absorbed energy was calculated from clearance rates, measured mean cell densities of 2000 *Rhodomonas* cells ml^{-1} with 45 pg C cell^{-1} and an absorption efficiency of 80% according to Riisgard 1981; mean±SD, n=4 aquaria with 2x3 mussels each.

The higher protein breakdown observed under elevated pCO_2 might be one reason for reductions of SfG and growth as it is energetically less efficient (Tedegren and Kautsky 1990). Additionally, increased NH_4^+ excretion implies also an enhanced nitrogen loss of the animals. In general, *M. edulis* assimilates nitrogen more efficiently than carbon (Kreeger et al. 1995, Kreeger et al. 1996, Smaal and Vonck 1997). When maintained at balanced protein breakdown and synthesis, 3.6% of body protein are degraded per day in *Mytilus edulis* but about 90% are directly recycled in the synthesis of new proteins in order to minimize the loss to the environment (Hawkins and Bayne 1991). Studies suggest that *Mytilus* growth is limited by nitrogen and especially amino acid supply. Therefore, ingested algae with low C:N facilitate growth (Kreeger and Langdon 1993, Kreeger et al. 1996). Nevertheless, also energy is a limiting factor and growing animals are characterized by a higher SfG than starving, non-growing animals (Hawkins et al. 1989, Hawkins and Banye 1991, van Haren and Kooijman 1993). Hawkins et al. (1991) reported relative smaller nitrogen loss in animals maintained at higher food concentration. They calculated higher recycling efficiency with increased energy supply (Hawkins et al. 1991). As these animals also exhibited higher growth, they were characterized by a higher SfG. Similarly, reduced SfG in *Mytilus* under elevated pCO_2 may reduce their ability to retain body nitrogen and therefore could cause enhanced nitrogen loss as indicated by higher NH_4^+ excretion rates. According to this hypothesis, protein degradation is not elevated but nitrogen recycling efficiency is reduced. As a consequence, growth reductions of mussels might be caused by SfG reduction and subsequent enhanced nitrogen loss. Therefore, adverse effects of pCO_2 might be drastically enhanced in studies conducted with insufficient food supply (and consequent low SfG) and may finally cause elevated mortality (Berge et al. 2006, Dickinson et al. 2012). Additionally, the high costs required for calcification are often ignored, as this process also includes the energy consuming production of organic components. Especially in young thin shelled mussels, the energetic costs required for shell production exceed those for somatic growth (publication 3). Consequently, during unfavorable abiotic conditions, calcification might be the process which is down regulated at first as it is no directly related to the survival of a mussel and energy is allocated to more essential processes.

Therefore, adequate nutrition of mussels is a central aspect which determines the tolerance to abiotic stress. In filter feeding mussels the POC concentration available in the surrounding water column is the most important factor which determines the energy available for the organisms and therefore also growth (Page and Hubbard 1987, Stirling and Okumus 1994, Buck 2007). SfG decreases with increasing pCO_2, higher POC concentration may therefore support compensation of the negative impacts of ocean acidification. According to the laboratory experiment with crossed treatments of elevated pCO_2 and feeding regimes, food supply was much more important than pCO_2 levels up to 4000 µatm. At the pCO_2 levels encountered in the inner Kiel Fjord, SfG is not significantly affected by pCO_2. Therefore, high food availability outweighs the effects of elevated pCO_2 and the higher energy availability enabled much higher growth of mussels compared to the outer fjord area with lower pCO_2 but also much lower POC concentrations (publication 3). In accordance to the results of Melzner et al. (2011) higher energy availability supports the ability of mussels to overcome the negative impacts of ocean acidification.

The observation of increased ammonium excretion rates under elevated pCO_2 raised the question of the underlying excretion mechanisms and the potential physiological role in the acclimation process. The NH_3/NH_4^+ concentrations of haemolymph and tissue are much higher than in the seawater and correspond to values obtained for other marine species (Nawata et al. 2010, Martin et al. 2011). Relative NH_3 concentrations of haemolymph and tissues are low due to low haemolymph pH and the high pK of NH_3/NH_4^+. Nevertheless, due to the high total ammonia concentrations an outward directed pNH_3 gradient exists between tissue and water and also between haemolymph and water (Fig. 4.4D). This may enable an excretion of NH_3 across the large gill area. However, compared to the haemolymph, much higher NH_3/NH_4^+ concentrations were measured in the kidney fluid in cephalopods (Potts 1965) and also in a marine bivalve (Suzuki 1988). This suggests a key role of this organ in urine formation and excretion. So far, research on the *M. edulis* kidney focused on its role in storage and excretion of heavy metals (Pirie and George 1979, George and Pirie 1979). Due to the small volume of the kidney fluid/urine in *M. edulis* no determination of the NH_3/NH_4^+ concentration was possible within the frame work of this thesis. Nevertheless, kidney tissue (including the urine in the lumen) is characterized by relative high NH_3/NH_4^+ concentrations compared to other tissues (Fig. 4.4D). Especially, increased and high concentrations were observed compared to other tissues during exposure to high environmental ammonia (HEA, 663 µmol L^{-1} vs 35 µmol L^{-1} as a control). This may indicate a similar accumulation of NH_3/NH_4^+ in the lumen of the kidney. The fraction of H^+-ATPase and Na^+-K^+-ATPase activities and their gene expression were similar in all tissues (Fig. 4.4A,B). However, total ATPase activity was much higher in the kidney tissue compared to gill and mantle. The undefined high activity may indicate a potential for transport activity not related to sodium and potassium or proton transport. This may either be related to NH_3 excretion or to accumulation and excretion of heavy metals (George and Pirie 1979).

Rh proteins were indentified to play a crucial role in the ammonia excretion mechanism as they facilitate the transport of NH_3. This general pattern was observed in the mammalian kidney (Weiner and Verlander 2011) and also in the gill of teleost fish (Wright and Wood 2009) and crustaceans (Weihrauch et al. 2004). Changing expression of Rh isoforms under high environmental ammonia (HEA) and elevated pCO_2 are documented for fish (Nawata et al. 2010) and crustaceans (Martin et al. 2011). In the moderate HEA treatment (663 µmol L^{-1}) no significant changes of Rh mRNA expression were measured in *M. edulis* (Fig 4.4B). However, Rh and also Amt (ammonium transporter) mRNA are highly expressed in the kidney, but not in gill and foot. Similar to Rh, Amt forms a channel through the cell membrane and the resulting pore facilitates the gas exchange of NH_3 across the lipid bilayer (Khademi et al. 2004, Zidi-Yahioui et al. 2009). Subsequently, NH_3 is trapped as NH_4^+ in the boundary layer by a seperately transported H^+. Genes which might be related to NH_3 excretion were expressed much lower in gill and foot when compared to the kidney (Fig. 4.4B). This data reveals for the first time that *M. edulis* expresses Rh and Amt genes, which support NH_3 diffusion. The proton which is required for the acid-trapping is probably excreted by a H^+-ATPase and not by NHE as the inhibitor amiloride has no effect on ammonium excretion rates in *M. galloprovincialis* (Hunter and Kirschner 1986). *M. edulis* exhibits a well developed excretory system and ultrastructure of kidney cells indicates ion transport properties, although mussels do not excrete a hypo-osmotic urine (Pirie and George 1979). Derived from ultrastructure analyses, the haemolymph is modified by ultrafiltration by podocytes in the

pericard (Robinson and Morse 1994). The ultrafiltrate then enters the kidney through the renopericardial canal (Pirie and George 1979). In a second step, the primary urine is modified in the kidney by resorption and excretion before it is excreted via the excretory pore (Potts 1967). The high Rh and Amt expression levels and high NH_3 concentration in the kidney suggest that most probably, the gill is not the main site of excretion. The localization of both proteins is unclear; however, occurrence of two different ammonia channel proteins in the same tissue may enable an efficient regulation of basolateral ammonia uptake and apical excretion in epithelial cells. Additionally, the ubiquitous Na^+/K^+-ATPase may transport NH_4^+ on the basolateral site (Pagliarani et al. 2008).

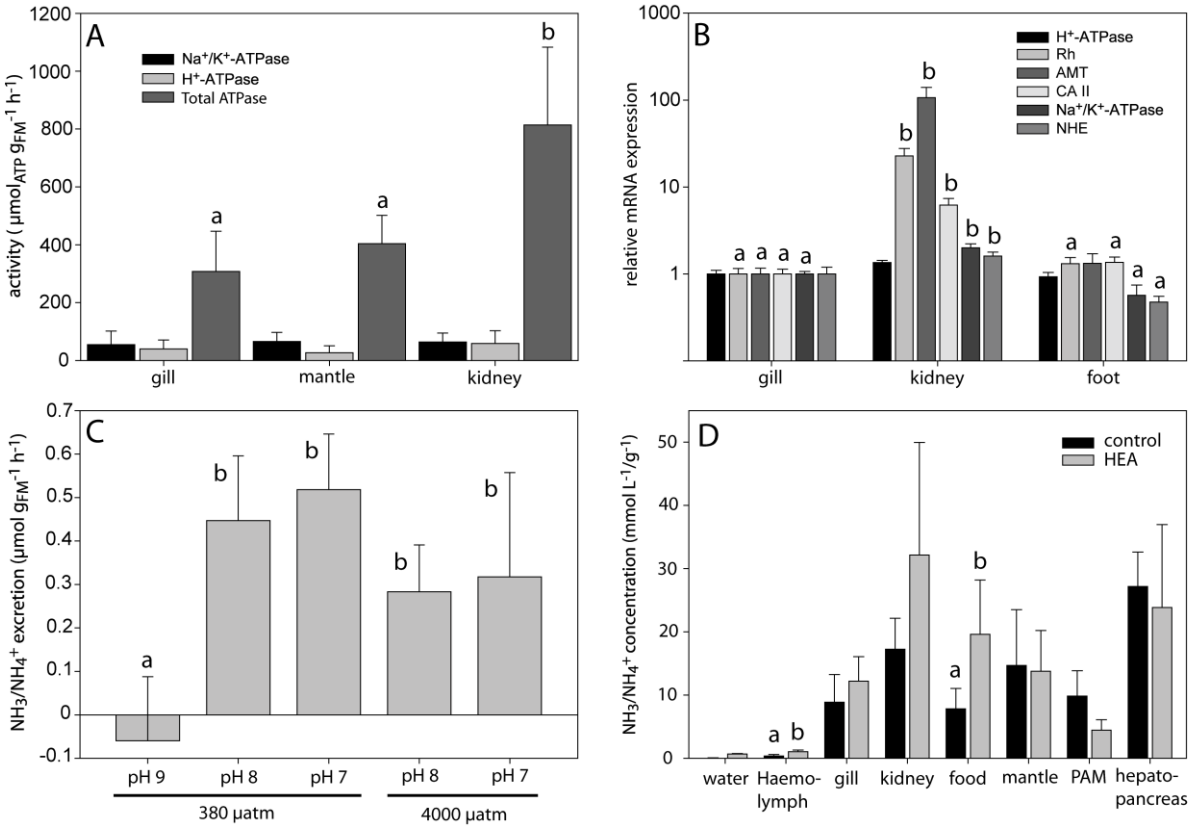

Figure 4.4: Activity of Na^+/K^+-ATPase, H^+-ATPase and Total ATPase in gill, mantle and kidney tissue mean±SD, n=3-5 (A), relative mRNA expression of genes suggested to be involved in NH_3/NH_4^+ excretion in gill, kidney and foot tissue mean±CF, n=9-12 (B), NH_3/NH_4^+ excretion rates under acute exposure (2 h) to 380 or 4000 µatm and pH values of 7, 8 and 9, mean±SD, n=4 (C), NH_3/NH_4^+ concentration of ambient water and haemolymph (in mmol L^{-1}) and tissues (in mmol g^{-1}, PAM=posterior adductor muscle) during control (35 µmol L^{-1} NH_3/NH_4^+, black) and high environmental ammonia (HEA, 663 µmol L^{-1} NH_3/NH_4^+, grey) condition (D), significant differences are indicated by letters.

It has been suggested that one mechanisms of net H^+ extrusion from the intracellular space is excretion of NH_4^+. Increased NH_3/NH_4^+ excretion rates have been observed in a number of species in response to short- and long-term elevated pCO_2 (Lindinger et al. 1984, Michaelidis et al. 2005, Hammer et al. 2011, Stumpp et al. 2012, publication 2). However, increased excretion may also result from passively enhanced acid-trapping due to lowered seawater pH. Determination of the NH_3/NH_4^+ net flux during an acute exposure (2 h) to lowered pH 7 at a pCO_2 of 380 µatm revealed a slight but insignificant increase of NH_4^+ excretion (Fig. 4.4C). In seawater of pH 9 adjusted by NaOH addition, ammonium excretion ceased completely. This data supports the hypothesis that also in mussels,

NH_3/NH_4^+ excretion is facilitated by an acid-trapping mechanism similar to the general model developed for crustaceans (Weihrauch et al. 2004). At a pCO_2 of 4000 µatm and 2 h incubation, excretion was not elevated but slightly lowered, which did not agree to other results for short-term exposure to elevated pCO_2 (Lindinger et al. 1984, Michaelidis et al. 2005) and may result from a short-term lowering of metabolic rates. After prolonged acclimation (5 to 8 weeks), increased protein breakdown takes place in bivalves and echinoderms, as indicated by lower O:N ratios and higher ammonia excretion rates (Stumpp et al. 2012, publication 2). NH_3 production may contribute to buffering of the cytosol as NH_4^+ is formed at intracellular pH values. However, Rh and Amt proteins transport only NH_3 and not NH_4^+ (Khademi et al. 2004). After removal of the NH_3 from the cytosol, the proton still needs to be removed from the cell lumen. This role is most likely fulfilled by the H^+-ATPase (Martin et al. 2004). As the proton pump transports only one H^+ per ATP it is energetically not as efficient as an NHE which exchanges one proton for about 1/3 ATP, since the Na^+-K^+-ATPase removes three Na^+ per ATP. From this point of view, elevated NH_4^+ excretion rates do not necessarily support intracellular acid-base regulation or at least are energetically not a more efficient pathway. But it may contribute to the excretion of protons from the bodyfluids. Also generation of HCO_3^- by breakdown of certain amino acids (aspartic and glutamic acid) may support pHi regulation (Langenbuch and Pörtner 2002).

4.3 *Mytilus* and the benthic community in a high pCO_2 ecosystem

In coastal habitats, which are characterized by elevated pCO_2 levels as a consequence of volcanic activity, the number of benthic calcifiers is decreased at low pH (Hall-Spencer et al. 2008, Fabricius et al. 2011). In Kiel Fjord, such a reduction is not observed. Similar to observations made earlier in this habitat, the benthic community is dominated by calcifying organisms and *M. edulis* in particular (Boje 1965, Enderlein and Wahl 2004). Although the mean pCO_2 levels and also pCO_2 variability drastically increased within the last 50 years due to eutrophication induced hypoxia, the dominant position of mussels in the benthic communities has not changed. During summer/autumn mean pCO_2 of 970 µatm were observed, the annual mean is about 700 µatm. Under experimental conditions, these levels have not been shown to significantly lower the survival of *M. edulis* larvae, but only affect calcification (Gazeau et al 2010, Gaylord et al. 2011). The high settlement rates of larvae and their fast growth rates in the inner Fjord enables the mussels to outcompete other species for space on artificial substrata (Enderlein and Wahl 2004). The primary effect of eutrophication is not increased pCO_2 but in particular enhanced primary production. Increased nutrient load of Kiel Fjord probably had a positive effect on the production of *M. edulis*. Due to their high filtering capacity, mussels are able to convert a huge fraction of the present POC content in coastal habitats into biomass (Clausen and Riisgard 1996). Filtration rates are known to decrease during prolonged exposure to high cell densities, but these levels are not observed in nature (Clausen and Riisgard 1996). As visible in Fig 4.4, filtration (absorbtion) and also metabolic rates are not significantly affected at mean pCO_2 levels encountered in inner Kiel Fjord. Only during acute upwelling events with values up to 2400 µatm, SfG can be significantly lowered. As these events do not last for more than a few days, it cannot be expected that

these levels significantly reduce the annual production under present conditions. Additionally, the past change of the carbonate system might have already affected their predators. In Kiel Fjord, the sea star *Asterias rubens* is the main predator of mussels (Dürr and Wahl 2004, Reusch and Chapman 1997). This species seems to be much more affected by elevated pCO_2 than mussels. Juvenile sea star specimens kept under elevated pCO_2 of about 1000 µatm exhibited significant reductions of feeding rates compared to control levels (Appelhans et al. in prep.). The observed pCO_2 increase in the recent past already might have affected sea star feeding rates. Therefore, *M. edulis* dominance in the Fjord might have become even more pronounced than in former times.

On the other hand, the atmospheric CO_2 increase expected for the end of the century and the resulting shift of the carbonate system will drastically elevated the mean pCO_2 levels. This increase is in particular expected for the main settlement and growth period in summer and autumn. The expected values might be high enough to cause larval malformation, enhance mortality and reduce settlement success (Kurihara et al. 2008a, Bechmann et al. 2011). Under prolonged elevated pCO_2 the expected reduced SfG may also cause significant reduction of annual the growth of *M. edulis* in Kiel Fjord. Nevertheless, the main predators *A. rubens* and *Carcinus maenas* will be probably even more affected by future pCO_2. Although survival was not impaired, feeding rates decreased at highly elevated pCO_2 (Appelhans et al. accepted). Additionally, the predicted desalination of the Baltic may have considerable impact on the diversity and species interaction. Whereas mussels are quite tolerant to lower salinities, sea stars might be strongly affected and abundances are expected to decline (Casties et al. in prep). Most probably, ocean acidification as a single factor will not substantially change the community or decrease *M. edulis* dominance in this habitat as the most abundant species tolerate increased pCO_2 (McDonald et al. 2009, Pansch et al. submitted).

This is in contrast to the predictions of reduced calcifier abundance as response to ocean acidification deduced from the data collected at Ischia (Hall-Spencer et al. 2008, Kroeker et al. 2011). Nevertheless, also in this habitat, e.g mussels transplanted into a high pCO_2 zones were able to survive and continued calcification (Rodolpho-Metalpa et al. 2011). Ablation of the periostracum causes similar external shell dissolution features as observed for Kiel Fjord animals (Rodolpho-Metalpa et al. 2011 supplementary information). In general, *M. galloprovincialis* seems to be similarly tolerant towards ocean acidification as *M. edulis*, as growth continued also at 5000 µatm and survival was not affected (Michaelidis et al. 2005). For another *Mytilus* species much more severe affects were hypothesized. Reduction of size and dominance of *M. californianus* in the coastal upwelling area at the American West coast were related to the upwelling of high pCO_2 water (Wootton et al. 2008, Feely et al. 2008). This process probably has been strongly enhanced by human activities and increased atmospheric CO_2 (Feely et al. 2009) and has great impact on this mussel population (Pfister et al. 2011). A number of bivalve species exhibited high sensitivity to elevated pCO_2 or under saturation and exhibited reduced growth and survival (Talmage and Gobler 2009, 2010, 2011, Miller et al. 2010). However, to a certain degree this low tolerance might be related to insufficient acclimation time and feeding (Waldbusser et al. 2010a,b, Dickinson et al. 2012). In general, at least the genus *Mytilus* seems to be relatively tolerant to high ambient pCO_2 (Michaelidis et al. 2005, Kurihara et al. 2008a, Rodolpho-Metalpa et al. 2011). To what extend the Kiel Fjord population has adapted to the past pCO_2

increase and has developed a higher resistance to elevated pCO_2 is not clear. Evolutionary responses are not well studied to date. Whereas current physiotypes might be susceptible to ocean acidification, evolutionary adaptation may enable much better performance in the future (Lobeck et al. submitted). Although the genetic and phenotypic variation is lower compared to a sea urchin species, simulated evolution suggests genetic adaptation potential of mussels to elevated pCO_2 within 50 years (Sunday et al. 2011). This corresponds to the time frame, in which the ecosystem of Kiel Fjord was subjected to much higher pCO_2 levels. The pCO_2 increase at the US coastline is probably more rapid and the rate exceeds the critical tolerance level of the inhabiting mussel species (Wootton et al. 2008).

The high energy availability in Kiel Fjord might be the main reason for the tolerance of calcareous invertebrates towards the adverse carbonate system. Most coastal habitats provide high POC concentrations similar to Kiel Fjord and thereby provide energy amounts which allow a certain tolerance towards ocean acidification (Werner et al. 2006, Buck 2007). In contrast, the Mediterranean Sea is an oligotrophic ocean and has a much lower POC concentration (Cauwet et al 1997). This might have enhanced the susceptibility of calcifiers to high pCO_2. Nevertheless, whereas the obtained mean pH values at some of the investigated stations at Ischia correspond to future CO_2 increase, the pCO_2 amplitude at these vents varies drastically and peak pCO_2 levels exceed realistic levels by far (Kroeker et al. 2011, Kerrison et al. 2011). Larvae drifted into these high pCO_2 areas, have no time to adapt to the ambient conditions and are probably not affected by moderate pCO_2 levels but suffer from the high pCO_2 peaks. These strongly elevated pCO_2 levels may cause responses on the species physiological level (metabolic depression) as well as on ecosystem level (absence of calcifiers) which will most probably not occur at realistic future CO_2 levels.

Ocean acidification will not act as a single stressor alone but is accompanied by ocean warming. Synergistic effects of high pCO_2 and temperatures may reduce the ability of marine animals to cope with future climate change. CO_2 has been show to reduce the thermal tolerance during acute exposure to high temperatures (Walther et al. 2009). In general, the thermal tolerance window may shrink at elevated pCO_2 (Pörtner 2010). Rodolpho-Metalpa and coworkers (2011) observed that mussels and corals were able to survive at the high pCO_2 site in Ischia. However, unusually high temperatures adversely affected these species and increased mortality rates (Rodolpho-Metalpa et al. 2011). Combined effects of increasing pCO_2 and temperature have been suggested to lower survival of barnacles (Findlay et al. 2010). In the Baltic, warming may have a similar effect on the local mussel population as temperature is expected to increase by approximately 3°C (Döscher and Meier 2004). During summer, very high temperatures which might be critical for *M. edulis* may coincide with elevated pCO_2. Therefore climate change which combines several abiotic stressors might have considerable impact on the benthic community in Kiel Fjord.

5. Conclusion and outlook

This work provides evidence that the blue mussel *M. edulis*, which is an important benthic calcifier, can cope with elevated pCO_2 levels which are expected for the 2300 due to future ocean acidification. In other naturally acidified habitats, calcifiers were affected the most by low pH and high pCO_2 (Hall-Spencer et al. 2008). Mussels were expected to be especially sensitive and future pCO_2 levels might decrease calcification rates and finally dissolve mussel shells (Gazeau et al. 2007).

The results of the experiments conducted in the frame of this thesis, revealed that adequate nutrition and acclimation time seems to be sufficient to allow *M. edulis* compensation of the negative effects of elevated pCO_2. According to these results, predictions of the fate of an ecosystem which are only based on projected pCO_2 may not be reliable as other biotic and abiotic factors such as energy availability may have substantial effects. Further, present experimental results cannot mimic the adaptation which may take place within multiple generations (Sunday et al. 2011, Lohbeck et al. submitted). The study of naturally acidified habitats may provide the best possibility to investigate these adaptation potential. However, due to the small size of these areas affected by volcanic activity (Hall-Spencer et al. 2008), in most cases present day physiotypes are rapidly subjected to unnatural high pCO_2 levels. Larvae passively drifted into a high pCO_2 plume experience drastic changes of the carbonate chemistry within a very short time period similar to laboratory experiments (Kroeker et al. 2011, Kerrison et al. 2011). Therefore, experiments as well as these study sites most probably do not reflect the responses of animals after multi generation adaptation to ocean acidification. The study site in Kiel Fjord may resemble a more realistic scenario, as the amplitude of pCO_2 change is much lower and the area larger. The results imply, that calcification of mussels per se is not necessarily impacted and an adaptation potential ameliorates the responses to elevated pCO_2. Further, Kiel Fjord *M. edulis* population might have been already adaptated to elevated pCO_2. Therefore, experiments need be repeated with *M. edulis* populations from a more stable habitat with less pCO_2 fluctuations. The comparison of the results would allow to asses acclimation and adaptation potential and their importance for the tolerance to ocean acidification stress.

The experiments performed in the field and in the laboratory revealed the importance of nutrition on the tolerance to ocean acidification. Higher energy availability enables a much higher tolerance which emphasizes the importance of the physiological responses of an organism to elevated pCO_2. Within twelve months of acclimation, the responses (e.g. increased vs. unchanged metabolic rates) differ drastically, but in both cases the scope for growth was reduced. Future research needs to elucidate the energy budget and allocation within an organism in response to elevated pCO_2. However, even in closely related (therefore physiologically comparable) echinoderm species the responses to elevated pCO_2 drastically differ between 100% mortality (Dupont et al. 2008), slowdown of development (Stumpp et al. 2011a) and faster, more successful development (Dupont et al. 2010). Therefore the physiological mechanisms which underlie the tolerance to ocean acidification need to be clarified. For instance, the hypothesis that the extracellular acid-base status determines the performance aerobic metabolism (Pörtner et al. 2005) needs to be revised. Similarly, the extracellular ion regulatory

capacity does not necessarily determine the ability of an organism to withstand ocean acidification stress (Melzner et al. 2009, Nilsson et al. 2012).

Ocean acidification is only one aspect of global change and will be always accompanied by warming and in the Baltic Sea by desalination. Synergistic stress effects by ocean acidification and warming have been already observed (Pörtner 2008, Rodolpho-Metalpa et al. 2011). The combination of two or even three stressors at the same time may also alter the tolerance of *M. edulis* in the Kiel Fjord. Therefore, future studies need to address the combined effects of multiple stressors.

6. References

Addadi, L., Raz, S. & Weiner, S. (2003). Taking advantage of disorder: amorphous calcium carbonate and its roles in biomineralization. *Advanced Materials*, *15*(12), 959-970.

Ameyaw-Akumfi, C. & Hughes, R. (1987). Behaviour of *Carcinus maenas* feeding on large *Mytilus edulis*. How do they assess the optimal diet? *Marine Ecology Progress Series*, *38*(3), 213-216.

Babenerd, B. (1991). Increasing oxygen deficiency in Kiel Bay (Western Baltic), *Meeresforschung*, *33*, 121-140.

Bach, L.T., Riebesell, U. & Schulz, K.G. (2011). Distinguishing between the effects of ocean acidification and ocean carbonation in the coccolithophore *Emiliania huxleyi*. *Limonology And Oceanography*, *56*(6), 2040-2050.

Bamber, R. (1990). The effects of acidic seawater on three species of lamellibranch molluscs. *Journal of Experimental Marine Biology and Ecology*, *143*(3), 181-191.

Bayne, B.L. (1965). Growth and the delay of metamorphosis of the larvae of *Mytilus edulis* (L.). *Ophelia, 2*, 1-47.

Bayne B.L. & Hawkins A.J.S. (1997) Protein metabolism, the costs of growth, and genomic heterozygosity: Experiments with the mussel *Mytilus galloprovincialis* Lmk. *Physiological Zoology*, *70*, 391-402

Bayne, B.L, & Widdows, J. (1978). The physiological ecology of two populations of *Mytilus edulis* L. *Oecologia*, *37*(2), 137-162.

Bechmann, R.K., Taban, I. C., Westerlund, S., Godal, B. F., Arnberg, M., Vingen, S., Ingvarsdottir, A. & Baussant, T. (2011). Effects of ocean acidification on early life stages of shrimp (*Pandalus borealis*) and mussel (*Mytilus edulis*). *Journal of Toxicology and Environmental Health Part A*, *74*(7), 424-38.

Beldowski, J., Löffler, A., Schneider, B. & Joensuu, L. (2010). Distribution and biogeochemical control of total CO_2 and total alkalinity in the Baltic Sea. *Journal of Marine Systems*, *81*(3), 252-259.

Beniash, E, Ivanina, A, Lieb, N., Kurochkin, I, & Sokolova, I.M. (2010). Elevated level of carbon dioxide affects metabolism and shell formation in oysters *Crassostrea virginica* (Gmelin). *Marine Ecology Progress Series*, *419*, 95-108.

Bentov, S., Brownlee, C. & Erez, J. (2009). The role of seawater endocytosis in the biomineralization process in calcareous foraminifera. *Proceedings of the National Academy of Sciences of the United States of America*, *106*(51), 21500-21504.

Berge, J.A., Bjerkeng, B., Pettersen, O., Schaanning, M.T. & Oxnevad, S. (2006). Effects of increased sea water concentrations of CO_2 on growth of the bivalve *Mytilus edulis* L, *62*(4), 681-687.

Bishop, J.M., Verlander, J.W., Lee, H.W., Nelson, R.D., Weiner, A.J., Handlogten, M.E. & Weiner, D. (2010). Role of the Rhesus glycoprotein, Rh B glycoprotein, in renal ammonia excretion. *American Journal of Physiology-Renal Physiology*, *299*(5), F1065-F1077.

Booth, C.E., McDonald, D.G. & Walsh, P.J. (1984). Acid-base-balance in the sea mussel, *Mytilus edulis* .1. Effects of hypoxia and air-exposure on hemolymph acid-base status, *5*(6), 347-358.

Borges, A.V. & Frankignoulle, M. (1999). Daily and seasonal variations of the partial pressure of CO_2 in surface seawater along Belgian and southern Dutch coastal areas. *Journal of Marine Systems*, *19*(4), 251-266.

Borges, A.V. & Gypens, N. (2010). Carbonate chemistry in the coastal zone responds more strongly to eutrophication than to ocean acidification. *Limonology And Oceanography*, *55*(1), 346-353.

Boron, W.F. (2004). Regulation of intracellular pH. *Advances in Physiology Education*, *28*(1-4), 160-179.

Boutilier, R.G. & St-Pierre, J. (2000). Surviving hypoxia without really dying. *Comparative biochemistry and physiology Part A Molecular integrative physiology*, *126*(4), 481-490.

Brasse, S., Nellen, M., Seifert, R. & Michaelis, W. (2002). The carbon dioxide system in the Elbe estuary. *Biogeochemistry*, *59*(1), 25-40.

Brey, T., Rumohr, H. & Ankar, S. (1988). Energy content of macrobenthic invertebrates: general conversion factors from weight to energy. *Journal of Experimental Marine Biology and Ecology*, *117*(3), 271-278.

Bubel, A. (1973). An electron- microscope study of periostracum formation in some marine bivalves. II. The cells lining the periostracal groove. *Marine Biology*, *20*, 222-234.

Buck, B.H. (2007). Experimental trials on the feasibility of offshore seed production of the mussel *Mytilus edulis* in the German Bight: installation, technical requirements and environmental conditions. *Helgoland Marine Research*, *61*(2), 87-101.

Burnett, L.E. (1997). The challenges of living in hypoxic and hypercapnic environment. *Comparative and General Pharmacology*, *640*, 633-640.

Bustnes, J.O. & Erikstad, K.E. (1990). Size selection of common mussels, *Mytilus edulis*, by common eiders, *Somateria mollissima*: Energy maximization or shell. *Canadian Journal of Zoology*, *68*(11), 2280-2283.

Böhle, B. (1972). Effects of adaptation to reduced salinity on filtration activity and growth of mussels (*Mytilus edulis* L.). *Journal of Experimental Marine Biology and Ecology*, *10*(1), 41-47.

Büdenbender, J, Riebesell, U, & Form, A. (2011). Calcification of the Arctic coralline red algae *Lithothamnion glaciale* in response to elevated CO_2. *Marine Ecology Progress Series*, *441*, 79-87.

Cai, W.J., Hu, X., Huang, W.J., Murrell, M.C., Lehrter, J.C., Lohrenz, S.E., Chou, W.C., Zhai, W., Hollibaugh, J.T., Wang, Y., Zhao, P., Guo, X., Gundersen, K., Dai, M. & Gong, G.C. (2011). Acidification of subsurface coastal waters enhanced by eutrophication. *Nature Geoscience*, *4*(11), 1-5.

Caldeira, K, & Wickett, M.E. (2005). Ocean model predictions of chemistry changes from carbon dioxide emissions to the atmosphere and ocean. *Journal of Geophysical Research*, *110*(C9), 1-12.

Cao, L. & Caldeira, K. (2008). Atmospheric CO_2 stabilization and ocean acidification. *Geophysical Research Letters*, *35*(19), 1-5.

Cauwet, G., Miller, A., Brasse, S., Fengler, G., Mantoura, R. & Spitzy, A. (1997). Dissolved and particulate organic carbon in the western Mediterranean Sea. *Deep Sea Research Part II: Topical Studies in Oceanography*, *44*(3-4), 769-779.

Checkley, D.M., Dickson, Andrew G., Takahashi, M., Radich, J. A., Eisenkolb, N. & Asch, R. (2009). Elevated CO_2 enhances otolith growth in young fish. *Science*, *324*(5935), 1683. AAAS.

Cigliano, M., Gambi, M C, Rodolfo-Metalpa, R, Patti, F.P. & Hall-Spencer, J.M. (2010). Effects of ocean acidification on invertebrate settlement at volcanic CO_2 vents. *Marine Biology*, 157(11), 2489-2502.

Clausen, I. & Riisgård, H. (1996). Growth, filtration and respiration in the mussel *Mytilus edulis*:no evidence for physiological regulation of the filter-pump to nutritional needs. *Marine Ecology Progress Series*, *141*(1981), 37-45.

Comeau, S., Gorsky, G., Jeffree, R., Teyssi, J.L. & Gattuso, J.P. (2009). Key Arctic pelagic mollusc (*Limacina helicina*) threatened by ocean acidification. *Biogeoscience*, 6(1), 2523-2537.

Comeau S., Jeffree R., Teyssie J.L. & Gattuso J.P. (2010) Response of the arctic pteropod *Limacina helicina* to projected future environmental conditions. *PlosONE*, *5*, e11362

Conley, D.J., Carstensen, J., Ærtebjerg, G., Christensen, P.B., Dalsgaard, T., Hansen, J.L.S. & Josefson, A.B. (2007). Long-term changes and impacts of hypoxia in Danish coastal waters. *Ecological Applications*, *17*(sp5), S165-S184.

Crenshaw, M.A. & Neff, J.M.(1969). Decalcification at the mantle-shell interface in molluscs. *American Zoologist*, *9*, 881-885.

Cummings, V., Hewitt, J., Van Rooyen, A., Currie, K., Beard, S., Thrush, S., Norkko, J., Barr, N., Heath, P., Halliday, N.J., Sedcole, R., Gomez, A., McGraw, C. & Metcalf, V. (2011) Ocean acidification at high latitudes: potential effects on functioning of the antarctic bivalve *Laternula elliptica*. *PLoS ONE*,*6*(1): e16069

Dankers, N. & Zuidema, D.R. (1995). The role of the mussel (*Mytilus edulis* L.) and mussel culture in the Dutch Wadden Sea. *Estuaries*, *18*(1), 71.

Davenport, J. (1979). Is *Mytilus edulis* a short term osmoregulator? *Comparative Biochemistry and Physiology Part A: physiology, 64*(1), 91-957.

De Nooijer, L.J., Toyofuku, T. & Kitazato, H. (2009). Foraminifera promote calcification by elevating their intracellular pH. *Proceedings of the National Academy of Sciences of the United States of America*, *106*(36), 15374-15378.

Deigweiher, K., Hirse, T., Bock, C., Lucassen, M. & Pörtner, H.O. (2010). Hypercapnia induced shifts in gill energy budgets of Antarctic notothenioids. *Journal of comparative physiology B Biochemical systemic and environmental physiology*, *180*(3), 347-359.

Deigweiher, K., Koschnick, N., Pörtner, H.O. & Lucassen, M. (2008). Acclimation of ion regulatory capacities in gills of marine fish under environmental hypercapnia. *American journal of physiology Regulatory integrative and comparative physiology*, *295*(5), R1660-R1670.

Diaz, R.J. & Rosenberg, R. (2008). Spreading dead zones and consequences for marine ecosystems. *Science*, *321*(5891), 926-929.

Dickinson, G.H., Ivanina, A.V., Matoo, O.B., Pörtner, H.O., Lannig, G., Bock, C., Beniash, E. & Sokolova, I.M. (2012). Interactive effects of salinity and elevated CO2 levels on juvenile eastern oysters, *Crassostrea virginica*. *Journal of Experimental Biology*, *215*, 29-43.

Dickson, A.G. (1981). An exact definition of total alkalinity and a procedure for the estimation of alkalinity and total inorganic carbon from titration data. *Deep Sea Research Part A Oceanographic Research Papers*, *28*(6), 609-623.

Dickson, A.G. (1990). Standard potential of the reaction - $AgCl_S$+1/2 H_2 = Ag_S+HCl_{Aq} and the standard acidity constant of the ion HSO_4- in synthetic sea-water from 273.15-K to 318.15-K. *Journal of Chemical Thermodynamics*, *22*(2), 113-127.

Dickson, A.G., Afghan, J.D. & Anderson, G.C. (2003). Reference materials for oceanic CO2 analysis: a method for the certification of total alkalinity. *Marine Chemistry*, *80*(2-3), 185-197.

Dickson, A.G. & Millero, F.J. (1987). A comparison of the equilibrium-constants for the dissociation of carbonic-acid in seawater media, *34*(10), 1733-1743.

Dickson, A.G., Sabine, C.L. & Christian, J.R. (2007). *Guide to best practices for ocean CO_2 measurements* (Vol. 3, p. 191). PICES Special Publications .

Dixson, D.L, Munday, P.L. & Jones, G.P. (2010). Ocean acidification disrupts the innate ability of fish to detect predator olfactory cues. *Ecology Letters*, *13*(1), 68-75.

Donelson, J.M., Munday, P.L, Mccormick, M.I. & Nilsson, G.E. (2010). Acclimation to predicted ocean warming through developmental plasticity in a tropical reef fish. *Global Change Biology*, *17*(4), 1712-1719.

Doney, S.C., Fabry, V.J., Feely, R.A. & Kleypas, J.A. (2009). Ocean Acidification: The Other CO_2 Problem. *Annual Review of Marine Science*, *1*(1), 169-192.

Döscher, R. & Meier, H.E.M. (2004). Simulated sea surface temperature and heat fluxes in different climates of the Baltic Sea. *AMBIO: ajournal of human environment*, *33*, 242-248.

Dupont, S, Havenhand, J., Thorndyke, W., Peck, L. & Thorndyke, M. (2008). Near-future level of CO_2-driven ocean acidification radically affects larval survival and development in the brittlestar *Ophiothrix fragilis*. *Marine Ecology Progress Series*, *373*, 285-294.

Dupont, S., Lundve, B. & Thorndyke, M. (2010). Near future ocean acidification increases growth rate of the lecithotrophic larvae and juveniles of the sea star *Crossaster papposus*. *Journal of experimental zoology Part B Molecular and developmental evolution*, *314*(5), 382-389.

Dürr, S. & Wahl, M. (2004). Isolated and combined impacts of blue mussels (*Mytilus edulis*) and barnacles (*Balanus improvisus*) on structure and diversity of a fouling community. *Journal of Experimental Marine Biology and Ecology*, *306*(2), 181-195.

Ellington, W.R. (1993). Studies of intracellular pH regulation in cardiac myocytes from the marine bivalve mollusk, *Mercenaria campechiensis*. *Biological Bulletin*, *184*(2), 209.

Enderlein, P. & Wahl, M. (2004). Dominance of blue mussels versus consumer-mediated enhancement of benthic diversity, *Journal of Sea Research*, *51*(2), 145-155.

Evans, D.H., Piermarini, P.M. & Choe, K.P. (2005). The multifunctional fish gill: dominant site of gas exchange, osmoregulation, acid-base regulation, and excretion of nitrogenous waste. *Physiological Reviews*, *85*(1), 97-177.

Fabricius, K.E., Langdon, C., Uthicke, S., Humphrey, C., Noonan, S., De'ath, G., Okazaki, R., Muelheimer, N., Glas, M.S. & Lough, J.M. (2011). Losers and winners in coral reefs acclimatized to elevated carbon dioxide concentrations. *Nature Climate Change*, *1*(6), 1-5.

Falini, G., Albeck, S., Weiner, S, & Addadi, L. (1996). Control of aragonite or calcite polymorphism by mollusk shell macromolecules. *Science*, *271*(5245), 67-69.

Famme, P. (1980). Effect of shell valve closure by the mussel Mytilus edulis on the rate of oxygen consumption in declining oxygen tension. *Comparative Biochemical Physiology*, *67*, 167-170

Feely, R.A, Sabine, C.L, Hernandez-Ayon, J.M., Ianson, D. & Hales, B. (2008). Evidence for upwelling of corrosive "acidified" water onto the continental shelf, *Science, 320*(5882), 1490-1492.

Feely, R.A, Sabine, C L, Lee, K, Berelson, W., Kleypas, J., Fabry, V.J. & Millero, F.J. (2004). Impact of anthropogenic CO_2 on the $CaCO_3$ system in the oceans, *Science, 305*(5682), 362-366.

Feely, R.A, Alin, S.R., Newton, J., Sabine, C.L., Warner, M., Devol, A., Krembs, C. & Maloy, C. (2010). The combined effects of ocean acidification, mixing, and respiration on pH and carbonate saturation in an urbanized estuary. *Estuarine, Coastal and Shelf Science*, *88*(4), 442-449.

Fehsenfeld, S., Kiko, R., Appelhans, Y., Towle, D.W., Zimmer, M. & Melzner, F. (2011). Effects of elevated seawater pCO_2 on gene expression patterns in the gills of the green crab *Carcinus maenas*. *BMC Genomics*, *12*(1), 488.

Feng, Q.L., Li, H.B., Pu, G., Zhang, D.M., Cui, F.Z. & Li, H.D. (2011) Crystallographic alignment of calcite prisms in the oblique prismatic layer of *Mytilus edulis* shell. *Journal of Materials Science*, *35*, 3337-3340.

Findlay, H.S., Burrows, M.T., Kendall, M.A., Spicer, J.I. & Widdicombe, S. (2010) Can ocean acidification affect population dynamics of the banacle Semibalanus balanoides at its southern range edge? *Ecology*, *91*, 2931-2940.

Franke, A. & Clemmesen, C. (2011) Effect of ocean acidification on early life stages of Atlantic herring (*Clupea harengus* L.). *Biogeoscience*, *8*, 3697-3707.

Frankignoulle, M, Abril, G., Borges, A., Bourge, I., Canon, C., DeLille, B., Libert, E. & Theate, J.M. (1998). Carbon dioxide emission from european estuaries, *Science*, *282*(5388), 434-436.

Frankignoulle, M, Bourge, I. & Wollast, R. (1996). Atmospheric CO_2 fluxes in a highly polluted estuary (the Scheldt). *Limonology And Oceanography*, *41*(2), 365-369.

Frankignoulle, M, & Canon, C. (1994). Marine calcification as a source of carbon-dioxide - positive feedback of increasing atmospheric CO_2. *Limonology and Oceanography*, *39*(2), 458-462.

Frommel, A., Schubert, A., Piatkowski, U. & Clemmesen, C. (2012) Egg and early larval stages of Baltic cod, *Gadus morhua*, are robust to high levels of ocean acidification. *Marine Biology*, online first

Gattuso, J. (1998). Effect of calcium carbonate saturation of seawater on coral calcification. *Global and Planetary Change*, *18*(1-2), 37-46.

Gaylord, B., Hill, T.M., Sanford, E., Lenz, E.A., Jacobs, L.A., Sato, K.N., Russell, A.D. & Hettinger, A. (2011). Functional impacts of ocean acidification in an ecologically critical foundation species. *Journal of Experimental Biology*, *214*, 2586-2594.

Gazeau, F., Quiblier, C., Jansen, J.M., Gattuso, J.P., Middelburg, J.J. & Heip, C.H.R. (2007). Impact of elevated CO_2 on shellfish calcification. *Geophysical Research Letters*, *34*(7), 1-5.

Gazeau, F., Gattuso, J.P., Dawber, C., Pronker, A.E., Peene, F., Peene, J, Heip, C.H.R. & Middelburg, J.J. (2010). Effect of ocean acidification on the early life stages of the blue mussel *Mytilus edulis*. *Biogeosciences*, *7*(7), 2051-2060.

Gazeau, F., Gattuso, J. P., Greaves, M., Elderfield, H., Peene, J., Heip, C.H.R. & Middelburg, J.J. (2011). Effect of carbonate chemistry alteration on the early embryonic development of the Pacific Oyster (*Crassostrea gigas*). *PLoS ONE*, *6*(8), 8.

George, S.G. & Pirie, B.J.S. (1979). The occurrence of cadmium in sub-cellular particles in the kidney of the marine mussel, *Mytilus edulis*, exposed to cadmium: The use of electron microprobe analysis . *Biochimica et Biophysica Acta (BBA)-Protein Structure*, *580*(2), 234-244.

Gibbs, A. & Somero, G.N. (1990). Na^+/K^+ -adenosine triphosphatase activities in gills of marine teleost fishes: changes with depth , size and lomotory activity level. *Marine Biology*, *106*, 315-321.

Gidhagen, L. (1987) Coastal upwelling in the Baltic Sea - Satellite and *in situ* measurements of sea-surface temperatures indicating coastal upwelling. *Estuarine, Coastal and Shelf Science*, *24*, 449-462.

Gilek, M., Tedengren, M. & Kautsky, N. (1992). Physiological performance and general histology of the blue mussel, *Mytilus edulis* L, from the Baltic and North Seas, *30*, 11-21.

Gilles, R. (1972). Osmoregulation in three molluscs: *Acanthochitona discrepans* (Brown), *Glycymeris glycimeris* (L.) and *Mytilus edulis* (L.). *The Biological Bulletin*, *142*(1), 25-35.

Gillikin, D.P. Hutchinson, K.A. & Kumai, Y. (2009). Ontogenetic increase of metabolic carbon in freshwater mussel shells (*Pyganodon cataracta*) . *Journal of Geophysical Research*, *114*, G01007.

Green, M.A., Jones, M.E., Boudreau, C.L., Moore, R.L. & Westman, B.A. (2004) Dissolution mortality of juvenile bivalves in coastal marine deposits. *Limnology and Oceanography*, *49*, 727-734.

Green, M.A., Waldbusser, G.G., Reilly, S.L., Emerson, K. & O´Donnell, S. (2009) Death by dissolution: sediment saturation state as a mortality factor for juvenile bivalves. *Limnology and Oceanography*, *54*, 1037-1047.

Guppy, M. & Withers, P. (1999). Metabolic depression in animals: physiological perspectives and biochemical generalizations. *Biological Reviews of the Cambridge Philosophical Society*, *74*(1), 1-40.

Gutowska, M.A, Pörtner, H.O. & Melzner, F. (2008). Growth and calcification in the cephalopod *Sepia officinalis* under elevated seawater pCO_2. *Marine Ecology-Progress Series*, *373*, 303-309.

Gutowska, M.A., Melzner, F., Langenbuch, M., Bock, C., Claireaux, G. & Pörtner, H.O. (2010a). Acid-base regulatory ability of the cephalopod (*Sepia officinalis*) in response to environmental hypercapnia. *Journal of comparative physiology B Biochemical systemic and environmental physiology*, *180*(3), 323-335.

Gutowska, M.A., Melzner, F, Pörtner, H.O. & Meier, S. (2010b). Cuttlebone calcification increases during exposure to elevated seawater pCO_2 in the cephalopod *Sepia officinalis*. *Marine Biology*, *157*(7), 1653-1663.

Hall-Spencer, J.M., Rodolfo-Metalpa, R., Martin, S., Ransome, E., Fine, M., Turner, S. M., Rowley, S.J., Tedesco, D. & Buia, M.C. (2008). Volcanic carbon dioxide vents show ecosystem effects of ocean acidification. *Nature*, *454*(7200), 96-99.

Hand, S.C. (1998). Quiescence in *Artemia franciscana* embryos: reversible arrest of metabolism and gene expression at low oxygen levels. *Journal of Experimental Biology*, *201*(Pt 8), 1233-1242.

Hansen, H.P., Giesenhagen, H.C. & Behrends, G. (1999). Seasonal and long-term control of bottom-water oxygen deficiency in a stratified shallow-water coastal system, *56*, 65-71.

Harper, E. M. (1997). The molluscan periostracum: An important constraint in bivalve evolution. *Palaeontology*, *40*(1), 71-97.

Hawkins, A.J.S, Bayne, B.L. & Clarke, K.R. (1983) Co-ordinated rhythms of digestion, absorption and excretion in *Mytilus edulis* (Bivalvia: Mollusca), *Marine Biology*, *74*, 41-48.

Hawkins A.J.S., Widdows J. & Bayne B.L. (1989) The relevance of whole-body protein-metabolism to measured costs of maintenance and growth in *Mytilus edulis*. *Physiological Zoology*, *62*, 745-763

Hawkins, A.J.S. & Bayne, B.L. (1991) Nutrition of marine mussels: factors influencing the relative utilizations of protein and energy. *Aquaculture*, 94, 177-196.

Haynert, K., Schönfeld, J., Riebesell, U. & Polovodova, I. (2011). Biometry and dissolution features of the benthic foraminiferal species *Ammonia aomoriensis* at high pCO_2. *Marine Ecology Progress Series*, *432*, 53-67.

Heinemann, A., Fietzke, J., Eisenhauer, A. & Zumholz, K. (2008). Modification of Ca isotope and trace metal composition of the major matrices involved in shell formation of *Mytilus edulis*. *Geochemistry Geophysics Geosystems*, *9*(1), Q01006.

Heinemann, A., Fietzke, J., Melzner, F., Böhm, F., Thomsen, J. Garbe-Schönberg, D. & Eisenhauer, A. (2012) Conditions of *Mytilus edulis* extracellular body fluids and shell composition in a pH-treatment experiment: Acid-base status, trace elements and $\delta^{11}B$. *Geochemistry Geophysics Geosystems*, *13*,Q01005.

HELCOM (1990). Baltic Sea Environment Proceedings No. 35 B. Second Periodic Assessment of the State of the Marine Environment of the Baltic Sea, 1984-1988; Backround Document. Baltic Marine Environment Protection Commission -Helsinki Commission-.

HELCOM (2003). Baltic Sea Environment Proceedings No. 87. The Baltic Sea environment: 1999-2002. Baltic Marine Environment Protection Commission -Helsinki Commission-.

HELCOM (2009). Baltic Sea Environment Proceedings No. 115 B. Eutrophication in the Baltic Sea – An integrated thematic assessment of the effects of nutrient enrichment and eutrophication in the Baltic Sea region.

Hernroth, B., Baden, S., Thorndyke, M. & Dupont, S. (2011). Immune suppression of the echinoderm *Asterias rubens* (L.) following long-term ocean acidification. *Aquatic toxicology*, *103*(3-4), 222-224.

Hofmann, G.E., Smith, J.E., Johnson, K.S., Send, U., Levin, L.A., Micheli, F., Paytan, A., Price, N.N., Peterson, B., Takeshita, Y., Matson, P.G., Crook, E.D., Kroeker, K.J., Gambi, M.C., Rivest, E.B., Frieder, C.A., Yu, P.C. & Martz, T.R. (2011). High-frequency dynamics of ocean pH: a multi-ecosystem comparison. *PLos One*, *6*(12), e28983.

Hu, M.Y., Sucré, E., Charmantier-Daures, M., Charmantier, G., Lucassen, M., Himmerkus, N. & Melzner, F. (2010). Localization of ion-regulatory epithelia in embryos and hatchlings of two cephalopods. *Cell and Tissue Research*, *339*(3), 571-583.

Hu, M.Y., Tseng, Y.-C., Stumpp, M., Gutowska, M. A., Kiko, R., Lucassen, M. & Melzner, F. (2011). Elevated seawater pCO_2 differentially affects branchial acid-base transporters over the course of

development in the cephalopod *Sepia officinalis*. *American journal of physiology Regulatory integrative and comparative physiology*, *300*(5), R1100-R1114.

Hunter, K.C., & Kirschner, L.B. (1986). Sodium absorption coupled to ammonia excretion in osmoconforming marine invertebrates. *American Journal of Physiology- Regulatory, Integrative and Comparative Physiology*, *251*(5), 957-962.

Innes, D.J., & Haley, L.E. (1977). Genetic aspects of larval growth under reduced salinity in *Mytilus edulis*. *Biological Bulletin*, *153*(2), 312-321.

Ishii, M., Kosugi, N., Sasano, D., Saito, S., Midorikawa, T. & Inoue, H. Y. (2011). Ocean acidification off the south coast of Japan: A result from time series observations of CO_2 parameters from 1994 to 2008. *Journal of Geophysical Research*, *116*(C6), 1-9.

Jacob, D.E., Soldati, A.L., Wirth, R., Huth, J., Wehrmeister, U. & Hofmeister, W. (2008). Nanostructure, composition and mechanisms of bivalve shell growth. *Geochimica et Cosmochimica Acta*, *72*, 5401-5415.

Jacob, D.E., Wirth, R., Soldati, A.L., Wehrmeister, U. & Schreiber, A. (2011). Amorphous calcium carbonate in the shells of adult Unionoida. *Journal of Structural Biology*, *173*(2), 241-249.

Jobling, M. (1983). Towards an explanation of specific dynamic action (SDA). *Journal of Fish Biology*, *23*(5), 549-555.

Jörgensen, C. (1976). Growth efficiencies and factors controlling size in some mytilid bivalves, especially *Mytilus edulis* L.: Review and interpretation. *Ophelia*, *15*(2), 175-192.

Kautsky, N. & Evans, S. (1987). Role of biodeposition by *Mytilus edulis* in the circulation of matter and nutrients in a Baltic coastal ecosystem. *Marine Ecology Progress Series*, *38*(1952), 201-212.

Kautsky, N., Johannesson, K. & Tedengren, M. (1990). Genotypic and phenotypic differences between Baltic and North-Sea populations of *Mytilus edulis* evaluated through reciprocal transplantations .1. growth and morphology. *Marine Ecology-Progress Series*, *59*(3), 203-210.

Kerrison, P., Hall-Spencer, J.M., Suggett, D., Hepburn, L.J. & Steinke, M. (2011). Assessment of pH variability at a coastal CO_2 vent for ocean acidification studies. *Estuarine, Coastal and Shelf Science*, *94*(2), 129-137.

Khademi, S., O'Connell, J., Remis, J., Robles-Colmenares, Y., Miercke, L.J.W. & Stroud, R.M. (2004). Mechanism of ammonia transport by Amt/MEP/Rh: structure of AmtB at 1.35 A. *Science*, *305*(5690), 1587-1594.

Khademi, S. & Stroud, R.M. (2006). The Amt/MEP/Rh family: structure of AmtB and the mechanism of ammonia gas conduction. *Physiology Bethesda Md*, *21*, 1548-9213.

Kim, H.C. & Lee, K. (2009). Significant contribution of dissolved organic matter to seawater alkalinity. *Geophysical Research Letters*, *36*(20), 1-5.

Knepper, M.A. (2008). Courier service for ammonia. *Nature*, *456*(7220), 336-337.

Kniprath, E. (1981). Larval development of the shell and the shell gland in *Mytilus* (Bivalvia). *Wilhems Roux´s Archives*, *188*, 201-204.

Koehn, R.K. (1991). The genetics and taxonomy of species in the genus *Mytilus*. *Aquaculture*, *94*(2-3), 125-145.

Koeve, W., Kim, H.C., Lee, K. & Oschlies, A. (2011). Potential impact of DOC accumulation on fCO_2 and carbonate ion computations in ocean acidification experiments. *Biogeosciences Discussions*, *8*(2), 3797-3827.

Kreeger, D.A., Hawkins, A.J.S. & Bayne, B.L. (1996). Use of dual-labeled microcapsules to discern the physiological fates of assimilated carbohydrate, protein carbon, and protein nitrogen in suspension-feeding organisms. *Limnology Oceanography*, *46*, 208-215.

Kroeker, K.J., Kordas, R.L., Crim, R.N. & Singh, G.G. (2010). Review and synthesis: Meta-analysis reveals negative yet variable effects of ocean acidification on marine organisms. *Ecology Letters*, *13*(11), 1419-1434.

Kroeker, K.J., Micheli, F., Gambi, M.C. & Martz, T.R. (2011). Divergent ecosystem responses within a benthic marine community to ocean acidification. *Proceedings of the National Academy of Sciences of the United States of America*, *108*(35), 14515-14520.

Kurihara, H., Kato, S. & Ishimatsu, A. (2007). Effects of increased seawater pCO_2 on early development of the oyster *Crassostrea gigas*. *Aquatic Biology*, *1*(1), 91-98.

Kurihara, H., Asai, T., Kato, S. & Ishimatsu, A. (2008a). Effects of elevated pCO_2 on early development in the mussel *Mytilus galloprovincialis*. *Aquatic Biology*, *4*, 225-233.

Kurihara, H. (2008b). Effects of CO_2-driven ocean acidification on the early developmental stages of invertebrates. *Marine Ecology Progress Series*, *373*, 275-284.

Langdon, C, Takahashi, T, Sweeney, C., Chipman, D., Goddard, J., Marubini, F., Aceves, H., Burnett, H. & Atkinson, M.J. (2000). Effect of calcium carbonate saturation state on the calcification rate of an experimental coral reef, *14*(2), 639-654.

Langenbuch, M. & Pörtner, H.O. (2002). Changes in metabolic rate and N excretion in the marine invertebrate *Sipunculus nudus* under conditions of environmental hypercapnia: identifying effective acid-base variables. *Journal of Experimental Biology*, *205*, 1153-1160.

Lannig, G., Eilers, S., Pörtner, H.O., Sokolova, I.M. & Bock, C. (2010). Impact of ocean acidification on energy metabolism of oyster, *Crassostrea gigas*—Changes in metabolic pathways and thermal response. *Marine Drugs*, *8*(8), 2318-2339.

Larsen, B.K., Pörtner, H.O. & Jensen, F.B. (1997). Extra- and intracellular acid-base balance and ionic regulation in cod (*Gadus morhua*) during combined and isolated exposures to hypercapnia and copper. *Marine Biology*, *128*(2), 337-346.

Lefèvre, N., Aiken, J., Rutllant, J., Daneri, G., Lavender, S. & Smyth, T. (2002). Observations of pCO_2 in the coastal upwelling off Chile : Spatial and temporal extrapolation using satellite data. *Journal of Geophysical Research*, *107*, 1-15.

Lehmann, A. & Myrberg, K. (2008). Upwelling in the Baltic Sea — A review. *Journal of Marine Systems*, *74*, S3-S12.

Lindinger, M.I., Lauren, D.J. & McDonald, D.G. (1984). Acid-base-balance in the sea mussel, *Mytilus edulis*. 3. Effects of environmental hypercapnia on intracellular and extracellular acid-base-balance, *Marine Biology Letters*, *5*(6), 371-381.

Lischka, S., Büdenbender, J, Boxhammer, T. & Riebesell, Ulf. (2010). Impact of ocean acidification and elevated temperatures on early juveniles of the polar shelled pteropod *Limacina helicina*: mortality, shell degradation, and shell growth. *Biogeosciences*, *7*(4), 8177-8214.

Lorens, R.B. & Bender, M.L. (1977). Physiological exclusion of magnesium from *Mytilus edulis* calcite. *Nature*, *269*, 793-794.

Madshus, I.H. (1988). Regulation of intracellular pH in eukaryotic cells. *The Biochemical journal*, *250*(1), 1-8.

Mandic, M., Todgeham, A.E. & Richards, J.G. (2009). Mechanisms and evolution of hypoxia tolerance in fish. *Proceedings of the Royal Society B*, *276*, 735-744.

Manzello, D.P. (2010). Ocean acidification hot spots : Spatiotemporal dynamics of the seawater CO_2 system of eastern Pacific coral reefs. *Marine Biology*, *55*(1), 239-248.

Marin, F., Luquet, G., Marie, B. & Medakovic, D. (2008). Molluscan shell proteins: primary structure, origin, and evolution. *Current Topics in Developmental Biology*, *80*(7), 209-276.

Martin, M., Fehsenfeld, S., Sourial, M.M. & Weihrauch, Dirk. (2011). Effects of high environmental ammonia on branchial ammonia excretion rates and tissue Rh-protein mRNA expression levels in seawater acclimated Dungeness crab *Metacarcinus magister*. *Comparative biochemistry and physiology Part A Molecular integrative physiology*, *160*(2), 267-277.

Martin, S., Richier, S., Pedrotti, M.L., Dupont, S., Castejon, C., Gerakis, Y., Kerros, Y.G., Oberhänsli, F., Teyssie, J.L., Jeffree, R. & Gattuso, J.P. (2011). Early development and molecular plasticity in the Mediterranean sea urchin *Paracentrotus lividus* exposed to CO_2-driven acidification. *Journal of Experimental Biology*, *214*, 1357-1368.

Matsushiro, A. & Miyashita, T. (2004). Evolution of hard-tissue mineralization: comparison of the inner skeletal system and the outer shell system. *Journal of Bone and Mineral Metabolism*, *22*(3), 163-169.

McConnaughey, T. A. & Gillikin, D.P. (2008). Carbon isotopes in mollusk shell carbonates. *GeoMarine Letters*, *28*(5-6), 287-299.

McDonald, J. H., Seed, R. & Koehn, R.K. (1991). Allozymes and morphometric characters of three species of *Mytilus* in the Northern and Southern Hemispheres. *Marine Biology*, *111*, 323-333.

McDonald, M., McClintock, J., Amsler, C., Rittschof, D, Angus, R., Orihuela, B. & Lutostanski, K. (2009). Effects of ocean acidification over the life history of the barnacle *Amphibalanus amphitrite*. *Marine Ecology Progress Series*, *385*, 179-187.

Medakovic, D, Popovic, S., Grzeta, B., Plazonic, M. & Hrs-Brenko, M. (1997). X-ray diffraction study of calcification processes in embryos and larvae of the brooding oyster *Ostrea edulis*. *Marine Biology*, *129*(4), 615-623. .

Medakovic, D. (2000). Carbonic anhydrase activity and biomineralization process in embryos, larvae and adult blue mussels *Mytilus edulis* L. *Helgoland Marine Research*, *54*(1), 1-6.

Meier, H.E.M., Feistel, R., Piechura, J., Arneborg, L., Burchard, H., Fiekas, V., Golenko, N., Kuzimina, N., Mohrholz, V., Nohr, C., Paka, V.T., Sellschopp, J., Stips, A. & Zhurbas, V. (2006). Ventilation of the Baltic Sea deep water: A brief review of present knowledge from observations and models. *Oceanologia*, *48*, 133–164.

Melzner, F., Gutowska, M.A, Langenbuch, M., Dupont, S., Lucassen, M., Thorndyke, M.C., Bleich, M. & Pörtner, H.O. (2009a). Physiological basis for high CO_2 tolerance in marine ectothermic animals: pre-adaptation through lifestyle and ontogeny? *Biogeosciences*, *6*(10), 2313-2331.

Melzner, F., Göbel, S., Langenbuch, M, Gutowska, M.A., Pörtner, H.O. & Lucassen, M. (2009b). Swimming performance in Atlantic Cod (*Gadus morhua*) following long-term (4-12 months) acclimation to elevated seawater pCO_2. *Aquatic Toxicology*, *92*(1), 30-37.

Melzner, F., Stange, P., Trübenbach, K., Thomsen, J., Casties, I., Panknin, U. & Gutowska, M.A. (2011). Food supply and seawater pCO_2 impact calcification and internal shell dissolution in the blue bussel *Mytilus edulis*. *PLoS ONE*, *6*(9), e24223.

Michaelidis, B., Ouzounis, C., Paleras, A. & Pörtner, H.O. (2005). Effects of long-term moderate hypercapnia on acid-base balance and growth rate in marine mussels *Mytilus galloprovincialis*. *Marine Ecology-Progress Series*, *293*, 109-118.

Michaelis, H. (1978). Zur Morphologie und Ökologie von *Polydora ciliata* und *P. ligni* (Polychaeta, Spionidae). *Helgoländer Wissenschaftliche Meeresuntersuchungen*, *31*(1-2), 102-116.

Miles, H., Widdicombe, S., Spicer, J. & Hall-Spencer, J.M. (2007). Effects of anthropogenic seawater acidification on acid-base balance in the sea urchin *Psammechinus miliaris*. *Marine Pollution Bulletin*, *54*(1), 89-96.

Miller, A.W., Reynolds, A.C., Sobrino, C. & Riedel, G.F. (2010). Shellfish face uncertain future in high CO_2 world: influence of acidification on oyster larvae calcification and growth in estuaries. *PLoS ONE*, *4*, e5661.

Mingliang, Z., Jianguang, F., Jihong, Z., Bin, L., Shengmin, R., Yuze, M. & Gao, Y. (2011). Effect of marine acidification on calcification and respiration of *Chlamys farreri*. *Journal of Shellfish Research*, *30*(2), 267-271.

Misogianes, M.J. & Chasteen, N.D. (1979). A chemical and spectral characterization of the extrapallial fluid of *Mytilus edulis*. *Analytical Biochemistry*, *100*(2), 324-334.

Miyamoto, H., Miyashita, T, Okushima, M., Nakano, S., Morita, T., & Matsushiro, A. (1996). A carbonic anhydrase from the nacreous layer in oyster pearls. *Proceedings of the National Academy of Sciences of the United States of America*, *93*(18), 9657-9660.

Munday, P., Crawley, N, & Nilsson, G. (2009a). Ocean acidification impairs olfactory discrimination and homing ability of marine fish. *Proceedings of the National Academy of Sciences of the United States of America*, *106*, 1848-1852.

Munday, P., Crawley, N, & Nilsson, G. (2009b). Interacting effects of elevated temperature and ocean acidification on the aerobic performance of coral reef fishes. *Marine Ecology Progress Series*, *388*, 235-242.

Munday, P., Gagliano, M., Donelson, J., Dixson, D. & Thorrold, S. (2011). Ocean acidification does not affect the early life history development of a tropical marine fish. *Marine Ecology Progress Series*, *423*, 211-221.

Musa-Aziz, R., Chen, L. M., Pelletier, M.F. & Boron, W.F. (2009). Relative CO_2/NH_3 selectivities of AQP1, AQP4, AQP5, AmtB, and RhAG. *Proceedings of the National Academy of Sciences of the United States of America*, *106*(13), 5406-5411.

Myrberg, K. & Andrejev, O. (2003). Main upwelling regions in the Baltic Sea — a statistical analysis based on three-dimensional modelling. *Boreal Environment Research*, *8*, 97-112.

Nawata, C.M., Hirose, S., Nakada, T., Wood, C.M. & Kato, A. (2010). Rh glycoprotein expression is modulated in pufferfish (*Takifugu rubripes*) during high environmental ammonia exposure. *Journal of Experimental Biology*, *213*(18), 3150-3160.

Neff, J.M. (1972). Ultrastructure of the outer epithelium of the mantle in the clam *Mercenaria mercenaria* in relation to calcification of the shell. *Tissue cell*, *4*(4), 591-600.

Newell, R.I.E. (1989) Species profile: life histories and environmental requirements of coastal fishes and invertebrates (North and Mid-Atlantic) - blue mussel. U*.S. Fish and Wildlife Service Biological Report* , *82*, 1-21.

Nienhuis, S., Palmer, A.R. & Harley, C.D.G. (2010). Elevated CO_2 affects shell dissolution rate but not calcification rate in a marine snail. *Proceedings of the Royal Society B: Biological Sciences*, *277*(1693), 2553-2558.

Nilsson, G. E., Dixson, D.L., Domenici, P., McCormick, M.I., Sørensen, C., Watson, S.A. & Munday, P.L. (2012). Near-futurew carbon dioxide levels alter fish behaviour by interfering with neurotransmitter function. *Nature Climate Change*,

Norling, P., & Kautsky, N. (2008). Patches of the mussel *Mytilus* sp. are islands of high biodiversity in subtidal sediment habitats in the Baltic Sea. *Aquatic Biology*, *4*, 75-87.

Okumus, I, & Stirling, H.P. (1994). Physiological energetics of cultivated mussel (*Mytilus edulis*) populations in two Scottish west coast sea lochs. *Marine Biology*, *119*(1), 125-131.

Olafsson, J., Olafsdottir, S.R., Benoit-Cattin, A., Danielsen, M., Arnarson, T.S. & Takahashi, T. (2009). Rate of Iceland Sea acidification from time series measurements. *Biogeosciences*, *6*(11), 2661-2668.

Owen, E., Wanamakerjr, A., Feindel, S., Schone, B. & Rawson, P. (2008). Stable carbon and oxygen isotope fractionation in bivalve (*Placopecten magellanicus*) larval aragonite. *Geochimica et Cosmochimica Acta*, *72*(19).

Page, H.M. & Hubbard, D.M. (1987). Temporal and spatial patterns of growth in mussels *Mytilus edulis* on an offshore platform: relationships to water temperature and food availability. *Journal of Experimental Marine Biology and Ecology*, *111*(2), 159-179.

Pagliarani, A., Bandiera, P., Ventrella, V., Trombetti, F., Manuzzi, M.P., Pirini, M. & Borgatti, A.R. (2008). Response of Na^+-dependent ATPase activities to the contaminant ammonia nitrogen in *Tapes philippinarum*: Possible ATPase involvement in ammonium transport. *Archives of Environmental Contamination and Toxicology*, *55*(1), 49-56.

Palmer, A.R. (1983). Relative cost of producing skeletal organic matrix versus calcification: evidence from marine gastropods. *Marine Biology*, *75*(2-3), 287-292.

Palmer, A.R. (1992). Calcification in Marine Mollusks - How Costly Is It. *Proceedings of the National Academy of Sciences of the United States of America*, *89*(4), 1379-1382.

Parker,L.M., Ross, P.M. & O´Connor, W.A. (2010) Comparing the effect of elevated pCO_2 and temperature on the fertilization and early development of two species of oyster. *Marine Biology*, *157*, 2435-2452.

Parker,L.M., Ross, P.M. & O´Connor, W.A. (2011) Populations of the Sydney rock oyster, Saccostrea glomerata, vary in response to ocean acidification. *Marine Biology*, *158*, 689-697.

Paulmier, A., Ruiz-Pno, D. & Garvon, V. (2011) CO_2 maximum in the oxygen minimum zone (OMZ). *Biogeoscience*, *8*, 239-252.

Pawlak, J.F., & Leppänen, J.M. (2006). Climate Change in the Baltic Sea area Draft HELCOM Thematic Assessment in 2006. *HELCOM Stakeholder Conference on the Baltic Sea Action Plan Helsinki Finland 7 March 2006*, 1-53. HELCOM.

Petit, J.R., Jouzel, J., Raynaud, D., Barkov, N.I., Barnola, J.M., Basile, I., Bender, M., Chapellaz, J., Davis, M., Delaygue, G., Delmotte, M. Kotyakov, V.M. Legrand, M., Lipenkov, V.Y. Lorius, C., pepin, L., Ritz, C., Saltzman, E. & Stievenard, M. (1999). Climate and atmospheric history of the past 420,000 years from the Vostok ice core, Antarctica. *Nature*, *399*(6735), 429-436.

Pfister, C.A., McCoy, S.J., Wootton, J.T., Martin, P.A., Colman, A.S. & Archer, D. (2011) Rapid environmental change over the past decade revealed by isotopic analysis of the california mussel in the Northeast Pacific. *PLoS ONE*, *6*(10): e25766.

Pirie, B.J.S. & George, S.G. (1979). Ultrastructure of the heart and excretory system of *Mytilus edulis* (L.). *Journal of the Marine Biological Association of the UK*, *59*(4), 819-829.

Potts, W. T. (1965). Ammonia excretion in *Octopus dofleini*. *Comparative biochemistry and physiology*, *14*, 339-355.

Potts, W.T. (1967). Excretion in the molluscs. *Biological Reviews*, *42*(1), 1-41.

Pörtner, H.O., RWebber, D.M., Boutilier, R.G. & O´Dor R.K. (1991) Acid-base regulation in exercising squid (Ilex illecebrosus, Loligo pealei). *American journal of physiology Regulatory integrative and comparative physiology*, *261*, 239-246.

Pörtner, H.O. (1994) ACoordination of metaolism, acid-base regulation and haemocyanin function in cephalopods. *Marine and Freshwater Behaviour and Physiology*, *25*, 131-148.

Pörtner, H.O., Reipschläger, A. & Heisler, N. (1998) Acid-base regulation, metabolism and energetics in *Sipunculus nudus* as a function of ambient carbon dioxide level. *Journal of Experimental Biology*, *201*, 43-55.

Pörtner, H.O., Bock, C. & Reipschläger, A. (2000) Modulation of the cost of pHi regulation druing metabolic depression: a ^{31}P-NMR study in invertebrate (*Sipunculus nudus*) isolated muscle. *Journal of Experimental Biology*, *203*, 2417-2428.

Pörtner, H.O., (2000) Biological impact of elevated CO_2 concentrations: Lessons from animal physiology and earth history. *Journal of Oceanography*, *60*, 705-718.

Pörtner, H.O., Langenbuch, M. & Reipschläger, A. (2004) Biological impact of elevated CO_2 concentrations: lessons from animal physiology and earth history. *Journal of Oceanography*, *60*, 705-718.

Pörtner, H.O. (2008) Ecosystem effects of ocean acidification in times of ocean warming: a physiologist´s view. *Marine Ecology Progress Series*, *373*, 203-217.

Pörtner, H.O. (2010) Oxygen- and capcity-limitation of thermal tolerance: a matrix for integrating climate-related stressor effects in marine ecosystems. *Journal of Experimental Biology*, *213*, 881-893.

Provoost, P., Van Heuven, S., Soetaert, K., Laane, R. W.P.M. & Middelburg, J.J. (2010). Seasonal and long-term changes in pH in the Dutch coastal zone. *Biogeosciences*, *7*(11), 3869-3878.

Reusch, T.B.H. & Chapman, A.R.O. (1997). Persistence and space occupancy by subtidal blue mussel patches. *Ecological Monographs*, *67*(1), 65-87.

Riebesell, U., Zondervan, I., Rost, B., Tortell, P. D., Zeebe, R.E. & Morel, F.M. (2000). Reduced calcification of marine plankton in response to increased atmospheric CO_2. *Nature*, *407*(6802), 364-7.

Ries, J.B., Cohen, A.L., & McCorkle, D.C. (2009). Marine calcifiers exhibit mixed responses to CO_2-induced ocean acidification. *Geology*, *37*(12), 1131-1134.

Riginos, C. & Cunningham, C.W. (2005). Local adaptation and species segregation in two mussel (*Mytilus edulis* x *Mytilus trossulus*) hybrid zones. *Molecular Ecology*, *14*(2), 381-400.

Robinson, W E, & Morse, M. P. (1994). Biochemical constituents of the blood plasma and pericardial fluid of several marine bivalve mollusks - Implication for ultrafiltration. *Comparative Biochemistry and Physiology B-Biochemistry & Molecular Biology*, *107*(1), 117-123.

Rodhe, J. (1998). Chapter 24. The Baltic and North Seas: A process-oriented review of the physical oceanography coastal segment. *The Sea* (p. 699).

Rodolfo-Metalpa, R., Houlbrèque, F., Tambutté, É., Boisson, F., Baggini, C., Patti, F.P., Jeffree, R., Fine, M., Foggo, A., Gattuso, J.P. & Hall-Spencer, J.M. (2011). Coral and mollusc resistance to ocean acidification adversely affected by warming. *Nature Climate Change*, *1*(9), 1-5.

Roy, R., Roy, L., Vogel, K., Porter-Moore, C., Pearson, T., Good, C., Millero, F.J. & Campbell, D.M. (1993). The dissociation constants of carbonic acid in seawater at salinities 5 to 45 and temperatures 0 to 45°C. *Marine Chemistry*, *44*(2-4), 249-267.

Sabine, C.L, Feely, R.A., Gruber, N., Key, R.M., Lee, K., Bullister, J.L., Wanninkhof, R., Wong, C.S., Wallace,D.W.R, Tilbrook,T., Millero, F.J., Peng, T.H., Kozyr, A., Ono,T. & Rios, A.F. (2004). The oceanic sink for anthropogenic CO_2, *305*(5682), 367-371.

Sadok, S., Uglow, R.F. & Haswell S.J. (1997). Haemolymph and mantle fluid ammonia and ninhydrin positive substances variations in salinity-challenged mussels (*Mytilus edulis* L.). *J Ex Mar Biol Ecol*, *211*(2), 195-212.

Salonen, K., Sarvala, J., Hakala, I. & Viljanen, M. (1976). The relation of energy and organic carbon in aquatic invertebrates. *Limnology and Oceanography*, *21*(5), 724-730.

Saranchova, O.L., & Flyachinskaya, L.P. (2001). The influence of salinity on early ontogeny of the mussel *Mytilus edulis* and the starfish *Asterias rubens* from the White Sea. *Text*, *27*(2), 87-93.

Sarma, V.V.S.S. (2003). Monthly variability in surface pCO_2 and net air-sea CO_2 flux in the Arabian Sea. *Journal of Geophysical Research*, *108*(C8), 3255.

Scardino, A., De Nys, R., Ison, O., O'Connor, W., & Steinberg, P. (2003). Microtopography and antifouling properties of the shell surface of the bivalve molluscs *Mytilus galloprovincialis* and Pinctada imbricata. *Biofouling*, *19*, 221-230.

Schiettecatte, L.S., Gazeau, F., van der Zee, C., Brion, N. & Borges, A.V. (2006). Time series of the partial pressure of carbon dioxide (2001–2004) and preliminary inorganic carbon budget in the Scheldt plume (Belgian coastal waters). *Geochemistry Geophysics Geosystems*, *7*, Q06009.

Schneider, B, Nausch, G., Kubsch, H., & Petersohn, I. (2002). Accumulation of total CO_2 during stagnation in the Baltic Sea deep water and its relationship to nutrient and oxygen concentrations. *Marine Chemistry*, *77*(4), 277 - 291.

Schönitzer, V. & Weiss, I.M. (2007). The structure of mollusc larval shells formed in the presence of the chitin synthase inhibitor Nikkomycin Z. *BMC Structural Biology*, *7*(71), 71. BioMed Central.

Schwartz, A., Allen, J.C. & Harigaya, S. (1969). Possible involvement of cardiac Na^+, K^+-adenosine triphosphatase in the mechanism of action of cardiac glycosides. *The Journal of Pharmacology and Experimental Therapeutics*, *168*, 31–41.

Sharp J.H. (1974). Improved analysis for “particulate” organic carbon and nitrogen from seawater. *Limnology and oceanography*, *19*(6), 984-989.

She, J., Berg, P. & Berg, J. (2007). Bathymetry impacts on water exchange modelling through the Danish Straits. *Journal of Marine Systems*, *65*(1-4), 450-459.

Shirayama, Y. & Thornton, H. (2005). Effect of increased atmospheric CO_2 on shallow water marine benthos, Jouranl of Geophysical Research, *110*, C9S08.

Siegel, H., Gerth, M., Rudloff, R. & Tschersich, G. (1994) Dynamic features in the western Baltic Sea investigated using NOAA-AVHRR data. *Ocean Dynamics*, *46*, 191-207.

Silva, A. L. & Wright, S. H. (1994a). Short-term cell volume regulation in *Mytilus californianus* gill. *Journal of Experimental Biology*, *194*, 47-68.

Silverman, J., Lazar, B., Cao, L., Caldeira, K. & Erez, J. (2009). Coral reefs may start dissolving when atmospheric CO 2 doubles. *Geophysical Research Letters*, *36*(5), 1-5.

Smaal, A. & Vonck, A. (1997). Seasonal variation in C, N and P budgets and tissue composition of the mussel *Mytilus edulis*. *Marine Ecology Progress Series*, *153*, 167-179.

Smith, F.A. & Raven, J.A. (1979). Intracellular pH and its regulation. *Annual Review of Plant Physiology*, *30*(1), 289-311.

Soupene, E., King, N., Feild, E., Liu, P., Niyogi, K.K., Huang, C.H. & Kustu, S. (2002). Rhesus expression in a green alga is regulated by CO_2. *Proceedings of the National Academy of Sciences of the United States of America*, *99*(11), 7769-7773.

Spicer, J.I., Raffo, A. & Widdicombe, S. (2007). Influence of CO_2-related seawater acidification on extracellular acid-base balance in the velvet swimming crab *Necora puber*. *Marine Biology*, *151*(3), 1117-1125.

Spicer, J.I., Taylor, A.C. & Hill, A.D. (1988). Acid-base status in the sea urchins *Psammechinus miliaris* and *Echinus esculentus* (Echinodermata, Echinoidea) during emersion. *Marine Biology*, *99*(4), 527-534.

Stirling, H.P. & Okumus, I. (1994). Growth, mortality and shell morphology of cultivated mussel (*Mytilus edulis*) stocks cross-planted between two Scottish sea lochs. *Marine Biology*, *119*(1), 115-123.

Stuckas, H., Stoof, K., Quesada, H. & Tiedemann, R. (2009). Evolutionary implications of discordant clines across the Baltic Mytilus hybrid zone (*Mytilus edulis* and *Mytilus trossulus*). *Heredity*, *103*(2), 146-156.

Stumpp, M., Wren, J., Melzner, F., Thorndyke, M.C. & Dupont, S. (2011a). CO_2 induced seawater acidification impacts sea urchin larval development I: Elevated metabolic rates decrease scope for growth and induce developmental delay. *Comparative Biochemistry and Physiology Part A, 160*, 331-340.

Stumpp, M., Dupont, S., Thorndyke, M.C. & Melzner, F. (2011b). CO_2 induced seawater acidification impacts sea urchin larval development II: Gene expression patterns in pluteus larvae. *Comparative biochemistry and physiology Part A Molecular integrative physiology*, *160*(3), 320-330.

Stumpp, M., Trübenbach, K., Brennecke, D., Hu, M.Y. & Melzner, F. (2012) Resource allocation and extracellular acid-base status in the sea urchin *Strongylocentrotus droebachiensis* in response to CO_2 induced seawater acidification. *Aquatic Toxicology*, 110-111, 194-207.

Suffrian, K., Schulz, K. G., Gutowska, M.A., Riebesell, U. & Bleich, M. (2011). Cellular pH measurements in *Emiliania huxleyi* reveal pronounced membrane proton permeability. *New Phytologist*, *190*(3), 595-608.

Suzuki, M., Saruwatari, K., Kogure, T., Yamamoto, Y., Nishimura, T., Kato, T. & Nagasawa, H. (2009). An acidic matrix protein, Pif, is a key macromolecule for nacre formation. *Science*, *325*(5946), 1388-1390.

Suzuki, T. (1988). Ultrastructure of the excretory organs and urinary component of the marine bivalve, *Atrina* (S.) *pectinata*. *Comparative biochemistry and physiology. A.*, *90*(1), 79-83.

Takahashi, T. (2009). Climatological mean and decadal change in surface ocean pCO_2, and net sea–air CO_2 flux over the global oceans. *Deep Sea Research Part II: Topical Studies in Oceanography*, *56*(8-10), 554-577.

Takahashi, T., Sutherland, S.C., Feely, R.A. & Cosca, C.E. (2003). Decadal variation of the surface water pCO_2 in the western and central equatorial Pacific. *Science*, *302*(5646), 852-856.

Talmage, S.C. & Gobler, C.J. (2009). The effects of elevated carbon dioxide concentrations on the metamorphosis , size , and survival of larval hard clams (*Mercenaria mercenaria*), bay scallops (*Argopecten irradians*), and Eastern oysters (*Crassostrea virginica*). *Limnology and Oceanography*, *54*(6), 2072-2080.

Talmage, S.C. & Gobler, C.J. (2010). Effects of past, present, and future ocean carbon dioxide concentrations on the growth and survival of larval shellfish. *Proceedings of the National Academy of Sciences of the United States of America*, *107*(40), 17246-17251.

Talmage, S.C. & Gobler, C.J. (2011). Effects of elevated temperature and carbon dioxide on the growth and survival of larvae and juveniles of three species of Northwest Atlantic bivalves. *PLoSONE*, *6*(10), e26941.

Tedengren, M., Andre, C., Johannesson, K. & Kautsky, N. (1990). Genotypic and phenotypic differences between Baltic and North-Sea populations of *Mytilus edulis* evaluated through reciprocal transplantation 3. Physiology. *Marine Ecology-Progress Series*, *59*(3), 221-227.

Tedengren, M. & Kautsky, N. (1986). Comparative-study of the physiology and its probable effect on size in blue mussels (*Mytilus edulis* L) from the North-Sea and the northern Baltic proper, *25*(3), 147-155.

Thompson, R.J. & Bayne, B.L. (1972). Active metabolism associated with feeding in the mussel *Mytilus edulis* L. *Journal of Experimental Marine Biology and Ecology*, *9*, 111-124.

Thompson, R.J. & Bayne, B.L. (1974). Some relationships between growth, metabolism and food in the mussel *Mytilus edulis*. *Marine Biology*, *27*, 317-326.

Tomanek, L., Zuzow, M., Ivanina, A., Beniash, E. & Sokolova, I.M. (2011). Proteomic response to elevated pCO_2 level in eastern oysters, *Crassostrea virginica*: evidence for oxidative stress. *The Journal of Experimental Biology*, *214*, 1836-1844.

Truchot, J.P. (1976). Carbon dioxide combining properties of the blood of the shore crab *Carcinus maenas* (L): carbon dioxide solubility coefficient and carbonic acid dissociation constants. *Journal of Experimental Biology*, *64*(1), 45-57.

Truchot, J.P. & Duhamel-Jouve, A. (1980) Oxygen and carbon dioxide in the marine intertidal environment and tidal changes in rockpools. *Respiration Physiology* , *39*, 241-254.

Tunnicliffe, V., Davies, K.T.A., Butterfield, D.A., Embley, R.W., Rose, J.M. & Chadwick Jr., W.W. (2009). Survival of mussels in extremely acidic waters on a submarine volcano. *Nature Geoscience*, *2*(5), 344-348.

Uozumi, S. & Suzuki, S. (1979) "Organic membrane-shell" and initial calcification in shell regeneration. *Journal of the Faculty of Science*, *19*, 37-74.

Venn, A., Tambutté, E., Holcomb, M., Allemand, D. & Tambutté, S. (2011). Live tissue imaging shows reef corals elevate pH under their calcifying tissue relative to seawater. *PLoS ONE*, *6*(5), 9.

Vermeij, G.J. (1992). Trans-Equatorial Connections between Biotas in the Temperate Eastern Atlantic. *Marine Biology*, *112*(2), 343-348.

Väinölä, R. & Strelkov, P. (2011). *Mytilus trossulus* in Northern Europe. *Marine Biology*, *158*(4), 817-833.

Waite, J.H., Saleuddin A.S.M. & Andersen S.O. (1979). Periostracin- A soluble precursor of sclerotized periostracum in *Mytilus edulis* L. *Journal of Comparative Physiology B*, *130*, 301-307.

Waite, J.H. & Andersen, S.O. (1980). 3,4 Dihydroxyphenylalanine (DOPA) and sclerotization of periostracum in *Mytilus edulis* L. *Biological Bulletin*, *158*, 164-173.

Waldbusser, G.G., Bergschneider, H. & Green, M.A. (2010). Size-dependent pH effect on calcification in post-larval hard clam *Mercenaria* spp. *Marine Ecology Progress Series*, *417*, 171-182.

Waldbusser, G.G., Voigt, E.P., Bergschneider, H., Green, M.A. & Newell, R. I. E. (2010). Biocalcification in the eastern oyster (*Crassostrea virginica*) in relation to long-term trends in Chesapeake Bay pH. *Estuaries and coasts*, *34*, 221-231.

Walsh, P.J., McDonald, D.G. & Booth, C.E. (1984). Acid-base-balance in the sea mussel, *Mytilus edulis* .2. Effects of hypoxia and air-exposure on intracellular acid-base status. *Marine Biology Letters , 5*(6), 359-369.

Walther, K., Anger, K. & Pörtner, H. (2010). Effects of ocean acidification and warming on the larval development of the spider crab *Hyas araneus* from different latitudes (54° vs. 79°N). *Marine Ecology Progress Series*, *417*, 159-170.

Walther, K., Sartoris, F.J., Bock, C. & Pörtner, H. (2010). Impact of anthropogenic ocean acidification on thermal tolerance of the spider crab *Hyas araneus*. *Biogeoscience*, *6*, 12207-2215.

Wang, W. & Widdows, J. (1991). Physiological responses of mussel larvae *Mytilus edulis* to environmental hypoxia and anoxia. *Marine Ecology Progress Series*, *70*(1989), 223-236.

Weigelt, M. (1990). Oxygen conditions in the deep water of Kiel Bay and the impact of inflowing salt-rich water from the Kattegat. *Meeresforschung*, *33*(1),1-22.

Weihrauch, D., Becker, W., Postel, U., Riestenpatt, S. & Siebers, D. (1998). Active excretion of ammonia across the gills of the shore crab *Carcinus maenas* and its relation to osmoregulatory ion uptake. *Journal of Comparative Physiology B-Biochemical Systemic and Environmental Physiology*, *168*(5), 364-376.

Weihrauch, D. (2006). Active ammonia absorption in the midgut of the tobacco hornworm *Manduca sexta* L.: Transport studies and mRNA expression analysis of a Rhesus-like ammonia transporter. *Insect Biochemistry and Molecular Biology*, *36*(10), 808-821.

Weihrauch, D, Morris, S. & Towle, D.W. (2004). Ammonia excretion in aquatic and terrestrial crabs. *Journal of Experimental Biology*, *207*(26), 4491-4504.

Weiner, I.D. & Verlander, J.W. (2010). Molecular physiology of the Rh ammonia transport proteins. *Current Opinion in Nephrology and Hypertension*, *19*(5), 471-477.

Weiner, I.D. & Verlander, J.W. (2011). Role of NH_3 and NH_4^+ transporters in renal acid-base transport. *American journal of physiology Renal physiology*, *300*(1), F11-F23.

Weiner, S., Sagi, I. & Addadi, L. (2005). Structural biology. Choosing the crystallization path less traveled. *Science*, *309*(5737), 1027-1028.

Weiner, S. & Addadi, L. (2011). Crystallization pathways in biomineralization. *Annual Review of Materials Research*, *41*(1), 21-40.

Weiss, I.M. & Schönitzer, V. (2006). The distribution of chitin in larval shells of the bivalve mollusk *Mytilus galloprovincialis*. *Journal of Structural Biology*, *153*(3), 264-277.

Weiss, I.M., Tuross, N., Addadi, L. & Weiner, S. (2002). Mollusc larval shell formation: amorphous calcium carbonate is a precursor phase for aragonite. *The Journal of experimental zoology*, *293*(5), 478-491.

Weiss, R.F. (1974). Carbon dioxide in water and seawater: the solubility of a non-ideal gas. *Marine Chemistry*, *2*(3), 203-215.

Werner, U., Billerbeck, M., Polerecky, L., Franke, U., Huettel, M, van Beusekom, J.E.E. & De Beer, D. (2006). Spatial and temporal patterns of mineralization rates and oxygen distribution in a permeable intertidal sand flat (Sylt, Germany). *Limnology & Oceanography*, *51*(6), 2549-2563.

Wesslander, K., Omstedt, A., & Schneider, B. (2010). Inter-annual and seasonal variations in the air–sea CO_2 balance in the central Baltic Sea and the Kattegat. *Continental Shelf Research*, *30*(14), 1511-1521.

Westerbom, M., Kilpi, M. & Mustonen, O. (2002). Blue mussels, *Mytilus edulis* at the edge of the range: population structure, growth and biomass along a salinity gradient in the north-eastern Baltic Sea. *Marine Biology*, *140*(5), 991-999.

Widdows, J. & Bayne, B.L. (1971). Temperature acclimation of *Mytilus edulis* with reference to its energy budget. *Journal of the Marine Biological Association of the United Kingdom*, *51*(4), 827-843.

Williams, R.J. (1979) Freezing tolerance in *Mytilus edulis*. *Comparative Biochemical Physiology*, *35*, 145-161.

Wood, H.L., Spicer, J.I. & Widdicombe, S. (2008). Ocean acidification may increase calcification rates, but at a cost, P*roceedings of the Royal Society B*, *275*(1644), 1767-1773.

Wootton, J.T., Pfister, C.A., & Forester, J.D. (2008). Dynamic patterns and ecological impacts of declining ocean pH in a high-resolution multi-year dataset. *Proceedings of the National Academy of Sciences of the United States of America*, *105*(48), 18848-18853.

Wright, P.A., & Wood, C.M. (2009). A new paradigm for ammonia excretion in aquatic animals: role of Rhesus (Rh) glycoproteins. *Journal of Experimental Biology*, *212*(15), 2303-2312.

Yamamoto-Kawai, M., McLaughlin, F.A., Carmack, E.C., Nishino, S. & Shimada, K. (2009). Aragonite undersaturation in the Arctic Ocean: effects of ocean acidification and sea ice melt. *Science*, *326*(5956), 1098-100.

Yin, Y., Huang, J., Paine, M. L., Reinhold, V.N. & Chasteen, N.D. (2005). Structural characterization of the major extrapallial fluid protein of the mollusc *Mytilus edulis*: implications for function. *Biochemistry*, *44*, 10720-10731.

Zange, J., Pörtner, H.O., Jans, W.H. & Grieshaber, M.K. (1990). The intracellular pH of a molluscan smooth muscle during a contraction-catch-relaxation cycle estimated by [^{14}C]DMO and by ^{31}P-NMR spectroscopy. *The Journal of Experimental Biology*, *150*, 81-93.

Zeebe, R.E. & Sanyal, A. (2002). Comparison of two potential strategies of planktonic foraminifera for house building: Mg^{2+} or H^{+} removal? *Geochimica et Cosmochimica Acta*, *66*(7), 1159-1169.

Zeebe, R.E. & Wolf-Gladrow, D.A. (2001). *CO_2 in seawater: equilibrium, kinetics, isotopes*. (D. Halpern, Ed.) *Elsevier Oceanography Series* (Vol. 65, p. 346).

Zidi-Yahiaoui, N., Callebaut, I., Genetet, S., Le Van Kim, C., Cartron, J. P., Colin, Y., Ripoche, P. & Mouro-Chanteloup, I. (2009). Functional analysis of human RhCG: comparison with *E. coli* ammonium transporter reveals similarities in the pore and differences in the vestibule. *American journal of physiology Cell physiology*, *297*(3), C537-C547.

Erklärung

Hiermit erkläre ich gemäß § 9, dass ich diese Abhandlung, abgesehen von der Beratung durch meinen Betreuer, nach Form und Inhalt selbständig erarbeitet habe und keine anderen als die von mir aufgeführten Quellen und Hilfsmittel verwendet wurden. Diese Arbeit ist unter Einhaltung der Regeln guter wissenschaftlicher Praxis der Deutschen Forschungsgemeinschaft enstanden und wurde weder ganz noch in Teilen an anderer Stelle im Rahmen eines Prüfungsverfahrens eingereicht.

Kiel, März 2012 Jörn Thomsen